

Soil Spatial Scaling: Modelling variability of soil properties across scales using legacy data

S. E. Paterson

A thesis submitted in fulfilment of the requirements for the degree of Doctor
of Philosophy

2018

Faculty of Science

School of Life and Environmental Sciences

The University of Sydney

Declaration

This is to certify that to the best of my knowledge, the content of this thesis is my own work. This thesis has not been submitted for any degree or other purposes.

I certify that the intellectual content of this thesis is the product of my own work and that all the assistance received in preparing this thesis and sources have been acknowledged.

Stacey E. Paterson

Date:18-09-05

Thesis Summary

This thesis is concerned with the scaling properties of soil spatial variability. There is a need for better understanding of soil variability in space to allow more efficient sampling and mapping. In this thesis, we develop our understanding of the scaling behaviour of soil variability relies on using legacy data to develop empirically-based scaling theories. In the introduction, we highlight how understanding spatial variability informs digital soil mapping and spatial sampling and review existing studies of spatial variability. Our review highlights the practical problem of collecting sufficient data to develop a comprehensive theory of soil spatial scaling, and the associated knowledge gap. We propose to address this problem by using large legacy datasets to investigate the scaling properties of soil. We identify three major aims: First, a general characterisation of soil variability scales ranging from field to global. Second, the development of a general model of variability across scales, finally, to test the variability of soils compared to other environmental variables. We work towards each of these aims in Chapters 2 to 6 as outlined below.

Chapter 1 sets the context and significance of scaling issues related to soil science and describes the importance of scales of observation for understanding soil processes, in particular for digital soil mapping. We review soil variability across different scales and identify a major knowledge gap. Studies that describe soil variability at several fine scales commonly find variability dominated by variation within just a few meters. Studies that consider variability across a landscape scale tend to find useful measures of variability at these scales too. Largely due to the expense and difficulty of collecting data there are few studies that consider the scaling properties of variability between the sub field and regional scale. We proposed that legacy data might be a useful and as yet underused resource for addressing this gap.

In Chapter 2, we used soil texture legacy data from across the Australian continent as the basis for a description of soil variability at different scales. First, we employed empirical variogram calculation from classical geostatistics to model the soil variability at different scales by simultaneously varying the bin size and the extent. We further developed our theory of spatial scaling by combining the variograms into a composite that measured variability across scales. Using the ‘variogram method’ we investigated the possibility of a power scaling law, or the existence of a fractal dimension to describe roughness across scales. We found that the change in variability between scales was not well described by a fractal model, or even a traditional multifractal model. Instead we propose a new measure of roughness. Our new framework is conceptually linked to the multifractal model, but allows a gradual change in stochasticity or variability as the scales change. Our results suggest that a more

gradual approach to soil variability is more appropriate than the traditional multifractal framework, which proposes regions of self-similarity punctuated by rapid change.

In our third chapter, we use a radiometric dataset to investigate the effects of sampling distribution on the shape of the variogram and the roughness index. Radiometric data makes a useful proxy for soil texture as the radiometric signal is linked to clay. The Radiometric dataset has more even coverage (although a wider support) than the soil texture legacy data. This allows us to sample across the continent, and also allows us to investigate different sampling designs which may be useful for estimating scaling properties.

To investigate the claim that soil is more variable at fine scales than other environmental properties, we assemble a range of legacy data and remotely observed data for a number of environmental variables. Using the methods developed in Chapter 2, and the alternative sampling design developed in Chapter 3 for the remotely observed data, we compare variability between properties across scales. We find that contrary to popular mythology there are several environmental variables that show similar levels of stochasticity across most scales.

In order to test the limits of our proposed model of scaling of soil properties, we access a global dataset and use it to model global clay variograms. Unlike variability at the other scales, we find that the global clay variogram is strongly isotropic, and the variograms do not fit well with the model of spatial scaling developed for the Australian continent. This might imply that the spatial scaling model we develop in Chapter 2 applies only up to continental scales. Surprisingly, the global variograms do not show more variability than the continental variograms.

In our final investigative chapter, we seek to better understand the scaling properties of the soil at the field and sub field scale. Because of the importance of these scales for agricultural decision making, there is a significant amount of data available at these scales. This data is currently under used. We compile precision agriculture variograms from the literature and investigate whether they are useful for prediction of field scale variability. There is some similarity in the range (the majority of field scale variograms reach the sill at less than 100m) but the shape and the other variogram properties vary widely. The existing literature does not provide a useful guide to the expected variability of soil properties at the field scale. Further, the extremely short range, and high sill that is found at these scales suggests that further work is to be done to understand how the 'local sill' and the 'global sill' interact in practice.

The final chapter of this thesis presents conclusions and areas of future work to further improve our understanding of soil spatial scaling. Recommended areas of future work broadly included a greater

focus on developing an understanding of how the scaling patterns of variability differ between regions, and the links between variability in soil properties and other environmental properties.

Acknowledgements

“Sometimes success demands a certain refined insanity.”

Isobelle Carmody, The Keeping Place

The first acknowledgement needs to go to my supervisors Alex McBratney and Budiman Minasny. Alex and Budi possess a wealth of knowledge about Pedometrics. Over the last four years I have enjoyed many moments of insight, clarity or humour from conversation with them. I thank you both for the opportunity to approach this intriguing topic, for your ideas, your practical help and your guidance.

Of course, a PhD is rarely finished without input from many sources. What follows is an acknowledgement of many, but by no means all of the individuals who have helped me along the way.

Nathan Odgers’ time and willingness to help me learn some of the finer points of managing and manipulating spatial datasets was invaluable to me early in my thesis. Thom Bishop has always been willing to share his knowledge of geostatistics (and more than willing to share his knowledge on the best way to approach a conference). Brendan Malone read early drafts, and provided useful comments on some chapters of this thesis (as did Nathan). From my first week in Sydney Uta Stockmann has been a source of warmth, wisdom and an exemplar of German competency. Kanika Singh and Vanessa Pino have also provided me with sound practical advice. Brett Whelan engaged in many useful discussions as I wrote Chapter 6. Damien, Stephen, Willem, Balwant and Floris all leant me their varying expertise at different points in this process.

My dear friend Sanji. Thank you for the walks and talks, the sounding board, the technical trouble shooting. Niranjan (#1 Nice guy and my first official PhD friend), our whole office is the better for having you in it. My cubicle mates, Ignacio, YuXing and Jose. Supportive desk neighbours make a huge difference in quality of PhD life. Jose in particular has helped me with coding in R. I am grateful to have shared space with people happy to talk through ideas, laugh and have a friendly chat with. Liana Pozza my over the fence neighbour requires special mention. Thank you for keeping me on track, lending me your bean bag and your willing ear. Ed, Patrick, Jason, Mario, Jay, Wartini, Phil, James. I have learnt something from each of you.

Outside of the office, Matt Pringle was instrumental in writing Chapter 6. Ross Whelan provided the NSSC dataset which was the basis of Chapter 2. Richard Webster and Ana Tarquis made useful suggestions on conference presentations that ultimately helped to improve the content in this chapter. Ischani Wheeler provided emergency tech assistance at my first Pedometrics conference, and

has since provided occasional (but invaluable remote guidance). Brooke and Claire, Tessa and Kelly your combined wisdom (about life in general and PhDs in particular) has been invaluable to me, for much of the last decade and especially the last few years and months.

To the climbers, all the climbers: Thank you for your company, thank you for catching me, thank you for pushing me, thank you for taking me to the beautiful places, and thank you especially providing me with the perspective and balance I needed to persevere. Jacob, you taught me how to haul myself up a hundred meter cliff face, and how useful such a skill can be for regaining perspective. Ange, you rescued me when I couldn't work out how to rescue myself.

To everyone who has laughed, danced, argued, philosophised, shared food or drink, with me, helped me move, lived with me – thank you for helping to keep me whole and keep me sane. My life has been the richer for you.

Finally, I want to thank my family, especially my parents. I am lucky to come from a family where love and support were taken as a given. I am lucky to come from a home where questions were encouraged and answers were rarely prescriptive. I am lucky to have you in my life. I love you very much.

Thank you all,

I am grateful.

Chapter 2 of this thesis is published as Paterson S. Minasny B. McBratney, A. Spatial variability of Australian Soil texture: A multiscale analysis. *Geoderma*, 309, 60-74

Chapter 6 of this thesis is published as Paterson S. McBratney A. Minasny B. Pringle M. (2018) Variograms of Soil Properties for Agricultural and Environmental Applications. In Alex McBratney, Budiman Minasny and Uta Stockmann (Eds.) *Pedometrics* (pp 623-667) London, Springer.

Table of contents

Contents

General introduction	1
1.1 Soil and Scale.....	2
1.2. Soil Spatial Scaling and the Soil Map.....	5
1.2.1 Spatial scale and sampling design.....	6
1.2.2 Spatial scale and change of support	6
1.2.3 Studies of soil spatial variability at different scales	7
1.3. Legacy data: An opportunity for improving our understanding of soil spatial scaling.....	9
1.4. Our Questions	9
A list of important spatial terms.....	15
Spatial Variability of Australian Soil Texture: A multiscale analysis	17
2.1. Introduction.....	19
2.2 Methods.....	20
2.2.1 Conceptual overview	20
2.2.2 NSSC soil texture data	21
2.2.3 Experimental Variograms – modelling at multiple scales.....	23
2.2.4 Experimental Variograms - improving fit using spatial declustering	24
2.2.5. Measures of roughness: The Hausdorff Besicovitch Dimension and the Hurst Exponent	26
2.2.6. The ‘Variogram Method’ for calculating the D Value	29
2.2.7. D values: Comparing variability across scales.....	30
2.2.8. The Hausdorff Besicovitch Dimension: An adaption of the ‘Variogram Method’ for continuous estimates of ‘roughness index’	31
2.2.9 Implications of the two methods.....	37
2.3 Results and Discussion	37
2.3.1 Empirical Variograms – Variability across scales and the impact of spatial declustering ...	37
2.3.2 The Roughness Index – Variability across scales	42

2.3.3. D values: Comparison of methods	43
2.3.4. Changes in Soil variability with depth	46
2.3.5. Spatial variability increases with depth: Possible mechanistic explanations	47
2.3.6 Contribution to spatial scaling literature	47
2.3.7 Future work.....	48
2.4 Conclusions.....	50
Assessing the impact of sampling distribution on the Variogram and roughness index.....	55
3.1 Introduction.....	57
3.2 Methods.....	57
3.2.1 Data	57
3.2.2 Sampling Design.....	58
3.3. Results and Discussion	62
3.3.1 Clustered observations, declustering and the variogram.....	62
3.3.2 Alternative sampling designs, and the roughness index	64
3.4 Conclusions.....	67
New Data for Old Questions: Is soil more variable than other environmental properties?	69
4.1 Introduction.....	71
4.2 Methods.....	72
4.2.1 The roughness Index	72
4.2.2. Applying roughness index to different data structures	72
4.2.3. Point Data	74
4.2.4. Calculating an experimental variogram from coverage data	77
4.2.4.2. Coverage datasets – summary of key parameters	77
4.3. Results and Discussion	80
4.3.1. Curve Fit	80
4.3.2. Overview of results.	85
4.3.3. Topographic variables.....	90
4.3.4 Radiometrics	91

4.3.5 Rainfall	92
4.3.6 Enhanced Vegetation Index	92
4.4. Implications and Conclusions	93
4.4.1. Implications.....	93
4.4.2. Conclusions	95
Calculating the Global Variogram. Modelling soil variability beyond the continental scale	99
5.1 Introduction.....	101
5.2 Methods.....	101
5.2.1. Calculating the Global Variogram	101
5.2.2 The data	102
5.3. Results and Discussion	107
5.3.1. Global Variability.....	107
5.3.2 Limits of continuous change model	108
5.3.3. Global Anisotropy	108
5.3.4. Global Non-stationarity.....	109
5.3.5. Global Variability with Depth.....	110
5.4 Conclusions.....	111
Variograms of Soil Properties for Agricultural and Environmental Applications.....	113
6.1. Geostatistics and precision agriculture	115
6.2. Soil survey, the variogram and kriging	115
6.3. Key components of the variogram	116
6.4 Soil survey design: capturing spatial variability	118
6.5. Variograms from the precision agriculture literature.....	119
6.5.1. Field scale soil variograms: key trends.....	120
6.5.2. Field scale soil variograms: methodological differences	121
6.5.3. Field scale soil variograms: a compilation	123
6.6 Estimation of the variogram from proportional variograms	132
6.7 Estimation of the variogram from average variograms.....	132

6.8 Ancillary information.....	133
6.9 Expert Knowledge	133
6.10 Quick variograms.....	134
6.11 Recommendations.....	136
Concluding Remarks and Future work	168
7.1 Overview.....	169
7.1.1 How variable is the soil at different spatial scales?	169
7.1.2. Can we develop a general model to describe how soil variability changes across spatial scales?	170
7.1.3 How variable is the soil compared to other soil properties?.....	171
7.2 Future work.....	172
7.3 Final remarks.....	175

List of figures

Figure 1.1. Soil structure schematic, based on Dijkman’s (1974) hierarchy	2
Figure 1.2. Overview on the scale-dependent hierarchy of drivers and indicators for SOC storage (MAT = mean annual temperature, MAP = Mean annual precipitation, TWI = topographic wetness index, SSA = specific surface area). Figure from Wiesmeier et al. (2019)	3
Figure 1.3. The sampling scale triplet of spacing, extent and support for a regularly spaced two dimensional case. (Figure taken from Skøien & Blöschl, (2006)).	5
Figure 2.1. The distribution of the NSSC dataset. Each black dot represents an individual soil observation.	22
Figure 2.2. Power curve variograms and simulated 2 dimensional surfaces. D values are: 2.5, 2.8 and 2.95 top to bottom.....	28
Figure 2.3. Composite Variogram, top soil clay	32
Figure 2.4. Composite variogram, top soil clay, \log_{10} - \log_{10} scale	33
Figure 2.5. Composite variogram, top soil clay, \log_{10} - \log_{10} scale – fitted curve	34
Figure 2.6. Derivative of the composite variogram curve – plotted against $\log_{10}(h)$ (log to the base 10 separation distance).	35
Figure 2.7. Derivative of the composite variogram curve – plotted against h (separation distance), top soil clay.....	35
Figure 2.8. Roughness Index calculated from the composite variogram curve: plotted against separation distance (h)	36
Figure 2.9. Empirical variograms calculated across varying spatial extents. Data from the NSSC dataset: Clay content (% fraction); soil depth 0-5cm. Black dots represent individual bins. Red lines are the fitted power curves. Other coloured lines indicate expansion.....	39
Figure 2.10. Empirical variograms calculated across varying spatial extents using declustering. Data from the NSSC dataset: Clay content (% fraction); soil depth 0-5cm. Black dots represent individual bins. Red lines are the fitted power curves. Other coloured lines indicate expansion.	40
Figure 2.11. Empirical variograms calculated across varying spatial extents using declustering. Data from the NSSC dataset: Sand content (as percentage): soil depth 0-5cm. Black dots represent individual bins. Red lines are the fitted power curves. Other coloured lines indicate expansion.	41
Figure 2.12. Hausdorff Besicovitch Dimension plotted against separation distance. Sand and Clay topsoil and subsoil	44

Figure 2.13. \log_{10} - \log_{10} variograms with fitted curves. Sand and Clay topsoil and subsoil. The blue squares shown are the data points from the composite variograms. The red curves are the fitted models (equation and R2 shown on chart).....45

Figure 2.14. D values mapped against spatial extent for clay (top) and sand (bottom) 46

Figure 3.1. Left Panel: Radiometric sampling density (Minty et al. 2009) Right Panel: Potassium layer from the radiometric map of Australia (original source Geoscience Australia). 58

Figure 3.2 The distribution of the NSSC dataset. Each black dot represents an individual soil observation. (Duplicated from Figure 2.1)..... 59

Figure 3.3. Schematics showing the paired observations for 10km lag and 100km lag (right). Original random sample (1 to 720) are shown in black. Paired observations (isotropic condition) are shown in red. Note the greater separation distance in the right hand panel results in more observations falling outside of the boundaries of the continent..... 61

Figure 3.4. a-c Experimental variograms calculated from Radiometrics data using different sampling design schemes and methodologies..... 63

Figure 3.5 a-c Log-log experimental variograms calculated from Radiometrics data using different sampling design schemes and methodologies. 65

Figure 3.6. Comparison of sampling designs, roughness index value against distance 0-10km.....66

Figure 3.7. Comparison of sampling designs, roughness index value against distance 0-1000km.....66

Figure 4.1. The distribution of the NSSC dataset. Each black dot represents an individual soil observation. 75

Figure 4.2. Distribution of the Bureau of Meteorology rainfall observations 2001-2010 (10 year average) 76

Figure 4.3. Left Panel: Radiometric sampling density (Minty et al. 2009) Right Panel: Potassium layer from the radiometric map of Australia (original source Geoscience Australia). 79

Figure 4.4. Log-log empirical semivariogram (DEM), with increasing exponential decay model fitted 81

Figure 4.5. Log-log empirical semivariogram (relief), with increasing exponential decay model fitted 82

Figure 4.6. Log-log empirical semivariogram (elevation – 300m focal range), with increasing exponential decay model fitted..... 82

Figure 4.7. Log-log empirical semivariogram (Radiometrics), with increasing exponential decay model fitted..... 83

Figure 4.8. Log-log empirical semivariogram, (EVI) with increasing exponential decay model fitted . 83

Figure 4.9. Log-log empirical semivariogram (Clay topsoil), with increasing exponential decay model fitted.....	84
Figure 4.10. Log-log empirical semivariogram (Sand topsoil), with increasing exponential decay model fitted.....	84
Figure 4.11. Log-log empirical semivariogram (Rainfall), with increasing exponential decay model fitted.....	85
Figure 4.12. Roughness index: 0-1000km for multiple environmental properties	86
Figure 4.13. Roughness index: 0-10km across scales for multiple environmental properties.....	86
Figure 4.14. Roughness index across scales: average annual rainfall, selected years.....	88
Figure 4.15. Roughness index across scales	90
Figure 5.1. Distribution of WoSIS and NSSC dataset	103
Figure 5.2. Percentage clay fraction statistics by latitude (North-South). Average per degree of latitude in left panel, variance per degree of latitude in right panel.	104
Figure 5.3. Percentage clay fraction statistics by longitude (East-West). Average per degree of latitude in left panel, variance per degree of latitude in right panel.	104
Figure 5.4. Percentage clay fraction against latitude. On the left panel each red point represents an observation. On the right panel each red point represents the average of the % clay fraction observations collected in that degree of longitude. The black line is the same on both panels	105
Figure 5.5. Percentage clay fraction statistics calculated from residual data by latitude (North-South). Average per degree of latitude in left panel, variance per degree of latitude in right panel.....	105
Figure 5.6. Global Variogram North South, calculated from original data (blue points) and residual data (red points).....	106
Figure 5.7. Global variogram – East West calculated from original data (blue points) and residual data (red points).....	106
Figure 5.8. Experimental semivariograms calculated from the residuals (detrended clay % fraction data), with composite variogram from Chapter 2 overlain.	107
Figure 5.9. Koppen climate classification, source: Rubel & Kottek, 2010	109
Figure 5.10. Clay (0-2 micro meter) mass fraction % at 5cm depth. Source soilgrids.org	110
Figure 5.11. Global variogram calculated at increasing depth intervals	111
Figure 5.12. Global variogram calculated at increasing depth intervals	111
Figure 6.1. Stylised diagram, showing the three most important indicators of spatial structure, the nugget, sill and the range.....	116
Figure 6.2. <i>Compilation of field scale variograms for Clay.</i> The bold black line represents the average variogram. Summary details and references for each variogram (a-ag) are given in Table 6.1.....	124

Figure 6.3. *Compilation of field scale variograms for Sand* The bold black line represents the average variogram. Summary details and references for each variogram (a-r) are given in Table 2. 125

Figure 6.4. *Compilation of field scale variograms for pH.* The bold black line represents the average variogram. Summary details and references for each variogram (a-ag) are given in Table 6.3..... 126

Figure 6.5. *Compilation of field scale variograms for Carbon.* The bold black line represents the average variogram. Summary details and references for each variogram (a-al) are given in Table 6.4..... 127

Figure 6.6. *Compilation of field scale variograms for Available Nitrogen.* The bold black line represents the average variogram. Summary details and references for each variogram (a-m) are given in Table 6.5. 128

Figure 6.7. *Compilation of field scale variograms for Total Nitrogen.* The bold black line represents the average variogram. Summary details and references for each variogram (a-h) are given in Table 6.6. 129

Figure 6.8. *Compilation of field scale variograms for Phosphorus.* The bold black line represents the average variogram. Summary details and references for each variogram (a-ab) are given in Table 6.7. 130

Figure 6.9. *Compilation of field scale variograms for Potassium.* The bold black line represents the average variogram. Summary details and references for each variogram (a-ad) are given in Table 6.8. 131

Figure 6.10. *Sampling approach for estimating a ‘rough’ variogram.* Here, it is shown that sampling is recommended in 8 locations (4 widely spaced points, each with a closely spaced pair, i.e. A-B, C-D, E-F and G-H). Each letter represents a sampling location. 135

List of tables

Table 2.1. Percentage Clay fraction: Summary statistics	22
Table 2.2. Percentage Sand fraction: Summary statistics	23
Table 2.3. Extent and bin size combinations for empirical variograms	24
Table 2.4. Extent, bin size and grid size combinations for declustered empirical variograms	26
Table 2.5. Extent, bin and grid size for declustered empirical variograms used in calculation of D values	30
Table 2.6. Power curve parameters and Roughness Index values from variograms of clay and sand content at 0 – 5cm depth interval.	41
Table 3.1. Comparison of roughness index value against extent for different sampling designs	66
Table 4.1. Advantages and disadvantages of point and coverage data used in this analysis	72
Table 4.2. Summary of key metadata properties of datasets we used.	73
Table 4.3. Percentage Clay fraction: Summary statistics	74
Table 4.3. Roughness Index Values: selected distances	88
Table 5.1. Summary statistics of splined composite WOSIS and NSSC dataset	103
Table 6.1. Compilation of key properties for clay variograms	136
Table 6.2. Compilation of key properties for sand variograms	140
Table 6.3. Compilation of key properties for pH variograms	142
Table 6.4. Compilation of key properties for carbon variograms	146
Table 6.5. Compilation of key properties for available nitrogen variograms	149
Table 6.6. Compilation of key properties for total nitrogen variograms	151
Table 6.7. Compilation of key properties for phosphorus variograms	153
Table 6.8. Compilation of key properties for potassium variograms	157

Chapter 1

General introduction

Tell the truth through whichever veil comes to hand — but tell it.
Zadie Smith

1.1 Soil and Scale

Our understanding of any property or process is influenced by the scale of our observation. When studying a particular soil property, it is critical that investigation occurs at a level of resolution which is appropriate for the model we are trying to construct (Hoosbeek & Bryant, 1992). In some cases, we can be guided by the structure of the soil itself. Dijkerman (1974) emphasises the hierarchical nature of soil organisation: the soil can be subdivided into smaller and smaller subsystems of decreasing complexity: the landscape can be divided into the profile, which can be divided into the pedon.

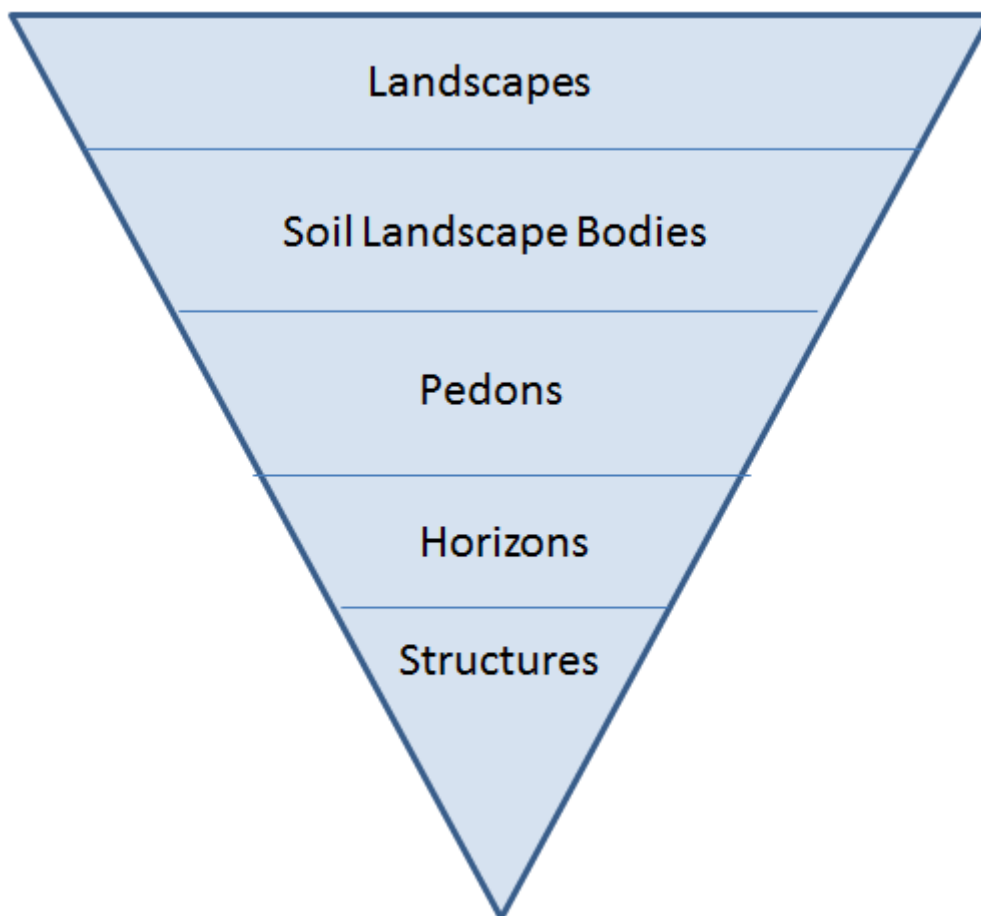


Figure 1.1. Soil structure schematic, based on Dijkerman's (1974) hierarchy

Soil formation is dependent upon the interaction of environmental variables such as climate, parent material, vegetation, human influence, topography and time (Heuvelink & Webster, 2001; Jenny, 1941; R. Webster, 2000). Each of these factors will operate distinctly at different scales. For example, general climate trends are much easier to predict (more consistent) than the exact location and timing of a thunder storm (Costanza & Maxwell, 1994). These soil forming factors interact with each other

and with the soil in complex ways. For example, rainfall and climate drive the development of vegetation (in conjunction with the existing soil condition) and over time the vegetation affects not only the soil condition, but also the microclimate, and to some extent the macroclimate. This complexity means that while the behaviour of the soil is theoretically deterministic and, with enough information, should be possible to model mechanistically, in practice, we often cannot explain soil behaviour mechanistically. Or, if we can, we can only do so under certain specific scales. For example, Moni et al. (2010) find evidence that suggests the mechanisms that link iron and aluminum oxides to storage of organic carbon operate at the pedon scale, but not at the field scale. Wiesmeier et al. (2019) characterise key scale dependent drivers of soil carbon variability (Figure 1.2).



Figure 1.2. Overview on the scale-dependent hierarchy of drivers and indicators for SOC storage (MAT = mean annual temperature, MAP = Mean annual precipitation, TWI = topographic wetness index, SSA = specific surface area). Figure from Wiesmeier et al. (2019)

Our scales of observation and the statistical analysis employed can be expected to affect the results of any model we apply them to (Dungan et al., 2002). This is not always explicitly considered by soil scientists, but the underlying principle is well understood by the discipline: A simple example, likely to be well known is the practice of compositing soil samples. This practice reduces the impact of fine scale spatial variability. This deliberate removal of very fine scale spatial information (typically compositing occurs within a few meters) reduces fine scale stochasticity and reveals more general spatial trends. Another example which highlights the soil scientists understanding of the importance of scale is the pedological practice of breaking up soil profiles by horizons.

So far, we have used the term 'scale' without including a precise definition. The term scale is often used with different meanings between different disciplines¹. We introduce here some more precise terms which describe important components of scale: support, spacing and extent. These terms can be used to describe temporal variability (Blöschl & Sivapalan, 1995) or spatial variability in one or more dimensions (Young & Gotway, 2007). The focus of this thesis is on lateral spatial variability, so unless otherwise specified when we refer to scale, or the terms Support, Spacing and Extent we are referring to lateral spatial variability.

- **Spacing** refers to how far apart the observations are
- **Support** refers to the coverage of the observation
- **Extent (sampling)** the maximum distance between any two observations

As well as being used to describe the scale of observation, each of these terms can be used to describe the scale of the model output as well. When used to describe the model output the terms have a similar meaning.

- **Extent** refers to the maximum distance of the map or the model
- **Spacing** refers to how frequently the predictions occur and
- **Support** refers to the coverage of each prediction

It is common for spacing and support of a model output to be identical. When this is the case, support and spacing are often bundled together into a single term (**resolution**) or **grain size**.

¹ With reference to mapping, 'small scale' to describe a map which depicts a large territory, and therefore has been scaled down more. Large scale describes a map which depicts a small territory, and therefore which is drawn at scale not too far from the original. The terms small scale and large scale do not provide information about the resolution or the quality or detail of the information underlying the map.

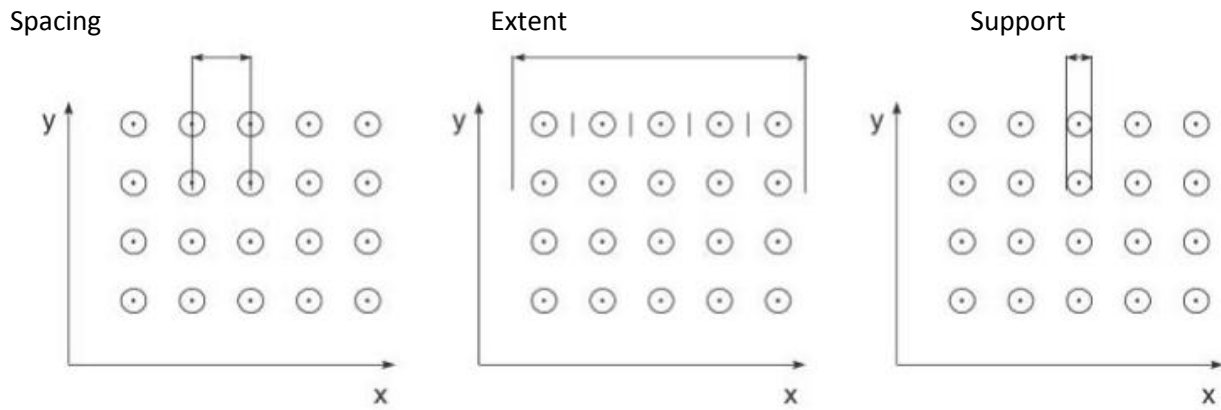


Figure 1.3. The sampling scale triplet of spacing, extent and support for a regularly spaced two dimensional case. (Figure taken from Skøien & Blöschl, (2006)).

These terms can also sometimes be usefully applied to the modelling or working scale.

1.2. Soil Spatial Scaling and the Soil Map

Scale is an important concept in soil science (and other areas of science). It has particular importance for the growing field of digital soil mapping. Over the last several decades there has been a proliferation of techniques being developed for digital soil mapping (Grunwald, 2011). Development of accurate soil maps at a range of scales will be required for addressing challenges of the future, in particular climate change and food security (Grunwald, 2011).

A major challenge faced by the digital soil mapper is using observations from one scale and converting it into information that is useful for decision making. For information to be useful it needs to be accurate and precise enough to meet the needs of the information user, and it also needs to be available at a spatial scale relevant for decision making (Lark, 2005; Malone, et al. 2013). This is an especially challenging problem when we are working with the soil resource, because the scale of observation is typically very far removed from the required scale of prediction. Current methods of soil sampling are expensive, time consuming and destructive. Our observation support is typically very small: a soil core typically has a lateral support of around 10cm, and with a few exceptions spacing is either sparse, or the extent is small. By contrast when we require information about the soil we require it to be continuous, and where possible detailed.

Geostatistics has provided us with a useful toolkit for predicting continuous soil properties from limited information. Despite this, the problem of how best to predict from different scales of observation is not yet fully understood. The soil is complex: it encompasses physical, chemical and biological processes which interact differently across spatial scales. This means that soil variability has

different characteristics at different scales (Lark & Webster, 1999)². Our understanding of how this variability changes between scales is limited by our ability to observe the soil. Our limited understanding of soil variability across scales is a problem because optimal sampling and modelling of the soil requires an understanding of how variability changes between scales. In particular, an accurate understanding of variability across scales will inform two practical questions commonly faced by the Digital Soil Mapper.

This leads to two practical questions for the Digital Soil Mapper:

1. How can we best sample (control the scale of observation) to get the most useful information for the least cost.
2. Given the information that we do have, how can we best use it to produce a useful map or model?

We describe in section 1.2.1 and 1.2.2. how a greater knowledge of the scaling properties of soil variability helps us to better address each of these questions.

1.2.1 Spatial scale and sampling design

Understanding soil variability at different scales allows us to create a more efficient sampling design (Kerry & Oliver, 2004; Lark, 2002; Pettitt & McBratney, 1993). There is always a trade off between the cost of sampling (time, money and soil destruction) and the benefit, information gained from the sampling. When we don't know how variability changes with scale, we cannot estimate ahead of time how much information we might gain from increasing the resolution of the sampling. We elaborate on this problem in Chapter 2.

1.2.2 Spatial scale and change of support

Understanding the detail required to make information 'relevant for decision making' requires not only an understanding of the decisions which are being made, but also an understanding of the underlying variability of the soil at any particular scale. The first part of this statement is perhaps intuitively obvious. A landholder who can manage their fertilizer application down to 1m is unlikely to

² When we use the term variability we follow Heuvelink & Webster, (2001); McBratney,(1992); Webster, (2001) who define soil variability as the potential or tendency for the soil to vary. Measures of variability for a particular property include the range, s.d. and the variance. Each of these measures is a method of quantifying the potential of a particular property to vary. In this thesis we tend use the semivariance, and the variogram to quantify variograms across scales. We also use statistics derived from the semivariogram to quantify how variability changes with scale.

be particularly interested in the difference between individual cm, or in the average variability across the whole field. The second part of this paragraph's opening statement: that the underlying variability at any given scale is an important determinant of the 'relevant' spatial scale is perhaps less obvious. Antle et al. (2003) highlight this with reference to different management regimes for soil carbon sequestration. Understanding how spatial variability changes between scales also allows us to understand how the representation of the soil resource in a given map compares to the underlying reality (El Maayar & Chen, 2006; Malone et al., 2013; Zhang et al. , 2002). All maps (like all other types of models) involve generalisations. Understanding how soil variability changes between scales allows us to understand how much information is lost in any particular generalisation.

1.2.3 Studies of soil spatial variability at different scales

There have been significant efforts made to develop our understanding of how soil variability changes across scales. The majority of these studies focus on understanding the scaling properties of variability at extents less than 50 km. This is in part due to the expense of wide extent field surveys, and in part because of the importance of understanding fine scale variability for precision agriculture applications.

The majority variograms of soil properties calculated at the field scale have a local sill at less than 100m (more detail in chapter 2). Beckett & Webster (1971) find that in general around half of the variability contained within a field can be found within a meter (when sampling using traditional soil cores). This emphasises the importance of very fine scale spatial variability. This tendency to find significant variability in soil at short extents is often also found in studies that focus more explicitly upon scaling. Smith's (1938) study of the variability in yield finds that as the size of the field increases the variability captured within it also increases but at a decreasing rate. Using an explicitly nested sampling design (optimal for capturing variability across scales (Le Guen et al., 2017) find that fine scale variability is significant and masks the effects of biochar application between fields. Combining fractal theory with the variogram, Burrough (1983) finds that soil pH and texture fraction exhibit notable short term stochasticity. Amico (2015) finds fine scale variability is driven by cryoturbation. Šamonil et al., (2011) find that that 70-80% of the sill (across a field) occurs within a distance of 10m.

Studies that consider the variability of soil at fine scales consistently find high levels of soil stochasticity. However, studies that measure the variability and spatial dependence of different soil properties at regional scales also tend to find patterns of dependence at extents up to hundreds of km. Liu et al. (2013) measure spatial dependence of Nitrogen and Phosphorous across the Loess plateau (an extent of ~ 1000km at the maximum East West direction) and find spatial dependence at extents of several hundred km. Hu, et al. (2014) and Liu et al. (2013) explicitly compare variability

between scales. Hu et al. find that soil organic matter and total nitrogen spatial dependence at scales of 30km extent and 400m spacing, are distinct from spatial dependence at fine scales (5km extent and 100m spacing). Liu et al. (2013) find something similar when they measure the spatial dependence of soil nutrients in an agricultural region of Eastern China at (12km and 84km). Xiaoni, et al. (2010) find scale dependence in their examination of scaling properties of heavy metals in agricultural soil. The difficulty of obtaining enough samples to accurately measure variability at regional scales means that these studies typically cannot consider variability across a wide range of scales. Each sample taken by Xiaoni et al. (2010) is made up of five samples within a 10m by 10m square. Hence, they are deliberately removing the fine scale variability that field scale studies are deliberately investigating. Yemefack et.al. (2005) use nested sampling and ANOVA analysis to compare variability at plot, field and regional scales, but their sample size is limited to only 134 points, which may not be sufficient for a comprehensive modelling of the scaling patterns. In a recent study, Lark et al., (2017) suggest that estimation of scale dependent variance components would require around 200-250 samples.

One field in which there have been studies linking scaling properties from the very fine to the continental scale is in microbiology. Green et al. (2004) find a power law relationship linking microbial biodiversity to area. Zhou et al. (2008) do not find a strong power law relationship between species richness and area. Van Der Gast et.al. (2011) find that arbuscular mycorrhizal fungi demonstrate scaling in turnover, but that this is dependent on human management. Based on the description of studies above we conclude the following:

- The majority of studies that consider field scale variability find significant variability reached at very short extents
- Studies that consider the spatial variability and dependence at regional scales often find spatial correlation at extents up to hundreds of km.
- There are few studies that compare spatial variability / dependence at more than one or two scales
- The high data requirements for describing variability across scales represent a significant barrier to accurately describing how variability changes with scale.
- There are significant knowledge gaps about how variability is related between scales. There is especially a lack of empirical studies that model the change in variability of soil properties between multiple scales.

1.3. Legacy data: An opportunity for improving our understanding of soil spatial scaling

There are significant data requirements for modelling the scaling properties of soil variability (Lark et al., 2017). These present a significant difficulty in the development of theory that describes how the statistical properties of the soil vary with scale. A general theory to describe how the variance of soil properties changes with spatial scale would allow more efficient sampling design and allow better use of existing soil information.

In the last ten years or so there have been significant undertakings aimed at compiling and synthesising soil legacy data (Ribeiro et al., 2015; Searle, 2014). These compiled data sources have been used for large scale (global and national) digital soil mapping projects. They are a potentially valuable resource for modelling variability across scales from the local to the global. This thesis aims to use these existing legacy data sources to model spatial variability across scales and investigate the possibility of developing a general theory of spatial scaling.

1.4. Our Questions

There is a significant knowledge gap around how the spatial variability of soil at fine scales and short extents is connected to the spatial variability of soils at coarser scales and greater extents. Fine scale studies (field extent or smaller) tend to find that variability is dominated by very fine scale variability (within a few meters), large scale studies often find trends in spatial variability occurring across hundreds of km. Due (in part) to the cost and difficulty of sampling across multiple scales there are limited studies that link variability at the sub field scale to variability at scales of more than a few km.

Our thesis addresses the following broad questions:

- *How variable is the soil at different spatial scales?*
- *Can we develop a general model to describe how soil variability changes across spatial scales?*
- *How does soil variability compare with the variability of other environmental properties across spatial scales?*

How variable is the soil at different spatial scales?

In our initial characterisation of soil variability at different spatial scales (Chapter 2), we calculate declustered variograms from a legacy dataset. By varying the bin size and spatial extent we are able to change the scale of variability that each variogram is modelling. We assess the impact of the

distribution of the dataset using a proxy variable (Chapter 3). We use the same method to calculate global variograms using a different legacy dataset (Chapter 5). We also include a meta-analysis of field scale variograms to examine the field and sub field variability of soil properties in more detail (Chapter 6).

Can we develop a general model to describe how soil variability changes across spatial scales?

In the second part of Chapter 2, we apply the 'empirical variogram method' of Burrough (1983) to the Australian legacy dataset. We find that a modification of this method provides a better characterisation of how variability changes across scales. When calculating the global variogram (Chapter 5) we find that the model does not extend to the global scale. We also find that while the model works well when applied to the sub-field scale based on the legacy dataset, individual field scale variograms are not well captured within this framework (Chapter 6).

How does soil variability compare with the variability of other environmental properties across spatial scales?

In Chapter 2, we develop a general model that describes spatial variability in soils from the field to the continental scale. In Chapter 4 we apply this model to other environmental variables. This allows us to compare the variability between environmental properties across multiple scales. It also allows us to consider the implications of different support and sampling distribution on the modelled results.

REFERENCES

- Amico, M. D., Gorra, R., & Freppaz, M. (2015). Catena Small-scale variability of soil properties and soil – vegetation relationships in patterned ground on different lithologies (NW Italian Alps). *Catena*, 135, 47–58.
- Antle, J., Capalbo, A. S., & Elliott, E. (2003). Spatial heterogeneity, contract design, and the efficiency of carbon sequestration policies for agriculture, *Journal of Environmental Economics and Management*, 46, 231–250.
- Beckett, P. H. T., & Webster, R. (1971). Soil Variability: A review. *Soils and Fertilisers*, 34, 1–15.
- Blöschl, G., & Sivapalan, M. (1995). Scale issues in hydrological modelling: A review. *Hydrological Processes*, 9 (September 1994), 251–290.
- Burrough, P. a. (1983). Multiscale sources of spatial variation in soil. I. The application of fractal concepts to nested levels of soil variation. *Journal of Soil Science*, 34, 577–597.
- Costanza, R., & Maxwell, T. (1994). Resolution and predictability : An approach to the scaling problem, 9(1), 47–57.
- Dijkerman, J. C. (1974). Pedology as a science: The role of data, models and theories in the study of natural soil systems. *Geoderma*, 11(2), 73–93.
- Dungan, J. L., Perry, J. N., Dale, M. R. T., Legendre, P., Citron-Pousty, S., Fortin, M. J., Rosenberg, M. S. (2002). A balanced view of scale in spatial statistical analysis. *Ecography*, 25(5), 626–640.
- El Maayar, M., & Chen, J. M. (2006). Spatial scaling of evapotranspiration as affected by heterogeneities in vegetation, topography, and soil texture. *Remote Sensing of Environment*, 102(1-2), 33–51.
- Green, J. L., Holmes, A. J., Westoby, M., Oliver, I., David, B., Dangerfield, M., Beattie, A. J. (2004). Spatial scaling of microbial eukaryote diversity. *Nature*, 432(105), 747–750.
- Heuvelink, G. B. M., & Webster, R. (2001). Modelling soil variation: Past, present, and future. *Geoderma*, 100, 269–301.
- Hu, K. L., Wang, S. Y., Li, H., Huang, F., & Li, B. G. (2014). Spatial scaling effects on variability of soil organic matter and total nitrogen in suburban Beijing. *Geoderma*, 226, 54–63.
- Jenny, H. (1941). *Factors of Soil Formation, A System of Quantitative Pedology*. New York: McGraw-Hill.
- Kerry, R., & Oliver, M. A. (2004). Average variograms to guide soil sampling. *International Journal of Applied Earth Observation and Geoinformation*, 5(4), 307–325.
- Lark, R. M. (2002). Optimized spatial sampling of soil for estimation of the variogram by maximum likelihood. *Geoderma*, 105(1-2), 49–80.

- Lark, R. M. (2005). Exploring scale-dependent correlation of soil properties by nested sampling. *European Journal of Soil Science*, 56(June), 307–317.
- Lark, R. M., Hamilton, E. M., Kaninga, B., Maseka, K. K., Mutondo, M., Sakala, G. M., & Watts, M. J. (2017). Nested sampling and spatial analysis for reconnaissance investigations of soil : an example from agricultural land near mine tailings in Zambia. *European Journal of Soil Science*, 68(September), 605–620.
- Lark, R. M., & Webster, R. (1999). Analysis and elucidation of soil variation using wavelets, (June), 185–206.
- Le Guen, M., Herrmann, L., Robain, H., Wiriyakitnateekul, W., Oliveira, T. De, Robin, A., Lesueur, D. (2017). Relevance of taking into account the fine scale soil variability to assess the effects of agricultural inputs on soil characteristics and soil microbial communities : A case study of biochar application in a rubber plantation in North East Thailand. *Geoderma*, 305 (July 2016), 21–29.
- Liu, Y., Lv, J., Zhang, B., & Bi, J. (2013). Spatial multi-scale variability of soil nutrients in relation to environmental factors in a typical agricultural region, Eastern China. *Science of the Total Environment*, 450-451, 108–119.
- Liu, Z. P., Shao, M. A., & Wang, Y. Q. (2013). Scale-dependent correlations between soil properties and environmental factors across the Loess Plateau of China. *Soil Research*, 51(2), 112–123.
- Malone, B. P., McBratney, A. B., & Minasny, B. (2013). Spatial Scaling for Digital Soil Mapping. *Soil Science Society of America Journal*, 77, 890.
- Mandelbrot, B., & Wallis, J. (1969). Some Long-Run Properties Geophysical Records. *Water Resources Research*, 5(2), 321–340.
- McBratney, a. B., & Pringle, M. J. (1999). Estimating Average and Proportional Variograms of Soil Properties and Their Potential Use in Precision Agriculture. *Precision Agriculture*, 1, 125–152.
- McBratney, A. (1992). On variation, uncertainty and informatics in environmental soil management. *Australian Journal of Soil Research*, 30(6), 913.
- Moni, C., Chabbi, A., Nunan, N., Rumpel, C., & Chenu, C. (2010). Spatial dependence of organic carbon-metal relationships. A multi-scale statistical analysis, from horizon to field. *Geoderma*, 158(3-4), 120–127.
- Pettitt, A N., & McBratney, A. B. (1993). Spatial Sampling Designs for Estimating Variance Components. *Journal of the Royal Statistical Society. Applied Statistics*, 42(1), 185–209.
- Ribeiro, E., Batjes, N. H., Leenaars, J. G. B., Oostrum, A. Van, & Jesus, J. M. De. (2015). Towards the standardization and harmonization of world soil data. *International Soil Reference and Information Service, World Soil Information*.
- Šamonil, P., Valtera, M., Bek, S., Šebková, B., Vrška, T., & Houška, J. (2011). Soil variability through spatial scales in a permanently disturbed natural spruce-fir-beech forest. *European Journal of Forest Research*, 130(6), 1075–1091.

- Searle, R. (2014). The Australian site data collation to support the GlobalSoilMap. In A. Arrouays, D; McKenzie, N; Hempel, J; DeForges, ACR; McBratney (Ed.), *GlobalSoilMap: Basis Of The Global Spatial Soil Information System* (pp. 127–132).
- Skøien, J. O., & Blöschl, G. (2006). Scale Effects in Estimating the Variogram and Implications for Soil Hydrology. *Vadose Zone Journal*, 5(1), 153.
- Smith, H. F. (1938). An empirical law describing heterogeneity in the yields of agricultural crops. *The Journal of Agricultural Science*, 28, 1.
- Van Der Gast, C. J., Gosling, P., Tiwari, B., & Bending, G. D. (2011). Spatial scaling of arbuscular mycorrhizal fungal diversity is affected by farming practice. *Environmental Microbiology*, 13(1), 241–249.
- Webster, R. (2000). Is soil variation random? *Geoderma*, 97(3-4), 149–163.
- Webster, R. (2001). Statistics to support soil research and their presentation. *European Journal of Soil Science*, 52(2), 331–340.
- Wiesmeier, M., Lützw, M. von, Wollschlaeger, U., Vogel, H. J., Garcia-Franco, N., Ließ, M., Koegel-Knabner, I. (2019). Soil organic carbon storage as a key function of soils - A review of drivers and indicators at various scales. *Geoderma*, under revision (November 2017), 149–162.
- Xiaoni, H., Hong, L., Danfeng, S., Liandi, Z., & Baoguo, L. (2010). Multi-scale spatial structure of heavy metals in agricultural soils in Beijing. *Environmental Monitoring and Assessment*, 164(1-4), 605–616.
- Yemefack, M., Rossiter, D. G., & Njomgang, R. (2005). Multi-scale characterization of soil variability within an agricultural landscape mosaic system in southern Cameroon. *Geoderma*, 125(1-2), 117–143. 7
- Young, L. J., & Gotway, Æ. C. A. (2007). Linking spatial data from different sources : the effects of change of support National Center for Environmental Health, 589–600.
- Zhang, X., Drake, N., & Wainwright, J. (2002). Scaling land surface parameters for global-scale soil erosion estimation. *Water Resources Research*, 38(9), 1–9.
- Zhou, J., Kang, S., & Schadt, C. W. (2008). Spatial scaling of functional gene diversity across various microbial taxa. *Proceedings of the National Academy of Sciences of the United States of America*, 105(22), 7768.

Chapter 1A:

A list of important spatial terms

We include below a list of closely related terms that are used throughout the thesis. Most of these terms are defined throughout the thesis as they occur. They are included here for convenience.

Variability: When we use the term variability we follow Heuvelink & Webster, (2001); McBratney,(1992); Webster, (2001) who define soil variability as the potential or tendency for the soil to vary. Measures of variability for a particular property include the range and the variance. The variogram (which relates variability to separation distance) is used frequently throughout this thesis.

Variation: In this thesis refers to the actual change in a particular property (i.e., where the soil is actually more variable) rather than the tendency for the soil to vary (variability).

Stochasticity: The term stochasticity in this thesis describes whether variability (of a particular property in space is more or less random. The more stochastic a property is, the more dominant the short range variability. A property with less stochasticity (noise, or random variation) will vary gradually in space and long term trends will be more important.

Hurst Exponent: The Hurst Exponent relates the autocorrelation of a series to the lag or separation of the series. Varying between zero and one, the closer the Hurst Exponent is to zero, the lower the autocorrelation, and the more stochastic or antipersistent the series. A Hurst exponent closer to one indicates stronger autocorrelation, and a less stochastic, more persistent series.

Hausdorff Besicovitch Dimension: the Hausdorff Besicovitch Dimension (or D value) can usefully be understood as a measure of roughness (Berry and Lewis, 1980) or stochasticity. The more significant the short range variability is, the higher the D value (Eghball et al., 1999). In the case of two dimensional data (i.e. spatial data) a D value of exactly 2.5 occurs if variability has a linear relationship with separation distance. This corresponds to Brownian motion and a Hurst Exponent of 0.5. D values > 2.5 imply that short range variability is more important than long range variability (antipersistence, and a Hurst exponent < 0.5). As the D value increases towards 3 the variogram approaches a pure nugget model (i.e. no spatial trend, pure white noise). D values lower than 2.5 suggest that long range variability is relatively more important than short range variability (persistence, and a Hurst exponent > 0.5).

Roughness Index: In this thesis we introduce a measure of stochasticity which we term the roughness index. Like the Hurst Exponent and the Hausdorff Besicovitch Dimension it quantifies the relative importance of short versus long range spatial variability (or stochasticity). The roughness index is distinct from the Hurst Exponent and Hausdorff Besicovitch Dimension because rather than assuming a constant fractal relationship it allows the measure of roughness to vary with separation distance or scale.

Chapter 2:

Spatial Variability of Australian Soil Texture: A multiscale analysis

Clearly the mind is always altering its focus, and bringing the world into different perspectives

Virginia Woolf

This chapter has been published as:

Paterson, S., Minasny, B., McBratney, A. (2018). Spatial variability of Australian soil texture: A multiscale analysis. *Geoderma*, 309, 60-74.

Abstract

Understanding how soil variability changes with spatial scale is critical to our ability to understand and model soil processes at scales relevant to decision makers. The compilation of large legacy data sets has opened up new possibilities to model spatial variability at the continental or even global scale. Using the National Soil Site Collation (NSSC) dataset of Australia we created empirical variograms for sand and clay fraction at extents from 1km to continental. The NSSC dataset is highly spatially clustered; a typical feature of legacy datasets. This leads to lumpy artefacts in the variograms. To reduce this lumpiness, we employed grid based declustering. We used the declustered empirical variograms to calculate the Hausdorff Besicovitch Dimension – a unitless measure of spatial roughness. We first fit a power model to each declustered variogram and calculated the Hausdorff Besicovitch dimension at each modelled scale. This allowed us to assess the roughness or variability at each modelled extent, however this assessment was somewhat coarse. We have proposed a new model that allows us to calculate the Hausdorff Besicovitch dimension continuously across all extents. The conceptual basis of this model moves away from a Multi-fractal framework typically used by soil scientists. It allows us to describe spatial variability or stochasticity as a continuous function of spatial separation. Both our new model and the continental scale variograms of texture emphasise the high degree of short range variability in soil spatial texture. Empirical variograms indicate that around 50 per cent of spatial variability occurs at less than 10km, and 30 % at less than 1 km. Spatial variability increases with depth consistently across all modelled extents and model types. Beyond extents of around 100km, the Hausdorff Besicovitch Dimension remains relatively stable. Soil spatial variability is highly stochastic at fine scales. Spatial variability may change gradually with extent and scale rather than abruptly.

2.1. Introduction

Our ability to understand and manage the soil resource is dependent on the scale at which we can observe and model soil characteristics and processes. As soil scientists, one of our key challenges is to produce information about soil quality and processes at a resolution and extent useful for decision makers (Lark, 2005; Malone et al., 2013). It may often be necessary to do this without the collection of additional data (Malone et al., 2013; Pongpattananurak et al., 2012). Modelling soil properties is challenging because a soil property at any given location is the result of a complex interplay of environmental and management factors over time. While these are in theory deterministic processes, the outcomes of these complex soil forming processes are often so unpredictable that they appear random (Heuvelink and Webster, 2001; Webster, 2000). The relative dominance and interactions of these different factors will vary with location and with the scale of observation (Heuvelink and Webster, 2001; Lark, 2011). This applies to both the deterministic and the ‘random’ component of soil variability. Capturing variability at relevant spatial scales is critical to production of useful models and maps, but is not a simple task. Without a priori knowledge of patterns in soil spatial variability it is easy to design a soil survey that misses important spatial variation either by sampling with spacing that is too broad or an extent that is too narrow. The importance of this issue has led to much work on the efficient design of soil surveys across multiple scales (Lark, 2005, 2011; Pettitt and McBratney, 1993; Webster et al., 2006). Even with these efficient methods, multiscale sampling strategies tend to be both time consuming and expensive and not always possible. It may be possible for the soil scientist to shape their expectations about the likely variability of soil at different scales from existing literature, but generally speaking our understanding of the variability of the majority of soil properties at different spatial scales is still limited. The availability of continental-scale soil data allows new avenues for approaching the question of how soil variability changes with scale. In this chapter:

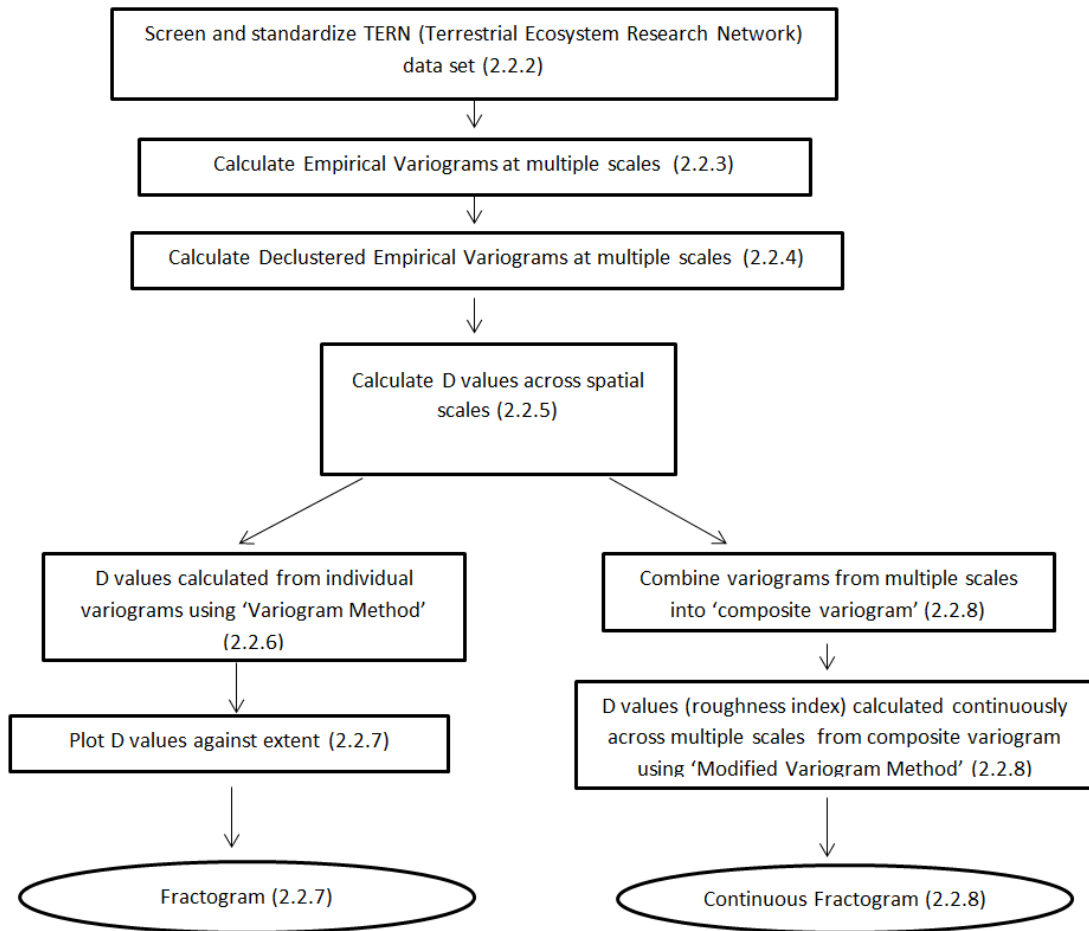
- We use legacy data to calculate empirical variograms at spatial extents ranging from continental to 1 km by varying bin size and extent. This illustrates the utility of the empirical variogram as a tool for exploiting large legacy datasets in investigation of scaling patterns (Sections 2.2.2, 2.2.3, 2.2.4 and 2.3.1).
- We describe two methods for calculating the spatial roughness for the quantitative assessment of spatial variability (Sections 2.2.5, 2.2.6, 2.2.7 and 2.2.8) and apply these methods to the empirical variograms we have calculated (Sections 2.3.2 and 2.3.3). This allows us to expand on the inferences we have drawn about changes in variability across scales (Sections 2.3.4, 2.3.5, 2.3.6, and 2.3.7).

2.2 Methods

2.2.1 Conceptual overview

Collaborative efforts to build large scale digital soil maps such as GlobalSoilMap have led to the creation of consolidated databases of soil information. These databases represent a significant resource for empirical characterization of soil spatial variability. Our idea was to take advantage of the inherent flexibility in the experimental variogram to create soil variograms at a range of spatial scales using compiled legacy data. By adjusting the bin size and extent of each variogram we adjusted the spatial scale so that each variogram captures a different magnitude of spatial variability. Creation of variograms across a range of spatial scales allowed the characterization of patterns of spatial variability with scale. We fit power curves to the empirical variograms across a range of modelled scales. The exponent parameter from the fitted power curve was used to calculate the Hausdorff Besicovitch Dimension or D value, a unitless measure for the roughness of an object. Burrough (1983) used this dimension to compare spatial variability between environmental properties. The 'variogram method' used by Burrough (1983) is rooted in the concept of Multifractals (regions of similar variability separated by 'zones of transition'). We introduce a differentiation-based method for estimating this dimension continuously across changing extents. Because the underlying conceptual framework for our model is distinct from the Multifractal framework we replace the term Hausdorff Besicovitch Dimension with the more general 'roughness index'. Because the roughness index is dependent upon the shape of the variogram but not the units, it provides a simple but useful quantitative tool for assessing spatial variability between properties and between scales. We calculated the 'roughness index' across different spatial extents and at several different depths using both methods.

The schematic below outlines the workflow of the chapter.



2.2.2 NSSC soil texture data

The soil texture data used in this analysis was compiled to support the Australian contribution to the GlobalSoilMap (Grundy et al., 2015). A collaboration of state and national government agencies and some universities worked together to produce the National Soil Site Collation or NSSC (Searle, 2014). The database includes geo-located soil observations collected by research and government agencies from the 1930s onwards. The NSSC is a composite of data from a variety of sources therefore it does not have a unified sampling design and the NSSC dataset reflects the research priorities of the different data collecting institutions at different times. The dataset is heavily focused in agricultural regions and includes areas of high density sampling and sparse sampling (Fig. 1). The complete database contains information on several soil properties including percentage clay and percentage sand fraction from almost 16,000 soil profiles. Percentage sand and clay fractions from this database are used in this study.

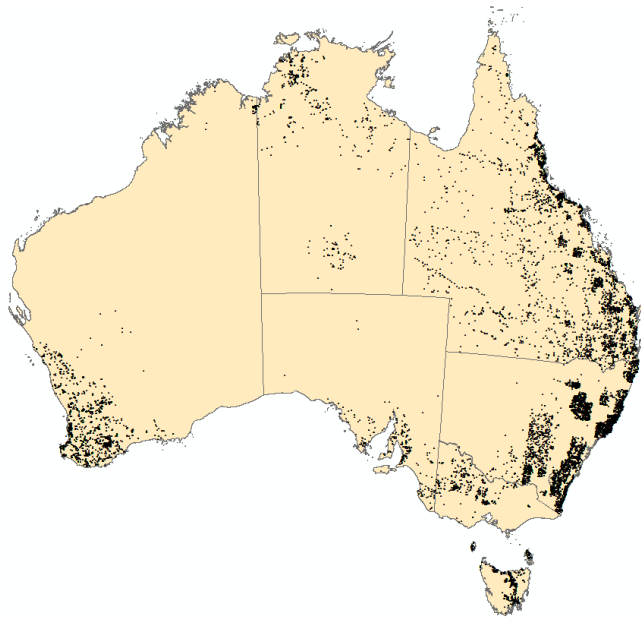


Figure 2.4. The distribution of the NSSC dataset. Each black dot represents an individual soil observation.

Observations in the NSSC database were not taken at consistent depths. Data was normalized using the generalized equal area spline depth function (Malone et al., 2009). Soil depth intervals were selected in line with the GlobalSoilMap depth intervals (0–5 cm, 5–15 cm, 15–30 cm, 30–60 cm, 60–200 cm³, Arrouays et al., 2014). Prior to applying the spline depth function, locations with no top soil measurement were discarded and locations with multiple observations or overlapping depths were deleted. The number of observations that were used at each interval are shown in Tables 2.1 and 2.2 below. The spline function does not return values at depths below the available data. The NSSC database contains more observations for the topsoil than the subsoil. This results in fewer data points observations available at lower depth intervals. Summary statistics for percentage Clay and Sand fraction are presented in Tables 2.1 and 2.2 below.

³ This depth combines 60-100 and 100-200.

Table 2.1. Percentage Clay fraction: Summary statistics

Soil Depth	Number of observations	Mean (% clay)	Median (% clay)	Standard deviation (% clay)	Skewness	Kurtosis
0-5 cm	13830	21.52	15.87	17.44	1.10	3.38
5-15 cm	13342	23.38	18.00	17.74	0.93	3.00
15-30 cm	9026	26.98	22.48	18.99	0.65	2.48
30-60 cm	7758	34.19	33.04	20.19	0.29	2.25
60-200 cm	5969	37.57	37.73	19.49	0.15	2.39

Table 2.2. Percentage Sand fraction: Summary statistics

Soil Depth	Number of observations	Mean (% sand)	Median (% sand)	Standard deviation (% sand)	Skewness	Kurtosis
0-5 cm	13258	63.17	66.83	22.74	-0.46	2.25
5-15 cm	13091	61.37	64.39	22.78	-0.37	2.16
15-30 cm	9012	57.82	58.86	23.43	-0.18	2.05
30-60 cm	7727	51.48	50.38	23.97	0.07	2.08
60-200 cm	5916	48.41	47.05	23.13	0.17	2.24

2.2.3 Experimental Variograms – modelling at multiple scales

We calculated experimental variograms using Matheron's (1963) method-of-moments estimator (Equation 1).

$$\hat{\gamma}(h) = \frac{1}{2M(h)} \sum_{j=1}^{M(h)} \{z(x_j) - z(x_j + h)\}^2 \quad \text{Equation 1}$$

In Equation 1 (above) the theoretical relationship between separation distance (lag or h) and semivariance, $\hat{\gamma}(h)$, is estimated by the function $\hat{\gamma}(h)$. $M(h)$ is the number of paired comparisons at a particular lag (h). $z(x_j)$ and $z(x_j + h)$ are the values of the property Z at places x_j and $x_j + h$ separated by

lag h . It is common practice for the lag h to cover a specified distance interval. For instance 1 km increments.

Use of method of moments to estimate semivariograms has been criticized for bias and for subjectivity (Lark, 2000). However, bias decreases as sample size increases (Oliver & Webster, 2014). Variograms are typically estimated based on tens to hundreds of data points, while this study uses several thousand. This significantly reduces problems of bias. Another reason to favour the use of Method of Moments in this context is the difficulty associated with using either REML (Restricted Maximum Likelihood) or MCMC (Markov Chain Monte Carlo) methods on very large datasets.

When using method of moments, the practitioner is required to select both bin size and extent. In relation to Equation 1, the bin sizes determine the interval over which the term spans. The intrinsic subjectivity of this method provided a convenient method for modelling variograms at different scales. Fixing the number of bins at 1,000, the maximum extent of the experimental variogram was gradually reduced. As the extent decreased, the bin size decreased proportionally. Combinations of bin size and extent are displayed in Table 2.3.

Table 2.3. Extent and bin size combinations for empirical variograms

Extent	1km	10km	100km	1000km	3,800km
Bin size	1m	10m	100m	1km	3.8km

2.2.4 Experimental Variograms - improving fit using spatial declustering

It has been established that empirical variograms calculated from spatially clustered data can be biased or lumpy (Emery, 2007; Marchant et.al., 2013; Richmond, 2002). This makes them less suitable for modelling variograms and for kriging because in clustered situations the variability at different lags is unequally characterised. As discussed above, the NSSC dataset used in this chapter has been compiled from a variety of government agencies and research bodies, and reflects the priorities of those bodies at the time of data collection. As such, the dataset is heavily clustered. Empirical variograms calculated with the method-of-moments exhibit strong lumpiness at spatial extents greater than 40km (you can see this lumpiness illustrated in figure 2.7). This is consistent with the pattern noted by Marchant et al. (2013) when using a similar dataset.

Methods for reducing this bias have been suggested by Emery (2007), Richmond, (2002) and Marchant et.al. (2013). We favour the last method as, unlike the first two, it is dependent only upon the spatial

location of the data and not upon the values of the data themselves. It is also easily computed and has intuitive appeal.

We use Marchant et al.'s (2013) modified declustering method of moments estimator (Equation 2) to recalculate the empirical variograms at the scales specified in Table 2.3. Deutsch (1989) describes the cell declustering procedure which Marchant et al. (2013) used to calculate weighting values. These methods are briefly summarized below.

1. A regular grid with cells of a fixed size and shape⁴ is projected over the study area.
2. The number of observations in each cell of the grid is calculated. This value which we can call c is assigned to each observation in the dataset.
3. Steps 1 and 2 are repeated several times, with the grid slightly offset each time. The average value of c from each repetition is calculated for each data point. We can call this value \bar{c} . This ensures that boundary effects do not dominate the calculation of declustering values.
4. Declustering weights, w , are set as inversely proportional to the value \bar{c} and then scaled so that the average declustering weight is equal to one. In this way, we ensure that isolated data points are given more weight than data points which are closely clustered with other data points.

The empirical variogram is then calculated using Equation 2:

$$\hat{\gamma}(h) = \frac{\sum_{j=1}^{M(h)} \{z(x_j) - z(x_{j+h})\}^2 \{w(x_j) \times w(x_{j+h})\}}{\sum_{j=1}^{M(h)} \{w(x_j) \times w(x_{j+h})\}} \quad \text{Equation 2}$$

The weighting values, w , in Equation 2 allow us to increase or decrease the importance of a particular observation when calculating the empirical variogram: $w(x_j)$ and $w(x_{j+h})$ are the weighting values associated with observations at location x_j , and x_{j+h} . The method can be compared to Cressie's (1985) weighted least squares calculation. Cressie (1985) weights each point on the empirical variogram by its variance. Intuitively, the smaller the error variance for a particular point, the more information it reveals, and hence the more important it is in variogram calculation. In Marchant et al.'s (2013) formulation (Equation 2), the weighting factor w is calculated exclusively from the spatial distribution of data points. The more isolated a data point, the more unique information it is expected to contain, and the greater the weight that is put upon it.

⁴ Typically square, but in some cases this can be rectangular

Effective use of this declustering method depends on selection of an appropriate cell size for the calculation of weighting values (w in Equation 2). A very fine grid size would result in all data points receiving a declustering weight of one. Conversely, a very coarse grid size would result in only a few highly weighted values.

Following Deutsch (1989), Marchant et al. (2013) suggest that an optimal grid size should allow the most isolated data points to be alone in a grid cell. Marchant et al. (2013) also suggest that a number of grid sizes be trialled, and the effects on the empirical variogram be assessed visually. As with bin size selection, there is a degree of practitioner subjectivity involved in the selection of appropriate grid sizes. There appears to be a trade-off between the removal of lumpiness and the precision of the empirical variogram. The larger the grid size is, the greater the reduction in lumpiness, but the more diffuse the overall shape of the empirical variogram.

We found that grid sizes suitable for removing declustering at one spatial extent were not necessarily appropriate at other extent. The final extent, bin size and grid size combinations that we selected are displayed in Table 2.4. Declustered variograms were calculated for all depths specified in Table 2.1 and 2.2. The maximum extent, bin size and grid cell size combinations in Table 2.4 were kept consistent for variograms calculated at each depth.

Table 2.4. Extent, bin size and grid size combinations for declustered empirical variograms

Extent	1km	10km	100km	1000km	3,800km
Bin size	1m	10m	100m	1km	3.8km
Grid size (m) ⁵	0.7km	0.7km	7km	70km	70km

2.2.5. Measures of roughness: The Hausdorff Besicovitch Dimension and the Hurst Exponent

The Hurst Exponent and the Hausdorff Besicovitch Dimension are related concepts which quantify the variability of a data series (spatial or temporal). The Hurst Exponent (Hurst, 1951) is commonly described as a measure of the long term memory of a series, while the Hausdorff Besicovitch Dimension (or D value) can usefully be understood as a measure of roughness (Berry and Lewis, 1980). The Hurst Exponent relates the autocorrelation of a series to the lag or separation of the series. Varying between zero and one, the closer the Hurst Exponent is to zero, the lower the autocorrelation, and the more stochastic or antipersistent the series. A Hurst exponent closer to one indicates stronger autocorrelation, and a less stochastic, more persistent series. There is an inverse linear relation between the Hurst Exponent and the D value. When calculated for two dimensional spatial data the

⁵ Length of one side of a square grid

D value will vary between 2 and 3. The more significant the short range variability is, the higher the D value (Eghball et al., 1999). In the case of two dimensional data (i.e. spatial data) a D value of exactly 2.5 occurs if variability has a linear relationship with separation distance. This corresponds to Brownian motion and a Hurst Exponent of 0.5. D values > 2.5 imply that short range variability is more important than long range variability (antipersistence, and a Hurst exponent < 0.5). As the D value increases towards 3 the variogram approaches a pure nugget model (i.e. no spatial trend, pure white noise). D values lower than 2.5 suggest that long range variability is relatively more important than short range variability (persistence, and a Hurst exponent > 0.5). Simulated surfaces were calculated for several D values using the Lower Upper decomposition matrix method (Davis, 1987). These are shown in Fig. 2.2 along with associated power curves.

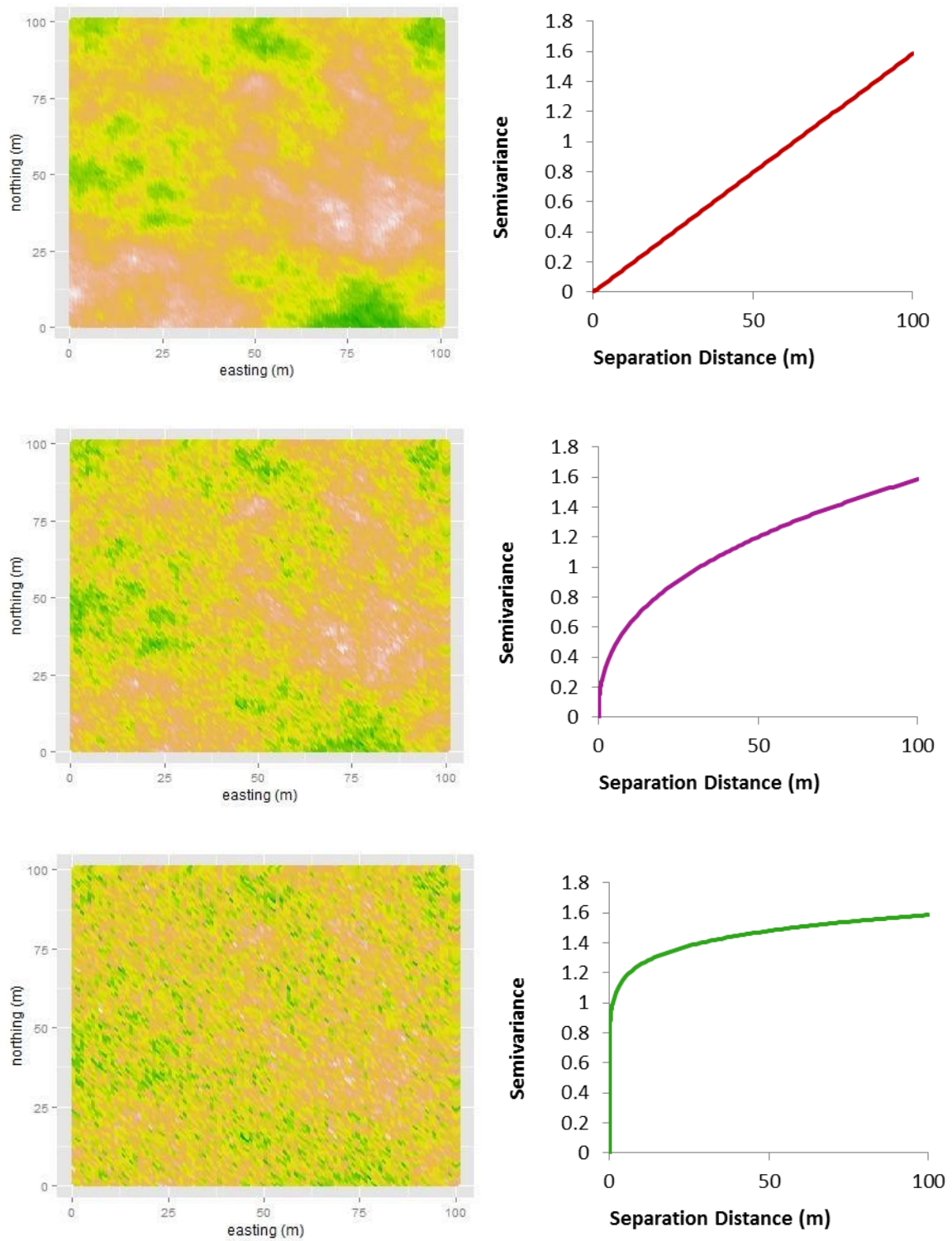


Figure 2.2. Power curve variograms and simulated 2 dimensional surfaces. D values are: 2.5⁶, 2.8 and 2.95 top to bottom

⁶This image was calculated using an alpha term of 0.999999 rather than 1 to ensure that the covariance matrix remained positive semidefinite.

2.2.6. The 'Variogram Method' for calculating the D Value

We use the variogram method introduced by Burrough (1983) to calculate the Hausdorff Besicovitch Dimension (henceforth called the D Value) for each empirical variogram. The method is computationally simple, and only requires two steps.

1. Fit a power curve (Equation 3) to experimental variograms and find the estimate of the exponent (ω)⁷.
2. Use the exponent term (ω) in a simple linear relationship (Equation 4) to estimate the D Value.

$$\gamma = bh^\omega \text{ Equation 3}$$

γ is the semivariance: $\gamma \geq 0$

h is the separation distance or lag between points: $h \geq 0$

ω and b are numerical constants: $2 \geq \omega \geq 0$ and $b \geq 0$

$$D = 3 - \frac{\omega}{2} \text{ Equation 5}$$

ω the exponent term from Equation 3: $0 \leq \omega \leq 2$

D is the Hausdorff Besicovitch Dimension for an isotropic property measured in two dimension: $2 \leq D \leq 3$

The original publication of the variogram method (Burrough, 1983) uses a slightly different equation (Eq. (5)). The Burrough (1983) paper uses variograms calculated from data on one dimensional transects while our variograms are calculated from two dimensional data. The equation we use (Eq. (4)), has the simple adjustment of a '+1' term. This allows the calculation of D values for two dimensional spatial data (Bez and Bertrand, 2011; Chan and Wood, 2000). This computationally trivial adjustment ensures that the D value remains between 2 and 3 (the appropriate range for two dimensional data). This adjustment relies on the assumption of isotropy. Calculation of directional empirical variograms at multiple scales across this dataset did not find evidence for anisotropy.

$$D^* = 2 - \frac{\omega}{2} \text{ Equation 5}$$

⁷ Because the paper by Burrough was published before non-linear least squares estimates were possible, he finds the estimate for (ω) by fitting a linear relationship to a plot of the variogram on a log-log scale and finding the slope.

ω is the exponent term from Equation 3: $0 \leq \omega \leq 2$

D^* is the Hausdorff Besicovitch Dimension for a property measured in one dimension: $1 \leq D \leq 2$

All of the analysis conducted in this chapter is on two dimensional data. Subsequent discussion of D values henceforth will refer to the two dimensional D values from Equation 4.

2.2.7. D values: Comparing variability across scales

We calculated D values from declustered empirical variograms for sand and clay percentage fractions using empirical variogram parameters shown in Table 2.5.

Table 2.5. Extent, bin and grid size for declustered empirical variograms used in calculation of D values⁸

Extent (km)	1	10	20	100	200	600	1000	2000
Bin Size (m)	1	10	20	100	200	600	1000	2000
Grid size (m) ⁹	0.7	0.7	0.7	7	7	70	70	70

As stated earlier, the roughness index expresses the relative importance of short range and long range variability. As the spatial extent of observations changes, the meaning of ‘short range’ and ‘long range’ also changes. Examining how D values change with scale has important implications for our understanding of variability. We will illustrate with three examples below.

- If the D value remains constant as resolution increases then relative importance of short range and long range variability remains constant. For instance if the D value remained the same as the extent of the variogram changed from 100m to 100km, this would imply that the relationship between variability at 1m and 100m is the same as the relationship between variability at 1km and 100km. It does not imply that the spatial pattern is the same, but that the degree of roughness is the same.
- If the D value *decreases* as the resolution increases, it implies that fine scale spatial trends exist and can only be detected as finer scales of observation become possible. At fine resolutions the spatial structure that is unobservable at coarser resolutions becomes short-

⁸ All variograms are calculated with all of the data in the data set. For instance in the 1km extent 1m bin size variogram the data point associated with the 5 m bin includes all of the pairs of data which are separated by 4.5- 5.5. m regardless of location or of orientation.

⁹ Length of one side of a square grid

range spatial structure, and the short-range structure at coarser resolutions becomes long-range structure. As a result, stochasticity reduces.

- If the D value *increases* as the resolution increases, it implies that spatial trends are not detectable at finer resolutions. As resolution becomes coarser (decreases), stochasticity reduces and the spatial trend increases. The very short range stochasticity is no longer observable, and the long range trends become observable.

Understanding which of these trends is likely to occur over particular spatial ranges has implications for sampling, modelling and understanding soil processes. If stochasticity is increasing as extent and bin size are increasing, point based sampling is less likely to provide useful information about medium to long range trends. If stochasticity reduces dramatically over a particular scale range, then sampling more finely is likely to provide useful information

The Hausdorff Besicovitch Dimension has been described as ‘scale invariant’ (Eghball et al., 1999). This does not mean that the spatial extent and resolution does not affect the value, but rather that the total magnitude of variability does not. The dimension measures only the relative importance of short range versus long range variance. As described above this makes the property useful for comparing roughness across spatial scales (as the meaning of long range and short range varies). It also makes the dimension a useful alternative to variograms for comparing between properties. Even where the units of measure are the same (e.g. sand percentage and clay percentage) variograms are influenced by the magnitude of the property they are measuring. This makes it difficult to compare directly between properties using variograms. The D value is derived from the variogram but depends only on the shape of the variogram curve so is not influenced by the magnitude or the unit of measure of the variability. A tool sometimes used to visualize how D values change with scale is the ‘fractogram’. This label is primarily used in ecology (Leduc et al., 1994; Schmid, 2000). The fractogram is simply a plot of D values against scale. The fractogram provides an effective illustration of how the D value changes with resolution. This aids our understanding of how the underlying spatial patterns might be affected by the scale of observation. The eight variograms described in Table 2.5 were included in the fractogram.

2.2.8. The Hausdorff Besicovitch Dimension: An adaption of the ‘Variogram Method’ for continuous estimates of ‘roughness index’

The methods described above create several distinct variograms at different extents in order to compare how variability changes between these distinct ranges (using both visual assessment and D values). We now introduce a method that assesses the relationship between variability and scale on a

continuous basis. We repeated this approach for sand and clay, topsoil and subsoil. We consider this approach to have two key advantages: 1. It removes a degree of arbitrary decision making in the selection of scales at which to model variograms 2. The ‘fractogram’ curve derived using these methods is calculated directly from a single composite variogram, rather than by linking together values calculated from individual variograms. It is based on a single fitted curve. This approach also has a different underlying conceptual framework, and will be discussed further in Section 2.2.9. Briefly, our method allows the characterisation of a change in the D values at all scales. This is a departure from the framework described by Burrough where regions of self-similarity are characterized by finding linear sections on a log-log variogram. The more continuous framework implies a more gradual change in stochasticity and therefore a more gradual change in the control of the variogram. Because of this shift in framework, we propose the use of the term ‘roughness index’ instead of D value. We outline details of this approach using an example (clay topsoil) below.

Step One: Composite Variogram

We created composite variograms using data points from declustered empirical variograms calculated with different bin sizes and extents. The composite variogram combines sections from variograms calculated at different scales so that it includes high resolution short scale information from the finest scale variograms and coarser resolution data calculated at larger extents. When combining this data we exercised a degree of subjectivity in inclusion and exclusion to ensure a smooth transition between scales. The composite variogram for top soil clay shown in Fig. 2.3.

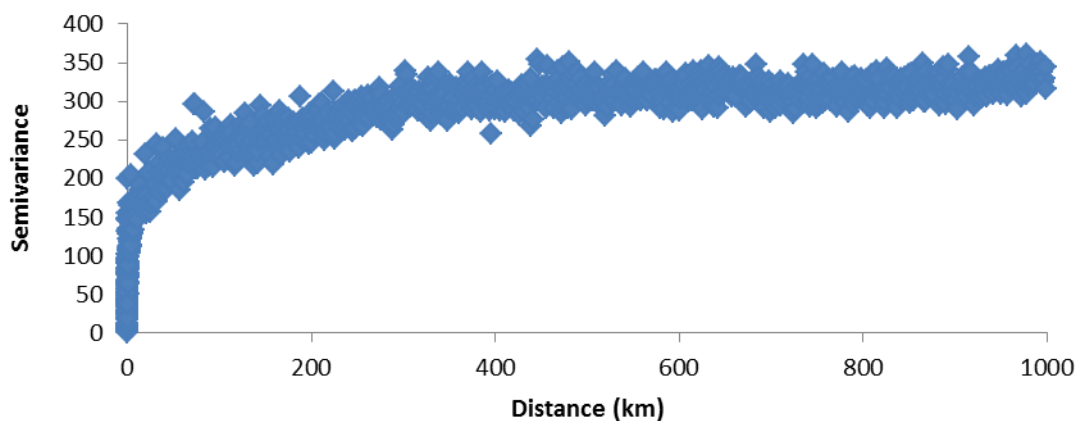


Figure 2.3. Composite Variogram, top soil clay

Step Two: log-log scale Composite Variogram

The power function (Eq. (3)) and Eq. (6) below are equivalent. This equivalence means that a power curve plotted on a log-log scale will appear as a straight line: The exponent term (ω) from the power curve will equal the slope of the log-log curve.

$$\log \gamma = \log(b) + \omega \log h \quad \text{Equation 6}$$

γ is the semivariance: $\gamma \geq 0$

h is the separation distance or lag between points: $h \geq 0$

ω is a numerical constants : $0 \leq \omega \leq 2$

Before rapid computational power became available it was common practice to estimate a power curve by plotting points on log-log paper and visually estimating a line of best fit (Burrough, 1983). Plotting variograms on a log-log scale (Fig. 4) and identifying linear sections is sometimes used as a tool for identifying regions of self-similarity. The slope (or derivative) of a linear section of a curve plotted on a log-log scale can be used to estimate ω .

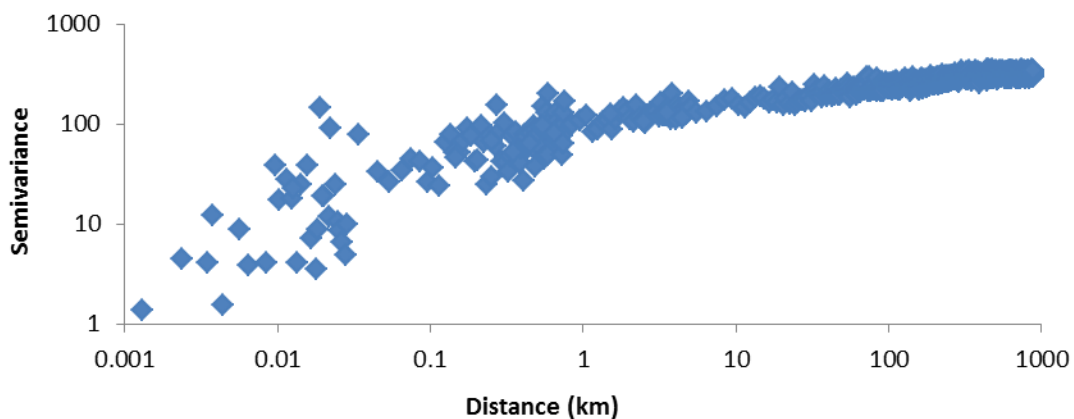


Figure 2.4. Composite variogram, top soil clay, \log_{10} - \log_{10} scale

Visual assessment of the composite variogram plotted on a log-log scale indicated that a curve might provide a better fit than a straight line or series of straight lines. While it is possible to imagine straight lines between 100 m and 1 km, 1 km and 100 km, 100 km and 1000 km there are no strongly linear sections and there does not appear to be strong evidence for self-similarity interspersed by transition zones. We propose that a curved line would be a better approximation for this shape.

Step Three: Fitting a curve to the composite variogram

We based our curve selection on visual inspection of fit and residual plots and R^2 . The exponential decay function (increasing) proved the best fit (Equation 7). Using non linear least squares we estimated values for the parameters, k , A and C . Estimates of these parameters as well as the shape of this curve are shown in Figure 2.5 below.

$$\log_{10} \gamma = C(1 - e^{-k \log_{10} h}) + A \quad \text{Equation 7}$$

γ is the semivariance: $\gamma \geq 0$

h is the separation distance or lag between points: $h \geq 0$

C , A and k are constants: $k > 0$, $C > 0$

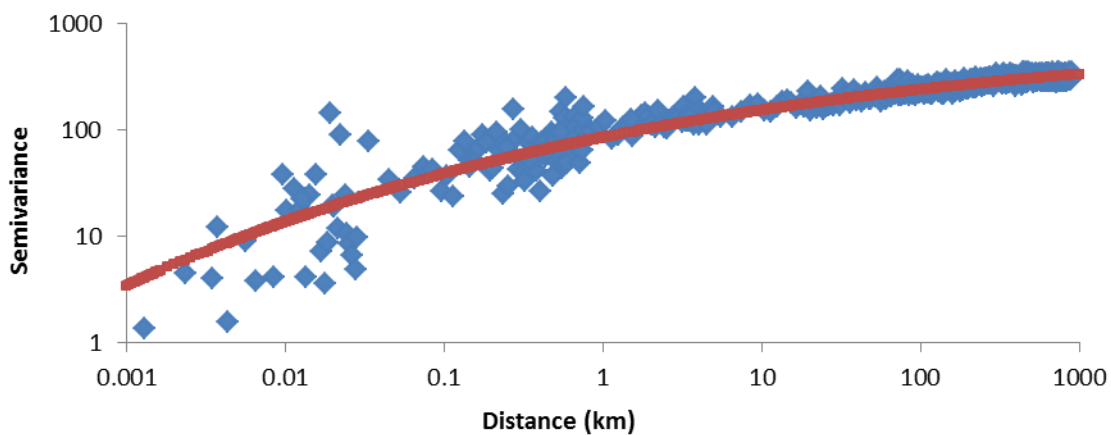


Figure 2.5. Composite variogram, top soil clay, \log_{10} - \log_{10} scale – fitted curve

Step Four: Calculating the derivative of the curve

Having fit a curve to the experimental variogram we then take the derivative of the curve.

The general form of the derivative of $\log_{10} \gamma$ with respect to $\log_{10} h$ is presented below (Equation 8).

$$C k e^{-k \log_{10} h} \quad \text{Equation 8}$$

γ is the semivariance: $\gamma \geq 0$

h is the separation distance or lag between points: $h \geq 0$

C and k are constants: $k > 0$, $C > 0$

$\omega = 0.29$

Using the estimates for C and K estimated in our worked example (1.04, 0.28 respectively) we can calculate the specific value for the derivative of the log-log curve. We include the curve and equation for the worked example (clay top soil) below in Figure 2.6 and 2.7.

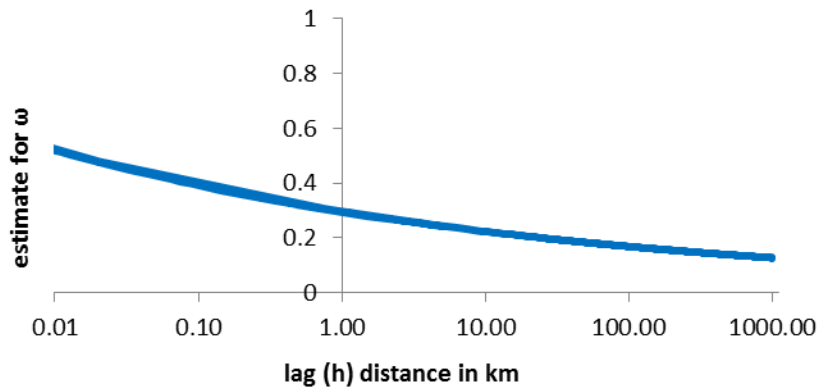


Figure 2.6. Derivative of the composite variogram curve – plotted against $\log_{10}(h)$ (log to the base 10 separation distance).

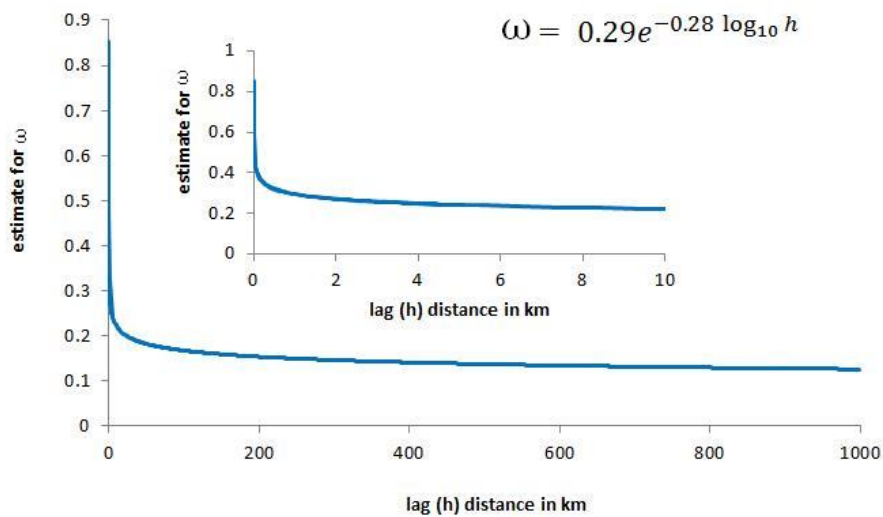


Figure 2.7. Derivative of the composite variogram curve – plotted against h (separation distance), top soil clay

Step Five : Estimating a continuous D value or Roughness Index

We use this derivative as an estimate for ω (in equation 5).

Substituting Equation 8 into Equation 5 to yield Equation 9 it is then trivial to solve for the D value as a function of h (separation distance or lag). (Plotted in Figure 2.8 below).

$$D = \frac{4-C(1+k(e^{-k \log(h)}))}{2} + 1 \quad \text{Equation 9}$$

γ is the semivariance: $\gamma \geq 0$

h is the separation distance or lag between points: $h \geq 0$

C and k are constants: $k > 0, C > 0$

$\omega = 0.29$

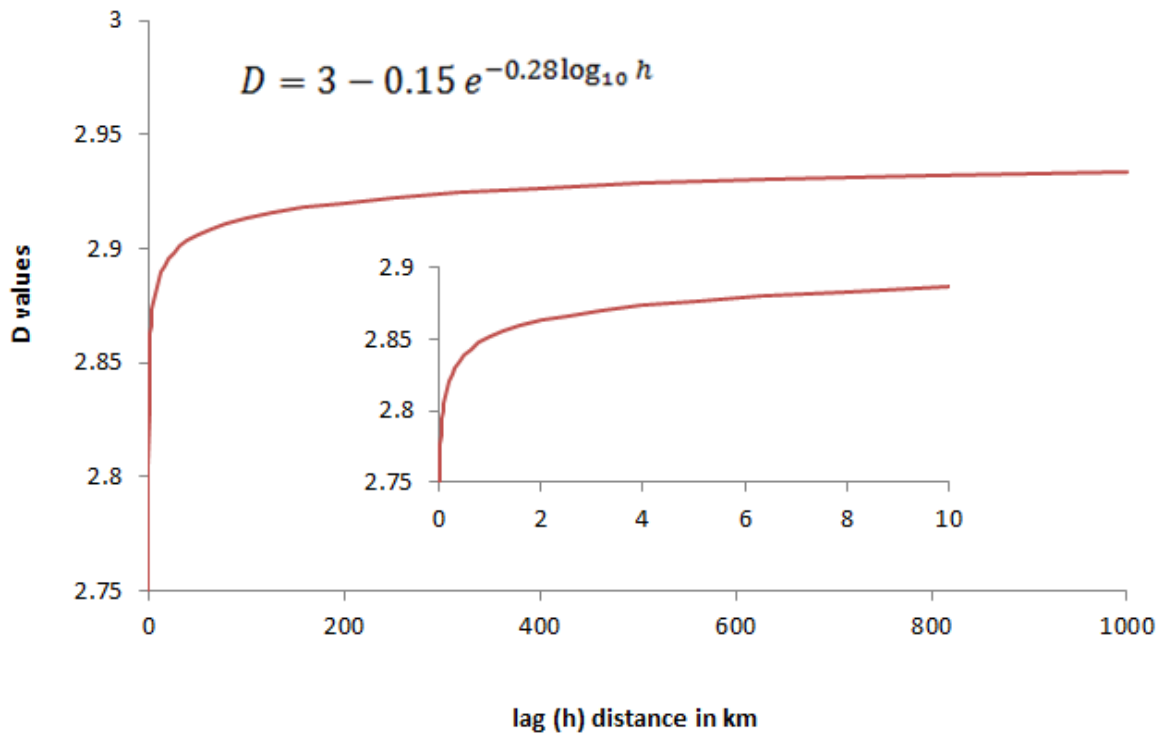


Figure 2.8. Roughness Index calculated from the composite variogram curve: plotted against separation distance (h)

The underlying premise of this method is the equivalence between the exponent of a power curve, and the derivative (or slope) of the same curve plotted on a log-log scale. When a variogram fits a power curve perfectly, the plot of that variogram on a log-log scale will be a straight line. If the plot of the variogram on a log-log scale does not fit a single straight line it can be divided up into shorter segments which have the same estimated slope (and therefore the same estimated Roughness Index). However it is rare for a curve to show strong linearity separated by obvious transition zones. On curvilinear lines one could imagine taking shorter and shorter line segments to estimate Roughness Index. At the limit of this idea, the line segments would be very small, and the line segments when viewed together would appear as a curve.

2.2.9 Implications of the two methods.

The variogram method is aligned with an underlying concept of soil variability as part of a multifractal system. Burrough (1983) hypothesises that different soil forming processes will dominant soil variability at different scales. For a particular spatial range which is dominated by a soil forming process, soil variability is likely to be self-similar in the sense that the relationship between separation distance and expected variability will be constant and predictable. Regions of self-similarity will be characterized by a linear variogram when plotted on a log-log scale. We would expect different processes to dominate at different scales. When the dominance is shifting from one process to another we can consider this a 'region of transition'. At these regions the slope of the line of the variogram will change. This framework is one of 'multifractals' — multiple fractal relationships layered upon each other. Another possibility is that change in roughness occurs more gradually. Rather than a multifractal framework with distinct regions of self-similarity separated by transition zones, the soil variability may change more gradually. This framework suggests a more gradual transition between different soil forming elements. Allowing the D Value (which measures the relative importance of short range variability) to change gradually implies that variability does not follow self-similar patterns over particular extents, but rather changes gradually. This may imply that the control between different environmental factors shifts gradually rather than abruptly over scales. Because of this shifting framework we suggest that a name such as 'roughness index' would be more appropriate than D value, which is closely tied to the concept of fractals. Understanding at which scales variability changes the most rapidly is of interest regardless of the underlying framework. Whether we are looking for distinct regions of transition separating self-similar variability, or a more gradual change, understanding where relative roughness changes most dramatically can allow us to better target our sampling and better model spatial variability.

2.3 Results and Discussion

2.3.1 Empirical Variograms – Variability across scales and the impact of spatial declustering

Fig. 9 displays variograms calculated for clay without declustering. Fig. 10 shows variograms calculated for clay at the same scales but using declustering. Declustered variograms were also calculated using the sand percentage dataset (Fig. 11). It is evident that a large proportion of total spatial variability in the property is realised at short extents. For both sand and clay around 30% of the variability is realised in the first kilometre, and around 50% in the first 10 km (Figs. 10 and 11). This similarity is unsurprising, because sand and clay fractions are not independent variables.

The effect of declustering on the empirical variograms is striking. Without declustering, variograms calculated for the three largest extents: 3800 km (full extent); 1000 km; and 100 km (Fig. 9) are very lumpy. Neither the 10 km nor the 1 km extent variograms exhibit lumpiness. Declustering removes the vast majority of this lumpiness for the 1000 km extent and the 100 km extent. At the largest extent (3800 km), the declustering methods did not remove lumpiness in the second half of the variogram. This is likely because this lumpiness is not due to spatial clustering, but rather a common feature of modelling variograms beyond half of the maximum extent. The lumpiness in the 100 km and 1000 km can be attributed to the strong spatial clustering in the dataset. Because of this strong spatial clustering, there are some lags (spatial separation distances) which are dominated by two densely sampled regions. If there is an above average variance between two dominant patches then the variogram will have an upward spike at that lag. A below average variability between the two patches will cause a downward peak. This does not indicate that the distribution is biased. There is no reason to expect that the average variability between these two regions would be the average variability for that separation distance across the dataset. Normal variability in the spatial distribution combined with patchy sampling can produce spikes or noise. Because this lumpiness is an artefact of the sampling distribution and not representative of a trend in the underlying spatial distribution, removing the lumpiness through the use of the declustering method is an improvement to the variograms (Marchant et al., 2013).

As noted above, the declustering does not remove all of the lumpiness in the maximum extent empirical variogram. The 1 km and 10 km extent variograms do not illustrate lumpiness, but declustering does produce variograms with a slightly different shape. Declustering has a smaller impact on the narrower because it's much less likely that densely sampled patches will create a strong spike over a relatively short spatial extent. But densely sampled patches may still exert a more subtle bias over the variogram, and declustering will work to reduce this influence. At these narrower extents it is less likely that there will be two dominant patches by these separation distances, but there will still likely be overrepresentation of some points (which will alter the shape). Power curves (Eq. (3)) were fitted to each variogram using the nonlinear least squares method. Parameters in the model¹⁰ are significant at $p < 0.01$ for all scales whether declustered or not (Table 2.6). The power curves are displayed as red lines in Figs. 9, 10 and 11. It is obvious from visual inspection that at the three largest extents (extent 3800 km, 1000 km and 100 km) the power curves fit the declustered empirical variograms better than the variograms calculated without declustering. Marchant et al. (2013) suggest that the removal of noise in the declustered empirical variograms results in fitted curves that much more closely describe the underlying spatial structure. The difference in the fit of the power curve at

¹⁰ This is more relevant for ω , as a value of 0 for b would create a null model

the 1 km and 10 km extent is marginal. There is no obvious lumpiness to be removed at these scales, but it may be possible that there is a degree of bias which has been removed by the declustering (i.e. reducing the impact of highly sampled areas). We assert that it is better to proceed with the declustered empirical variograms at all scales for the remaining analysis.

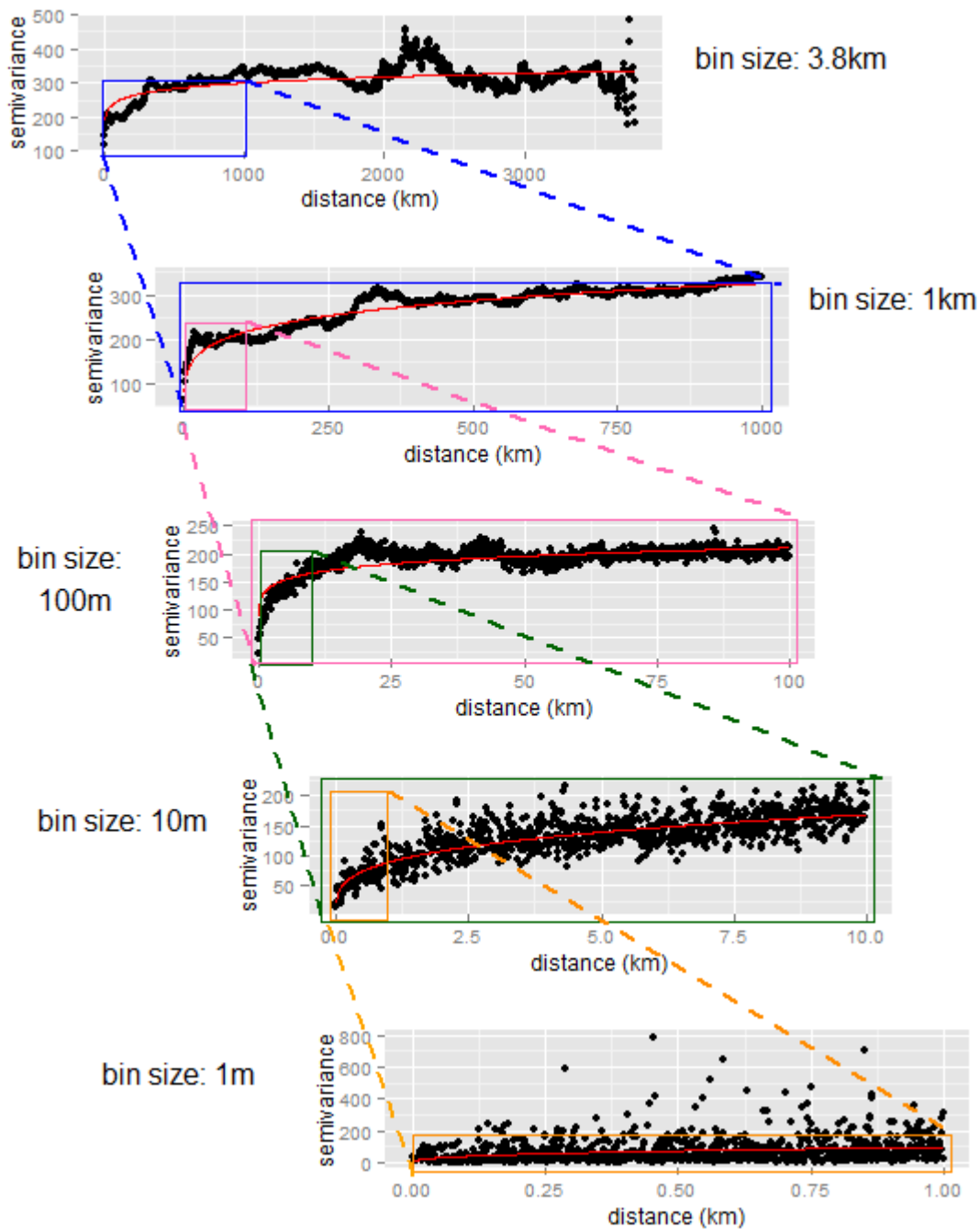


Figure 2.9. Empirical variograms calculated across varying spatial extents. Data from the NSSC dataset: Clay content (% fraction); soil depth 0-5cm. Black dots represent individual bins. Red lines are the fitted power curves. Other coloured lines indicate expansion.

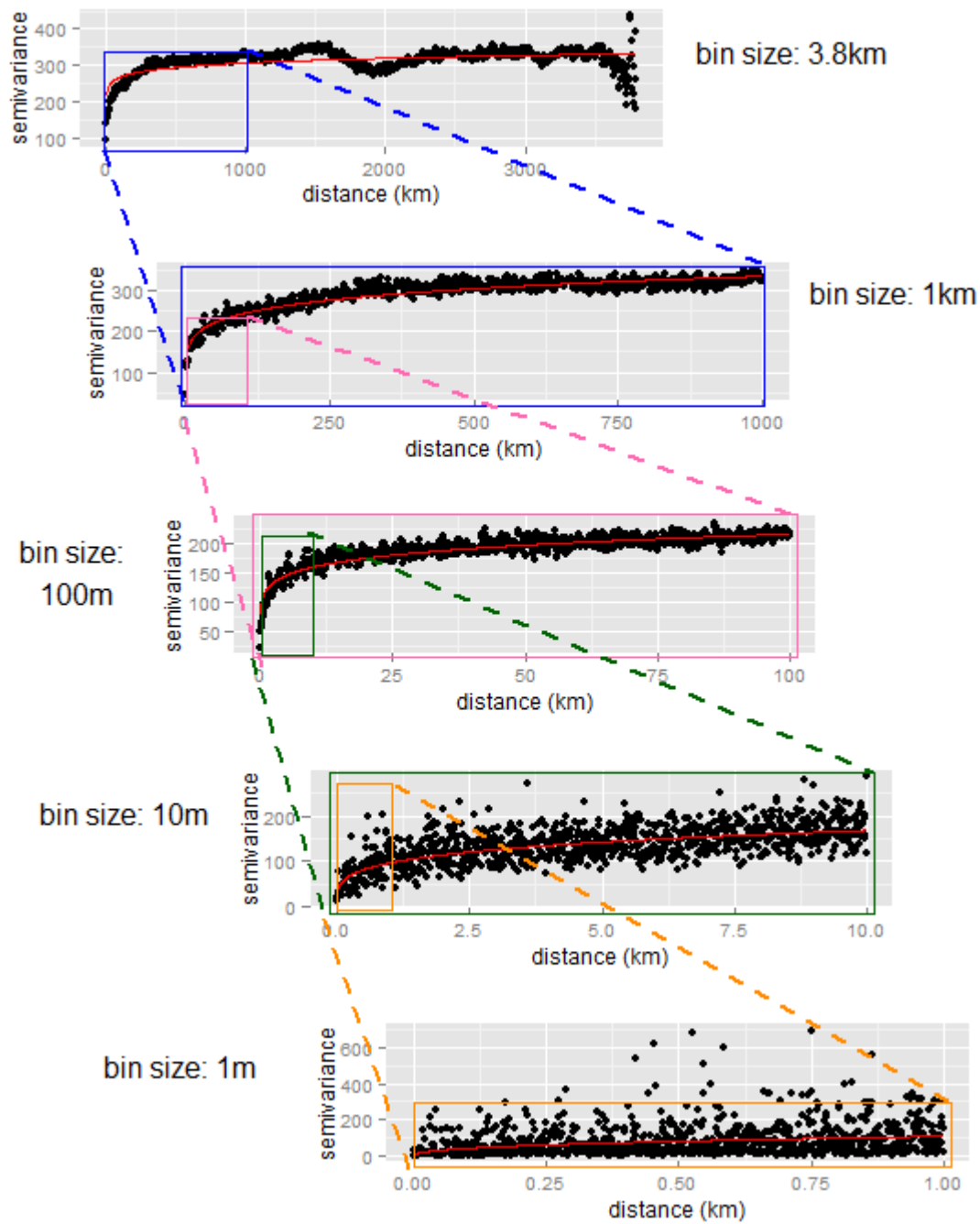


Figure 2.10. Empirical variograms calculated across varying spatial extents using declustering. Data from the NSSC dataset: Clay content (% fraction); soil depth 0-5cm. Black dots represent individual bins. Red lines are the fitted power curves. Other coloured lines indicate expansion.

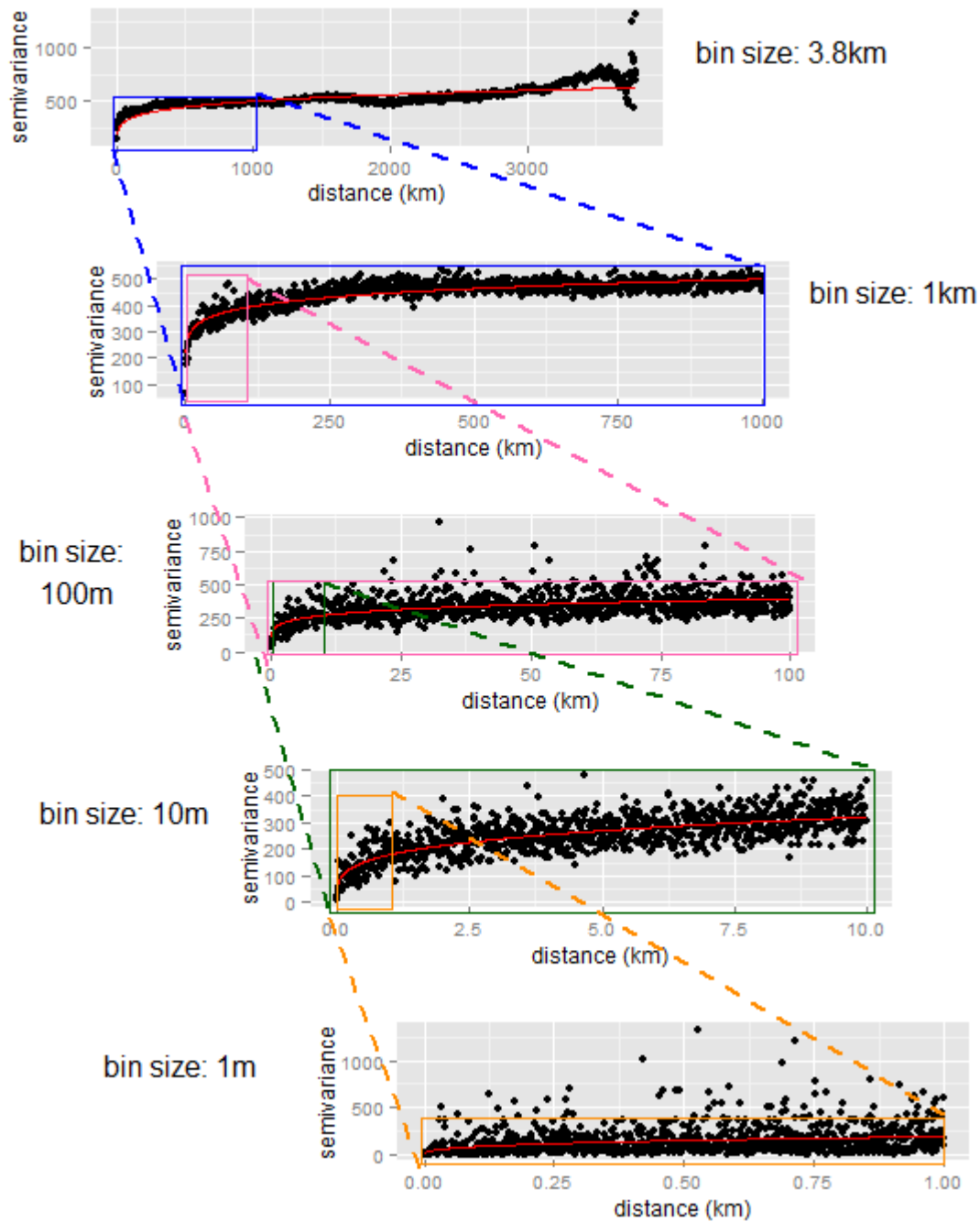


Figure 2.51. Empirical variograms calculated across varying spatial extents using declustering. Data from the NSSC dataset: Sand content (as percentage); soil depth 0-5cm. Black dots represent individual bins. Red lines are the fitted power curves. Other coloured lines indicate expansion.

Table 2.6. Power curve parameters and Roughness Index values from variograms of clay and sand content at 0 – 5cm depth interval.

parameter	variogram	extent (km)									
		3800		1000		100		10		1	
		estimate	se	estimate	se	estimate	se	estimate	se	estimate	se
ω	Clay % no declustering	0.08	0.004	0.18	0.002	0.10	0.00	0.27	0.01	0.40	
b		171	4	92	1.3	131	1.6	89	1.3	96	
RMSE		34.3		14.9		15.7		21.8		79.7	
D value		2.96		2.92		2.95		2.87		2.80	
ω	Clay % declustering applied	0.06	0.003	0.14	0.00	0.13	0.00	0.24	0.01	0.42	0.06
b		203.9	4.2	128.82	1.51	118.02	0.95	97.46	1.78	108.45	5.30
RMSE		24.6		13.94		9.98		30.81		86.92	
D value		2.97		2.93		2.93		2.88		2.79	
ω	Sand % declustering applied	.17	.005	0.11	.002	0.16	0.01	0.25	.009	0.36	0.05
b		158.7	6.07	238.0	3.16	185.7	7.49	180.0	2.86	192.0	8.76
RMSE		65.58		25.6		83.91		49.52		147.5	
D value		2.92		2.94		2.92		2.88		2.82	

2.3.2 The Roughness Index – Variability across scales

Fig. 12 shows D values obtained plotted against separation distance (i.e. a Fractogram) for sand and clay topsoil and subsoil. D values calculated from distinct variograms modelled at different extents (methods described in Sections 2.2.6 and 2.2.7) are represented as points. Continuous D values (roughness index) calculated from the derivative of the composite variogram on the log-log scale (methods described in Section 2.2.8) are shown as curved lines. The two methods show a similar trend in the change in D values with scale. D values are high (> 2.7) for sand and clay percentage fraction across all modelled extents (Table 2.6, Fig. 10). This is consistent with the high short range variability observable in the variograms in Section 2.3.2. Other studies which have estimated the fractal dimension of soils have also found high D values (Bai and Wang, 2011; Burrough, 1983; Eghball et al., 1999). The change in D values with scale is similar between sand and clay. There is a tendency for D values to decrease as the resolution of the modelling increases. The decrease in D values appears most dramatic at the narrowest bin sizes and extents modelled. This implies that much of the spatial structure of soil variability is organised at fine scales. The lowest values of around 2.8 for the finest variogram (1 m bin size, 1 km extent) increase to almost 2.9 by 10 m bin size 10 km extent. By 100 m

bin size 100 km extent, the D values appear to have reached a steady state. That is, the relationship between variability at 100 m and variability at 100 km is the same as the relationship between variability at 1 km and 1000 km. At the finest scale modelled (bin size 1 m, total extent 1 km) the D appear to still be decreasing (Fig. 10). This suggests that there is unresolved spatial variation at scales finer than those captured by the spacing of our data set (Burrough, 1983). The D value is usually calculated from a limited set of observations of a continuous process so the calculated D value reflects not only the underlying patterns in variation of a property, but also how well the particular sample captures this variation. A high D value might indicate a high level of stochasticity in the data, or it may indicate that the spacing is too wide to resolve short range patterns. If a D value remains high over a range of spatial scales it is indicative of a high level of roughness or stochasticity (at least over this range of scales). Alternatively, if the D value decreases as the spatial scale changes, then this suggests that the resolution is influencing the perceived stochasticity. The practical importance of this unresolved variation will depend on the end use of data. Management of soils at scales of < 1 m is often impractical, so information at scales finer than this may not have a strong practical use.

2.3.3. D values: Comparison of methods

There is a close correspondence between the values generated with the two methods (Fig. 10). The variogram method models a much noisier relationship between D value and distance than the 'continuous D value or Roughness Index'. This could be either a positive or a negative feature of the 'continuous variogram' method. The emphasis on fitting the model using an entire composite variogram ensures that the important broad trends are captured. One could also interpret this negatively: by creating a composite variogram, the opportunity to investigate shifts in roughness between scales, has been reduced. We lean towards the former explanation (provided that the curve fit to the composite variogram is good, with no trend in the residuals). Fig. 11 illustrates the fit of the exponential decay model (Eq. (7)) to the composite variograms on the log-log scale. The fit appears to be very good across for different separation distances and texture types. Another criteria that could be used to decide preferentially between the methods is the underlying belief in how the variability changes with scale. In Section 2.2.9 we discuss the underlying difference in frameworks between the two methods. Burrough (1983) hypothesised that it is likely that soil will have particular scales over which it behaves in a fractal-like manner (constant D values) separated by regions of transition. When a variogram representing a property with this behaviour was plotted on a log-log scale it would visualise as several straight lines of differing slopes. Another possibility is that change in roughness occurs more gradually. We believe the shape of the composite variogram is curved enough to favour the second option. However it is possible to imagine the data fitting Burrough's explanation. For

instance, divided into three segments (1 m to 100 m then 100 m to 10 km then 10 km to 1000 km) each segment could be close enough to linear to draw a straight line through it. The question of how linear is linear enough to meet the first hypothesis remains somewhat open (Figs. 13 and 14). The most significant argument (in our opinion) for the use of the variogram method for calculating D values presented is the background for its use. We were not able to find a precedent for the continuous method of calculating the D value across scales.

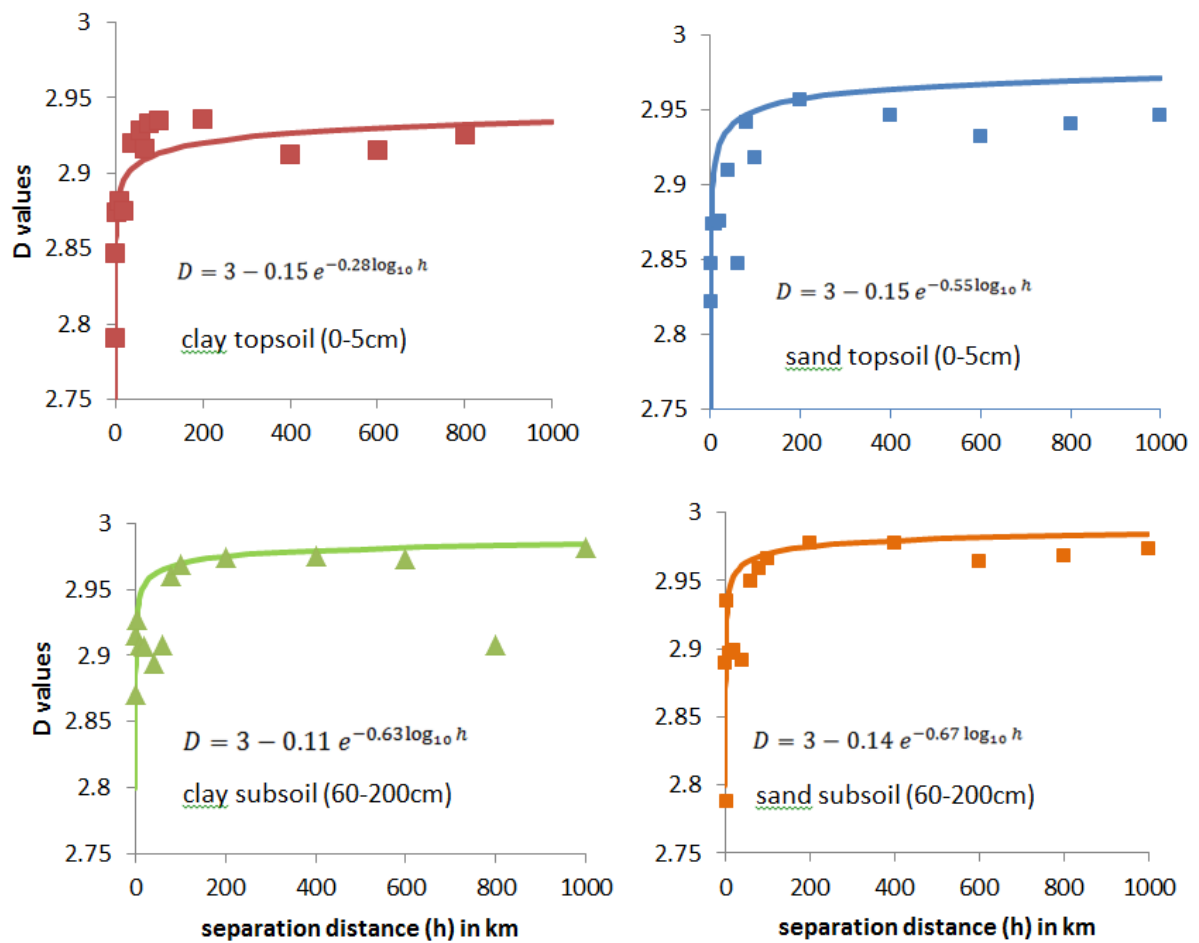


Figure 2.12. Hausdorff Besicovitch Dimension plotted against separation distance. Sand and Clay topsoil and subsoil

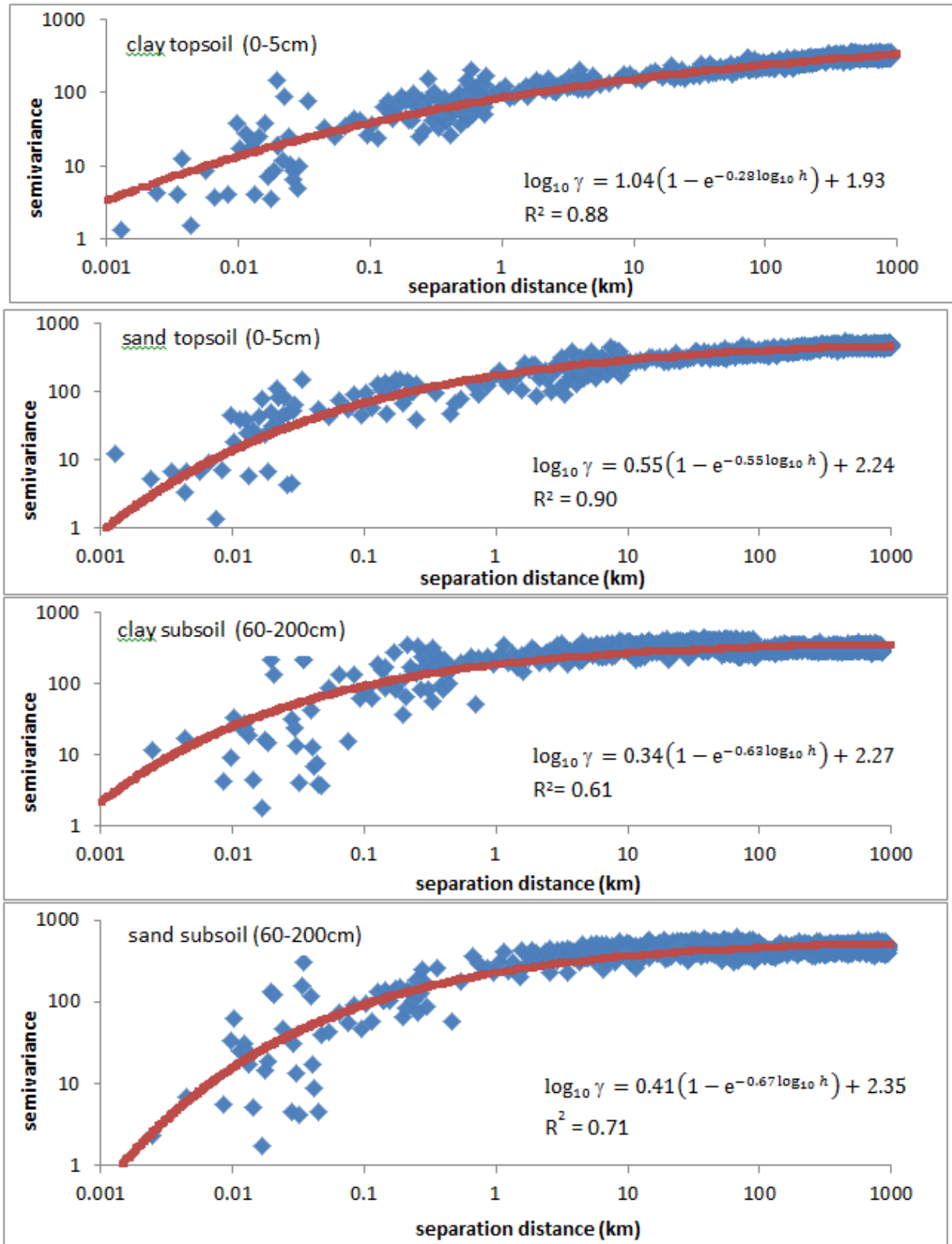


Figure 2.63. log₁₀-log₁₀ variograms with fitted curves. Sand and Clay topsoil and subsoil. The blue squares shown are the data points from the composite variograms. The red curves are the fitted models (equation and R² shown on chart)

2.3.4. Changes in Soil variability with depth

Declassified variograms were calculated across depths for a number of spatial extents. D values were fitted to these variograms using the power curve method, and fractograms are presented in Fig. 12. Variability increases with depth from 0 to 5 cm down to 30–60 cm at every extent modelled. As depth increases from 30 to 60 cm to 60–200 cm, the variability may increase or decrease depending on extent. The 1 km extent variogram, the semivariance of the subsoil layer increases more gradually than the 30–60 cm layer. In the variogram presented for 1000 km, the fitted power curve reaches peak variance almost instantaneously, resulting in the very high D value (Fig. 12).

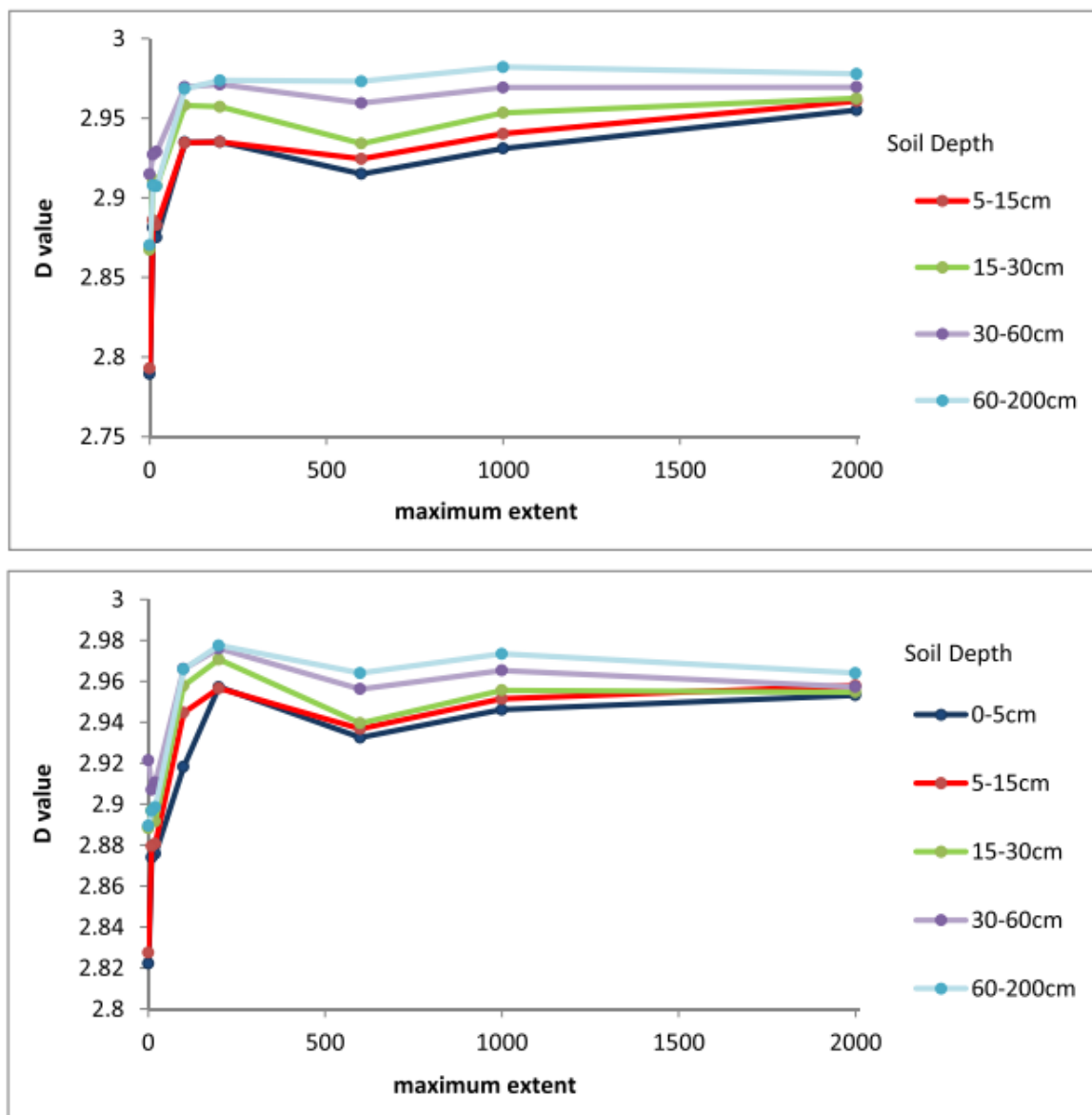


Figure 2.74. D values mapped against spatial extent for clay (top) and sand (bottom)

2.3.5. Spatial variability increases with depth: Possible mechanistic explanations

At all spatial extents we considered in this analysis, topsoil (0–5 cm and 5–15 cm) showed less variability than lower depths (15–30 cm, 30–60 cm and 60–200 cm). A thorough investigation into the causes of this trend is beyond the scope of this chapter, but we speculate on some possible mechanistic explanations below. The dominance of agricultural soils in the dataset must be noted. Anthropogenic influences, such as tilling, are likely to be a significant controlling factor in soil condition. Mechanical churning of the soil is likely to have a homogenizing effect on soil texture, and would be limited to the topsoil. The texture of deeper layers is likely to be more heavily influenced by the local parent material. In addition, Australian agricultural regions are typically dominated by duplex soils (soil with contrasting texture in the A and B horizons) and to a lesser extent by Vertosols (or Vertisols, WRB). Duplex (or texture contrast) soils are characterized by sandy loam top soils (A horizon), commonly extending up to 30 cm in depth, and clayey subsoils (B horizon). The increase in variability at depths > 15 cm may be due to a mix of A horizon and B horizon samples. It may also reflect increased variability in this depth range where the illuviation processes are more likely to be active. The mechanics of collecting soil data are another factor that could be contributing to the patterns of variability evident in the data. In particular, where soil is extremely clayey or extremely sandy, collecting soil becomes increasingly difficult with depth. Extreme observations at these depths may not have been recorded due to mechanical difficulties.

2.3.6 Contribution to spatial scaling literature

The question of how much soil varies across a given spatial extent is of fundamental interest to soil scientists. This article follows a number of others which describe soil spatial variability using formal mathematical relationships. Smith (1938) may have been the first to quantify soil spatial variability by formalizing the relationships he observed between plot size and yield variability with a logarithmic function. Green et al. (2004) were able to accurately characterize spatial diversity in soil eukaryotes over small to mid-ranges. McBratney (1992) considered the variability of magnesium at extents from field to continental but the conclusions are limited by lack of data. These contributions highlight both the possibility and the utility of developing a unified scaling theory for prediction. The spatial variability of many soil characteristics has been quantified over small extents and for particular biophysical regions (Bui et al., 2014; Ettema and Wardle, 2002; Garten et al., 2007; Tesfahunegn et al., 2011) among others. These studies have a strong advantage in their accurate description of soil scaling properties over small spatial extents. However the findings are specific to the regions they are conducted in so the results are difficult to generalise. The field of soil hydrology has made significant

achievements in consolidating smaller studies to develop a more general understanding of the scale effects on soil moisture properties. Efforts to consolidate understanding of scale effects in soil hydrology have led to a better understanding of the controls of soil moisture at different scales (Biswas et al., 2012; Crow et al., 2012; Western and Bloschl, 1999; Western et al., 2002) allowing improvements in predictive capacity. Our exploration of the spatial variability of soil texture across multiple scales moves us closer to answering the fundamental question: how variable is soil? There is a pronounced knowledge gap around the quantification of soil variability at mid to large scales. Our analysis considers spatial variability at extents from 1 km to several thousand kilometres and finds the following:

- Spatial variability of soil texture is greater at lower depths.
- Short range variability makes up a large proportion of total variability, around 50% of total soil variability is realised within 10 km and around 20% within 1 km.
- There is likely to be unresolved spatial variation at scales finer than those we have modelled.
- At extents > 100 km the relationship between variability and separation distance appears to reach a steady state.

These general results provide new information on soil spatial variability across scales. This information can be of use for informing soil survey design. Where site specific expectations about soil variability are not available, our results can suggest the extent of information lost or gained that could be expected from changing sampling density. An increased understanding of spatial variability in soils may also be useful for up and downscaling maps. Understanding how much more variability should be revealed as the resolution increases, and how much of this can be spatially modelled should assist digital soil mapping efforts, or at least assist in understanding the limitations of maps (i.e. where a downscaled map cannot include significantly more variability due to lack of information, but we expect that it should). The results from our analysis are also likely to be useful for simulations

2.3.7 Future work

Because the analysis presented in this chapter uses the complete (cleaned) dataset, all of the results presented in this chapter are of a general nature. We have characterised the average relationship between spatial extent and variability in primarily agricultural areas within Australia. We have not differentiated between different climatic regions, land uses or soil types. Splitting the dataset and repeating some or all of the analysis will improve our ability to use our results for prediction and to investigate how other factors might be driving soil variability. It may also be useful to conduct a similar

analysis on other properties. The Hausdorff Besicovitch Dimension is a useful tool for comparing spatial variability between properties and the methods used in this chapter lend themselves well to legacy datasets. Comparing the variability of other soil and other environmental properties across varying spatial extents is a logical extension of this work. The NSSC database has significant amounts of data available for pH and soil organic C, however as pH and SOC vary in time and in terms of response to testing procedure it will be more difficult to utilize the entire dataset than it was for texture. One of the limitations revealed by our work is the unresolved spatial variability at fine scales. Resolving trends in fine scale variability would require collection of additional data at these scales. Other trends suggested by our results: high levels of short range variability, scale invariance at medium to large extents and increasing variability with depth. Future work could and should test these trends with for purpose experimental design.

Because the analysis presented in this chapter uses the complete (cleaned) dataset, all of the results presented in this chapter are of a general nature. We have characterised the average relationship between spatial extent and variability in primarily agricultural areas within Australia. We have not differentiated between different climatic regions, land uses or soil types. Splitting the dataset and repeating some or all of the analysis will improve our ability to use our results for prediction and to investigate how other factors might be driving soil variability. It may also be useful to conduct a similar analysis on other properties.

The Hausdorff Besicovitch Dimension is a useful tool for comparing spatial variability between properties and the methods used in this chapter lend themselves well to legacy datasets. Comparing the variability of other soil and other environmental properties across varying spatial extents is a logical extension of this work. The NSSC database has significant amounts of data available for pH and soil organic C, however as pH and SOC vary in time and in terms of response to testing procedure it will be more difficult to utilize the entire dataset than it was for texture.

One of the limitations revealed by our work is the unresolved spatial variability at fine scales. Resolving trends in fine scale variability would require collection of additional data at these scales. Other trends suggested by our results: high levels of short range variability, scale invariance at medium to large extents and increasing variability with depth. Future work could and should test these trends with for purpose experimental design.

2.4 Conclusions

Our study highlighted two consistent trends around soil texture variability. The first is that variability increases with depth, as does roughness. The second is that a significant proportion of soil texture variability occurs at short extents. These results were indicated by the first part of the analysis (modelling empirical variograms across scales) and supported by the second part of the analysis (calculating D values from these empirical variograms). This supports evidence from other literature that soil is more variable than other environmental properties. The D values we calculated range from 2.79 to 2.96. This is consistent with, although on the high end of, other studies using D values to assess soil variability. The change in D values across different extents, (modelled in two different ways) indicates that there may be important unresolved variability in soil texture at finer resolutions than those included in this study.

- Empirical variograms calculated from large datasets are an effective and efficient tool for modelling variability across scales.
- Grid-based declustering is an effective strategy for reducing lumpiness in variograms resulting from clustered data distribution. When applying this method across scales, selection of appropriate grid sizes at each scale becomes important.
- Approximately half the continental variability of soil texture is realised within 10km. One third is realised in the first 1km.
- Soil texture variability and roughness tend to increase with depth across all scales up to depths of 60cm. Beyond 60cm the relationship becomes more complex.
- There is likely to be unresolved variability at scales finer than those we have modelled.
- When modelled across multiple spatial extents, soil texture variograms can be closely approximated by the function $\log_{10} \gamma = C(1 - e^{-k \log_{10} h}) + A$. This allows us to calculate a continuous relationship between D value and variability.

Acknowledgements

This work is supported by the ARC Discovery project DP140102283, A general soil spatial scaling theory. We thank Ross Searle (CSIRO) for providing data from the NSSC database, and we are grateful to all organisations involved in the compilation of the NSSC. We thank also Richard Webster for the suggestion to use declustering to improve the Empirical Variograms. We also thank Nathan Odgers, Brendan Malone and two anonymous reviewers for their constructive feedback on earlier versions of the chapter. We also thank Ana Tarquis for generously sharing her time and knowledge of fractal analysis. Discussions with her allowed significant improvements to this chapter.

REFERENCES

- Arrouays, D., McBratney, A., Minasny, B., Hempel, J., Heuvelink, G., MacMillan, R., ... McKenzie, N., 2014. The GlobalSoilMap project specifications. In: Arrouays, D., McKenzie, N., Hempel, J., de Forges, R.A., McBratney, A. (Eds.), *GlobalSoilMap: Basis of the Global Spatial Soil Information System*, pp. 9–12.
- Bai, Y.R., Wang, Y.K., 2011. Spatial variability of soil chemical properties in a jujube slope on the Loess Plateau of China. *Soil Science*. 176 (10), 550–558.
- Berry, M.V., Lewis, Z.V., 1980. In: On the Weierstrass Mandelbrot fractal function. *Proceedings of the Royal Society of London*. 370. pp. 459–484.
- Bez, N., Bertrand, S., 2011. The duality of fractals: roughness and self-similarity. *Theoretical. Ecology*. 4 (3), 371–383.
- Biswas, A., Zeleke, T.B., Si, B.C., 2012. Multifractal detrended fluctuation analysis in examining scaling properties of the spatial patterns of soil water storage. *Nonlinear Processes in Geophysics*. 19 (2), 227–238.
- Bui, E.N., Moran, C.J., Lark, R.M., Oliver, M.a., Webster, R., Zimmerman, D.L., McGuire, A.D., 2014. Spatial scaling effects on variability of soil organic matter and total nitrogen in suburban Beijing. *Geoderma* 9 (1), 2621–2627.
- Burrough, P.A, 1983. Multiscale sources of spatial variation in soil. I. The application of fractal concepts to nested levels of soil variation. *Journal of Soil Science*. 34, 577–597
- Chan, G., Wood, A., 2000. Increment-based estimators of fractal dimension for two-dimensional surface data. *Statistica. Sinica*. 10, 343–376.
- Cressie, N., 1985. Fitting variogram models by weighted least squares. *Mathematical. Geology*. 17 (5), 563–586.
- Crow, W.T., Berg, A.A., Cosh, M.H., Loew, A., Mohanty, B.P., Panciera, R., Walker, J.P., 2012. Upscaling sparse ground-based soil moisture observations for the validation of coarse-resolution satellite soil moisture products. *Review of Geophysics*. 50 (2), 1–21.
- Davis, M., 1987. Production of conditional simulation via the LU Triangular decomposition of the covariance matrix. *Mathematical. Geology*. 19 (2), 91–98.

- Deutsch, C., 1989. Declus: a fortran77 program for determining optimum spatial declustering weights. *Computational Geoscience*. 15 (3), 325–332.
- Eghball, B., Hergert, G.W., Lesoing, G.W., Ferguson, R.B., 1999. Fractal Analysis of Spatial and Temporal Variability. 88(12112). pp. 349–362.
- Emery, X., 2007. Reducing fluctuations in the sample variogram. *Stochastic Environmental Research and Risk Assessment* 21 (4), 391–403.
- Ettema, C.H., Wardle, D.a., 2002. Spatial soil ecology. *Trends in Ecology and Evolution* 17 (4), 177–183.
- Garcia Moreno, R., Diaz Alvarez, M.C., Saa Requejo, A., Valencia Delfa, J.L., Tarquis, A., 2010. Multiscaling analysis of soil roughness variability. *Geoderma* 160, 22–30.
- Garten, C.T., Kang, S., Brice, D.J., Schadt, C.W., Zhou, J., 2007. Variability in soil properties at different spatial scales (1 m–1 km) in a deciduous forest ecosystem. *Soil Biology and Biochemistry*. 39 (2007), 2621–2627.
- Green, J.L., Holmes, A.J., Westoby, M., Oliver, I., Briscoe, D., Dangerfield, M., Beattie, A.J., 2004. Spatial scaling of microbial eukaryote diversity. *Nature* 432 (7018), 747–750.
- Grundy, M.J., Viscarra Rossel, R.A., Searle, R.D., Wilson, P.L., Chen, C., Gregory, L.J., 2015. Soil and landscape grid of Australia. *Soil Res.* 53 (8), 835–844.
- Heuvelink, G.B., Webster, R., 2001. Modelling soil variation: past, present, and future. *Geoderma* 100 (3–4), 269–301.
- Hurst, H.E., 1951. Long term storage capacity of Reservoirs. *American Society of Civil Engineering*. 116, 770–799.
- Lark, R.M., 2000. Estimating variograms of soil properties by the method-of-moments and maximum likelihood. *European Journal of Soil Science* 51 (December), 717–728.
- Lark, R.M., 2005. Exploring scale-dependent correlation of soil properties by nested sampling. *European Journal of Soil Science*. 56 (June), 307–317.
- Lark, R.M., 2011. Spatially nested sampling schemes for spatial variance components: scope for their optimization. *Computational Geoscience* 37 (10), 1633–1641.
- Leduc, A., Prairie, Y.T., Bergeron, Y., 1994. Fractal dimension estimates of a fragmented landscape: sources of variability. *Landscape Ecology*. 9 (4), 279–286.

- Malone, B.P., McBratney, A.B., Minasny, B., Laslett, G.M., 2009. Mapping continuous depth functions of soil carbon storage and available water capacity. *Geoderma* 154 (1–2), 138–152.
- Malone, B.P., McBratney, A.B., Minasny, B., 2013. Spatial scaling for digital soil mapping. *Soil Science Society of America Journal* 77, 890.
- Marchant, B.P., Rossel, R.A.V., Webster, R., 2013. Fluctuations in method-of-moments variograms caused by clustered sampling and their elimination by declustering and residual maximum likelihood estimation *European Journal of Soil Science*. 64 (4), 401–409.
- Matheron, G., 1963. Principles of Geostatistics. *Econ. Geol.* 58, 1246–1266.
- McBratney, A., 1992. On variation, uncertainty and informatics in environmental soil management. *Australian Journal of Soil Resources*. 30 (6), 913.
- Oliver, M.A., Webster, R., 2014. A tutorial guide to geostatistics: computing and modelling variograms and kriging. *Catena* 113, 56–69..
- Pettitt, A.N., McBratney, A.B., 1993. Spatial sampling designs for estimating variance components *Applied Statistics-Journal of the Royal Statistical Society Series C* 42 (1), 185–209.
- Pongpattananurak, N., Reich, R.M., Khosla, R., Aguirre-Bravo, C., 2012. Modeling the spatial distribution of soil texture in the state of Jalisco, Mexico. *Soil Science Society of America Journal*. 76 (1), 199.
- Richmond, A., 2002. Two-point declustering for weighting data pairs in experimental variogram calculations. *Computational Geoscience*. 28, 231–241.
- Schmid, P.E., 2000. Fractal properties of habitat and patch structure in benthic ecosystems. *Advances in Ecological Research*. 30.
- Searle, R., 2014. The Australian site data collation to support the GlobalSoilMap. In: Arrouays, A., McKenzie, D., Hempel, N., DeForges, J., McBratney, A.C.R. (Eds.), *GlobalSoilMap: Basis of the Global Spatial Soil Information System*, pp. 127–132.
- Smith, H.F., 1938. An empirical law describing heterogeneity in the yields of agricultural crops. *Journal of Agricultural Science*. 28, 1.
- Tesfahunegn, G.B., Tamene, L., Vlek, P.L.G., 2011. Catchment-scale spatial variability of soil properties and implications on site-specific soil management in northern Ethiopia. *Soil Tillage Research* 117, 124–139. 5

Webster, R., 2000. Is soil variation random? *Geoderma* 97 (3–4), 149–163.

Webster, R., Welham, S.J., Potts, J.M., Oliver, M.A., 2006. Estimating the spatial scales of regionalized variables by nested sampling, hierarchical analysis of variance and residual maximum likelihood. *Computational Geoscience* 32 (9), 1320–1333.

Western, A.W., Blöschl, G., 1999. On the spatial scaling of soil moisture. *Journal of Hydrology*. 217 (3–4), 203–224.

Western, A.W., Grayson, R.B., Blöschl, G., 2002 Spatial Scaling of Soil Moisture: A review and Some recent results.

Chapter 3:

Assessing the impact of sampling distribution on the Variogram and roughness index

When you know better, you do better.
– Maya Angelou

Abstract

In this chapter we use a proxy dataset to test how different sampling designs affect the 'roughness index' developed in the previous chapter. We use a simple random average to test the effects of the biased sampling design in Chapter 2 on the variogram. We introduce a sampling design that selects independent pairs from the raster dataset. This aligns more closely with the sampling design typically used when calculating the Fractal Dimension or Hurst Exponent. We find that there is minimal difference in the results regardless of the sampling design used. This Chapter supports the conclusions drawn in Chapter 2, and introduces a sampling design used in Chapter 4.

3.1 Introduction

Sampling design is an important feature in variogram estimation. When using legacy data, it is not possible to control sampling design, and this may create bias or distortion in results. In this Chapter we use a Gamma Radiometric data as a proxy for soil texture to test different sampling designs. We use a simple random design to test the effect of bias, and a more complex random sampling design that avoids the reuse of observations across bins.

It is important to test the effect of sampling design, because while we are able to use declustering algorithm to remove noise in variogram estimation this declustering method cannot compensate for potential bias caused by a complete lack of data across large regions (as occurs in the NSSC dataset in Central Australia). The other important issue we are able to address here is the effect of reusing the same spatial observations in more than one bin. In Chapter 2, our method of calculating the variogram reuses observations, it is difficult to avoid this when using the legacy dataset. This is common practice when calculating an experimental variogram, but studies that consider D values and the Hurst exponent do not reuse observations¹¹. Because our roughness index is derived from these methods, it is worthwhile to consider the impact of this feature of variogram calculation.

We use the Gamma Radiometric dataset which covers the entire continent as a proxy for clay content. Because we have continental coverage we can experiment with sampling design. This allows us to evaluate:

1. The effect of the declustering;
2. The effect of the large areas with missing information on the variogram;
3. The effect of 'reusing' observations when calculating the variogram..

3.2 Methods

3.2.1 Data

We use percentage of Potassium (⁴⁰K) from the Radiometric map of Australia (Minty et al., 2009) as a proxy for soil mineralogy. The map provides levelled and merged composite grids of several radiometric elements over Australia at a 100m resolution. The raw data for the map comes from systematic airborne radiometric surveys undertaken over the last 40 years. The resolution of the airborne surveys is shown in Figure 3.1 (taken from Minty et al., 2009). The Radiometric data was

¹¹ Studies that use D values and the Hurst exponent will typically start with a for purpose survey design with pairs collected at specific intervals. Each of these pairs will only be used once. This means that the variance calculated at each separation distance is calculated from independent data.

aligned to a common datum, and older surveys were back calibrated using new field observations. Details of the alignment and calibration are available in Minty et al. (2009).

Significant additional information was collected during the Australia wide airborne geophysical survey. The survey was flown in 2007 at a nominal terrain clearance of 80 m above ground level. The north–south flight lines were spaced 75 km apart and the east–west flight lines spaced 400 km apart. A 33 L NaI (TI) detector was used in the survey (Milligan et al., 2009).

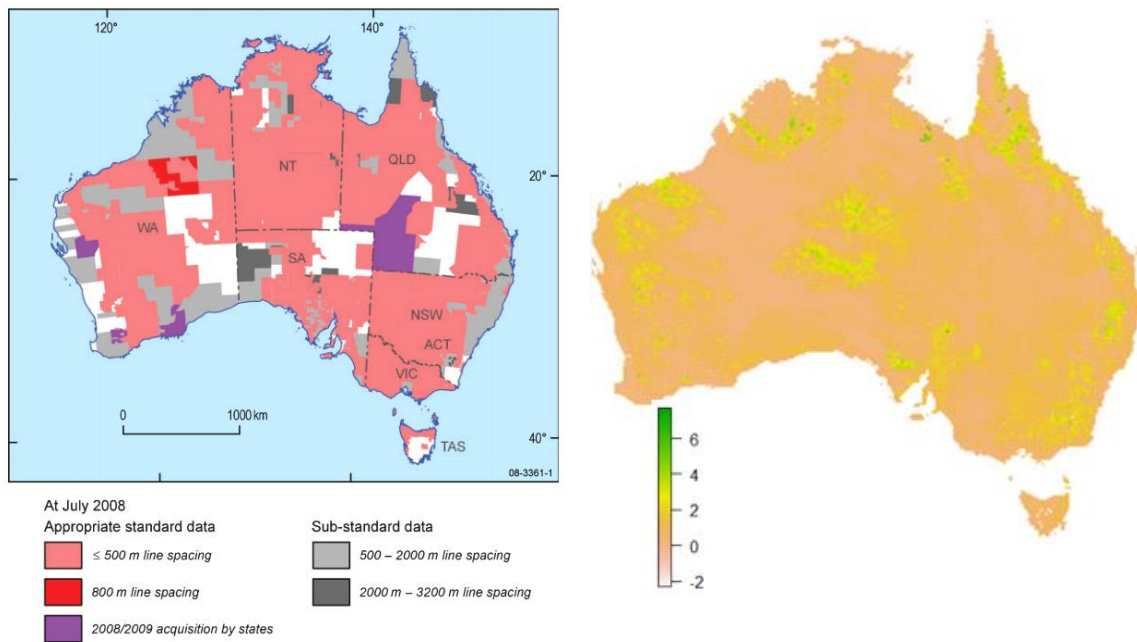


Figure 3.8. Left Panel: Radiometric sampling density (Minty et al. 2009) Right Panel: Potassium layer from the radiometric map of Australia (original source Geoscience Australia).

3.2.2 Sampling Design

We use three different sampling designs, detailed below: Comparisons between each of these reveals different information.

3.2.2.1 NSSC Sampling Design

We select ‘samples’ from the Gamma Radiometric raster using the same spatial locations contained within the NSSC dataset (13,830 observations).

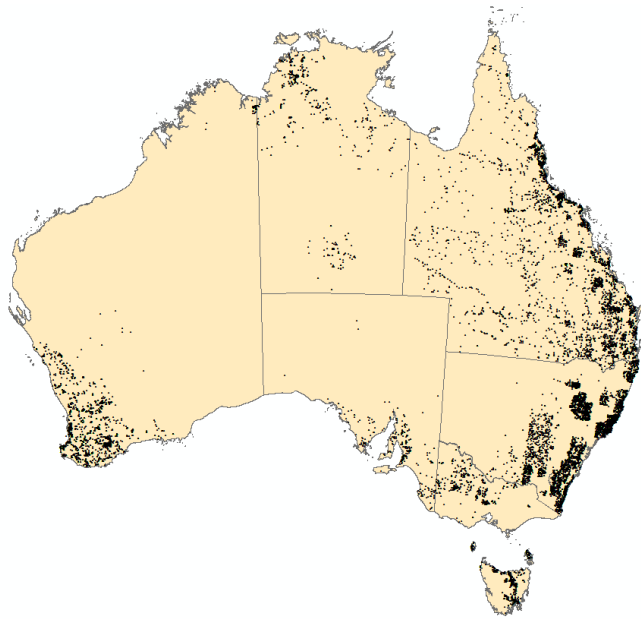


Figure 3.2. The distribution of the NSSC dataset. Each black dot represents an individual soil observation. (Duplicated from Figure 2.1).

3.2.2.2 Simple Random Sampling Design

We randomly select 13,000 samples from the Gamma Radiometric raster. We calculate empirical variograms using the same extent and bin size combinations used in Chapter 2. Following the methodology described in Chapter 2 we calculate composite variograms, by combining the variograms across bin sizes and calculating roughness index from it.

3.2.2.3 Random Pairs Sampling Design

The roughness index which we introduced in the previous chapter is derived from the composite variogram method of calculating the D value. It is also theoretically linked to the Hurst exponent. Both the variogram method and the calculations of the Hurst exponent are calculated so that each observation is used only once. That is, that any individual data point is used in only one 'bin' or 'lag'. In the previous chapter and in the two sampling conditions described above, we reused observations so that any individual spatial observation would be reused. Theoretically any given spatial observation could be used in every bin if it had a pair separated by the same distance.

The problems associated with this reuse of observations can be understood in a way that is similar to the problems associated with clustered sampling. The reuse of observations provides the opportunity

for these observations to exert a disproportionate influence on the variogram. An observation that is used in multiple bins will have an effect on each of those bins.

When calculating empirical variograms from the legacy dataset it is difficult to achieve this condition. However, when sampling from a raster grid which covers all of Australia, we have the luxury of being able to design our own sampling regime (without the added complication of additional costs).

We use this raster dataset to design a sampling scheme which meets the following conditions.

- Random sampling across the continent
- Observations are not used in more than one bin
- Pairs are distributed at a range that allows us to model a variogram on a log-log scale with good detail

The steps are as follows:

1. Specify q lag distances (h_1 to h_q) at appropriate intervals for modelling variogram across desired extent. We used the following intervals: .001, .025, .05, .075, .1, .15, .2, .25, .3, .35, .4, .5, .6, .7, .8, .9, 1, 1.25, 1.5, 1.75, 2, 2.5, 3, 3.5, 4, 5, 6, 7, 8, 9, 10, 15, 20, 25, 30, 40, 50, 75, 100, 200, 300, 400, 500, 600, 700, 800, 900, 1000 (km)
2. Randomly select n data points from raster grid. In this case we set $n = 720$ ¹²
3. Match each of the n (720) randomly selected data points with another point sampled from the raster. Each of these paired points will be h_1 separation distance away. For anisotropic sampling each degree angle from 1 to 360 degrees was represented twice¹³ ensuring an even coverage of angles. We also tested two anisotropic sampling schemes: For anisotropic (E-W) sampling the orientation has an equal chance of being 90 degrees or 270 degrees¹⁴. For anisotropic (N-S) sampling, the orientation has an equal chance of being 0 degrees or 180 degrees¹⁵.

¹²We chose 720 so that each an. This size sample was partly a matter of convenience (i.e. doubling the degrees) and partly because this number of observations was sufficient to obtain consistent values for the variance in each bin, but not so large to slow down the computation.

¹³ With the exception of cases where the paired observation fell outside of the bounds of the Australian continent, in which case the sample was excluded.

¹⁴ We used equal numbers of East and West lags so that the East and West coasts had similar representation.

¹⁵ We used equal numbers of North and South lags so that the North and South coasts had similar representation.

4. Repeat steps 2 and 3 for lags h_2 to h_q
5. Calculate the semivariance for each lag h_2 to h_q and plot

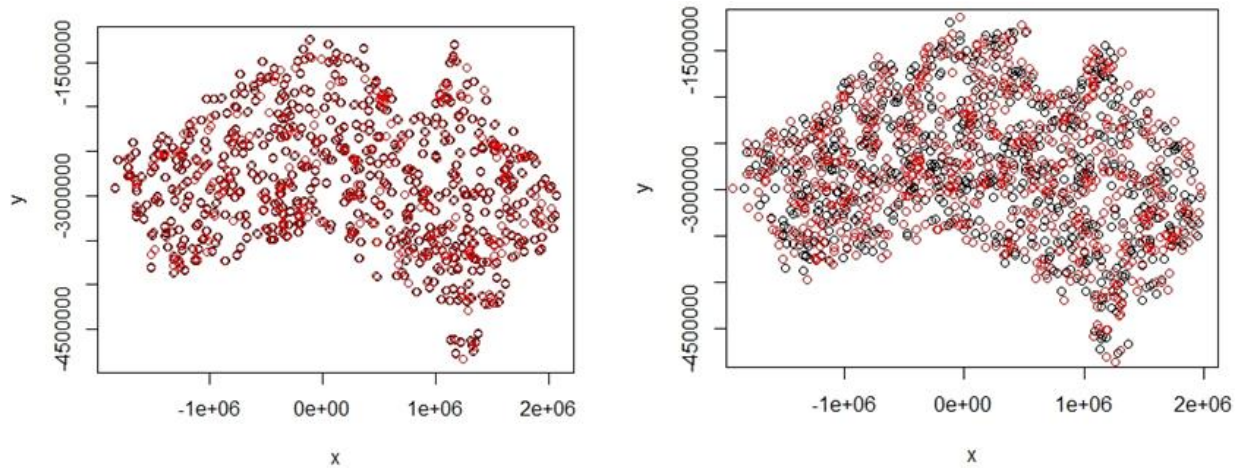


Figure 3.3. Schematics showing the paired observations for 10km lag and 100km lag (right). Original random sample (1 to 720) are shown in black. Paired observations (isotropic condition) are shown in red. Note the greater separation distance in the right hand panel results in more observations falling outside of the boundaries of the continent.

As the separation distance increases, the chances of the ‘paired point’ falling outside of the boundaries of the raster map of Australia also increases. This means that towards the largest separation distance (1000km) typically the number of pairs is around 360, compared to 720 for the smallest separation distances.

This sampling design has three major advantages.

- It means that each observation is only used once.
- The pairs are randomly selected.
- It is easy to control the direction of the pairs and calculate either isotropic or anisotropic variograms.

This sampling design does not address the issue of contiguous or overlapping pairs, but simulation studies have suggested that there is not a significant difference between the bias in these designs provided that there are enough observations (Ellis, 2007).

3.3. Results and Discussion

3.3.1 Clustered observations, declustering and the variogram.

In the previous chapter we describe the mechanism by which the patchiness in the sampling distribution creates the lumpiness in the variogram. We briefly reiterate here: A dense cluster of observations means that there is more information coming from the region where the dense observations occur. When there are two dense clusters of observations these two spatial regions become the dominant source of information about variability at this particular separation distance or lag. While the expected variance of any two observations does not depend on the location of these observations (under the assumption of second order stationarity), natural variability means that it is unlikely that the variability at these two locations is exactly the average variability for that lag over the whole continent. Where the two densely sampled areas have lower than average variation (between them) the overrepresentation of these two regions will result in a 'dip' in the variogram at that particular separation distance or lag. Where the densely sampled areas have higher than average variability (between them) the variogram will spike at that approximate lag. The grid-based declustering method addresses this trend by reducing the importance of the densely sampled observations in the calculation of the semivariogram. The method simply overlies a grid over the area, and computes the density of samples each of the cells within the grid. The declustering method is shown to be effective at removing the lumpiness in the variogram, this is consistent with Marchant et al. 2013 who introduce the method of grid based declustering as a tool for dealing with patchy sampling designs.

Using the Gamma Radiometric dataset to mimic the NSSC data distribution and the declustering process provides us with the opportunity to test the declustering process. Using the Gamma radiometric data as a proxy for soil texture is useful because of the relationship between clay texture and the Gamma radiometric signal (Rossel, Taylor, & McBratney, 2007). Our proxy can provide an indication of whether there is a bias created by the omission of large areas of the data from the sampling design. Declustering, while a useful tool for addressing the differences in sampling density, cannot address potential bias arising from absent observations. If the area missing is large enough and the variability contained within it different to the areas that have been sampled, then the lack of observations in central Australia are likely affect the shape of the variogram.

It was expected that the overall trend in the declustered variogram might differ from the overall trend in the random sample variogram due to bias. Large areas of the continent did not have any samples. However, the two variograms were similar with the exception of the slight dip (at around 400km).

The only visible 'lump' that the declustering does not appear to fully address is the slight dip at around 450 km. It is important to distinguish between natural bumps in the shape of the variogram (i.e. those that represent the true underlying spatial variability of the property in question) and artefacts of the data clustering. Because the variogram calculated from the 'simple random' does not show any sign of a bump, this suggests that this pattern is left over from the sampling distribution, rather than a feature of the underlying distribution. This indicates that the declustering, while a very useful tool, cannot entirely remove artefacts of a clustered sampling design. Another drawback of the declustering tool, is the coarse 'spread' of the declustered variogram. This highlights the cost (in terms of precision) of correcting for the sub optimal sampling design.

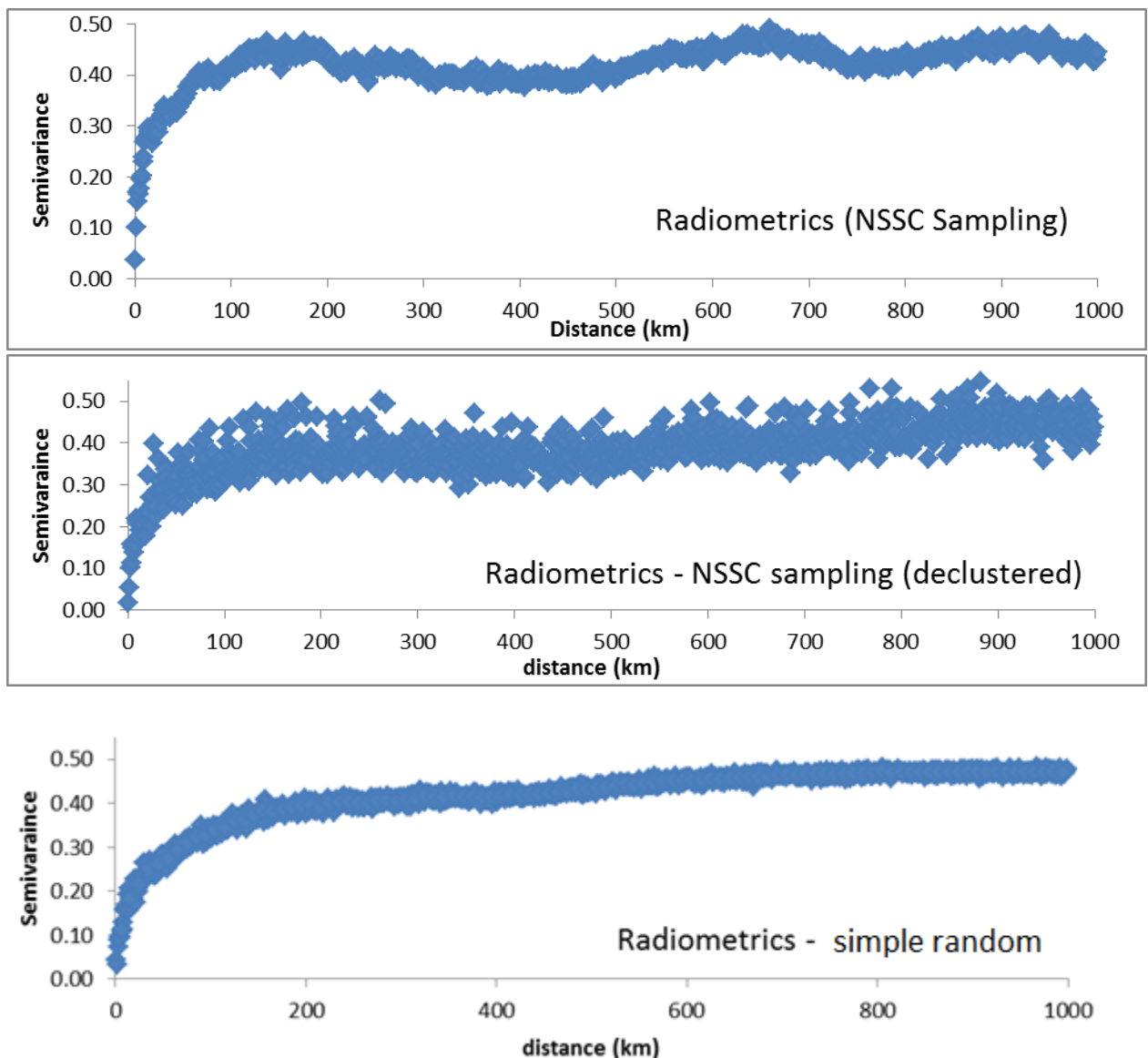


Figure 3.4. a-c Experimental variograms calculated from Radiometrics data using different sampling design schemes and methodologies.

The comparison of the declustered radiometrics variogram with the 'average' variogram reinforces the finding that declustering is an appropriate tool for reducing lumpiness that results from a clustered sampling design. The declustered Gamma Radiometric variogram has significantly less lumpiness than the variogram which is untreated, but there is still a very slight 'dip' in the variogram occurring at around 400km. This 'dip' is not present in the randomly sampled variogram, suggesting that it is a leftover feature from the sampling design rather than a true reflection of the spatial variability. The comparison with the variogram calculated from the random sample also highlights the fact that the declustering makes the variogram much more diffuse.

3.3.2 Alternative sampling designs, and the roughness index

In Section 3.3.1. the Gamma Radiometric raster was used as a proxy for soil texture to assess the effect of the patchy NSSC distribution, and declustering on the dataset. In this section we use the same Gamma Radiometric NSSC dataset to test its impact on the roughness index calculation.

Typically, studies that calculate the Fractal dimension or the Hurst exponent use non-overlapping observations, i.e. any given observation can only be used in one bin (Burrough, 1983). The roughness index that we describe in Chapter 2 is derived from the variogram method of calculating the D value and is conceptually similar to the Hurst Exponent. In Chapter 2, we reuse each sampling location. This is not consistent with the standard practice for D values and the Hurst exponent. We've introduced a sampling design that is random, provides control over the separation distance and which selects pairs of observations independently for each lag or separation distance. We compare the variogram calculated from these observations with the variograms calculated from the standard random sampling.

At extents greater than 100km the estimates of the roughness indices are very similar for all three sampling designs (Figure 3.7). At shorter extents however, there is a notable difference for the roughness indices calculated from the 'simple random' sampling design and the other two sampling designs (Figure 3.6). It is interesting that it is the average variogram, and not the NSSC design that is the most distinct of the three designs. The 'random pairs' design and the 'simple random' design both cover the whole continent. The 'NSSC' design and the 'simple random' design both reuse observations, while the 'random pairs' does not. The similarity between the NSSC and the 'random pairs' design is more evident when examining Figure 3.5a-c. The simple random design has very few 'bins' at separation distances of less than 500m. This means the spread of points at small lag values ' h ' will be

wider. This will affect the fit of the model at finer scales, and in turn lead to a very different shape of the roughness index curve.

Another advantage of this sampling regime is the discretion over the lags. By spacing the lags as we want them, we naturally create a multiscale variogram. This is a simpler and cleaner process than combining variograms calculated at different scales as we did in Chapter 2.

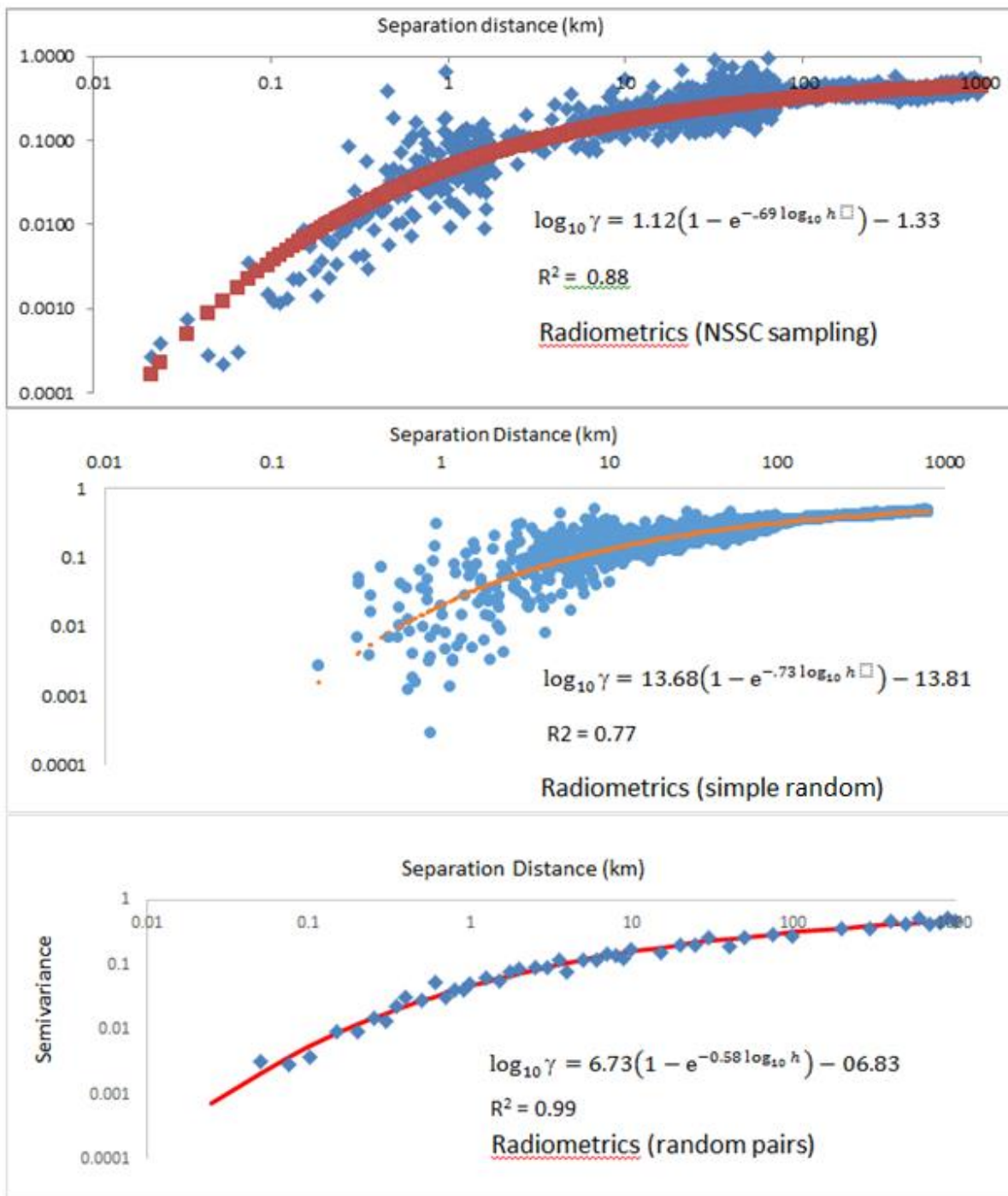


Figure 3.5. a-c Log-log experimental variograms calculated from Radiometrics data using different sampling design schemes and methodologies.

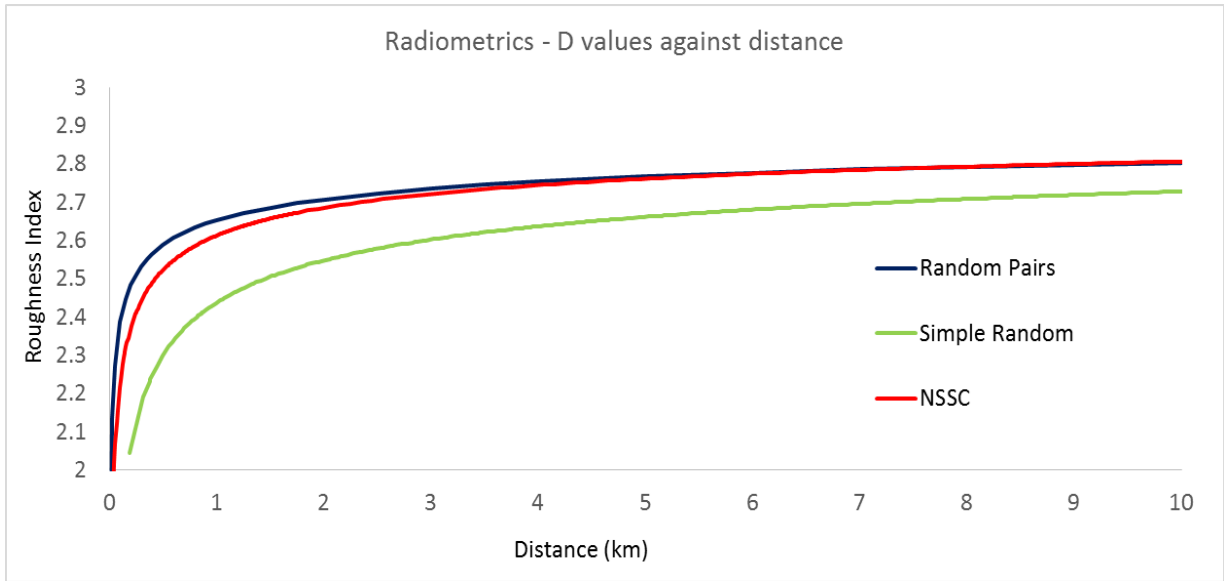


Figure 3.6. Comparison of sampling designs, roughness index value against distance 0-10km.

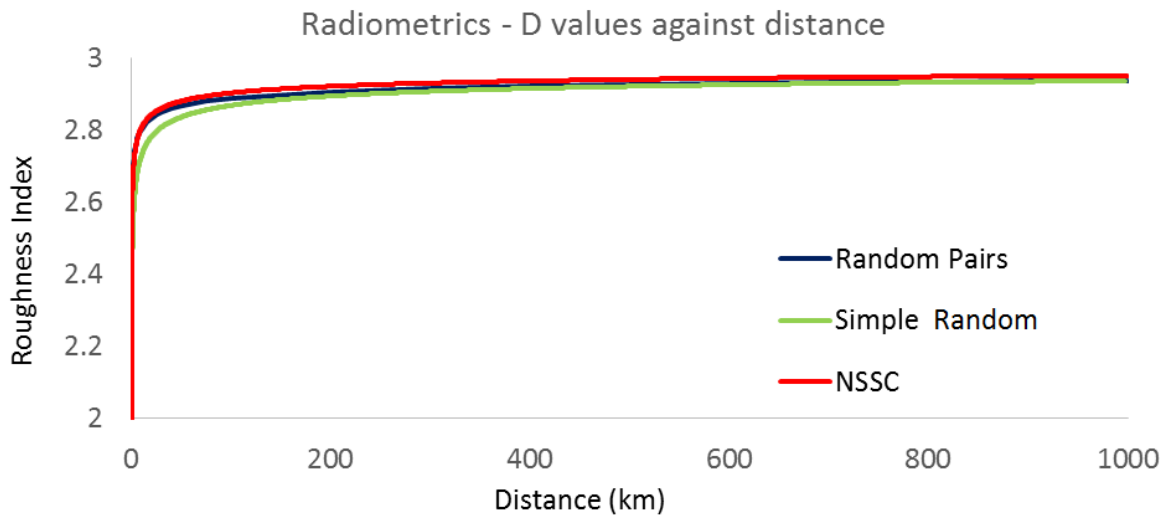


Figure 3.7. Comparison of sampling designs, roughness index value against distance 0-1000km.

Table 3.1. Comparison of roughness index value against extent for different sampling designs

Distance	NSSC	Simple random	Random Pairs
1km	2.61	2.44	2.65
10km	2.80	2.73	2.80
100km	2.90	2.87	2.89
1000km	2.95	2.94	2.94

3.4 Conclusions

- Declustering is a useful tool for handling highly clustered observations, but does not compensate fully for having a good sampling design in the first place.
- Nevertheless, the lack of observations in central Australia do not appear to have significantly affected the overall shape of the variogram.
- Having sufficient observations with a sufficiently fine scale sampling density appears to be a more important determinant of the ‘roughness index’ than either having randomly distributed observations, or having the semivariance calculated independently
- While there is little practical difference between the D values calculated from the NSSC and the ‘random pairs’ design in this case. The ‘random pairs’ design is easier to implement and theoretically better due to its random sampling and greater coverage.

These conclusions inform the work undertaken in the next Chapter.

REFERENCES

- Burrough, P. A. (1983). Multiscale sources of spatial variation in soil. I. The application of fractal concepts to nested levels of soil variation. *Journal of Soil Science*, 34, 577–597.
- Ellis, C. (2007). The sampling properties of Hurst exponent estimates. *Physica A: Statistical Mechanics and Its Applications*, 375(1), 159–173.
- Marchant, B. P., Viscarra Rossel, R. a., & Webster, R. (2013). Fluctuations in method-of-moments variograms caused by clustered sampling and their elimination by declustering and residual maximum likelihood estimation. *European Journal of Soil Science*, 64(August), 401–409.
- Milligan, P., Minty, B., Richardson, M., & Franklin, R. (2009). The Australia- Wide Airborne Geophysical Survey - Accurate Continental Magnetic Coverage. In ASEG Extended Abstracts 2009: 20th Geophysical Conference.
- Minty, B., Franklin, R., Milligan, P., Richardson, M., & Wilford, J. (2009). The Radiometric Map of Australia . *Exploration Geophysics*, 40(February), 325–333.
- Rossel, R. A. V., Taylor, H. J., & McBratney, A. B. (2007). Multivariate calibration of hyperspectral γ -ray energy spectra for proximal soil sensing. *European Journal of Soil Science*, 58(1), 343–353..

Chapter 4

New Data for Old Questions: Is soil more variable than other environmental properties?

Our origins are of the earth. And so there is in us a deeply seated response to the natural universe, which is part of our humanity

Rachel Carson

Abstract

Soil environment interactions are of intrinsic interest to natural scientists. Understanding how variation and variability in environmental properties interacts with the variation and variability in other environmental properties is of intrinsic interest. Further, developing an understanding of this relationship is likely to have practical implications for modelling and mapping purposes. Soil is commonly considered to be more complex at the finest scales than other environmental variables, although this may be in part due to the very fine support that is typically used to measure it.

In this chapter, we use the 'roughness index' to measure the stochasticity (or relative importance of short range and long range variability) over a range of scales. We find that the multi-scale variability of most of the properties we consider can be readily modelled using the roughness index.

At most scales we consider, soil appears to show similar stochasticity to fine scale elevation, and Enhanced Vegetation Index (a proxy for vegetation). Gamma Radiometrics is slightly less stochastic. Rainfall and long range elevation show significantly less stochasticity (more dependence on long range trend).

At the very finest scales soil does appear to show greater fine scale variability. Determining whether this result is an indication of the underlying nature of the soils, or a feature of the data itself required further work.

4.1 Introduction

The condition of the soil resource at any given location and moment is the result of a complex interplay of environmental and management factors. The relative dominance and interactions of these factors varies with location and with the scale of observation (Heuvelink & Webster, 2001a; Lark, 2011). In theory, these are deterministic processes, and many soil-environment interactions are well understood. However, the outcome of these multiple soil forming factors when combined is so unpredictable that the distribution of soil properties in space appears random (Heuvelink & Webster, 2001a; R. Webster, 2000). Our understanding of how different environmental factors affect the soil condition and of how soil condition affects environmental factors is far from complete. A major limitation in our understanding is the difficulty in collecting sufficient data to populate our models. Models of some mechanistic interactions between soil and other environmental properties have been well developed and when they exist can provide a firm basis for soil formation and integrated modelling. Empirical models of relationships between environmental properties can complement mechanistic models. However, data driven investigation into these interactions is usually limited to fine scales and specific environmental conditions. Even the most basic question: Are soils more variable than other environmental properties is not yet comprehensively answered.

In this chapter, we analyse the multiscale variability of a number of different environmental variables using the 'roughness index' approach introduced in Chapter 2. This approach derives from the empirical variogram method (Burrough, 1983) and the Hurst exponent for measuring spatial variability across scales.

In this chapter we:

- Illustrate that the roughness index is a useful measure of multiscale variability for several different environmental properties with data in different formats (Section 4.3.1 and 4.3.2).
- Compare the trends in spatial variability across scales and between environmental properties (Section 4.3.4. - 4.3.7.).
- Evaluate the effect of data on the 'roughness index'.

4.2 Methods

4.2.1 *The roughness Index*

In Chapter 2 we introduced a unitless measure for characterising spatial variability of a data series across scales, which we call the ‘roughness index’. We calculated this roughness index for soil texture using a legacy dataset of point observations.

Conceptually linked to the fractal dimension (Burrough, 1983) and the Hurst exponent, the ‘roughness index’ is calculated by plotting the variogram on a log-log scale, fitting a curve and taking the differential of this curve. The Roughness index is calculated from the slope (or derivative) of the fitted curve. It provides a continuous measure of the change in variability over space and represents the relative importance of short range and long range variability.

The value of the roughness index can fall between 2 and 3. Values approaching 2 imply a strong degree of long range variability. Values closer to 3 occur when short range variability is more dominant. A value of 3 is associated with a lack of spatial trend, or complete randomness. A key advantage of the roughness index is its abstraction from units. This makes it well suited to compare between properties and scales. In this chapter we calculate the roughness index for several different environmental properties. This allows us to describe how spatial variability changes over scale for a number of environmental properties. It also allows us to compare the relationship between soil variability and the variability of environmental properties.

4.2.2. *Applying roughness index to different data structures*

The major distinction we make between our datasets is whether they are point data or coverage data. For the remainder of this chapter, point data means that the data is collected manually at a specific location. The support for the two point datasets we use here is also small (typically less than 1m squared). We use two ‘point data’ sets, the NSSC soil texture dataset described in Chapter 2 (Searle 2014) and a point data rainfall dataset from the Australian Bureau of Meteorology (2017).

In this chapter, we use the term ‘coverage data’ to describe a raster dataset which covers the whole continent. The primary source of information for each of the ‘coverage datasets’ we use is from airborne surveys. These airborne surveys have a wider support (or footprint) than the point data surveys. The exact support or footprint depends largely on the height of the survey (the higher the survey the wider the footprint). For some properties the boundaries of the observation are diffuse which has a smoothing effect on representation of local variability. The strengths and weaknesses of

the different data forms are summarized in Table 4.1 below, and key properties summarized in Table 4.2.

Table 4.1. Advantages and disadvantages of point and coverage data used in this analysis

	Advantages	Disadvantages
Point Data	Potential to capture very short range variability accurately	Lack of observations in central Australia
	Well defined observation boundaries	Ad hoc design
		Noise in data
Coverage Data	Broad representation of properties over Australia	Less potential to measure very short range variability
	Control over sampling design	Observations influenced by surrounding area
	Better representation of long range trends?	Data support depends on the measurement

Table 4.2. Summary of key metadata properties of datasets we used.

Data Name	Description	Modelling	Output resolution
Digital Elevation Model Smooth (DEM-S)	Represents Ground surface topography with vegetation features removed.	Derived from 1 second resolution SRTM data acquired by NASA in February 2000.	3 arc seconds (approximately 90m) ¹⁶
Percentage slope	Slope measures the inclination of the land surface from the horizontal.	Derived from the DEM –S	3 arc seconds (approximately 90m)
elev_focalrange300 m_3s	The elevation range measures the full range of elevations within a 300m circular radius and can be used as a representation of local relief.	derived from the Smoothed Digital Elevation Model	3 arc seconds (approximately 90m)
PM Radiometrics – Potassium	The Radiometric Map of Australia Dataset - Potassium	Combined data from multiple airborne surveys	100m resolution

¹⁶ The 3 second resolution product was generated from the 1 second 300 m elevation range product and masked by the 3" water and ocean mask datasets

Enhanced Vegetation Index (EVI), MODIS TERRA	Modis Terra, 2000 to 2011	The EVI algorithm uses the 500m blue band to correct for residual atmospheric effects	250m, 16 day composite
Clay % (0-5cm)	Individual point observations collected from a variety of observations and collated	Data was cleaned and splined (Chapter 2 for details)	Point observations
Sand % (0-5cm)	Individual point observations collected from a variety of observations and collated	Data was cleaned and splined (Chapter 2 for details)	Point observations
Rainfall	Individual point observations collected by the Bureau of Meteorology	Data which was too incomplete was discarded	Point observations

4.2.3. Point Data

We describe here two point datasets. Soil texture and rainfall data.

Table 4.3. Percentage Clay fraction: Summary statistics

Soil Depth	Number of observations	Mean	Median	Standard deviation	Skewness	Kurtosis
Sand (%)	13830	21.52	15.87	17.44	1.10	3.38
Clay (%)	13258	63.17	66.83	22.74	-0.46	2.25
Rainfall (daily average in ml 2004-2013)	3512	1.82	1.61	1.18	2.89	16.21
Rainfall (daily average in ml, 1999)	4802	2.16	1.83	1.56	3.54	22.99
Rainfall (daily average in ml, 2004)	5547	1.90	1.69	1.30	3.14	19.90
Rainfall (daily average in ml, 2009)	5476	1.92	1.52	1.45	2.74	12.56
Rainfall (daily average in ml, 2014)	5037	1.79	1.57	1.18	3.27	20.18

4.2.3.1. Soil Texture Point Data : National Soil Site Collation Database

The soil texture data used in this analysis was compiled to support the Australian contribution to the GlobalSoilMap (Grundy et al., 2015). A collaboration of state and national government agencies and some universities worked together to produce the National Soil Site Collation or NSSC (Searle, 2014).

The NSSC is a composite of data from a variety of sources. Consequently, it does not have a unified sampling design, and the NSSC dataset reflects the research priorities of the different data collecting institutions at different times. The dataset is heavily focused in agricultural regions and includes areas of high density sampling and sparse sampling (Figure 4.1). The complete database contains information on several soil properties including percentage clay and percentage sand fraction from almost 16,000 soil profiles. Percentage sand and clay fractions for topsoil (0-5cm) are used in this study.

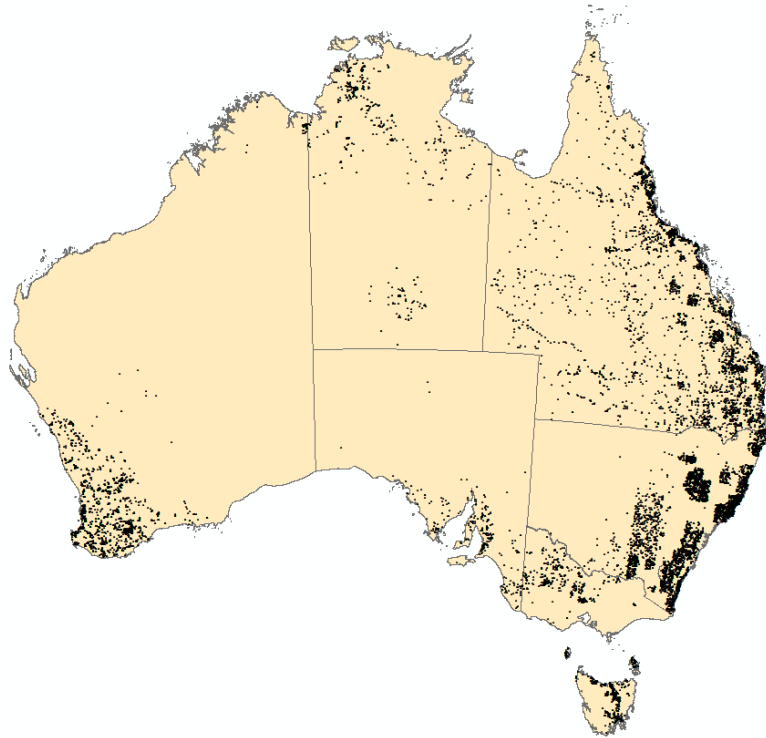


Figure 4.1. The distribution of the NSSC dataset. Each black dot represents an individual soil observation.

We employ the spatial declustering method of (Marchant et al., 2013), described in more detail in Chapter 2 to remove the lumpiness in the variogram. In very brief terms, the declustering process assigns additional weight to observations that are more spatially isolated, and reduces the weight of observations in densely sampled areas. This technique was also used for the rainfall data (Section 4.2.3.2).

4.2.3.2 Rainfall Point Data : Australian Bureau of Meteorology

We obtained point data collected from rainfall observation stations controlled by the Australian Bureau of Meteorology. The spatial distribution of these data is based on convenience legacy (more samples are taken close to populated areas).

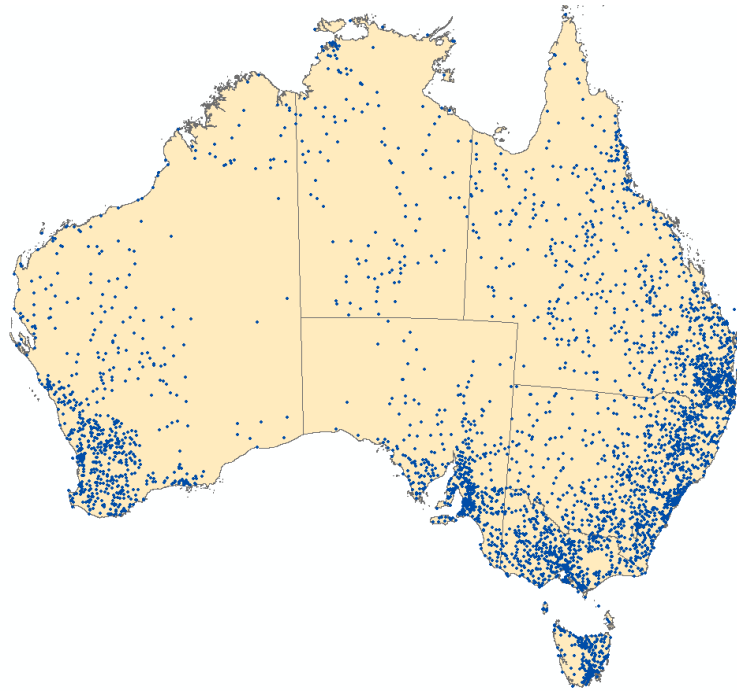


Figure 4.2. Distribution of the Bureau of Meteorology rainfall observations 2001-2010 (10 year average)

The best method for dealing with this (or the best choices to make to accurately represent the variability in rainfall over space) are still somewhat open to debate. The shorter the temporal support (i.e. the shorter the time window) the more stochasticity remains in the data. For example, fine scale temporal rainfall data (i.e. daily or weekly) tends to be highly stochastic, and may not accurately represent the spatial trends in rainfall. The temporal distribution of rainfall, as well as the annual average, can of course be important, but for the purposes of this chapter at least we are going to limit the analysis to broader temporal scales (annual and decadal).

We chose to discard locations where there were less than 300 daily observations for the year. Summary statistics for the NSSC soil data, a selected decadal average, and several annual averages for rainfall are shown in Table 4.3.

4.2.4. Calculating an experimental variogram from coverage data

As we mention in Section 4.2.1 and 4.2.2, the use of 'coverage data' provides us with the opportunity to subsample data to calculate the roughness index. We also sample from the raster dataset to reduce the computational load of calculating variograms.

The empirical variograms we calculate from the point data sources re use observations (as is typical of the classical empirical variogram). This is a departure from the preferred methods for calculating the Hurst exponent (from which the roughness index is derived). Typically studies that calculate the Hurst exponent use a sampling design that ensures that each pair of observations are used exclusively in a single bin.

Using coverage data allows us to control the sampling design in a way that we cannot when we are using legacy data. In the previous chapter we discuss some of the potential impacts of legacy data

By selecting unique pairs at pre-specified separation distances or lags, we can avoid potential issues with autocorrelation.

We use the 'random pairs' sampling design described in Chapter 3. This design ensures both that unique pairs are used for the calculation of pairs (avoiding the problem with autocorrelation¹⁷), and that the underlying distribution of points are random (avoiding potential problems with grid based sampling). This design also allows us to dictate the lags.

4.2.4.2. Coverage datasets – summary of key parameters

We selected coverage datasets that described properties of interest and that were suitable for our modelling. The calculation of the semivariogram (upon which our roughness index is based) requires that the data is numeric and ordinal, so we did not include categorical variables. We also required datasets with a reasonably fine support or resolution. For example, we chose not to use climate data available from the Australian Bureau of Meteorology comes at a 5km resolution which makes modelling below this resolution meaningless.

We present a brief summary of key properties of each of the coverage datasets that we use in Table 4.2 above, and more detail about each dataset in Sections 4.2.3.3. to 4.2.3.8.

¹⁷ There is still a minor issue with auto-correlation because pixels are not excluded after they have been sampled, so a small proportion of pixels will be resampled.

4.2.4.3. Digital Elevation Model – smoothed

A number of terrain models that model different features of terrain at high resolution have been developed by the Commonwealth Scientific and Industrial Research Organisation of Australia (CSIRO). All of these models ultimately derive from the Shuttle Radar Topography Mission (SRTM) satellite data collected by NASA during its 2000 space shuttle mission (Farr et al., 2007). We briefly describe the meaning of each layer and the basic processing/ modelling used below.

The digital elevation model represents ground surface topography. It has been filtered from vegetation features and is smoothed to reduce noise to better represent the surface shape (Geoscience Australia, accessed 2018). The smoothing processes mean that the DEM-Smooth supports calculation of local terrain shape attributes such as slope, aspect and curvature that cannot be reliably derived from the unsmoothed 1 second DEM because of artefacts (Gallant, 2011).

4.2.4.4. Percentage slope

Calculated from the smoothed digital elevation model, percentage slope measures the deviation from horizontal or flat of the land surface. Percentage slope provides information about likely run off and erosion potential.

4.2.4.5. Elevation focal range – 300m

Derived from the DEM – Smoothed data, the elevation range measures the full range of elevations within a circular window in this case 300m. This data can be used as a representation of local relief (CSIRO 2018).

4.2.4.6. Radiometric data

We use percentage of Potassium from the Radiometric map of Australia (Minty et al., 2009) as a proxy for soil mineralogy. Airborne Radiometric surveys have diffuse boundaries. The strongest signal comes from the area directly below the observation, but lateral observations continue to affect the signal. As lateral distance increases, the contribution to the signal decreases (Minty, 1997). This gradual reduction in signal influence with distance has a smoothing effect on local variability.

The map provides levelled and merged composite grids of radiometric regions of interests (ROIs) pertaining the potassium, thorium, uranium and total count over Australia at a 100m resolution. The

raw data for the map comes from systematic airborne radiometric surveys undertaken over the last 40 years. The resolution of the airborne surveys is shown below (Figure 4.3 taken from Minty et al., 2009). The Radiometric data was aligned to a common datum, and older surveys were back calibrated using new field observations. Details of the alignment and calibration are available in Minty et al., (2009).

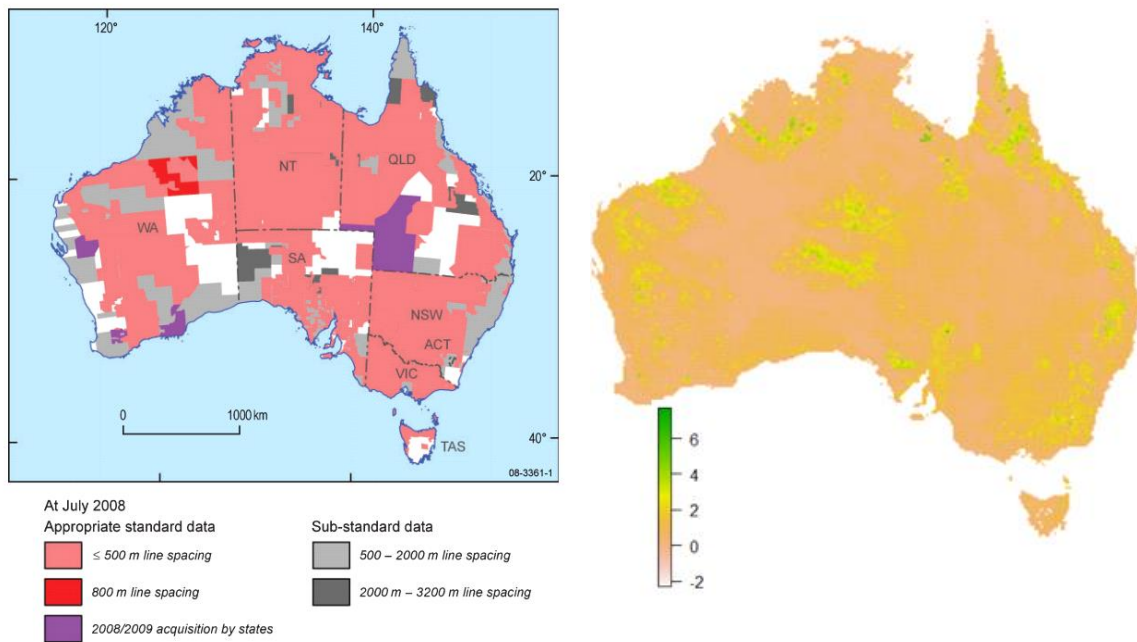


Figure 4.3. Left Panel: Radiometric sampling density (Minty et al. 2009) Right Panel: Potassium layer from the radiometric map of Australia (original source Geoscience Australia).

While the soil samples are observed to a given depth, sometimes >2 m, the radiometric data tends to observe only the top of the soil profile, typically the top 35cm (Minty, 1997). The footprint (which can be thought of loosely as the support) of an airborne radiometric survey will typically be around 50-100 meters, with diffuse boundaries due to the low linear attenuation co-efficient of air¹⁸.

¹⁸ The linear attenuation co-efficient describes how many atoms there are in a cubic cm volume of material. The lower the linear attenuation co-efficient, the wider the spatial range of materials that will affect the

4.2.4.5. Enhanced Vegetation Index

Enhanced Vegetation Index appears to be better than NDVI (the traditional vegetation indices) at discriminating in areas of high vegetation density (Didan, et al., 2015). EVI is calculated using visible and near visible spectrum (Didan et al., 2015):

$$EVI = G \frac{NIR - Red}{NIR + C1Red - C2Blue + L}$$

NIR, *Red*, and *Blue* are surface reflectance (full or partially atmospheric-corrected for Rayleigh scattering and ozone absorption). *L*, *C1*, *C2* and *G* are all coefficients. *L* is the canopy background adjustment for correcting the nonlinear, differential NIR and red radiant transfer through a canopy. *C1* and *C2* are the coefficients of the aerosol resistance term (which uses the blue band to correct for aerosol influences in the red band). *G* is a gain or scaling factor. The coefficients adopted for the MODIS EVI algorithm are, *L*=1, *C1*=6, *C2*=7.5, and *G*=2.5 (Didan et al., 2015).

The MODIS EVI that we use has a 16 day temporal resolution and a 250m spatial resolution. The best pixels from the 16 day temporal window are used. In some cases (e.g. where cloud cover is high), there will not be any quality information recorded in a given 16 day window (observations are taken daily) and the pixel values will be based on modelled data.

4.3. Results and Discussion

4.3.1. Curve Fit

Use of the log-log composite declustered variogram for estimating variability across scales depends on finding a model that closely fits the variogram when it's plotted on a log-log scale. The *D* values at any given extent are directly derived from the function fit to the log-log variogram. A poorly fitting model, would not provide useful information about the change in stochasticity. As is illustrated in Figures 4.4 through 4.11 the increasing exponential decay model ($y = C(1 - e^{-kt})$, $k > 0$) appears to fit very well. The weakest part of the fit is the small distances where the curvature in the data is stronger than the curvature in the function for a few properties (relief, clay and sand)

When applied to the point rainfall data sources (Figure 4.11), the function is very close to a linear function. We will discuss the implication of this for describing rainfall variability in sections 4.3.3 and

4.3.6. The increasing exponential decay function is quite flexible so that a number of spatial structures can be modelled with a single function. This strengthens the evidence that the trends illustrated in Figures 4.12 and 4.13 provide an accurate representation of the underlying trends.

All of the environmental properties we modelled (with the exception of rainfall) had a curvilinear trend (Figure 4.4 to Figure 4.11). The sole exception to this (from amongst the data we have modelled) is rainfall, which had a function very close to linear. This was the case for the 10 year average presented in Figure 4.11, as well as for each annual average that we calculated (Figure 4.14). There are limited observations available with short separation distances, so the experimental variogram illustrates a high degree of stochasticity at finer scales (Figure 4.11). This makes it difficult to confidently assign any particular values to the curve, and the linear trends shown in the rainfall data might be due to a lack of fine scale observations, rather than a true representation of the rainfall. There are several parameter combinations that return very similar Residual Sum of Squares values, and which appear to fit very similarly. While visually similar on the log-log scale, the different parameter combinations do affect the roughness index particularly at short scales.

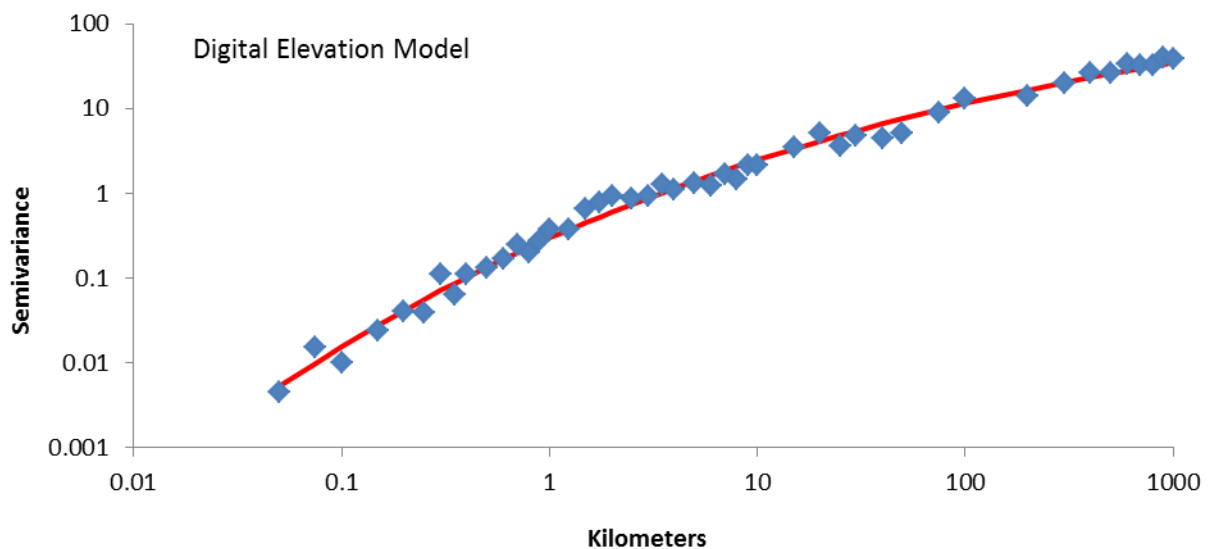


Figure 4.4. Log-log empirical semivariogram (DEM), with increasing exponential decay model fitted

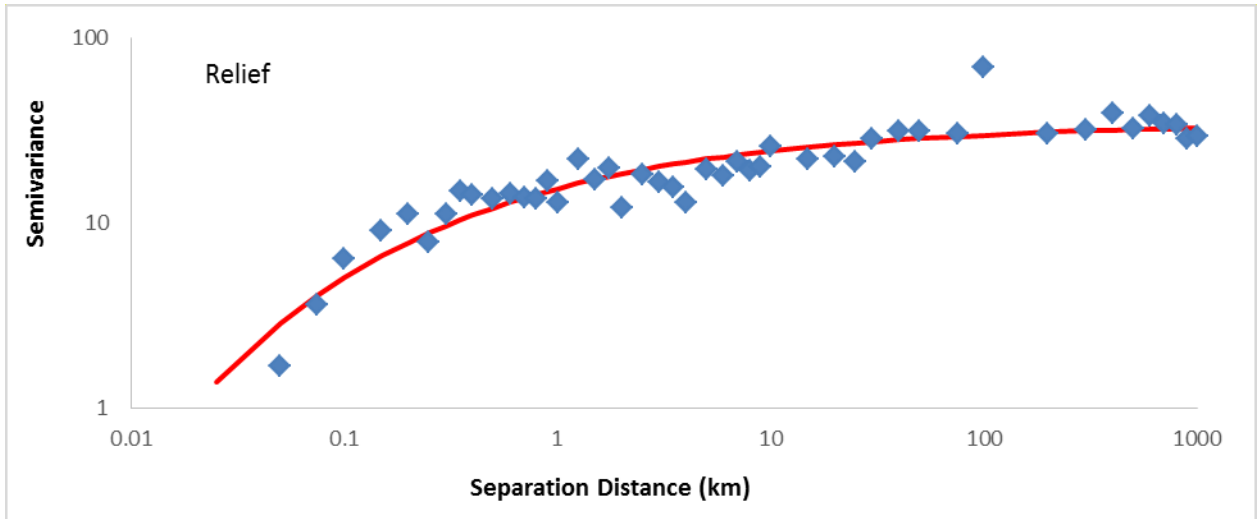


Figure 4.5. Log-log empirical semivariogram (relief), with increasing exponential decay model fitted

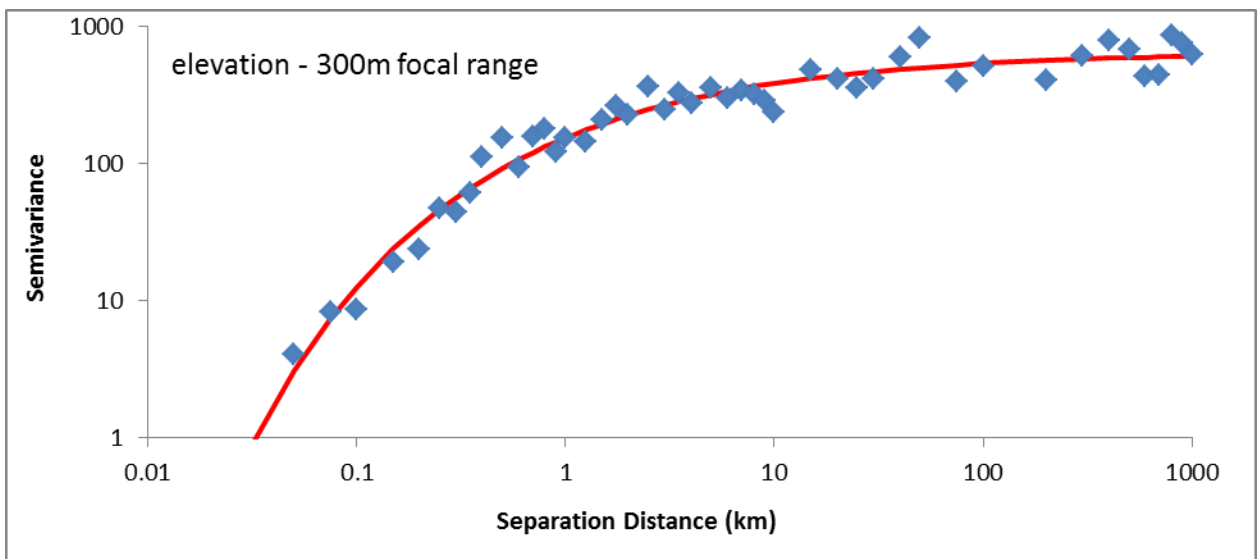


Figure 4.6. Log-log empirical semivariogram (elevation – 300m focal range), with increasing exponential decay model fitted

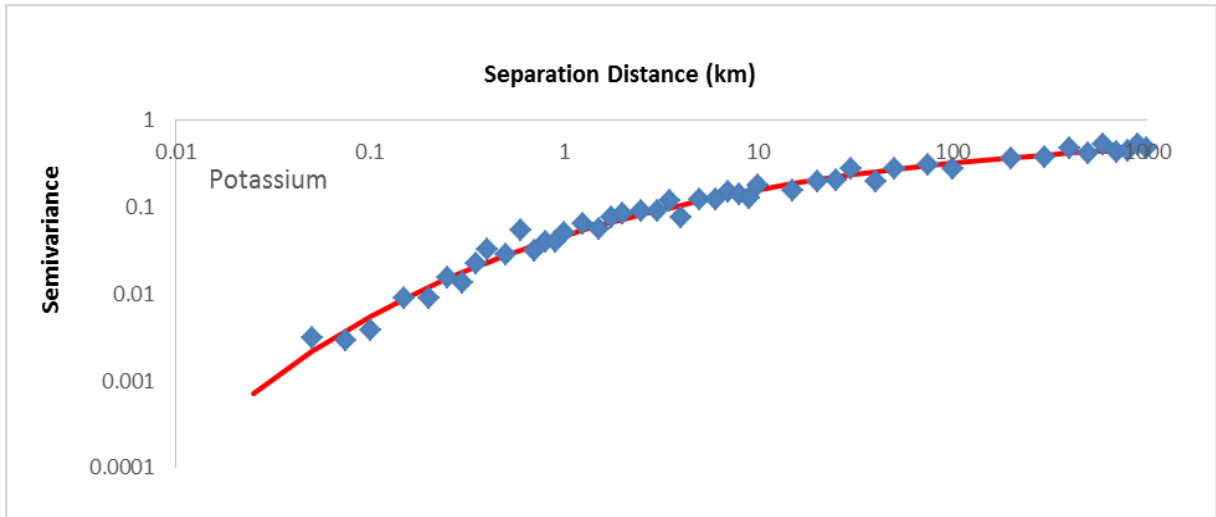


Figure 4.7. Log-log empirical semivariogram (Radiometrics), with increasing exponential decay model fitted

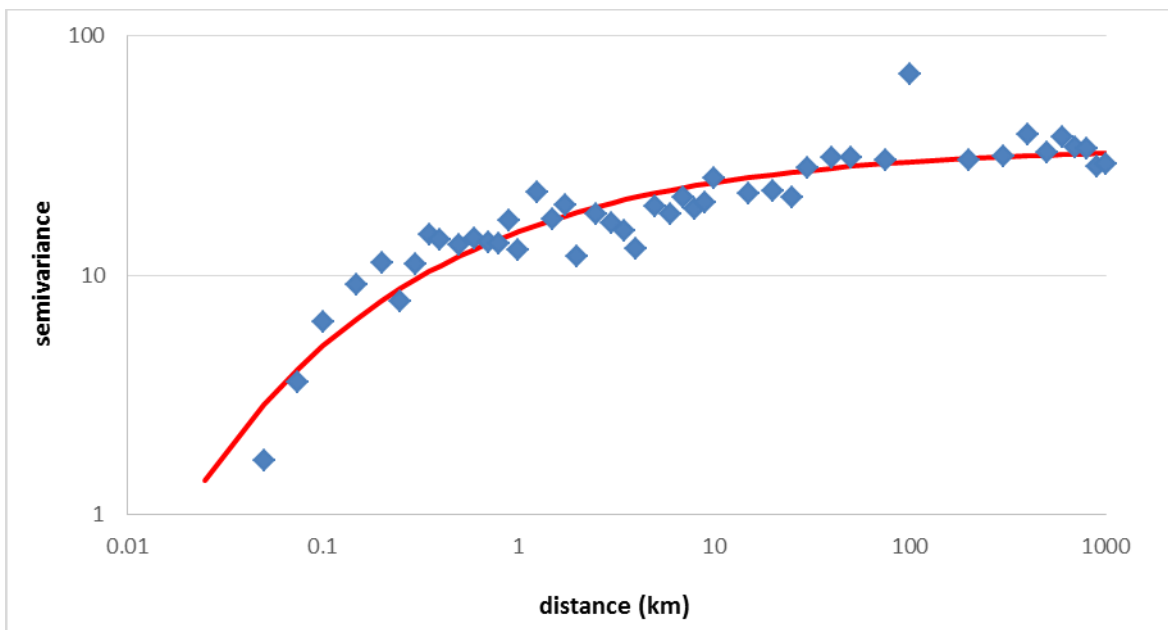


Figure 4.8. Log-log empirical semivariogram, (EVI) with increasing exponential decay model fitted

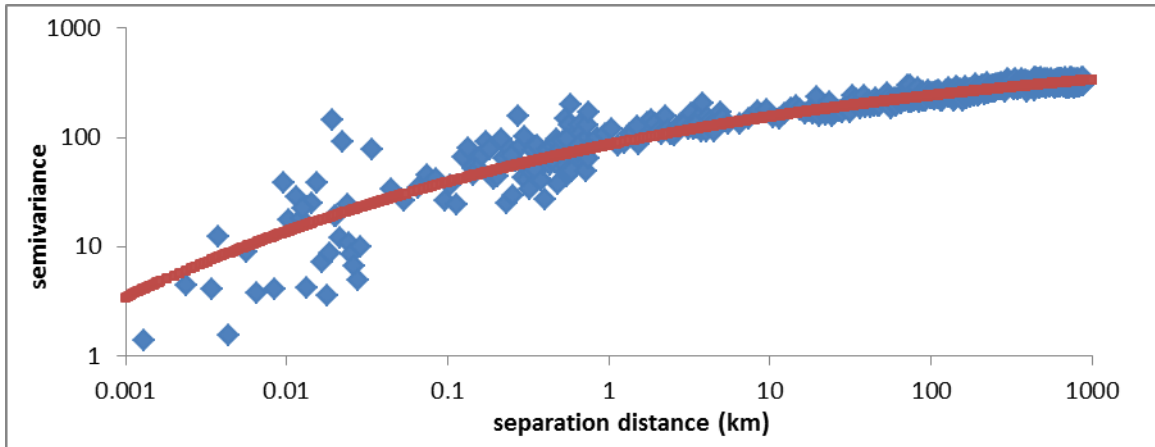


Figure 4.9. Log-log empirical semivariogram (Clay topsoil), with increasing exponential decay model fitted

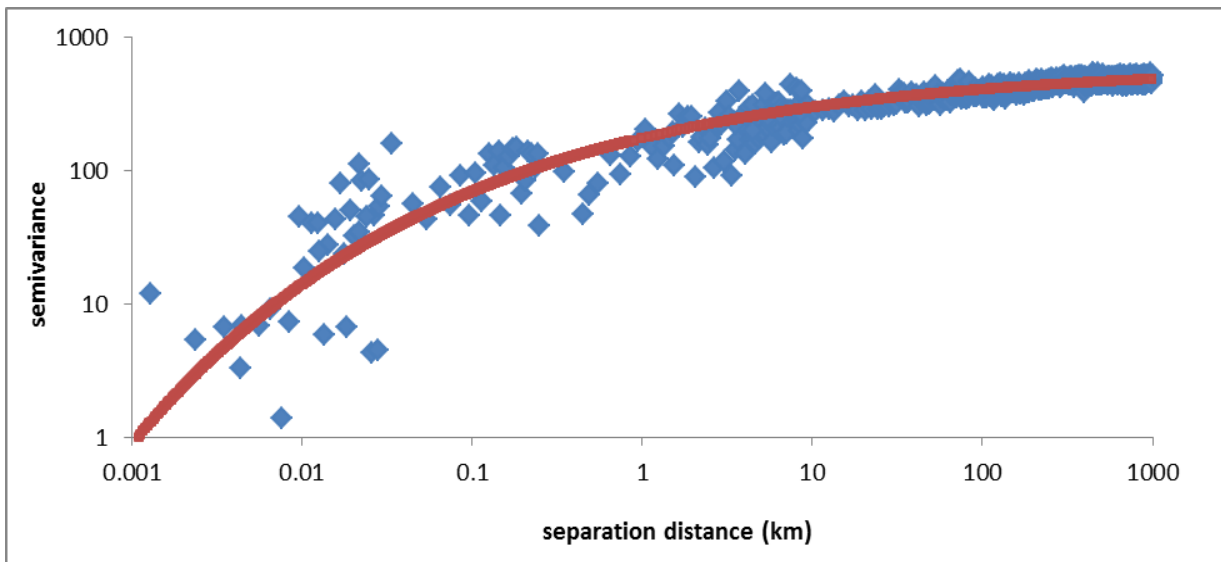


Figure 4.10. Log-log empirical semivariogram (Sand topsoil), with increasing exponential decay model fitted

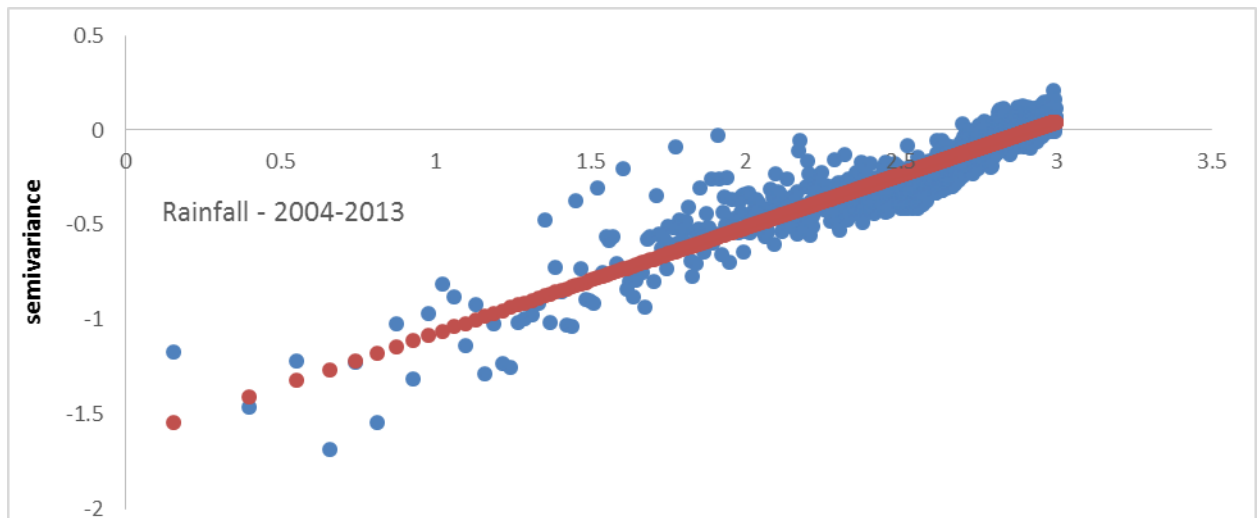


Figure 4.11. Log-log empirical semivariogram (Rainfall), with increasing exponential decay model fitted

4.3.2. Overview of results.

When considering figures 4.12, 4.13 and 4.15 it is useful to recall that the roughness index expresses the relative importance of short range and long range variability. As spatial extent changes, the meaning of ‘short range’ and ‘long range’ also changes.

The majority of environmental properties that we consider show a decreasing value for the roughness index as the resolution increases (i.e. the scale becomes finer). This implies that fine scale spatial trends exist and can only be detected as finer scales of observation become possible. At finer resolutions the spatial structure that is unobservable at coarser resolutions becomes short-range spatial structure, and the short-range structure becomes long-range structure. As a result, stochasticity reduces.

This overall trend is the same for most environmental properties, but the rate of change and the specific values of the roughness index vary between properties. The relative difference in these trends has implications for our understanding of the scales at which the most significant components of variability occur.

In the case of rainfall, the roughness index remains constant across all scales. This implies that the relative importance of short range and long range variability remains constant. It does not imply that the spatial pattern is the same, but that the degree of roughness is the same

None of the properties that we have modelled show an increase in D value as the resolution increases (finer scales).

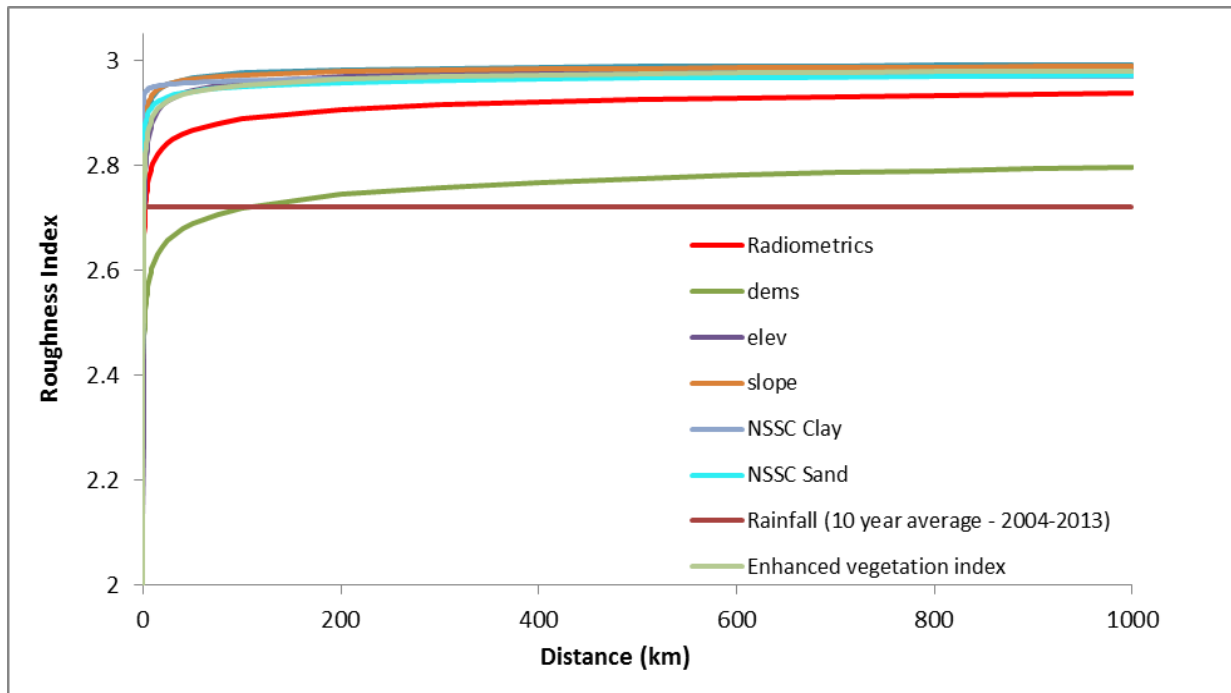


Figure 4.12. Roughness index: 0-1000km for multiple environmental properties

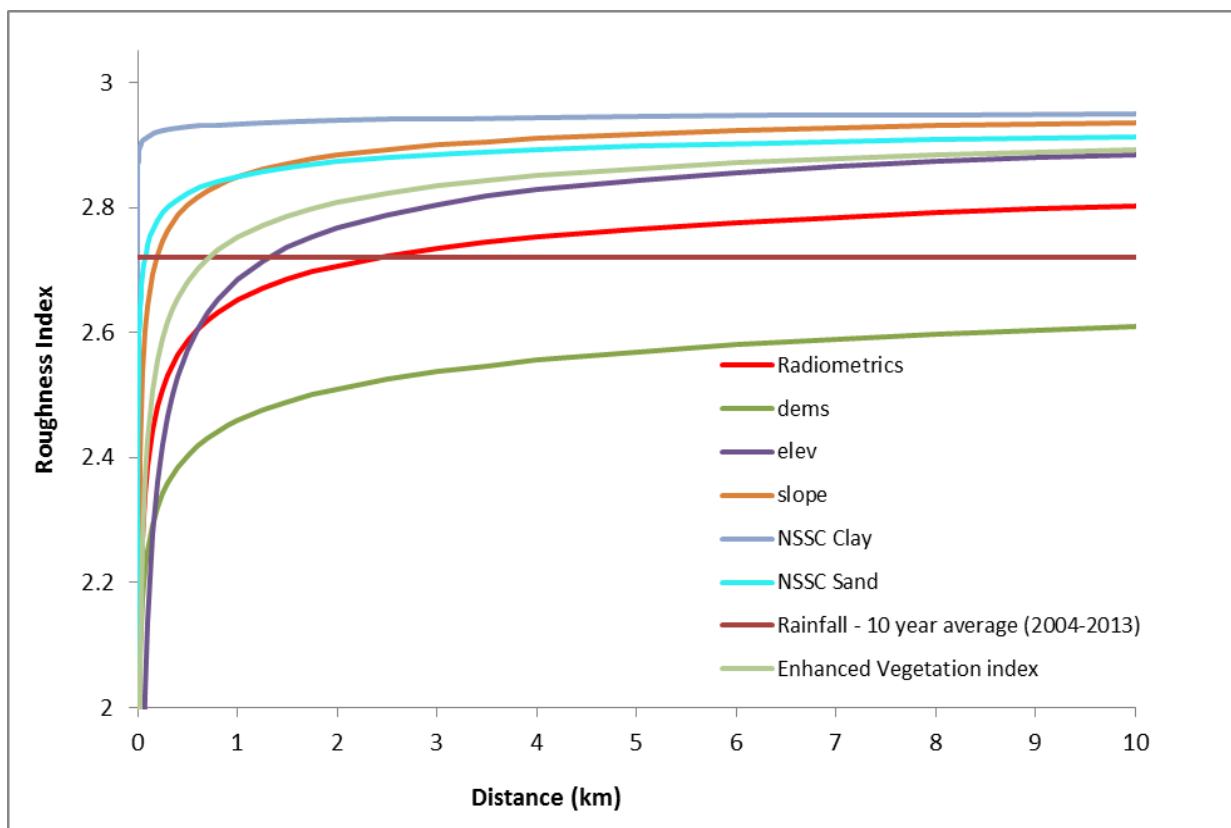


Figure 4.13. Roughness index: 0-10km across scales for multiple environmental properties

The roughness index increases with separation distance, in most cases fairly rapidly, before reaching a plateau or near plateau. As our scale of observation becomes finer (separation distance decreases), variation that appears stochastic at a coarser scale is revealed as a spatial trend. In a standard geostatistical analysis this trend would probably be modelled as a nugget effect, rather than as spatial trend. The differences between modelling as nugget or as short-range spatial correlation can be important particularly when block-support prediction is considered. With the exception of rainfall, each environmental property we model shows the same gradual change in D value or stochasticity. This is a departure from other analyses which tends to operate under a monofractal or multifractal framework.

Rainfall exhibits a different trend to the other properties. The roughness index for rainfall remains constant regardless of the scale change. This implies that the spatial variability of rainfall follows a mono-fractal trend: The variability in rainfall remains consistent regardless of the scale of observation. Taken together with the lower overall value for the roughness index, this suggest that rainfall has less short range variability than the other environmental properties, or that the variation in rainfall overall is more driven by long range trends.

Sand, Clay and Percentage slope all have very high roughness indices even at very fine scales. At a separation distance of 1km, the roughness index for each of these variables is greater than 2.8. At 100m separation distance, each of these properties has a roughness index value greater than 2.7. This suggests that there is still likely unresolved information at finer scales than this. Radiometrics exhibits a much more gradual change in roughness index value. At a 1km separation distance this roughness index is only 2.6 (a value, not significantly different from a random walk) suggesting moderate amounts of stochasticity. The roughness indices for Elevation Change (within a 300m radius) and Enhanced Vegetation Index increase more gradually than sand, clay and percentage slope, but less gradually than radiometrics. This suggests that more of the spatial variation is resolved at finer scales, or that variability at these scales appears less stochastic and more spatially driven.

Soil texture (as per the NSSC database), roughness, slope, elevation and gamma radiometric potassium all plateau to a similar roughness index (greater than 2.90). Beyond around 5km, only radiometrics is distinguishable within this group. A very high roughness index (i.e. greater than 2.9) suggests that short range variability is a much more important driver than long range variability. All of these properties can be considered highly stochastic.

The roughness index for elevation plateaus at a similar level to rainfall. This is much lower than the other environmental properties we consider, and indicates greater importance of long range trends in the variability of these two properties. .

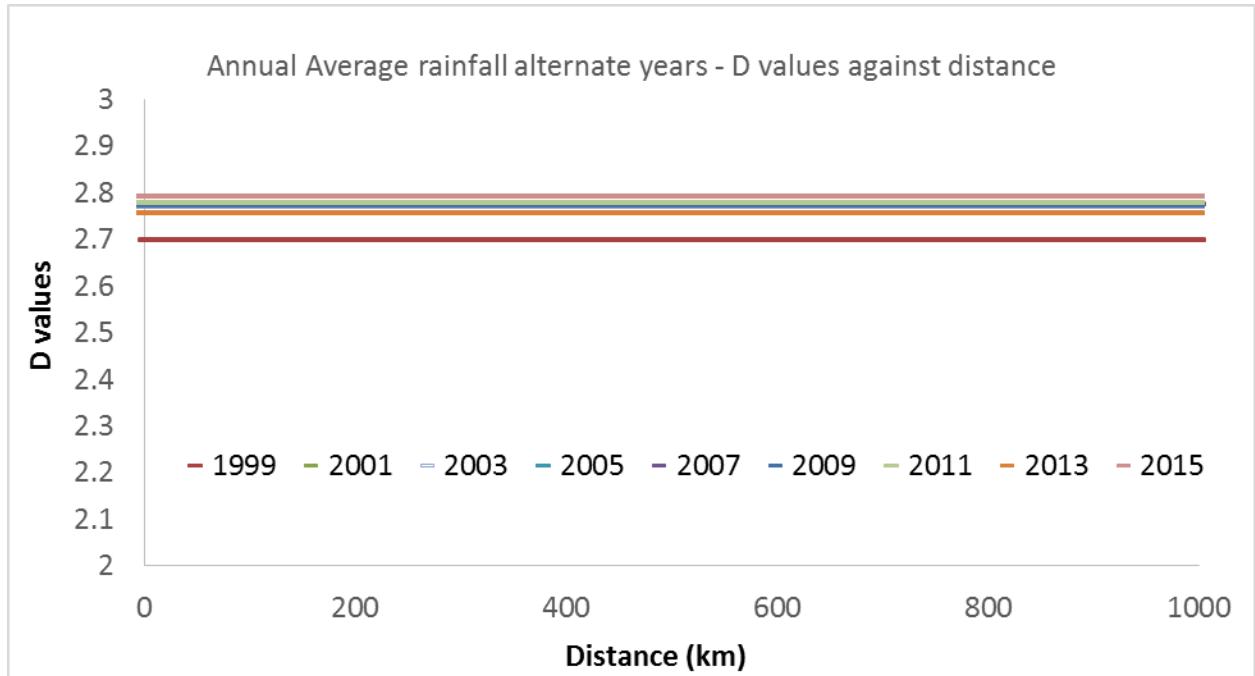


Figure 4.14. Roughness index across scales: average annual rainfall, selected years.

Table 4.3. Roughness Index Values: selected distances

	100m	1km	5km	10km	100km	1000km
Digital Elevation Model Smooth (DEM-S)	2.25	2.46	2.57	2.61	2.72	2.80
Percentage slope	2.64	2.85	2.92	2.94	2.97	2.99
elev_focalrange300m_3s	2.14	2.68	2.84	2.88	2.96	2.98
PM Radiometrics – Potassium	2.39	2.65	2.77	2.80	2.89	2.94
Enhanced Vegetation Index (EVI)	2.38	2.73	2.85	2.88	2.95	2.98
Sand	2.74	2.85	2.90	2.91	2.95	2.97
Clay	2.91	2.93	2.94	2.95	2.96	2.97
Rainfall (2004-2013 average)	2.72	2.72	2.72	2.72	2.72	2.72
Rainfall (1999)	2.71	2.71	2.71	2.70	2.70	2.69
Rainfall (2004)	2.78	2.78	2.78	2.78	2.78	2.78
Rainfall (2009)	2.77	2.77	2.77	2.77	2.77	2.77
Rainfall (2014)	2.77	2.77	2.77	2.77	2.77	2.77

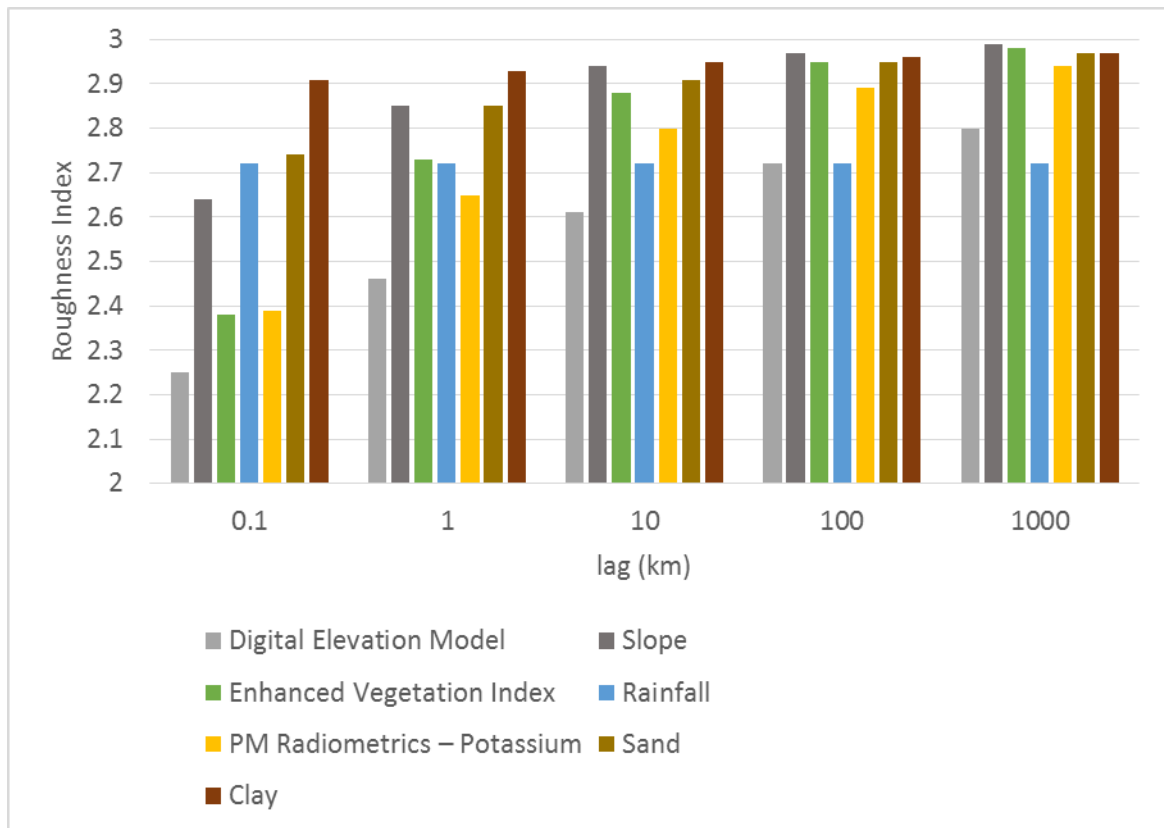


Figure 4.15. Roughness index across scales

4.3.3. Topographic variables

There are strong similarities in the roughness index that we calculate for local topographic variables and soil texture. Percentage slope measures the slope change over the calculated support (one ARC second approximately 30m). Focal elevation measures the elevation change over the adjacent 300m. The roughness index for both of these properties follows a very similar pattern to soil. A rapid increase over the first 10km and then a plateau to very high levels (over 2.95) in the first 100km.

Elevation (which measures height above sea level) has a much lower roughness index at all scales, and the rates of change in the roughness index are much lower.

Slope and 300m focal elevation change are calculated directly from the DEM. This means that any smoothing and modelling applied to calculate the DEM will also affect the slope and the 300m focal elevation change data. Any differences in roughness index for these properties come from how the elevation changes are measured. The percentage slope change is calculated for a 30m support and measures the exact change in slope over this 30m area. The grain size for the 300m focus elevation change is also 30m, but measures elevation change on the surrounding 300m. The DEM layer is measured on a 3 arc second (approximately 90m support). More importantly, this metric (meters

above sea level) captures the variation across the whole continent, while percentage slope change and focus elevation capture local variability. The DEM layer is much more heavily influenced by the change in elevation occurring with a mountain range, than by the smaller scale variations that might occur within the same mountain range. This is consistent with other studies that consider topographic variables. Green & Erskine, (2004) calculate the fractal dimension at fine scales (10-500m) for three fields and find the D value for elevation varies between 1.28 and 1.47 over three fields, and between 1.71 and 1.86 for slope over the same three fields (for each of these fields, the fractal dimension remains constant over the ranges considered). These results are consistent with our results in Table 4.3 (the relevant columns are 100m and 1km).

The roughness index for Percentage slope change, (percentage slope) is very similar to the roughness index for soil texture across all scales. This suggests that fine scale topographic variation is a more important determinant of soil variability than the large scale variation.

4.3.4 Radiometrics

As discussed in Chapter 3, radiometrics data is often used as a proxy for soil texture. The signals associated with radiometric data can be linked to clay particles, and so can be used as a proxy for the soil texture. The roughness index for the radiometric data shows a similar trend to the soil texture data, but is notably lower across all scales than the soil texture data (Figure 4.12, 4.13 and 4.15). The roughness index calculated from Radiometrics data is also notably lower than the elevation or EVI data. Gamma Radiometrics are often used as a proxy for soil parent material (Dickson & Scott, 1997) and soil texture so it is interesting that there are several other environmental properties that seem to have more similar levels of variability to soil texture.

One likely explanation for this difference in variability is the manner in which the radiometrics signal is detected. The grid size for the Radiometrics signal is 3 arc seconds ~ 90m. The observational support or 'footprint' for the Radiometrics signal is about 100m¹⁹. However, as explained in the methods, the Radiometrics observations do not have discrete boundaries. The Radiometrics signal incorporates information from the periphery of the observation at a rate that decreases with distance. A large support with discrete boundaries will already have some smoothing effect on a variogram, and reduce the appearance of short term stochasticity. The incorporation of a signal from adjacent areas will

¹⁹ In some areas the support will be much wider, due to wider flight line spacing (See Figure 4.1).

further enhance this effect. Proximal sensor with smaller footprints might be useful for more detailed mapping as suggested by Stockmann et al., (2015).

4.3.5 Rainfall

The lower stochasticity of the rainfall is also interesting to note. The rainfall data does not exhibit the same distinctive rapid increase in over the first several km. In fact, it is effectively flat across all scales. A completely constant roughness index is consistent with a monofractal (i.e. the variability is the same across all scales). However, given the limited availability of rainfall data at finer scales (which is where most of the curvature typically occurs) this results are not definitive. We can be more confident about the value of the roughness index at the greater extents.

We collated the rainfall data into annual averages for years from 1999 to 2015. Empirical variograms were calculated for each of these years (note these are not shown) and the exponential decay curve was fit to the log-log variogram of each year. Visual inspection of this variogram data suggests a strong positive correlation between distance and variability, but does not suggest a strong curvilinear relationship. The exponential decay functions which are fit to the curves emphasises this as they are close to linear. A linear fit to the log-log empirical variogram means a constant value of alpha which in turn implies a constant D value. With the exception of 1999 and 2000, all years have a D value between 2.75 and 2.8 across all scales (Figure 4.14). Even the slightly lower D values for 1999 and 2000 are still quite similar, with both close to 2.7. The ten year average has a similar value (2.72) despite the larger temporal scale²⁰. Mandelbrot & Wallis (1969) note the comparatively very low D values for annual precipitation, between 1.1 and 1.3²¹. However, these D values are calculated from Hurst Exponent calculated for time series rather than spatial data.

4.3.6 Enhanced Vegetation Index

The Enhanced Vegetation Index (EVI) stems from the visible and near visible spectrum. It measures changes in the growth status and type of vegetation. The high stochasticity of the EVI from medium scales is somewhat surprising. Intuitively we would have expected more wide scale emphasis as vegetation types change significantly over the continent. The very high stochasticity at fine scales might suggest that on average, the soil type, and slope have a significant control over vegetation status and type. It may also reflect the impact of human environment interactions where agricultural

²⁰ In general a larger support (temporal or spatial) reduces stochasticity.

²¹ For one dimension D value vary between 1 and 2 rather than 2 and 3.

developments, buildings, manmade parks, paths or other structures create sharp boundaries between vegetation types, or between vegetation and other surface structures.

Of all the datasets that we consider, the enhanced vegetation index has the coarsest grid size or support (250m). This will necessarily ensure that fine scale modelling shows less variability, as the chances of taking a subsample from within the same grid cell will be very high for fine separation distances.

4.4. Implications and Conclusions

4.4.1. Implications

Like the D value and the Hurst exponent, the roughness index has the advantage of abstracting from the scale of the units of measure. It is the relative rate of change, not the absolute magnitude that determines the roughness index. All three measures (Hurst, D value and roughness index) share this advantage when comparing between properties with different units.

The usefulness of the roughness index as distinct from either the Hurst exponent or the Fractal Dimension, lies in its ability to model change in stochasticity or 'roughness' on a continuous or gradual scale. This is a significant conceptual distinction from the traditional understanding of the fractal dimension as a mono-fractal, or multi-fractal. The results presented in Section 4.3.1. seem to indicate that this framework is useful for considering other environmental properties. In Sections 4.3.4 to 3.6 above we discuss the roughness indices for different environmental properties and speculate about possible causes and implications for the distinctions between them.

We calculate the roughness index to draw inferences about the change in variability across scales for different environmental variables. However, the discussion above highlights the fact that the roughness index that we calculate is affected by the form and structure of the data, not just the underlying distribution of the environmental properties. It is not possible to divorce the interpretation of the results from the form of the data that we have available.

The availability of high resolution data for different environmental properties has allowed us to investigate the spatial variability of different environmental variables across scales in an easily comparable way however the form of the data limits the comparisons we can make.

- Neither the soil nor the rainfall datasets have a statistically-based sampling design, which may lead to additional bias.

- There are limited closely spaced observations for rainfall, limiting our ability to model changes in variability across fine scales.
- Radiometrics data has very diffuse boundaries limiting capacity to model fine scale variability.

Despite these limitations, some noteworthy trends have emerged from this analysis.

Burrough (1983) found that soil exhibits more short range stochasticity than other environmental variables, such as annual rainfall and landform variables. Our results indicate a very high level of stochasticity for soil properties, but we find that this level of stochasticity is similar to some topographic variables.

We have compared the variability of environmental properties across multiple scales. We have observed that the majority of environmental properties we have modelled follow a similar overarching trend: Rapid increases in variability across fine scales, followed by a gradual plateau. The consistency of this pattern across several different properties highlights the importance of dealing with fine scale stochasticity when producing maps or models at coarser scales.

Despite the consistency in the general pattern of variability as the scale changes, there are marked differences in the roughness index between environmental properties. The roughness index changes at different rates for the different properties, and the plateau occurs at a different scale for different properties. These distinctions reveal where the most important changes in stochasticity occur, and provide a useful indication of the scale at which spatial variability can be modelled as a spatial trend rather than as noise.

There is a very close trend between slope, local relief and soil texture. While soil forming and controlling processes can be expected to operate differently in different landscapes (McKenzie & Ryan, 1999), the extremely close relationship might be indicative of a close relationship between these properties. The possibility is worth investigating further.

The roughness index of rainfall is distinct from the other environmental properties, as it does not change with scale. This may imply a monofractal relationship (i.e. one where the expected stochasticity or variability of the property is scale invariant). The constant value estimated for the roughness index may also result from the lack of observations at the scales where the greatest changes in variability appear to occur. We have not fully considered the question of how temporal variability and spatial variability interact. Rainfall, unlike the other environmental properties we have considered is a temporally dynamic property, and this may also be affecting our results.

4.4.2. Conclusions

- Most environmental properties reach high scales of stochasticity at short extents (around 10km). Variability remains fairly consistent at greater scales.
- Figure 4.14 shows that local topographic indicators (slope and local relief) and soil texture show similar characteristics in their spatial scaling behaviour. The roughness indices for these properties vary almost identically as the scale changes.
- Elevation and rainfall show significantly lower stochasticity than the other environmental properties modelled.
- At extents greater than around 100km, local elevation and vegetation indices show very similar stochasticity to soil. Radiometrics is only slightly less stochastic. Rainfall and elevation above sea level have noticeably lower levels of variability.
- At finer scales, soil is more variable than all properties except for slope which has a similar degree of variability. The higher apparent stochasticity at fine scales might be due to smaller support for soil measurements.

The comparison of how spatial variability changes across scale for different properties are of intrinsic interest. It provides another system of considering natural systems and how they interact.

In practical terms our results suggest useful directions for future research. They suggest that gamma radiometric data may not capture fine scale variability in soil texture. Whether this is largely due to the large footprint/ support and diffuse boundaries would be worth testing, especially with the increasing availability of proximal soil sensors and associated libraries.

Similarly, the extremely close relationship between local topography and soil variability is striking. Whether this relationship holds up in specific regions and at specific scales would be of great interest to note.

REFERENCES

- Australian Bureau of Meteorology (2017). Station rainfall data provided by the Australian Bureau of Meteorology on request, <http://reg.bom.gov.au/data-access/3rd-party-attribution.shtml>
- Burrough, P. A. (1983). Multiscale sources of spatial variation in soil. I. The application of fractal concepts to nested levels of soil variation. *Journal of Soil Science*, 34, 577–597.
- CSIRO (2018), Data Access Portal <https://data.csiro.au/dap/landingpage?pid=csiro:5589>, accessed March 2018
- Dickson, B. L., & Scott, K. M. (1997). Interpretation of aerial gamma-ray surveys-adding the geochemical factors, *Reviews of Geophysics* 17(2), 187–200.
- Didan, K., Munoz, A. B., & Huete, A. (2015). MODIS Vegetation Index User's Guide (MOD13 Series). *Vegetation Index and Phenology Lab*
- Farr, T. G., Rosen, P. A., Caro, E., Crippen, R., Duren, R., Hensley, S., Alsdorf, D. (2007). The Shuttle Radar Topography Mission, *Reviews of Geophysics* (2005), 1–33.
- Gallant, J. (2011). Adaptive smoothing for noisy DEMs. *Geomorphometry*, 37–40. Retrieved from <https://pdfs.semanticscholar.org/1575/2afefd0a43d5126752ba686375ac1522f13b.pdf>
- Geoscience Australia (2018) <http://www.ga.gov.au/scientific-topics/national-location-information/digital-elevation-data>
- Green, T. R., & Erskine, R. H. (2004). Measurement, scaling, and topographic analyses of spatial crop yield and soil water content. *Hydrological Processes*, 18(8), 1447–1465.
- Grundy, M. J., Viscarra Rossel, R. A., Searle, R. D., Wilson, P. L., Chen, C., & Gregory, L. J. (2015). Soil and landscape grid of Australia. *Soil Research*, 53(8), 835–844.
- Heuvelink, G. B. ., & Webster, R. (2001). Modelling soil variation: past, present, and future. *Geoderma*, 100(3-4), 269–301.
- Lark, R. M. (2011). Spatially nested sampling schemes for spatial variance components: Scope for their optimization. *Computers & Geosciences*, 37(10), 1633–1641.
- Mandelbrot, B., & Wallis, J. (1969). Some Long-Run Properties Geophysical Records. *Water Resources Research*, 5(2), 321–340.
- Marchant, B. P., Rossel, R. A. V, & Webster, R. (2013). Fluctuations in method-of-moments variograms caused by clustered sampling and their elimination by declustering and residual maximum likelihood estimation. *European Journal of Soil Science*, 64(4), 401–409.
- McKenzie, N. J., & Ryan, P. J. (1999). Spatial prediction of soil properties using environmental correlation. *Geoderma*, 89(1–2), 67–94.
- Minty, B. (1997). Fundamentals of airborne gamma-ray spectrometry. *Journal of Australian Geology and Geophysics*, 39–50.
- Minty, B., Franklin, R., Milligan, P., Richardson, M., & Wilford, J. (2009). The Radiometric Map of Australia . *Exploration Geophysics*, 40(February), 325–333.
- Paterson, S., Minasny, B., & McBratney, A. (2018). Geoderma Spatial variability of Australian soil texture : A multiscale analysis. *Geoderma*, 309(April 2017), 60–74.

- Searle, R. (2014). The Australian site data collation to support the GlobalSoilMap. In A. Arrouays, D; McKenzie, N; Hempel, J; DeForges, ACR; McBratney (Ed.), *Globalsoilmap: Basis Of The Global Spatial Soil Information System* (pp. 127–132).
- Stockmann, U., Malone, B. P., McBratney, A. B., & Minasny, B. (2015). Geoderma Landscape-scale exploratory radiometric mapping using proximal soil sensing. *Geoderma*, 239-240, 115–129.
- Webster, R. (2000). Is soil variation random? *Geoderma*, 97(3-4), 149–163.

Chapter 5:

Calculating the Global Variogram. Modelling soil variability beyond the continental scale

All of my creation is an effort to weave a web of connection with the world

Anais Nin

Abstract

In this chapter, we extend our analysis by modelling the global variability in soil texture. We find that the composite variogram model does not readily extend to the global scale.

Surprisingly we find that the maximum variability in global soil texture (as modelled by a global variogram) is not greater than the maximum variability in soil texture found within the Australian continent. At the global scale we find pronounced anisotropy, possibly driven by large scale climate trends. This anisotropy indicates that the 'roughness index model' we've used does not extend to the global scale.

5.1 Introduction

In this Chapter we approach the question of soil global variability. A number of global soil models exist, and are increasingly being incorporated into models of environmental variability. In Chapter 2, we modelled the spatial variability of soil texture at extents from 1km to continental. Our aims for this Chapter are twofold. First, to describe global soil variability. Second to test whether the model multiscale model developed for the Australian continent in Chapter 2 can usefully be extended to the Global Scale. Modelling global variograms also allows us to find a 'global sill' for soil texture variability, and to compare the variability that we found at the finest scales in Chapter 2 (1km extent) to global variability. We also test whether the tendency for soil texture variability to increase with depth holds at a global scale. This analysis is facilitated by the existence of compiled legacy datasets.

5.2 Methods

5.2.1. *Calculating the Global Variogram*

We use data from the World Soil Information System (Wosis) provided by Batjes, et al. (2016) to calculate global empirical variograms.

As in Chapter 2, we increase the bin size in line with the extent. In this analysis, we use bin sizes of 200km, and present an extent of 10,000km. We also use grid-based declustering method. Using latitude and longitude projections, we split the globe into 500 segments. Longitude is split into 25 segments, and latitude is split into 20 segments.

Around the equator the approximate grid size is 1,600km in an East-West direction and 1,000km in a North-South direction²². The NS grid length remains constant regardless of location, but the East-West separation gets smaller further from the equator. At 50° north or South, the declustering grids are approximately 1,000 square km. As in Chapter 2, the weight we use for each observation is inverse to the number of observations that occur within the same grid²³. As in Chapter 2 we check for anisotropy calculating directional variograms. Unlike Chapter 2, we find strong evidence for anisotropy and therefore present the directional variograms. We calculate variograms in the East West (EW) direction and the North South (NS) direction with a 45 degree tolerance on each direction.

Because of the strong anisotropy we do not extend the roughness index model from previous chapters. The analysis presented in this chapter is based on empirical variograms.

²² Estimates based on each degree being approximately 111 km

²³ The actual weight used is calculated from 9 slightly offset averages to avoid arbitrary cut off points.

As we are operating on a sphere, rather than a two-dimensional grid, as in Chapter 2, an additional step is required to calculate separation distance. For each pair of observations, we convert degrees to radians using a trigonometric function and we calculate separation distance in meters using the haversine formula.

5.2.2 The data

We use the World Soil Information System (Wosis) dataset provided by Batjes et al. (2016) supplemented with the Australian NSSC dataset described in Chapter 2. In this chapter we analyse percentage clay content.

In the North South direction, the dataset is concentrated between -50° and 50° latitude (a separation distance of around 11,000 km). The maximum latitudinal (North-South) separation is around 16,000 km (Figure 5.1 and Figure 5.2 left panel). There is very limited data collected in the Arctic or the Antarctic. In the East West direction, there is a region of very sparse data collection from around 150° to -150° longitude (Figure 5.1 and 5.3 left panel). This corresponds with the north and south pacific oceans where there is limited land mass, and where data collection is sparse over the land masses that do occur at these longitudes. Other notable (but shorter) gaps in the East West data occur at around -30° to -20° and 50° to 70° . The density of sampling is by far the greatest at longitudes of -120° to -80° , this corresponds with North America (Figure 5.1 and Figure 5.4 left panel).

5.2.2.1. Data Cleaning

The raw Wosis dataset contains around 80,000 points with observations for percentage clay fraction.

In order to harmonise the data for depth, we needed to clean the data. In addition to removing negative values and observations where the summation of the sand and clay fraction was greater than 100, we also removed observations where:

- the topsoil observation did not start at depth 0 cm ;
- If there was a gap between the layers ; and
- If there was an overlap between the layers.

These data treatments allowed fitting of the Spline function.

We harmonised the depth data using the equal area spline with the `ea_spline` function in the `itir` package (Malone, Minasny, & McBratney, 2017) using the same depth intervals as we used in Chapter 2. We combined the global data with the NSSC Australian data. This left us with 55,562 profiles 35,988 were from the US, another 2,101 were from Mexico, 89 from Canada, and the rest from different parts of the world (151 from Australia). The North American continent dominates the WOSIS dataset. The cleaned and splined NSSC dataset described in Chapter 2 was added to these observations, contributing another 13,830 observations from Australia (Figure 5.1). Summary statistics for the splined data of clay content in Table 5.1.

Table 5.1. Summary statistics of splined composite WOSIS and NSSC dataset

depth	count	average	s.d.	skewness	kurtosis
0-5 cm	69415	20.49	15.28	1.27	1.50
5-15 cm	68953	21.78	15.50	1.15	1.12
15-30 cm	64520	24.91	16.55	0.88	0.43
30-60 cm	62156	29.22	17.88	0.60	-0.04
60-200 cm	56141	29.81	18.33	0.60	-0.09

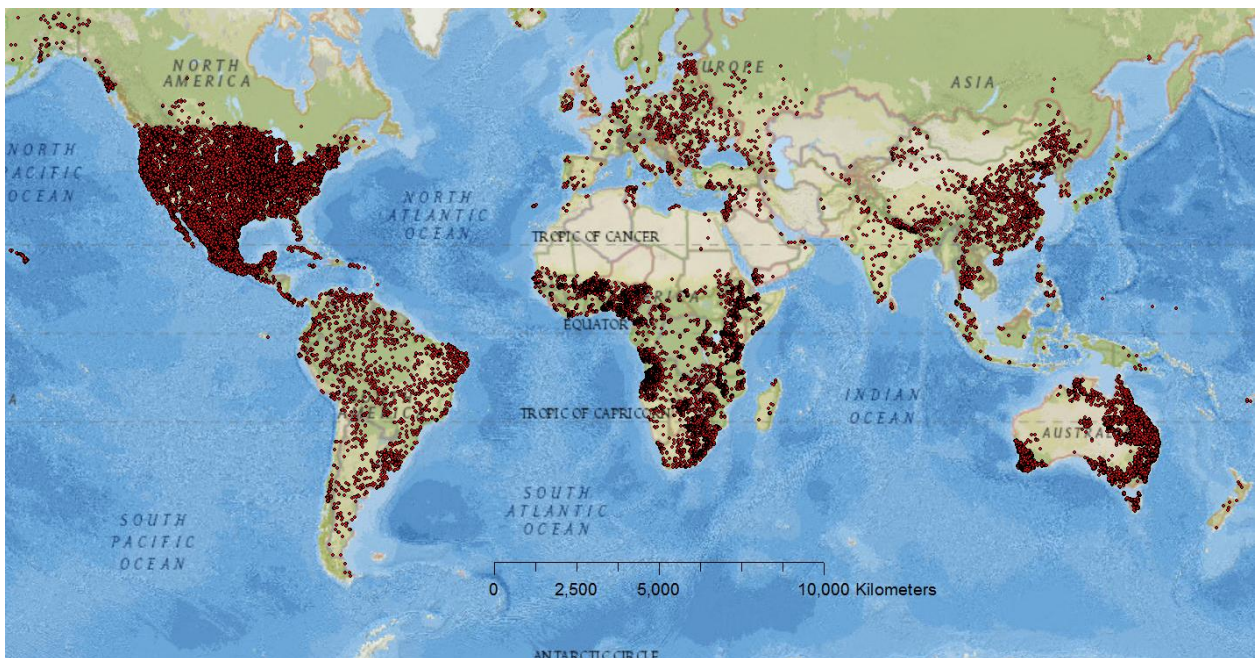


Figure 5.1. Distribution of WoSIS and NSSC dataset

5.2.2.2. Global Non-Stationarity

We find evidence for non-stationarity about the mean and the variance in the global soil texture data in the North South direction (Figure 5.2). We do not find evidence of non-stationarity in the East-West variogram. There is a region of lower variability, and lower mean values from around -140 to 100, but this does not represent a strong trend (Figure 5.3).

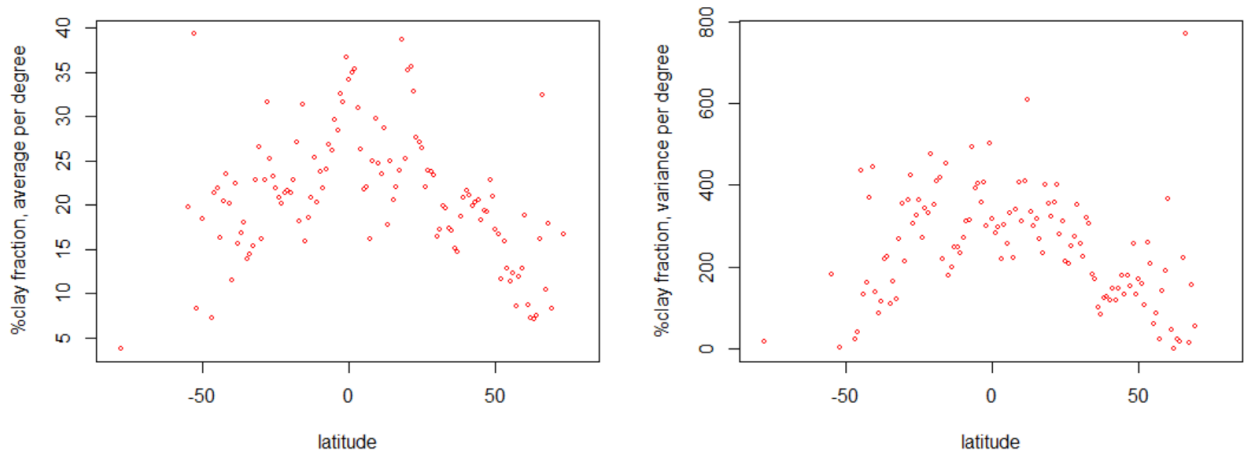


Figure 5.2. Percentage clay fraction statistics by latitude (North-South). Average per degree of latitude in left panel, variance per degree of latitude in right panel.

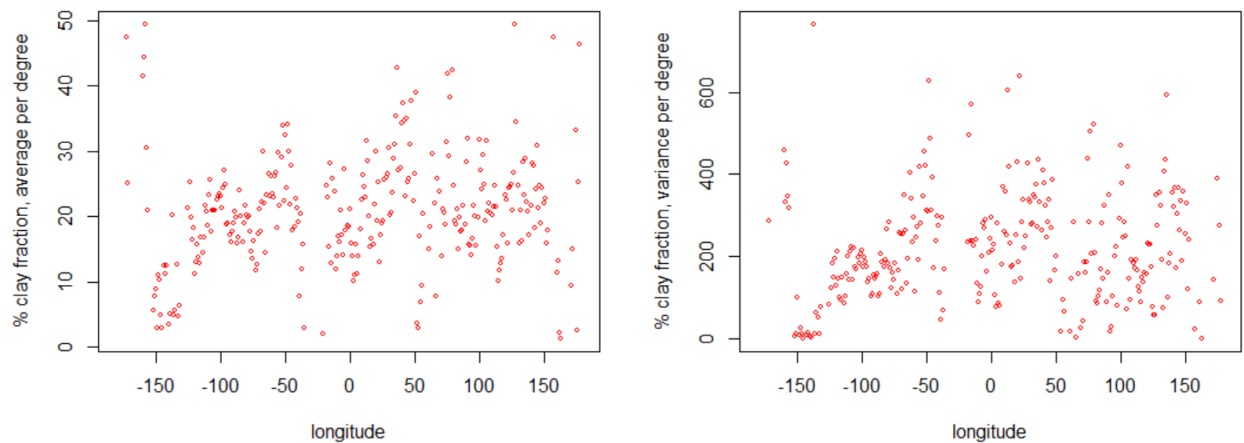


Figure 5.3. Percentage clay fraction statistics by longitude (East-West). Average per degree of longitude in left panel, variance per degree of longitude in right panel.

A common approach for dealing with non-stationarity about the mean is the removal of the trend. We try this approach. The N-S mean trend appears as though it could be well fit by a quadratic function (Figure 5.2 left panel). We select the quadratic function and fit it to the raw data (Figure 5.4 left panel).

It is difficult to visualize the fit on the raw data, but it appears to be a good fit against the the mean (Figure 5.4 right panel). From this fitted curve we calculate the residuals (Figure 5.5).

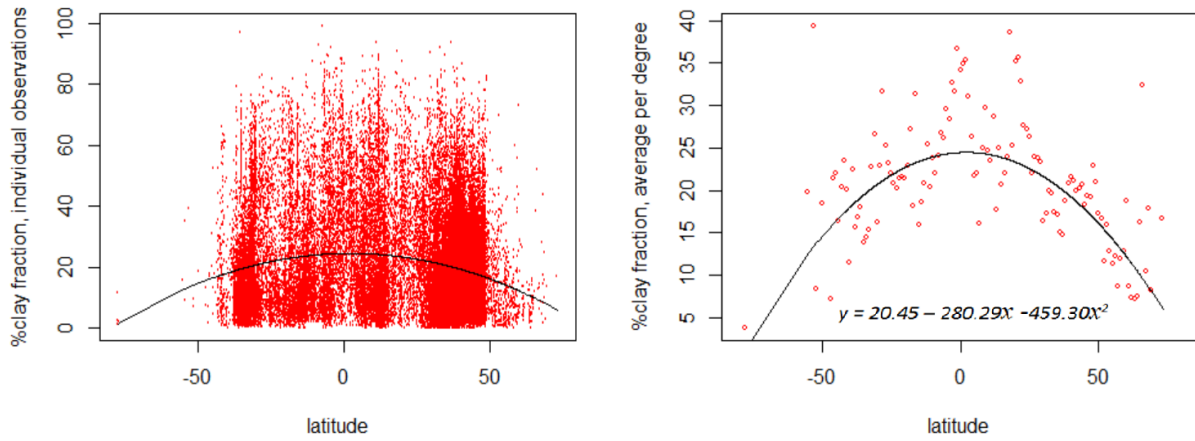


Figure 5.4. Percentage clay fraction against latitude. On the left panel each red point represents an observation. On the right panel each red point represents the average of the % clay fraction observations collected in that degree of longitude. The black line is the same on both panels

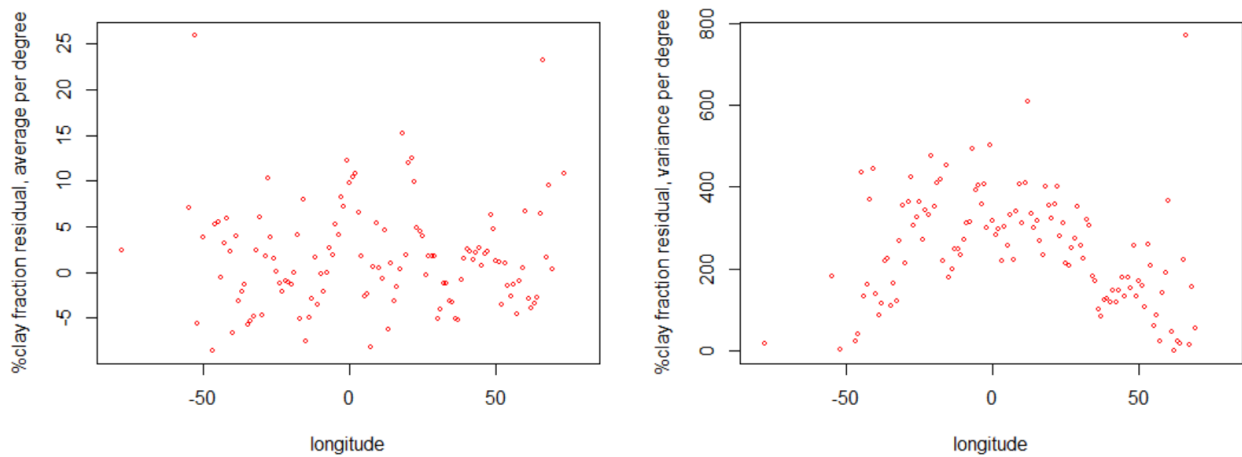


Figure 5.5. Percentage clay fraction statistics calculated from residual data by longitude (North-South). Average per degree of longitude in left panel, variance per degree of longitude in right panel.

Removal of the mean trend does not affect the stationarity about the variance (Figure 5.5 left panel), or the shape of the empirical semivariograms (Figure 5.6 and 5.7).

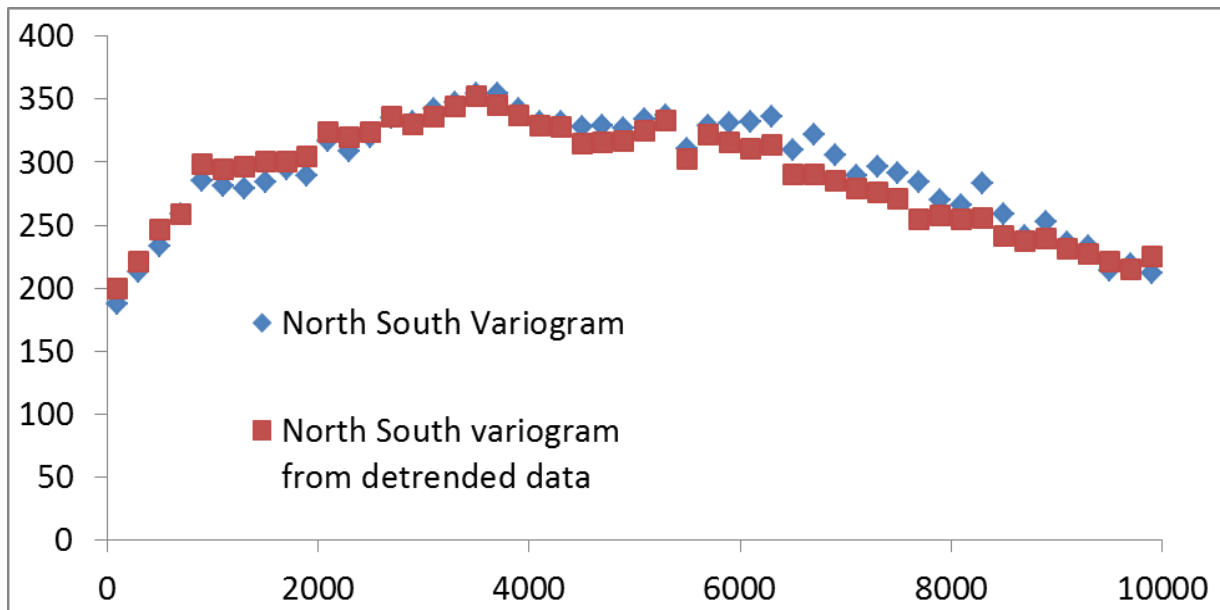


Figure 5.6. Global Variogram North South, calculated from original data (blue points) and residual data (red points)

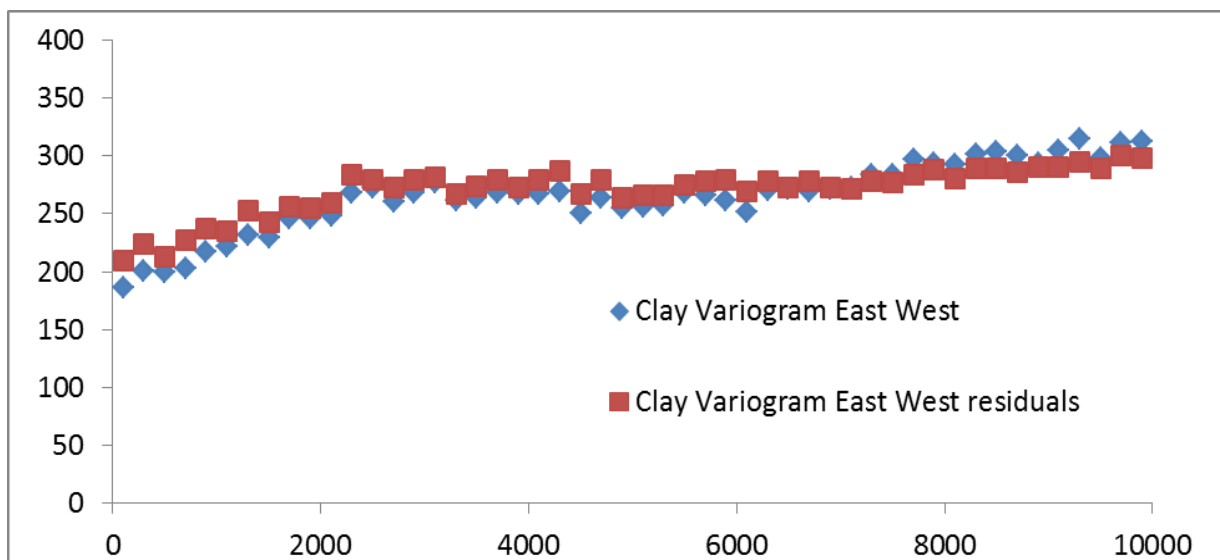


Figure 5.7. Global variogram – East West calculated from original data (blue points) and residual data (red points)

Dealing with non-stationarity about the variance is a more difficult problem than dealing with non-stationarity about the mean. The pronounced trend in the variance violates the second assumption of weak stationarity (i.e. the variance in this case is dependent not only on separation distance between two observations, but also on direction and location of these observations). Methods exist for modelling variograms when the variance is non-stationary (e.g. Lark, 2009; Meul & Van Meirvenne, 2003), but these approaches are not compatible with empirical variogram modelling at a global scale. In the results and discussion below, we proceed with the original data and discuss potential drivers

for the non-stationarity and associated anisotropy. It is necessary to deal with non-stationarity about the variance to create accurate estimates of the prediction error when using variograms for kriging and mapping (Lark, 2009), but the underlying non-stationarity does not prevent us from drawing inferences about global trends in variability from the global variograms.

5.3. Results and Discussion

5.3.1. Global Variability

We calculate semi-variograms from both the original dataset and the detrended residuals (Figure 5.8). Unlike the variograms calculated in Chapter 2 we find distinct anisotropy in the variograms calculated from the raw data and in the variograms calculated from the residuals.

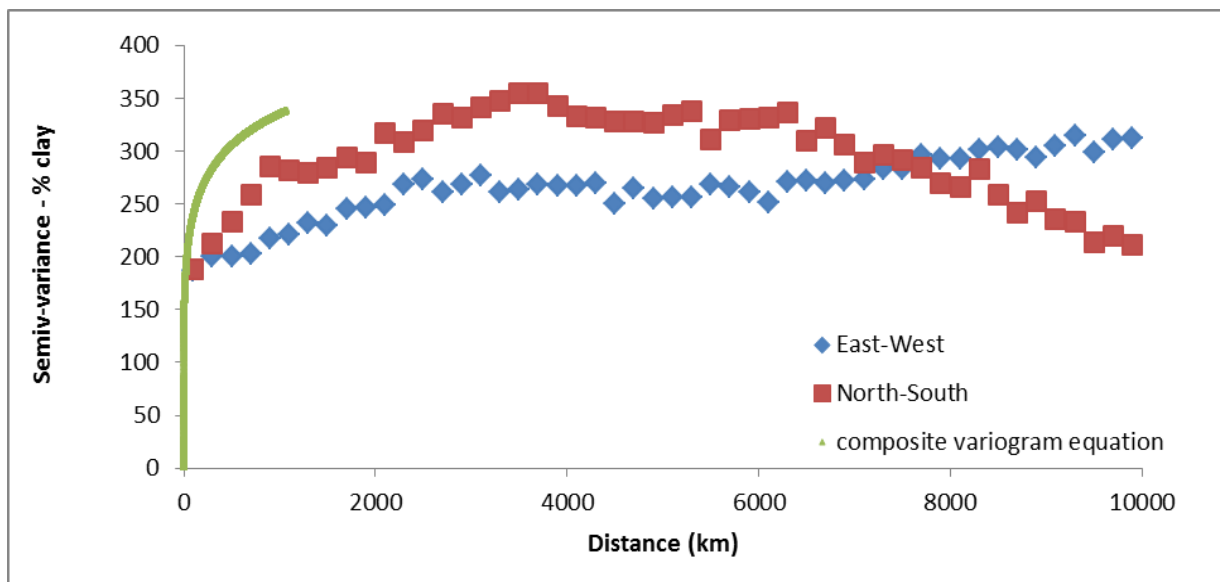


Figure 5.8. Experimental semivariograms calculated from the residuals (detrended clay % fraction data), with composite variogram from Chapter 2 overlain.

Despite the much greater extent the global variogram does not show a greater maximum variance than the continental variogram. At 10,000km separation distance, both the East-West and the North-South variogram show less variability than the Australian variogram showed at 1,000km. This result is surprising. Intuitively we would expect there to be more variability between continents than within them. It is possible that the method of measurement of soil texture variability (% fraction) is limiting the description of variability of soil texture. Measuring a percentage of an arbitrarily determined grain size interval reduces the variability that can be described. The Australian and US classification (used in

the WOSIS dataset) for clay content is 2 μm . The percentages presented in this chapter (and throughout the thesis) do not capture variation within 0-2 μm . It is possible that a more nuanced description of the data, such as that trialled in multifractal measures of soil texture (Grout, et al. 1998, Millán, et al. 2003; Neyshabouri, et.al., 2011) would allow a more accurate picture of the trend to be developed.

5.3.2 Limits of continuous change model

In Chapter 2, we find that variograms for percentage clay at a range of scales can be well approximated by power curves. Further, we find that when a multi-scale variogram is calculated and plotted on a log-log scale it can be well approximated by an exponential decay curve. This allows us to describe the change in variability across scales with a single equation. In Chapter 4 we find that this holds for a number of environmental properties. However, when we model the global variogram, the same pattern does not continue. Because we find strong anisotropy in the global models, they do not fit with the framework we use to describe our model in Chapter 2. It is not surprising that the model does not continue to fit well at this scale. When we consider the global scale factors such as continental drift, extremely different climate regimes and large separation distances, all come in to play.

5.3.3. Global Anisotropy

The East-West variogram shows a much more gradual increase in variability than the north south. It also continues to increase across the entire calculated range (up to 10,000km) although this rate of increase declines with increasing distance. By contrast the North-South variogram (relatively) quickly reaches a peak (at around 4,500 km) and then variability begins to decrease again, and continues to decrease until the maximum range of the calculated variogram (10,000km).

The variogram calculated in the North-South direction reaches maximum variance before 5,000 km, and then the variance begins to decline. For context, the circumference of the globe is about 40,000 km, and the distance from the equator to either pole is around 10,000 km. The distance between the tropic of cancer and the tropic of Capricorn is about 10,000 km. We suspect the anisotropy is driven by the same factors as the non-stationarity. The Shape of the North-South variogram, shows a very similar pattern to the pattern in the non-stationarity about the mean and the variance. In Section 5.3.4 we discuss potential drivers of the non-stationarity.

5.3.4. Global Non-stationarity

The N-S non-stationarity about the mean and variance follow a similar spatial trend. Both the average % clay fraction and the % clay variance are greater in the equatorial region than the temperate regions.

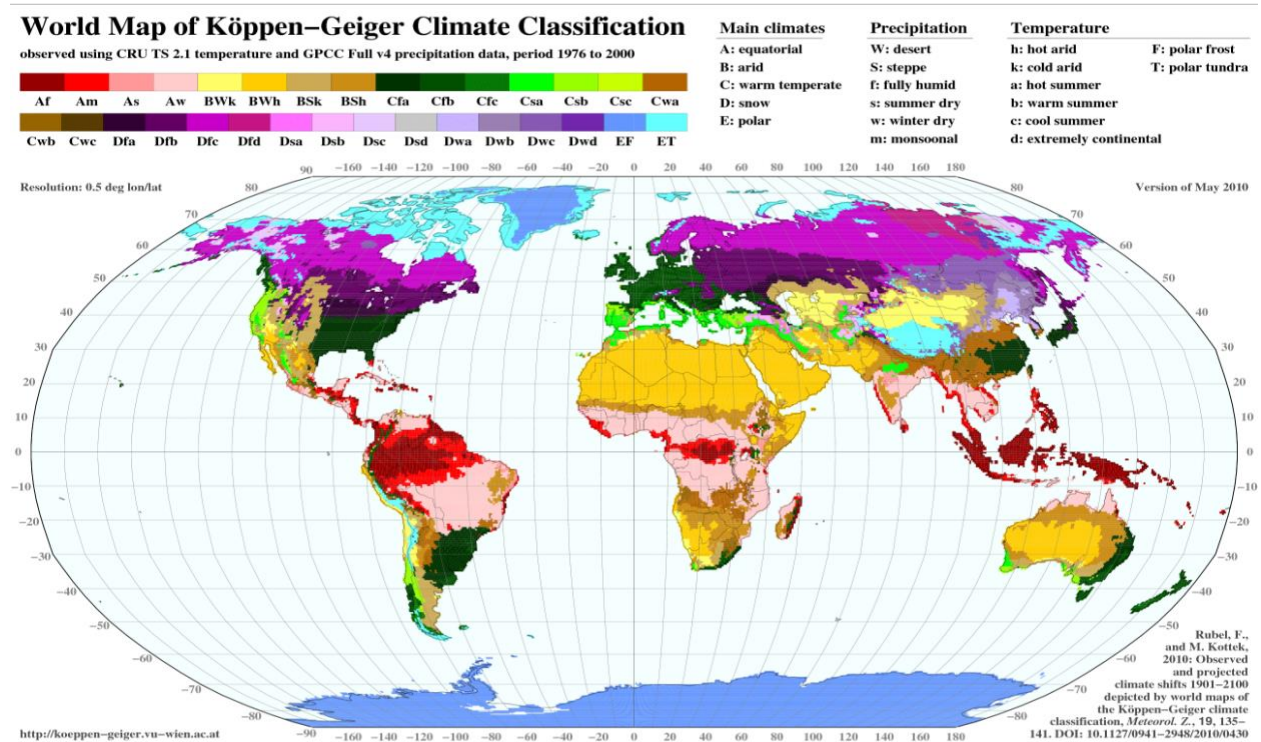


Figure 5.9. Koppen climate classification, source: Rubel & Kottek, 2010

There appears to be a relationship between this non-stationarity and major global climatic zones. Around the equator (longitude of zero) there is a tropical zone that extends approximately 4000km (or 20 degrees north and 20 degrees south). On either side of this tropical zone there are arid or temperate regions. Beyond these arid and temperate regions there are cold or arctic regions (Figure 5.9). Our dataset is heavily focused in the tropical and temperate regions with limited observations in the cold or arctic regions. Figure 5.10 (modelled clay content) shows a similar although less pronounced N-S trend, with a higher clay fraction closer to the equator.

A number of studies find a relationship between climate and weathering at global scales although these relationships are not always found at regional scales (Turner et al. 2010). Discerning the effects of temperature on weathering remains a difficult problem because the weathering rates are controlled by other factors (rainfall, and lithology) and related factors such as evapotranspiration and

plant growth (Turner et al., 2010). Temperature and water exposure are generally held to be key drivers of rates of weathering, which in turn contributes to the texture of the soil.

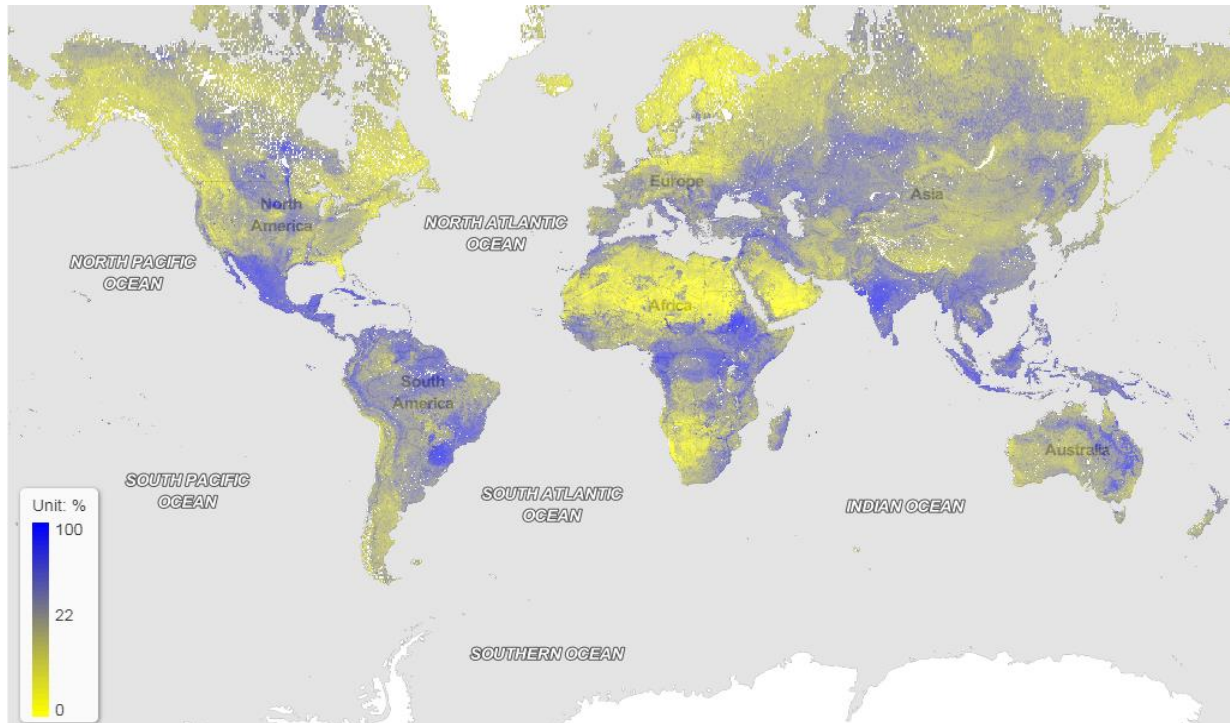


Figure 5.10. Clay (0-2 micrometer) mass fraction % at 5cm depth. Source soilgrids.org

5.3.5. Global Variability with Depth

Modelled across different depths, the broad patterns of the global variogram appear quite similar. Some minor fluctuations appear at different depths, but the major trends are similar for both of the directional variograms. There also appears to be the same tendency for variability to increase with depth that was noted in the multi-scale analysis of Australian soil texture in Chapter 2. As with the Australian soil texture this trend increases until the 60-200cm depth. In the scales we considered in Chapter 2, we found that this depth was sometimes less and sometimes more variable than the upper depths. In Figure 5.11 and 5.12 below we can see that the 60-200cm depth interval is less variable across the entire variogram. As discussed in Chapter 2, the drivers for this increased variability with depth might be to do with a greater homogenisation of surface soil due to surface processes including agricultural processes.

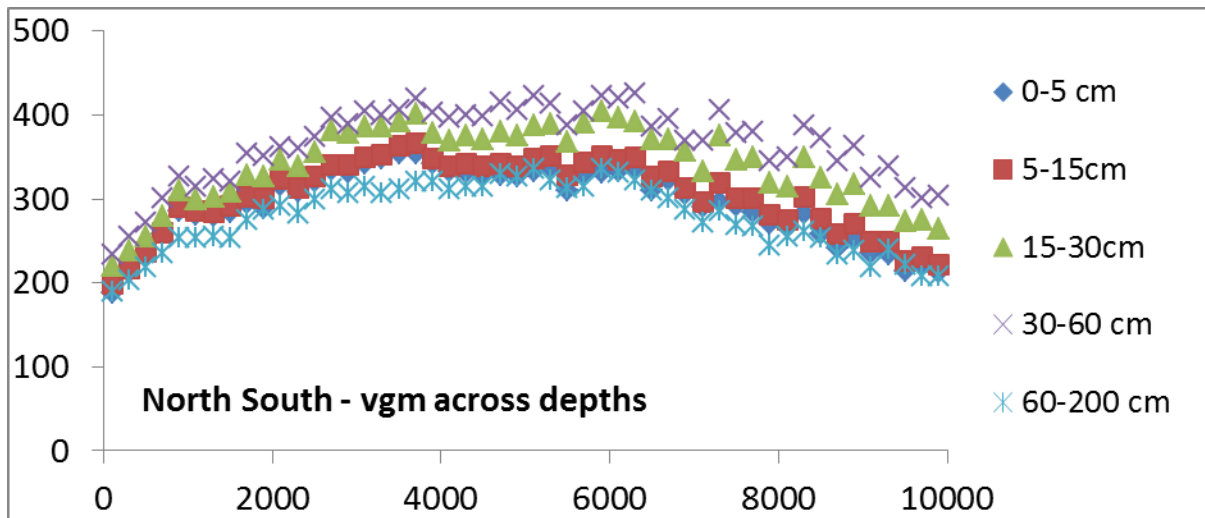


Figure 5.11. Global variogram calculated at increasing depth intervals

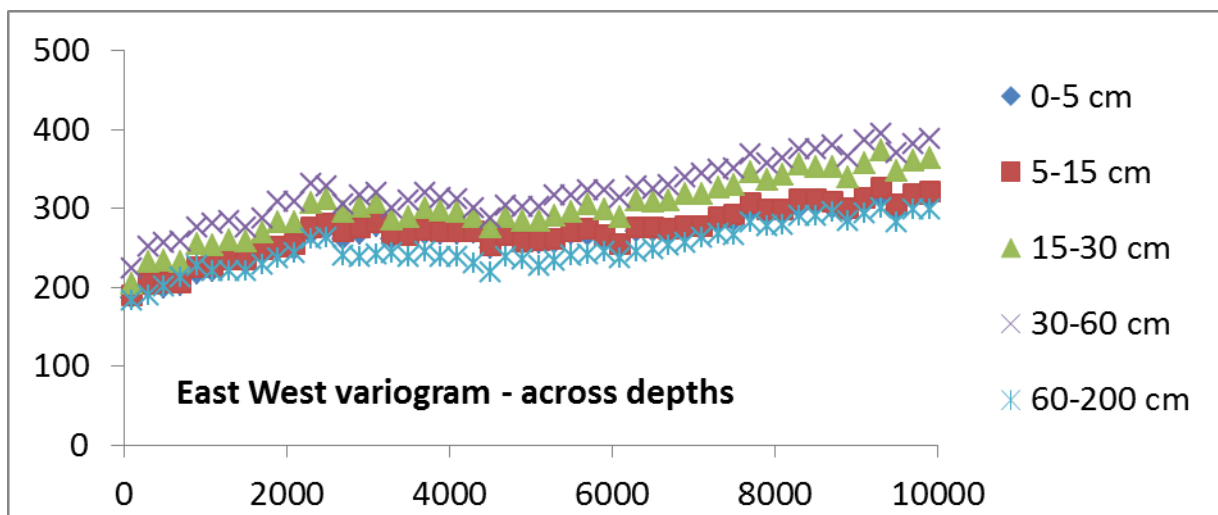


Figure 5.12. Global variogram calculated at increasing depth intervals

5.4 Conclusions

- The maximum variability found in clay percentage texture at the global scale was similar to the maximum variability found in clay percentage texture at the continental scale. This might imply a limit to spatial variability is found at the continental scale.
- The multiscale model that we developed in Chapter 2 appears to reach its limits for clay content at the continental scale. It might be possible to transform the data to allow this model to be extended.
- At the global scale, soil texture variability is non-stationary and anisotropic.
- Soil texture roughness increases with depth up to around 60cm at the global scale. This result is similar across scales from the field to the global.

REFERENCES

- Batjes, N. H., Ribeiro, E., van Oostrum, A., Leenaars, J. A., & Jesus de Mendes, J. (2016). Standardised soil profile data for the world (*WoSIS, July 2016 snapshot*).
- Lark, R. M. (2009). Kriging a soil variable with a simple nonstationary variance model. *Journal of Agricultural, Biological, and Environmental Statistics*, 14(3), 301–321.
- Grout, H., Tarquis, A. M., & Wiesner, M. R. (1998). Multifractal Analysis of Particle Size Distributions in Soil. *Environmental Science and Technology*, 32(9), 1176–1182.
- Malone, B. P., Minasny, B., & McBratney, A. B. (2017). Using R for digital soil mapping. *Progress in Soil Science*.
- Meul, M., & Van Meirvenne, M. (2003). Kriging soil texture under different types of nonstationarity. *Geoderma*, 112(3-4), 217–233.
- Millán, H., González-Posada, M., Aguilar, M., Domínguez, J., & Céspedes, L. (2003). On the fractal scaling of soil data. Particle-size distributions. *Geoderma*, 117(1-2), 117–128.
- Neyshabouri, M. R., Ahmadi, A., Rouhipour, H., Asadi, H., & Irannajad, M. (2011). Soil texture fractions and fractal dimension of particle size distribution as predictors of interrill erodibility. *Turkish Journal of Agriculture and Forestry*, 35(1), 95–102.
- Rubel, F., & Kottek, M. (2010). Observed and projected climate shifts 1901-2100 depicted by world maps of the Köppen-Geiger climate classification. *Meteorologische Zeitschrift*, 19(2), 135–141.
- Turner, B. F., White, A. F., & Brantley, S. L. (2010). Effects of temperature on silicate weathering: Solute fluxes and chemical weathering in a temperate rain forest watershed, Jamieson Creek, British Columbia. *Chemical Geology*, 269(1-2), 62–78.

Chapter 6:

Variograms of Soil Properties for Agricultural and Environmental Applications

Think left and think right and think low and think high. Oh, the things you can think up if only you try! – Dr Suess

This chapter has been published as: Paterson, S., McBratney, A., Minasny, B., Pringle, M. (2018). Variograms of Soil Properties for Agricultural and Environmental Applications. In Alex McBratney, Budiman Minasny and Uta Stockmann (Eds.), *Pedometrics*, (pp. 623-667). London: Springer.

Abstract

In this Chapter, we investigate solutions to the specific problem of efficient sampling design when fine scale variability is unknown. Focusing on eight soil properties commonly sampled in precision agriculture studies (Clay, Sand, pH, Carbon, Available Nitrogen, Total Nitrogen, Phosphorous, Potassium), we compile variograms from existing literature to evaluate whether an 'average' or a 'proportional' variogram can provide a good a priori estimate of field scale variability.

We do not find sufficient trend to allow the use of the proportional variogram, and advise caution in the use of the average variograms. We explore a range of other strategies for improving the knowledge of field scale variability prior to sampling.

6.1. Geostatistics and precision agriculture

Precision agriculture can be used to improve farm management to achieve economic and environmental benefits (Whelan, 2018). Short range differences in soil attributes mean that spatially differentiated management can create economic or environmental benefits. Effective precision agriculture requires accurate soil mapping at sub field scales so that management practices can be modified. Improvements in farming technology, for instance GPS controlled farm equipment, decrease the difficulty and cost associated with spatially differentiated management. This improves the ease of implementation and makes high resolution soil maps more valuable.

A key challenge for geostatistics in precision agriculture is the detection of soil variability at important sub field scales and the systematic incorporation of this variability into accurate field scale soil maps.

6.2. Soil survey, the variogram and kriging

Soil attributes are typically difficult and expensive to observe. As a result, soil attribute maps made for the purpose of precision agriculture are typically created from point observations which represent a small proportion of the area to be mapped. Estimates of soil attributes in unknown areas are based on the observations and an expectation of the regions between them. This process of predicting attributes in unobserved areas is known as kriging (explained in more detail in Lark, 2018). Assumptions about spatial variability are described quantitatively in the variogram, which links spatial separation distance to expectations about variability. Lark (2018) and Marchant (2018) explain the variogram, its uses and the different methods of calculating the variogram in more detail.

The variogram is sometimes called the 'cornerstone of geostatistics'. Accurate estimation of the variogram is critical to the production of accurate soil maps. Because of the hidden nature of most soil attributes, we can usually only directly observe a small proportion of an area of interest. In Lark (2018), the distinction between the experimental or empirical variogram and the model variogram is described in some detail. The empirical variogram plots the average variance against separation distance for a number of distinct lags. The model variogram uses the information from the empirical variogram to estimate the expected variability at all lags. The purpose of the model variogram is to estimate the true underlying spatial variation at a level of detail that allows useful predictions.

Interpolation of results into unobserved points depends on the spatial structure estimated by the variogram. The closer the estimated variogram to the underlying spatial structure the more accurate the subsequent interpolation. In general, a variogram computed from samples with finer spacing and more observations will estimate the underlying spatial structure more accurately than a variogram

computed from samples with coarser spacing. Finer spacing allows the detection of spatial structure across more scales. The extent to which this is true will depend on the interaction of the spacing with the underlying spatial structure. For example, if there is no spatial relationship between points more than 5 m apart, then decreasing spacing from 50 m of separation distance to 10 m will not improve the variogram. We pause here to explain some key components of the variogram and how they are affected by survey design.

6.3. Key components of the variogram

While the variogram can take many forms, there are three components which are typically considered the most important indicators of spatial structure. Shown in the stylised diagram in Figure 6.1 and subsequently described, these components are the nugget, the sill and the range. The estimation of each of these parameters depends strongly on the sampling design.

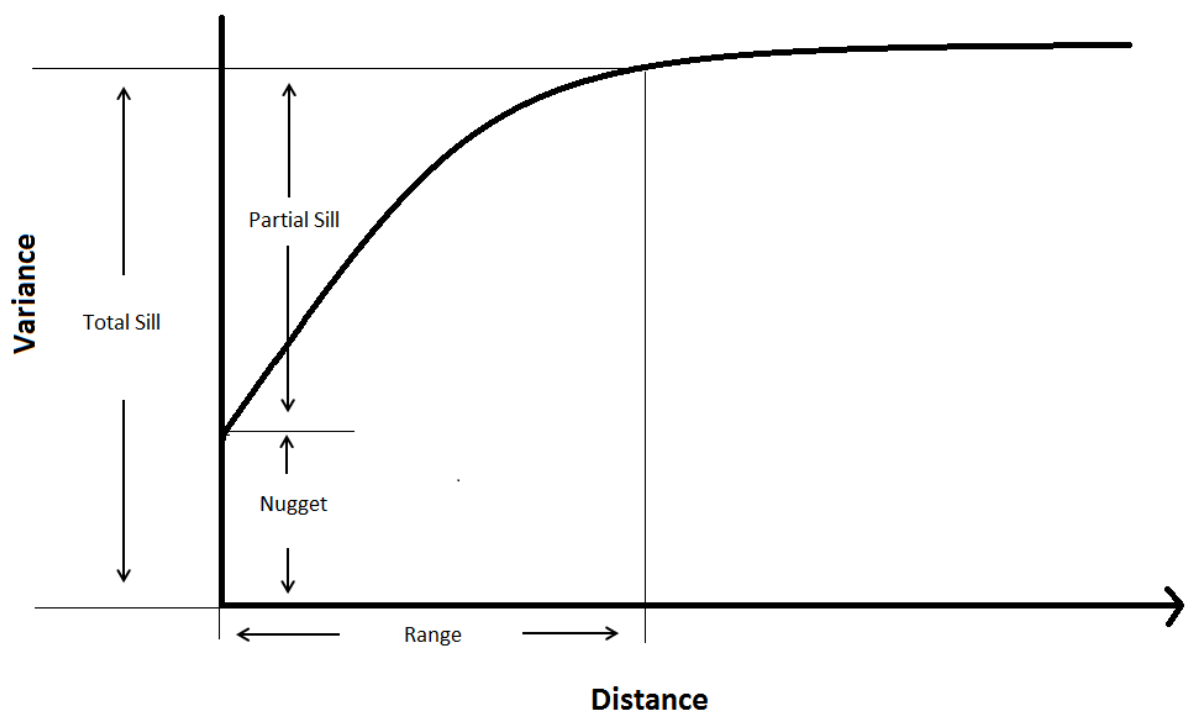


Figure 6.1. Stylised diagram, showing the three most important indicators of spatial structure, the nugget, sill and the range.

Nugget

In principle the nugget effect captures non spatial variation: measurement error; random variation. However, in practice the nugget will also capture spatial variation that occurs at scales less than the smallest sampling interval. If the sampling interval is wider than an important scale of spatial variation

then this will increase the nugget. Aliquotting (pooling of samples) will decrease the nugget. A larger support (area over which the sample is taken) will also decrease the nugget.

Total Sill

The total sill is defined as the maximum variability that can be expected for a particular soil property. Beyond a certain separation distance (the range, see below) the expected variability will not increase past the value of the total sill (or in some cases will increase only very slowly and slightly past the sill). Only bounded variogram models have a sill. The total sill is more likely to be affected by the number of samples and the wider separation distance than the minimum sampling spacing. When modelling spatial variability at a field scale, it is unlikely that the maximum variability of the soil will be reached. However unbounded models are rarely fit. In the context of precision agriculture, we can think of the total sill as being the maximum variability within this particular context, or a local maximum. If we extended the sampling to a regional level it is likely we would reach another magnitude of variability.

Partial Sill

The difference between the nugget and the sill is known as the partial sill. The partial sill is the component of variation that can be spatially attributed. In Figure 6.1, the semivariance increases linearly with distance at short separation distances. As the separation distance increases, the rate of increase in the semivariance decreases, before eventually reaching a plateau as the semivariance reaches the total sill. This pattern is commonly found in variogram models. (see Chapter 9 for more detail on the functional forms). Accurately determining the change in variability between the nugget and the sill requires sufficiently dense sampling at appropriate scales of variability.

Range

Like the nugget and the sill, the range estimated by the theoretical variogram will be strongly affected by the sampling design. As the lag increases, the confidence intervals (around the estimated empirical variogram) widen (Oliver and Webster, 2014) which can make it difficult to accurately fit a variogram at lags approaching the full extent. Precision agriculture surveys are typically conducted over areas from a few hectares to a few hundred hectares. This precludes them from capturing landscape or continental scale variability. Despite this, the majority of variogram fits from precision agriculture studies are bounded. The modelled range and sill can be thought of as the 'local sill' associated with the 'local range' associated with the particular extent and spacing of that survey. It is very likely that if the extent of the survey was increased another degree of variability would be found. It is critical to

consider the potential effect of both, the extent and the spacing on the range when considering precision agriculture studies, and how their findings may inform your own work.

6.4 Soil survey design: capturing spatial variability

The task of ensuring that a soil survey captures the necessary scales of variability is not a trivial one. The expense of a soil survey, and the commonly destructive nature of soil sampling creates a pressure to reduce the number of sampling points as much as possible. However, if sampling is insufficient or too sparse (relative to the underlying spatial structure) it will compromise the variogram, and thus the accuracy of the maps which are calculated from it. It is noted in Lark (2018) that one of the chief difficulties associated with the design of a soil survey for estimating a variogram is that the underlying spatial structure is unknown at the time the survey is designed. If the underlying spatial structure of a soil attribute is known, we can design a soil survey sufficiently to create a map at a particular level of detail.

Where budget allows it, the best practice is to undertake a preliminary soil survey to estimate important scales of variation before a more comprehensive soil survey is designed. This survey should be nested in its design to increase the chances of capturing important scales of variability (Pettitt & McBratney, 1993; Webster & Oliver, 2001). However, a preliminary survey will rarely be economically feasible. If it is not possible to conduct a preliminary survey, a soil survey design is likely to benefit from the consultation of alternative sources of information about soil variability, such as existing literature or covariates.

Budget or practical pressures may be sufficient to impede the collection of sufficient data to reliably calculate an empirical variogram. A stable variogram calculated from classical geostatistical methods (as described in Chapter Lark 2018) requires around 100 observations. More modern methods (as described in Marchant 2018) typically require around 50, although closer to 100 is still preferred (Webster and Oliver 2008). It is not possible to estimate spatial variability at distances less than the minimum separation distance. In cases where there are few, or widely spread soil observations alternative sources of information may be useful for the calculation of a variogram for kriging.

The expense of gathering soil observations creates a need for cheaper sources of information about soil variability, either to assist in the planning of a soil survey, or to use in the process of kriging itself. Many authors have identified sources and strategies for the production of this information.

6.5. Variograms from the precision agriculture literature

Variograms calculated for the same soil attribute may be a useful source of information. However, variograms calculated for the same property can vary significantly for a number of reasons that should be carefully considered. As outlined in Malone (2018), parent material, soil type, land use, and climate will all have an effect on soil spatial variability. Consideration of these factors will be important in the selection of a variogram. Unfortunately, knowledge about soil spatial variability does not extend to the quantification of which of these factors are most important for determining spatial variability of different soil attributes.

The underlying variability of soil attributes might be different for the reasons mentioned above. In addition, the methods used to detect soil variability might create differences in the shape of the variogram. Different projects may focus on detecting variability at different scales for management or budget reasons. Even if the soil type is similar between two studies, the spatial variability might not be measured in a way that provides useful information.

It is also very important that the statistical methods used are assessed critically, before results are used or duplicated. There are a number of variograms included in Tables 6.1 to 6.8 which appear to use insufficient sample numbers for variogram estimation. There are several variograms which appear to assign spatial structure at a magnitude that appears to be meaningless relative to the units (i.e. total sill of less than 1 % for the soil texture fraction)²⁴. These results have been included for completeness, but we wish to draw the readers' attention to the fact that some of the variograms included in this collection may have issues associated with them.

We describe below some key trends we have noted in the compilation of soil variograms and include a graphical summary of the variograms we have compiled. This Chapter builds on the 1999 summary of precision agriculture literature by McBratney and Pringle. Variograms from McBratney & Pringle (1999) are included as well as those we have collected from the intervening period. Summary details and references for each variogram are given in Tables 6.1 to 6.8. We encourage the reader to consult each source directly for more detail about the sampling design and process.

Variograms for the same soil attribute from existing literature can be a useful source of information about field scale soil. It is important to exercise caution when consulting this literature, as variograms have been created from different soil types, for different purposes and possibly with important methodological limitations.

²⁴ In some cases the magnitude of the nugget and partial sill is extremely small compared to the magnitude of the standard deviation. This may suggest that the data has been transformed in some way before the variogram has been fit. We have reported the results as in the original article. These results should be interpreted with particular caution.

6.5.1. Field scale soil variograms: key trends

Variogram forms

Across all soil properties, a number of functional forms were fit to variograms. For each soil property at least one study found no spatial structure (i.e. pure nugget) to be the best fit. This suggests that either the spatial structure occurs at scales finer than those surveyed, or that the variability in the property in question is less than the experimental error. Spherical and exponential variograms were commonly used. Some papers described the functional form as 'experimental'. These models were fit with an exponential model for simplicity.

Total sill

Between studies the total sill (nugget plus partial sill) changes by several orders of magnitude for each property. As expected, this variability is the least pronounced for bounded properties (pH, OM %, Sand % and Clay %) and much more pronounced for micronutrients, which vary by around 3 -5 orders of magnitude.

Variability in total sill is similar to that observed by McBratney & Pringle, (1999). Inspection of the summary tables (Table 6.2 to 6.9) indicates that for the majority of soil properties, the range of values in the total sill is similar for the variograms collected by McBratney & Pringle (1999) and the more recently collected properties. The maximum variability reached within 1km has remained within an order of magnitude for all properties. For soil pH, organic Carbon and Potassium the maximum variability found in the more recent literature search is two to three times greater than the maximum variability found in the literature reviewed by McBratney and Pringle (1999)The other properties have a very similar maximum.

Nugget

Like McBratney and Pringle (1999) we find wide variability (several orders of magnitude) in the nugget parameter. McBratney & Pringle (1999) suggest that this variability is largely due to the strong effect of sampling design on the nugget. A variogram can only model the spatial structure that is detectable by the sampling design. In general, the wider the spacing, the more spatial variability will be attributed to the nugget component of the model. If the survey spacing is wider than the spatial structure the variogram will appear as a pure nugget model. A wider support and the use of aliquotting will reduce the 'noise' in the data and decrease the nugget. It has been often proposed, and is quite likely, that

the majority of soil properties would have more than one layer of soil structure. The differences in estimated nugget likely reflect both the underlying differences in spatial structure at the field scale and the capacity of different survey designs to capture this variability.

Range

The vast majority of modelled variograms found a range. Carbon had one linear and one nugget model, as did Potassium and available Nitrogen. pH had two models with zero ranges (one nugget, on experimental). Phosphorous had one linear model fitted, and clay and sand had one nugget model each.

Table 6.1. summarises the ranges that were found for the various models. Around half of the modelled variograms we gathered had a range of less than 100m for the eight soil properties. Almost all of the modelled soil properties had a range of less than 500m.

Range	Carbon	Potassium	Total N	Available N	pH	Phosphoros	Clay	Sand
NA or absent	5%	3%	0%	8%	0%	4%	0%	0%
0 (nugget model)	2%	3%	0%	8%	9%	0%	3%	6%
<100m	44%	41%	56%	42%	35%	57%	52%	56%
100 - 500m	34%	50%	44%	50%	53%	36%	36%	28%
500m - 1,000m	10%	3%	0%	0%	3%	4%	3%	6%
>1,000m	5%	0%	0%	0%	0%	0%	6%	6%

Table 6.1. Summary of range distances found in precision agriculture variograms

This emphasises the importance of fine scale variability in the overall soil variability.

6.5.2. Field scale soil variograms: methodological differences

Survey design

Another substantial difference between the survey designs was whether or not aliquotting was used. This is particularly significant when comparing these spatial studies because some studies model the range at distances that other studies were combining soil at. This is typically done for samples taken within 1 m of each other. This practice is likely to reduce the nugget (or white noise) and also to reduce any short term spatial trends which might be occurring.

There is significant variation in the survey design which may influence the mapping of spatial variability. Nested designs are better placed to capture spatial trends across a variety of scales than designs with even spacing; however, because of the additional costs associated with these, they are less common.

Model-fitting process

Oliver & Webster (2014) wrote an explanatory piece of work, describing the best methods for soil scientists to model variograms for kriging. They also described common mistakes made by soil scientists when calculating variograms. The majority of papers we assess do not follow all of Oliver and Webster's recommendations for reporting methods. This makes it difficult to assess how well a fitted variogram captures underlying spatial variability. Few papers report summary statistics for a variety of models and few papers present variogram clouds to illustrate the utility of the fit. This does not necessarily mean that the fitted models are not accurate, but it does make it difficult to assess the model.

Another point worth considering is the possibility that trends are being overfitted. Perhaps some of the models presented in this chapter would have been better represented by a nugget. These issues around model quality are not new, but a degree of caution is required when interpreting the results.

The more recent literature has included studies which have found much lower values for the total sill for several soil attributes. For clay the lowest value found for the total sill is two orders of magnitude lower than the lowest value reported by Petit and McBratney. Sand is one order of magnitude lower. Some modelled variograms occur over a very tiny range of variability relative to the magnitude of the property they are measuring. Whether it is necessary or feasible to model a spatial structure of less than one percent for soil texture properties is questionable.

Measurement methods

The properties we have included here are commonly measured soil properties with known agronomic implications. However, measurement of these properties is rarely simple or consistent. Differences in measurement methods and differences in which component of the property is being measured will influence both the shape and magnitude of the variogram.

pH is an extremely commonly measured property. However, within the studies we have assessed there are differences in the solution, the dilution rate and the equipment used to measure the pH. This problem becomes more complex when considering more difficult-to-measure properties such as Potassium and Phosphorus. Different studies have used different extractants to target different fractions for these nutrients.

The variogram is affected by the distribution of the property it is being calculated for. The variograms calculated for Potassium and Phosphorus show the greatest differences in total sill. We expect that this is because the target of the measurements varies as well as the measurement method used.

Some articles were found which estimated total carbon, or inorganic carbon. However, there were relatively few such studies, so we have not included them here. We have included studies which measured organic matter as a proxy for organic carbon. We converted these using the van Bemmelen factor (1.724). Pribyl (2010) illustrates that an accurate conversion factor for different soils can vary from 1.4 to 2.5. Error in the conversion will be small relative to the overall spread of the variograms.

6.5.3. Field scale soil variograms: a compilation

Figures 6.2 to 6.9 provide a visual compilation of field scale variograms for each of the soil properties initially examined by McBratney and Pringle (1999). We include both the original variograms used by McBratney and Pringle and variograms published since then. We only include variograms which were calculated from untransformed data and which were based on physical observations (i.e. not from remotely observed data). The black bold lines represent the average variogram. Tables 6.1 to 6.8 correspond to each Figure and include reference details and key parameters for each variogram. Because of the wide range of values of the source variograms the scales used in the figures cannot include all of them and some low sill variograms have not been included. We include the details in the Tables for completeness, but suspect that they are unlikely to provide useful information. The figures affected and the number of source variograms not included is:- pH 1, Carbon 3, Total Nitrogen 1, Potassium 2.

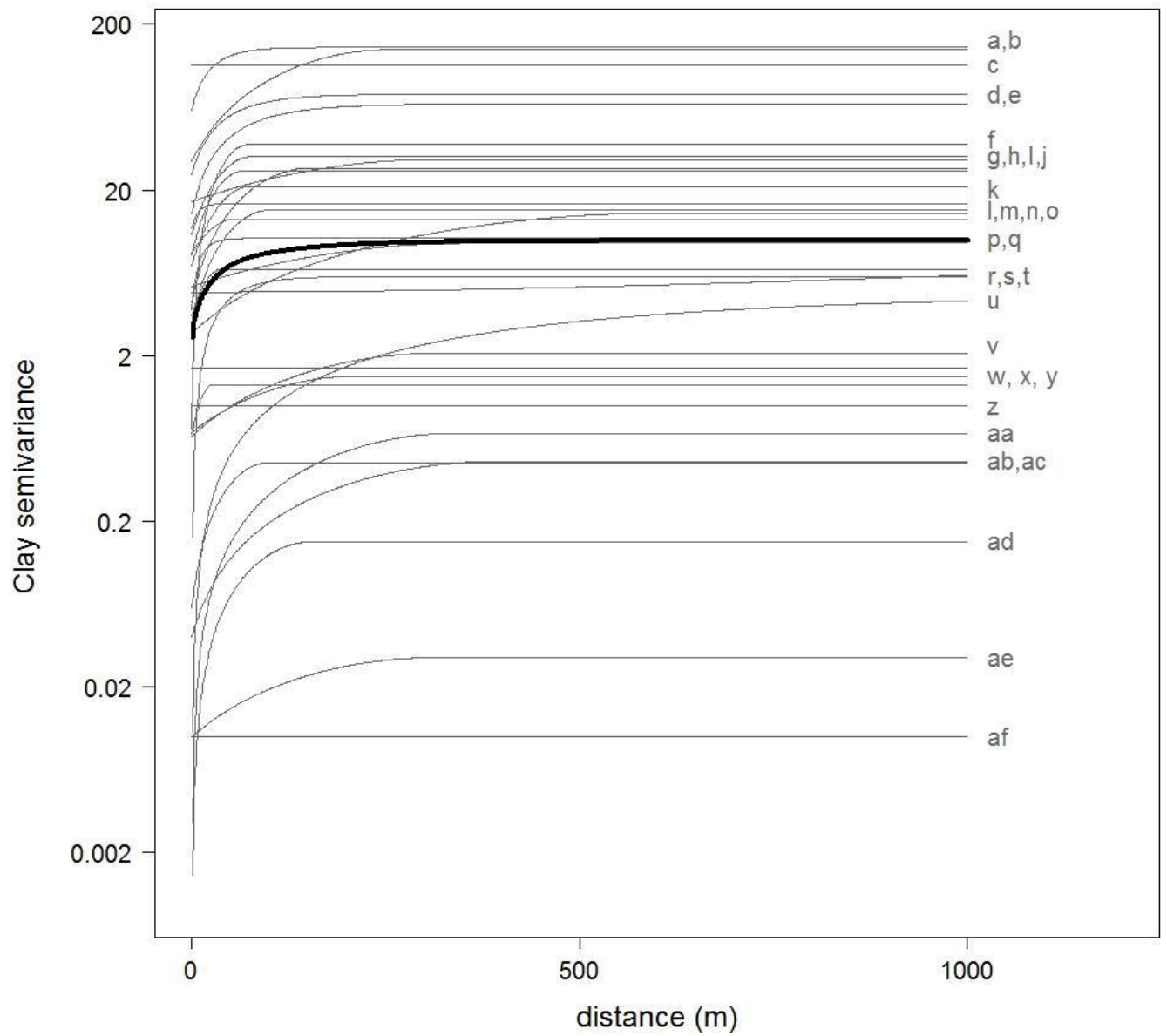


Figure 6.2. *Compilation of field scale variograms for Clay.* The bold black line represents the average variogram. Summary details and references for each variogram (a-ag) are given in Table 6.1.

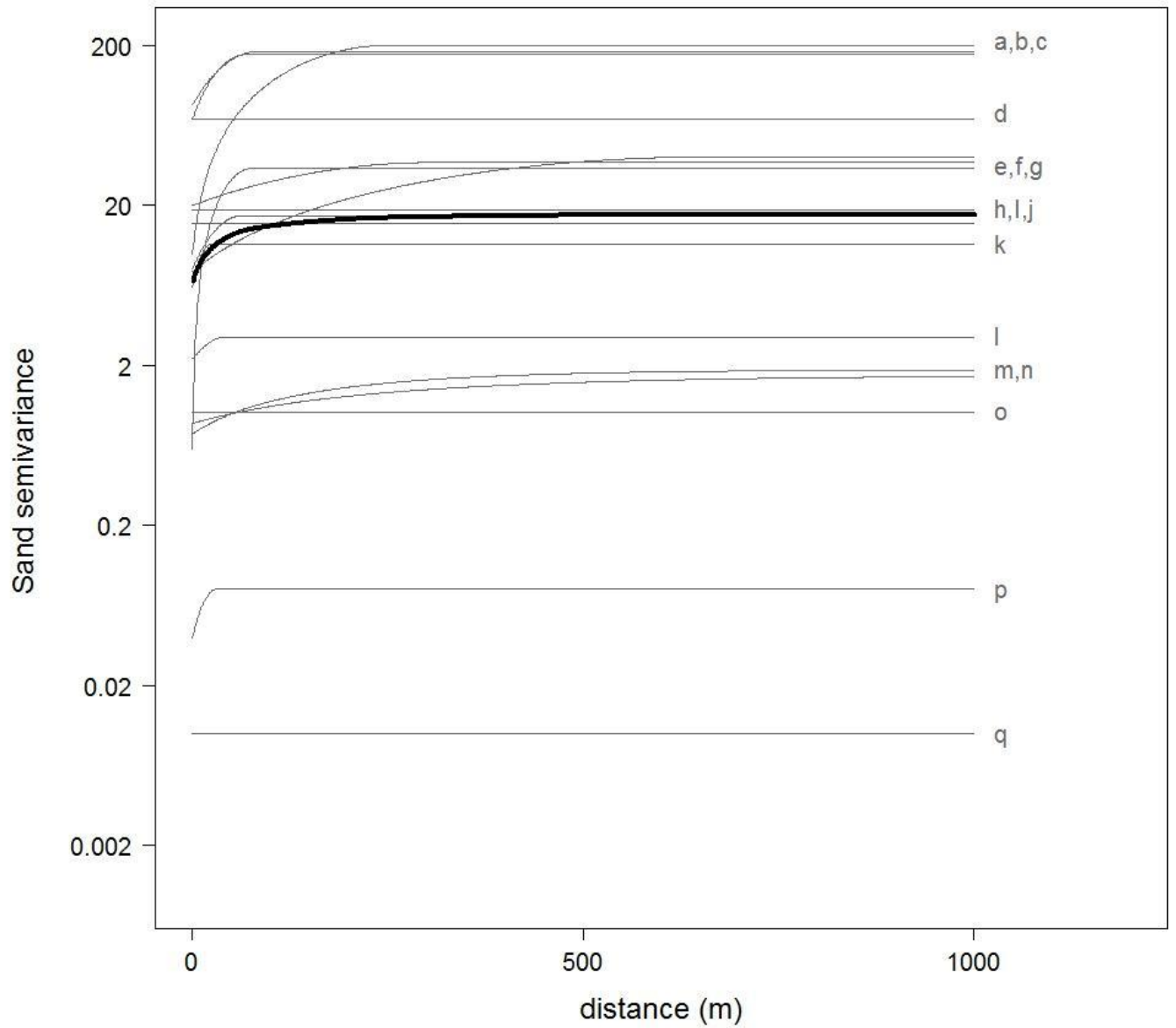


Figure 6.3. *Compilation of field scale variograms for Sand* The bold black line represents the average variogram. Summary details and references for each variogram (a-r) are given in Table 2.

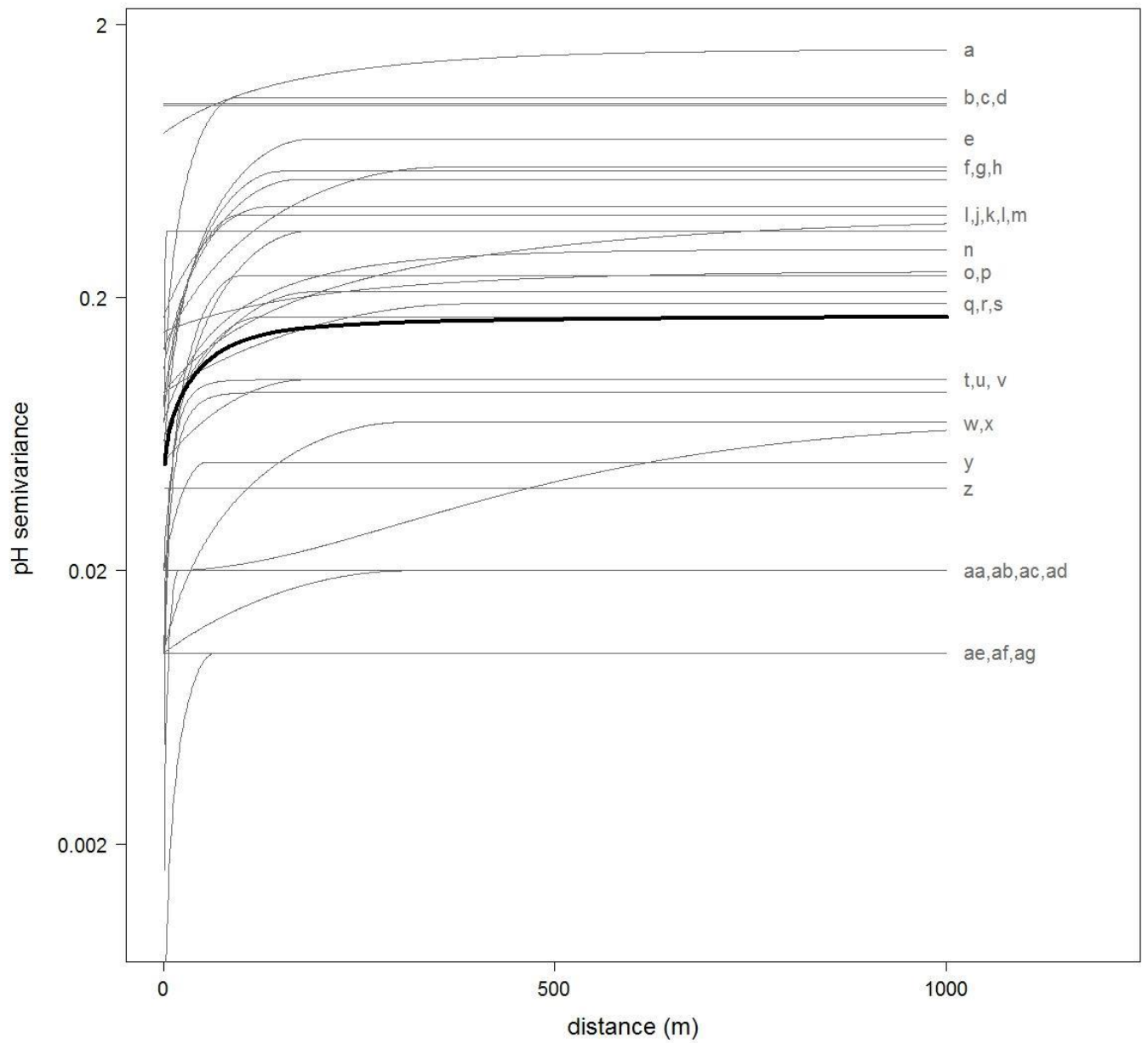


Figure 6.4. *Compilation of field scale variograms for pH.* The bold black line represents the average variogram. Summary details and references for each variogram (a-ag) are given in Table 6.3.

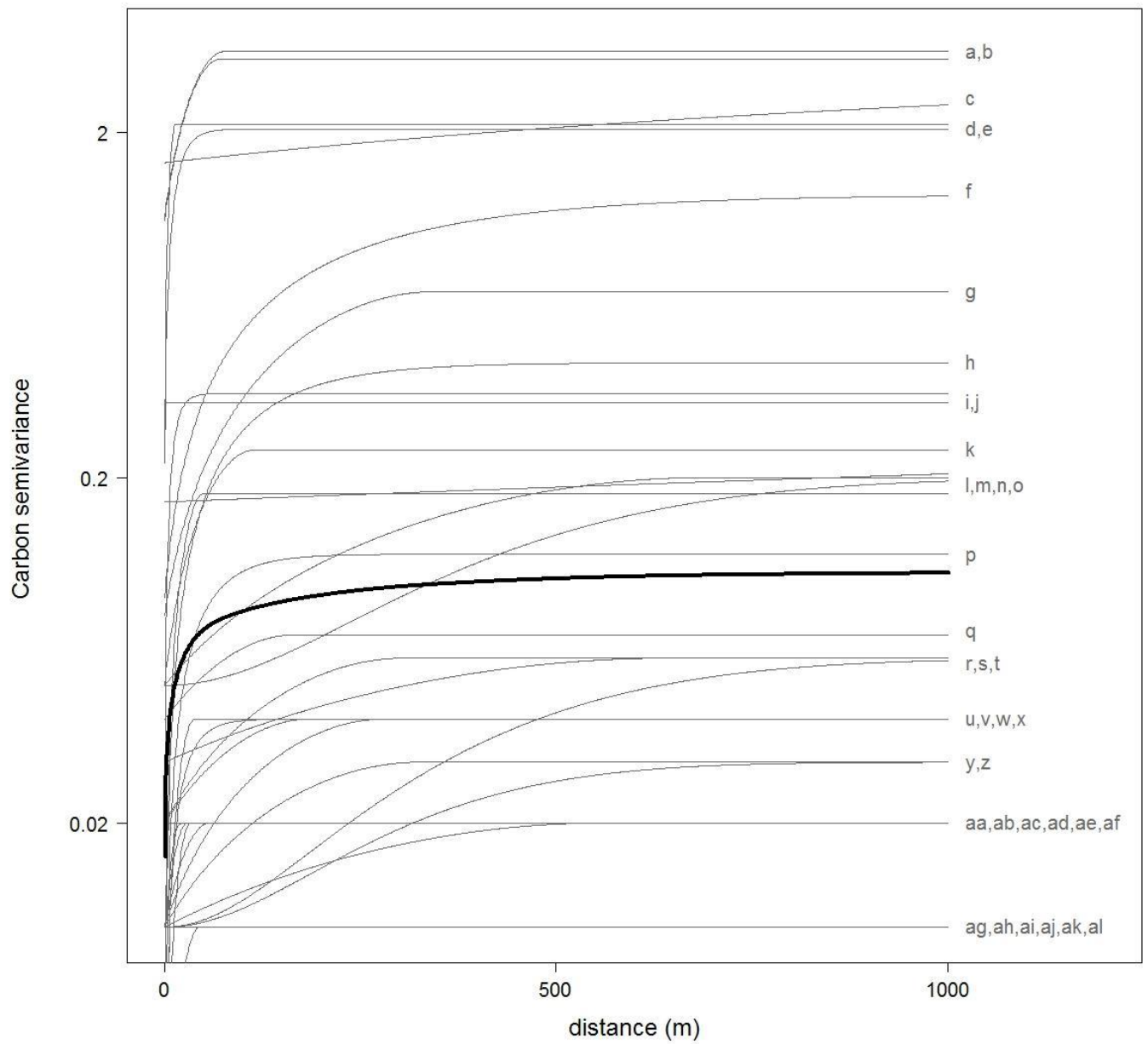


Figure 6.5. *Compilation of field scale variograms for Carbon.* The bold black line represents the average variogram. Summary details and references for each variogram (a-al) are given in Table 6.4.

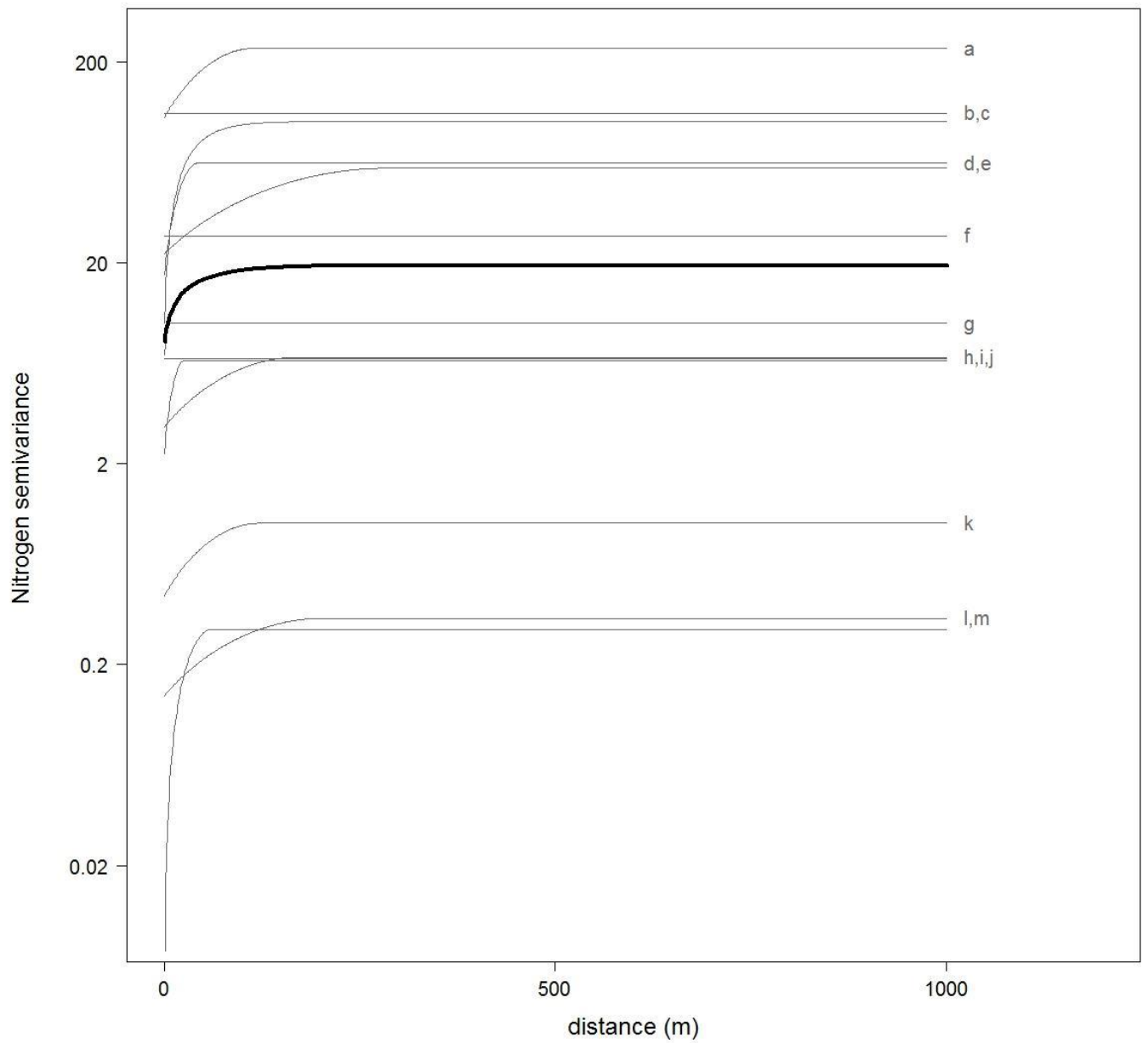


Figure 6.6. *Compilation of field scale variograms for Available Nitrogen.* The bold black line represents the average variogram. Summary details and references for each variogram (a-m) are given in Table 6.5.

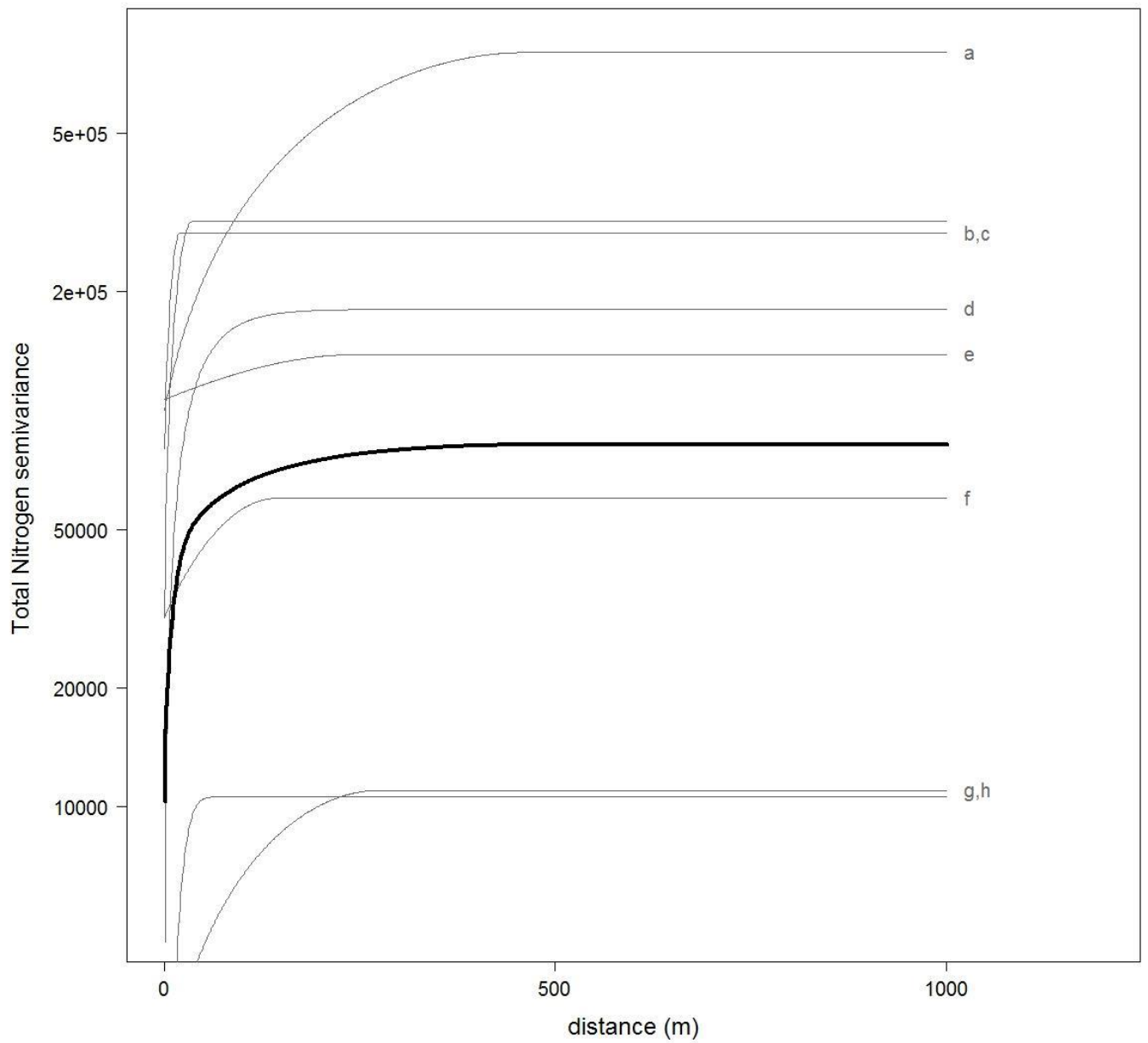


Figure 6.7. *Compilation of field scale variograms for Total Nitrogen.* The bold black line represents the average variogram. Summary details and references for each variogram (a-h) are given in Table 6.6.

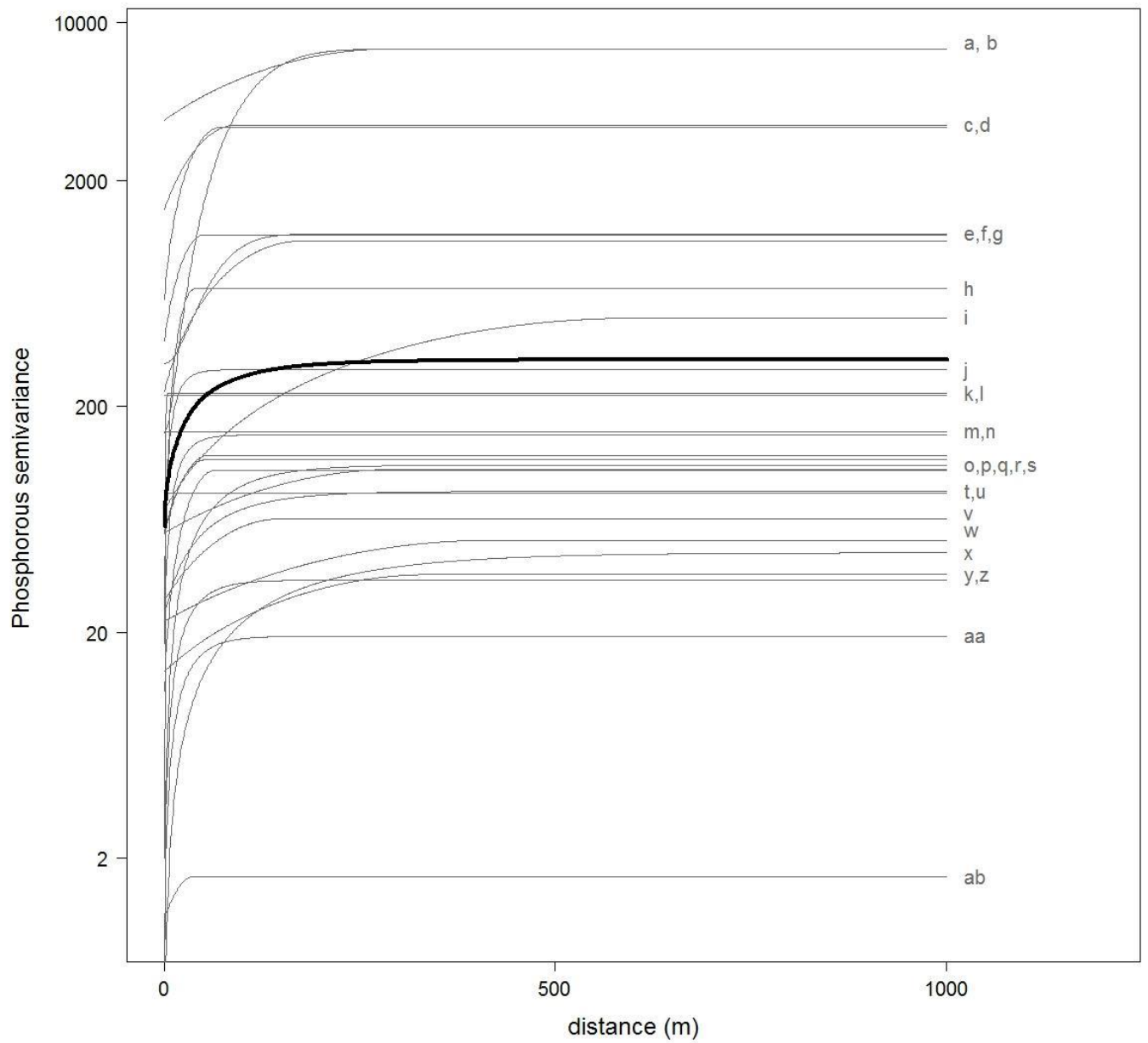


Figure 6.8. Compilation of field scale variograms for Phosphorus. The bold black line represents the average variogram. Summary details and references for each variogram (a-ab) are given in Table 6.7.

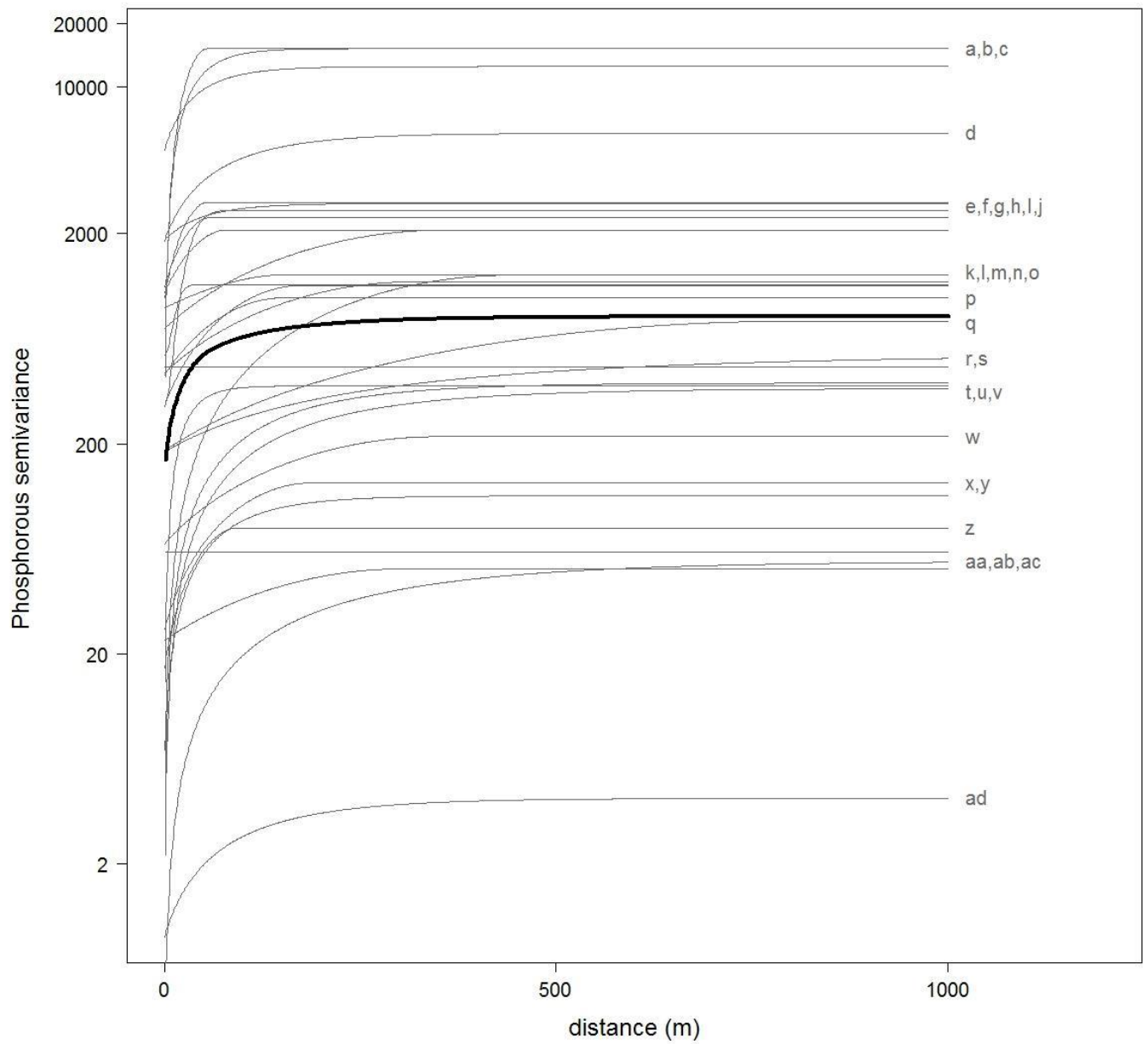


Figure 6.9. Compilation of field scale variograms for Potassium. The bold black line represents the average variogram. Summary details and references for each variogram (a-ad) are given in Table 6.8.

6.6 Estimation of the variogram from proportional variograms

McBratney and Pringle (1999) observe a strong relationship between mean squared and variance for several soil properties and develop a method for estimating a 'proportional variogram'. This method has the advantage of capturing the much higher levels of variability that tend to occur when the mean values of the property are extreme. Similar to McBratney and Pringle (1999), we find that some soil properties (Phosphorus, Nitrogen, Potassium and Carbon) appear to have a strong linear relationship between the mean and the standard deviation. This could imply that the calculation of a proportional variogram would be useful for these properties. However, closer interrogation reveals that this relationship is largely driven by high leverage points. It is not possible to fit a robust curve to link the mean and standard deviation. Proportional variograms are based on the relationship between the mean and the variance. Because we cannot be confident about this relationship, it is not prudent to calculate proportional variograms.

We advise against the use of proportional variograms as an estimate for variability, and as such do not update McBratney and Pringle's 1999 estimates of proportional variograms.

6.7 Estimation of the variogram from average variograms

McBratney and Pringle (1999) calculate average variograms for seven soil properties. These average variograms are calculated from the sample of variograms they compile. The fourth root transform of each approximated by the spherical model is taken, the models are averaged, and then the average is back transformed²⁵. Exponential or Spherical models are fitted to the back transformed average.

McBratney and Pringle (1999) note the broad spread of variability in the variograms they collected, and suggest that this might make the 'average' variograms less useful. Despite this, they suggest that the average variogram is a useful starting point where no other information is available. Kerry and Oliver (2003) find evidence that average variograms can be useful for prediction when parent material and soil forming factors are similar, but emphasise that they do not expect a global average variogram to provide much useful information.

We do not believe a global average provides useful information for predictive purposes. However, as McBratney and Pringle (1999) suggested, the average variogram does provide a useful reference for those interested in soil variability. We produce average variograms for illustrative purposes (by averaging the fourth-root transform of each variogram at finely spaced intervals, then plotting the back transformed values) but we do not fit these with a functional form.

²⁵ By taking the average from the fourth transform very high and low values carry less weight.

As suggested by McBratney and Pringle (1999) and illustrated by Kerry and Oliver (2004) the concept of the average variogram has the most use for prediction when it is calculated from a select subset of existing variograms. The diversity of climate regimes, soil types and land use for which field scale variograms have been calculated means that discretion is essential in the selection process. Differences in sampling regime, soil measurement protocols and geostatistical methods add another layer of complexity that needs to be navigated in appropriate selection. We discuss these issues further in the next section.

We advise against the use of the ‘global average’ variogram as an estimate of local soil variability. Instead, where suitable variograms are available, an average of variograms with similar conditions is taken. Discretion and expert knowledge will need to be used in this selection process. The process outlined by McBratney and Pringle (1999) for calculation of an average variogram can be followed.

6.8 Ancillary information

Kerry and Oliver have written several papers investigating the potential of using cheaper more densely available ancillary information to supplement expensive and sometimes sparse soil survey data. In 2004, they compared the spatial structure of a number of ancillary data sources to the spatial structure of a number of fixed soil properties. They found that variograms calculated from aerial colour photographs of 3.4 m ‘sampling density’ can estimate range with sufficient accuracy to helpfully guide sampling density of the soil survey. Their 2008 paper extends the use of ancillary information to kriging. They suggest that the primary requirement for using data is that the ancillary variogram has a similar sill to- nugget ratio to the property being studied.

Where it is available, ancillary information can be a useful source of information. Care must be taken in the selection of appropriate ancillary information. It may be useful to consult a range of ancillary variables.

6.9 Expert Knowledge

Truong et al. (2013) propose the use of expert knowledge as a means to estimate the variogram when there are not enough observations to calculate a reliable variogram using geostatistics. They point to an increasing realisation from other disciplines that experts’ knowledge provides a useful source of information that can be incorporated into statistical models, in particular through Bayesian approaches. Truong et al. (2013) also suggest that expert knowledge may be useful when there is no data available, or even when the available data for some reason are unreliable or unsuitable.

Truong et al. (2013) propose a strict methodology for eliciting knowledge from experts in order to construct a variogram. Their methods are designed to avoid bias. This process is still in the prototype stage. Currently, those seeking to supplement data with expert knowledge will not be able to avoid some bias. However, in many cases, subjective expert knowledge may be the best available option. Even when there are data available, a degree of subjectivity will be required to assess the usefulness and representativeness of these data. Where possible, it will obviously be preferred that these subjective decisions are informed by those with expertise in the area of interest (geographical or topical).

We strongly encourage the use of expert knowledge in the selection of appropriate datasets for the modelling of spatial variability. Where datasets are unavailable or deemed inappropriate, it may be necessary to rely entirely on expert knowledge to estimate the variogram. Eventually, it may be possible to elicit expert knowledge using a formal process such as that described by Truong et al. (2013).

6.10 Quick variograms

There may be situations when ancillary information, variograms from literature or even expert knowledge are unavailable or unreliable. In these cases, we would like to propose the following sampling approach that can be used to estimate a rough variogram at very low cost. The method proposed will necessarily be imprecise, but is a better alternative than not having any information. We anticipate that this method would be particularly useful in cases where alternative sources of information are available but unreliable.

We suggest sampling in 8 locations (4 widely spaced points, each with a closely spaced pair as per the diagram shown in Figure 6.10). Obviously, the sampling design will be affected by the shape of the field. We advise that sampling occurs as close to the boundaries as possible while avoiding the edge effect.

In Figure 10, one can calculate 4 bin sizes.

Close spacing (proxy for nugget): 4 pairs A-B, C-D, E-F, G-H

Maximum spacing (proxy for sill): 8 Pairs (A-G, A-H, B-G, B-H, C-E, C-F, D-E, D-F)

Intermediate spacing 1: 8 Pairs A-C, A-D, B-C, B-D, E-G, E-H, F-G, F-H

Intermediate spacing 2: 8 Pairs A-E, A-F, B-E, B-F, C-G, C-H, D-G, D-H

The close spacing (the close pairs) can be used as a proxy for the nugget, and the maximum spacing (the diagonals) can be used as a proxy for the total sill.

If the nugget and the sill are similar, we can assume that the appropriate model is the nugget model.

If the nugget and the sill are different, we will need to estimate the range and select a model for the variability.

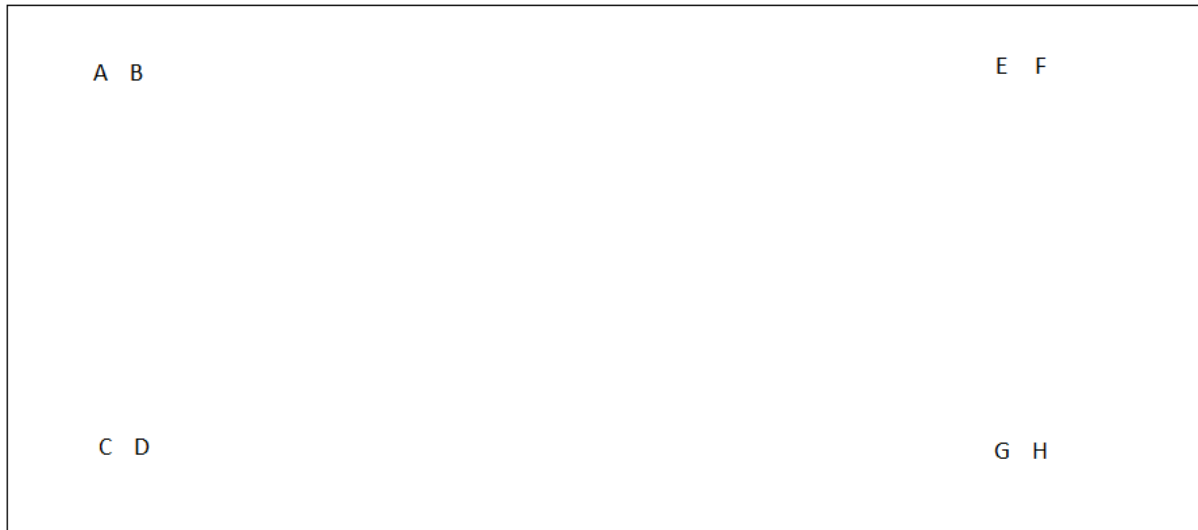


Figure 6.10. Sampling approach for estimating a 'rough' variogram. Here, it is shown that sampling is recommended in 8 locations (4 widely spaced points, each with a closely spaced pair, i.e. A-B, C-D, E-F and G-H). Each letter represents a sampling location.

There is no obvious proxy for the range that can be calculated from a small number of data points.

The two intermediate spacings may be useful to indicate where the range should occur. If they are similar to the total sill, then the range should be less than the intermediate spacings. If they are smaller than the total sill then the range should be greater than the intermediate spacings.

We suggest that the intermediate spacings be used to determine the limits of where the range could occur. The range should then be taken as the halfway point between the limits.

For example, if the smallest intermediate bin has a variance similar to the sill, then we should set the range to be equal to the halfway point between the nugget and the smaller intermediate bin. If both of the intermediate bins have variances smaller than the sill, we should set the range to be equal to halfway between the total sill and the intermediate bin.

Modelling a range larger than the maximum separation distance is always unlikely in variograms, because of the tendency of models to break down beyond half of the field extent. We do not think that unbounded models (i.e. ranges greater than the maximum separation distance) are necessary to consider here.

Quick variograms are not able to provide a precise estimation of soil variability. Their primary and important advantage is that they are calculated from data for the property of interest in the location of interest. Quick variograms provide a useful source of information when either: (i) there are no other sources of information available; or (ii) for checking alternative sources of information against a reference point.

6.11 Recommendations

- Where it is economically and practically feasible, best practice for estimating variograms is to conduct a preliminary survey and then a comprehensive field survey at the spatial scales of interest.
- Where resources for field survey are limited, it is desirable to find a variogram for the same property which has been calculated for a similar soil type. This variogram may be useful as a source of information for survey design. It may also be possible to use this variogram for kriging. Due to the large variability in soil variograms calculated for each soil property, it is critical to use discretion in this selection process.
- If more than one existing variogram from a similar soil type is identified, the information from both should be used. An averaging process may be a useful way to combine this information. Alternatively, they could be used separately to provide a range of predictions.
- Ancillary information (such as that from aerial photographs) should be considered to estimate variograms for soil properties. It can be used for survey planning and for kriging. Care must be taken to ensure that these variograms have a similar nugget to sill ratio to the property of interest. If available, it is preferred to use information from soil survey over ancillary information.
- If it is not possible to find a variogram for a similar area, other options are available. For example, expert knowledge could be consulted. Consultation of expert knowledge may occur in a formal process-based manner, or in a more informal way.
- Quick field surveys, with limited sampling may provide a cost-effective way to estimate rough variograms where other information is unavailable. These methods may also be useful when it is desirable to supplement information with observations directly from the field.
- Variograms are useful for designing detailed sampling surveys for agricultural and environmental purposes.

Table 6.2. Compilation of key properties for clay variograms

	Reference	Location	Climate ²⁶	Soil Type	Land Use	Timing	Measurement Method	Study Area (ha)	Sample Size	Mean	Standard Deviation	depth (cm)	Model	Nugget	Partial Sill	Range
a	Lopez-Granados 2002 (Site Two)	Caracol, Southern Spain		Vertic Xerochep	crop	before sowing	Bouyoucos densimeter	6	84	26.3	12	0-0.10	Exponential	61	84	29.9
b	Adderley et.al. 1997	Nigeria			Trees			30	480	25.8	9.1	0-0.10	Exponential	30	110	250
c	Lopez-Granados 2002 (Site One)	Monclova, Southern Spain		Alfisol	crop	before sowing	Bouyoucos densimeter	11.2	80	19.6	10.8	0-0.10	Nugget	113	0	0
d	Oliver and Webster 1987, (10-15)	Wyre forest, England		Acid brown loam	Forest			0.025	100			0-0.15	Exponential	24.9	50.7	51.6
e	Oliver and Webster 1987, (0-5)	Wyre forest, England		Acid brown loam	Forest			0.025	100	24.4	10.8	0 - 5	Exponential	14.34	51.8	65.7
f	Kerry & Oliver 2007							15	118	47.5	6.2		Spherical	0.72	36.72	71.48
g	Nolin et al. 1996	Quebec		Aquepts	crop			10	130	44.3	6	0 -15	Spherical	10.8	20.9	76
h	Shatar, 1996	Moree, Australia		Vertisol	crop			15	114	49	5.5	15 - 30	Spherical	17	13.5	310

²⁶ Unless otherwise specified mm refer to annual average rainfall, and C refers to average annual temperature

i	Kerry and Oliver 2007							44	294	17.9	7.3		Spherical	4.19	22.9	152	
j	Farooque, et al. 2012 (Site Two)	Nova Scotia, Canada		sandy loam, Orthic Humo-Ferric Podzols	orchard			Bouyoucos densimeter	1.6	86	9.6	4	0-15	Spherical	8.08	17.91	65.5
k	Miller et al. 1988.	Sacramento, California		Xererts, Xerochrepts	crop				8	99	37.1	4.6	Surface	Spherical	7	14	75
l	Shouse et.al. 1990	Texas, USA		Vertisol					0.3	203	40	3.9	0 - 30	Exponential	11.7	4.8	8.47
m	Kerry and Oliver, 2007	United Kingdom							10.5	205	30.2	5.8	0-15	Spherical	3.12	11.99	99.86
n	Liu et al. 2008	Henan Province, central China	monsoon climate 14.6C, 680mm	clay loam to loam	Tobacco Plantation	Before Sowing		Bouyoucos densimeter	87	81	41.7	3.4		Spherical	2.72	11.78	609
o	Williams, 1987 (4 directions average)	Oklahoma		Paleustolls	crop				1.62	108	22	2.3	0 - 30	Experimental	8.38	4.88	52.5
p	Shouse et al., 1990, (Field 1)	Texas, USA		Vertisol					0.3	182	51	3.1	0 - 30	Exponential	3.8	6.4	11.89
q	Shukla et al. 2004	Gross-Enzersdorf, Austria	510 mm, 10C	loam to sandy loam	crop	May		pipette method	6.25	60	46.8	4.6	0-15	Spherical	5.24	4.27	347
r	Shouse et al. 1990	Texas, USA		Vertisol					0.3	205	46.1	2.6	0 - 30	Spherical	3.5	3.1	36.58

s	Panagopoulos & Antunes 2008	Algarve region, south Portugal						400	81	32.7	7	0-20	Gaussian	4.83	5.77	1997.8	
t	Kristensen, et al. 1995	Riso, Denmark			Sandy loam/sandy clay loam	crop		10.9	270			0 - 25	Exponential	0	6	37	
u	Kristensen et al 1995 (Vindum)	Vindum, Denmark			Sandy loam	crop		10	302			0 - 25	Exponential	0	4.8	450	
v	Kilic, et al. , 2012, (5 years of cultivation)	Kaz Lake of Tokat, Turkey	436mm, 12C		Typic Ustifluent. Clay loam to sandy clay loam	crop/horticulture		Bouyoucos hydromete	0.8	46	21.7	6.3		Spherical	0.65	1.41	310.9
w	Tabor,et al. 1985	Arizona			Haplargid/Mollisol	crop		13	49	32.1	5.8	0 - 20	Linear	1.68	60.32	500	
x	Kilic et al., 2012	Kaz Lake of Tokat, Turkey	436mm, 12C		Typic Ustifluent. Clay loam to sandy clay loam	marshy plants		Bouyoucos hydromete	0.8	46	29.8	7.4	0-20	Spherical	0.69	0.81	207.8
y	Ayoubi, et al. 2007	Golestan province, Iran			fine, mixed, thermic, Fluventic Haploxerepts.	crop	before planting	Hydrometer method (Day, 1965);	1.8	101	56.3	1.1		Spherical	0.67	0.66	25.83
z	Kilic et al., 2012 cultivation	Kaz Lake of Tokat, Turkey	436mm, 12C		Typic Ustifluent. Clay loam to sandy clay loam	crop/horticulture		Bouyoucos hydromete	0.8	46	20.4	5.2		Linear	0.99	0	85.66
aa	de Souza 2010-Two	Araras, SouthEast Brazil	wet summer, dry winter		Oxisol (Typic Haplustox)	cropping	fall of 2004		22	90	34	0.2	0-20	Spherical	0	0.68	340

a	de Souza et al, 2010 - Site One	Araras, SouthEast Brazil	wet summer, dry winter	Oxisol (Typic cropping Haplustox)	fall of 2003	20	80	26.1	0.5	0-20	Spherical	0.04	0.42	393
ac	Kerry and Oliver, 2007					6.9	109	4.1	1		Spherical	0.06	0.39	96.17
a	Molin,et al. 2013- Field One	Sao Palo, southeast Brazil		Typic Dystrudoxes		19	42	21.5	5.1	0-20	Spherical	0	0.15	153
a	Molin et al., 2013 - Field Two	Sao Palo, southeast Brazil		Typic Hapludoxes		22	92	23.1	3.7	0-20	Spherical	0.01	0.02	307.3
af	Farooque et al., 2012: Site One	central Nova Scotia, Canada	sandy loam, Ferric Podzols			1	56	41.9	4.4	0-15	Linear	0.01	19.16	23.7

Table 6.3. Compilation of key properties for sand variograms

	Reference	Location	Climate	Soil Type	Land Use	Timing	Measurement Method	Study Area (ha)	Sample Size	Mean	Standard Deviation	depth (cm)	Model	Nugget	Partial Sill	Range
a	Adderly et al. 1997	Nigeria			Trees			30	157	56.8	10	0-10	Experimental	10	190	250
b	Lopez-Granados - 2002 Site Two	Caracol, Southern Spain		Vertic Xerochep	crop		Bouyoucos densimeter	6	84	33.4	13.4	0-10	Spherical	85	99	84.8
c	Farooque et al., 2012 - Site Two	central Nova Scotia, Canada		sandy loam, Orthic Humo-Ferric Podzols	orchard			1.6	86	48.7	12.5	0-15	Spherical	68.8	106.4	67.9
d	Granados - 2002 Site One	Moclova, Southern Spain		Alfisol	crop		Bouyoucos densimeter	11.2	80	57.4	8.5	0-10	Nugget	69	0	0
e	Liu et al., 2008	Henan Province, central China	monsoon 14.6C, 680mm	clay loam to loam,	Tobacco Plantation	Before Sowing	Bouyoucos densimeter	87	81	43.8	4.8	0-20	Spherical	7.7	32.43	657
f	Shatar (1996)	Moree, Australia		Vertisol	crop			15	114			15-30	Spherical	20	17	300
g	Miller et al. 1988	Sacramento, California		Xererts, Xerochrepts	crop			8	99	20.2	5.9	Surface	Spherical	0.6	33.4	75
h	Farooque et al., 2012: Site One	central Nova Scotia, Canada		sandy loam, Orthic Humo-Ferric Podzols	orchard			1	56	49.5	4.5	0-15	Linear	18.75	18.75	85.86

i	Williams et al. 1987, 4 directions averaged	Oklahoma, USA		Paleustolls	crop			1.62	108	27	4.8	0-30	Experimental	8	9.25	62.5
j	Tabor et al. 1985	Arizona, USA		Haplargid/Mollisol	crop			13	49	41.7	8.4	0-20	Linear	15.4	101.4	300
k	Shouse et al. 1990	Texas, USA		Vertisol				0.3	205	21.1	3.3	0-30	Spherical	6.2	5.2	22.86
l	Campbell 1977 Pawnee	Kansas, USA						1.6	160	8.5	2.9		Experimental	2.2	0.8	40
m	Kilic et al., 2012	Kaz Lake of Tokat, Turkey	436mm, 12C	Typic Ustifluent Clay loam to sandy clay loam	crop/horticulture		Bouyoucos hydrometer	0.8	46	25.5	9.7	0-20	Exponential	0.75	1.13	200.4
n	Kilic et al., 2012 - 5 years of cultivation	Kaz Lake of Tokat, Turkey	436mm, 12C	Typic Ustifluent. Clay loam to sandy clay loam	crop/horticulture		Bouyoucos hydrometer	0.8	46	33.5	10.3		Exponential	0.87	0.87	306
o	Kilic et al., 2012 - cultivation	Kaz Lake of Tokat, Turkey	436mm, 12C	Typic Ustifluent. Clay loam to sandy clay loam	crop/horticulture		Bouyoucos hydrometer	0.8	46	50.8	7.9		Linear	1.02	0	85.66
p	Campbell 1977 Ladysmith	Kansas, USA						1.6	160	1.2	0.3		Experimental	0.04	0.04	30
q	Ayoubi et al, 2007	Golestan province, Iran		fine, thermic, Fluventic Haploxerepts.	crop	before planting	Hydrometer method	1.8	101	2.2	0.1	0-30	Gaussian	0.01	0	91.41

Table 6.4. Compilation of key properties for pH variograms

	Reference	Location	Climate	Soil Type	Land Use	Timing	Measurement Method	Study Area (ha)	Sample Size	Mean	Standard Deviation	depth (cm)	Model	Nugget	Partial Sill	Range
a	Kilic et al., 2012 (unmodified)	Kaz Lake of Tokat, Turkey	436mm, 12C	Typic Ustifluent.	crop		Water 1:2.5	0.8	46	7.9	0.1	0-20	Exponential	0.8	0.82	209.6
b	Sidorova et al., 2012	Northwestern Russia			crop	before sowing	KCl		72	5.6	0.2	23	Spherical	0.08	1	93.1
c	Kilic et al., 2012 (20 year)	Kaz Lake of Tokat, Turkey	436mm, 12C	Typic Ustifluent.	crop		Water 1:2.5	0.8	46	8.1	0.2	0-20	Linear	1.03	0	85.66
d	Kilic et al., 2012 (5 year)	Kaz Lake of Tokat, Turkey	436mm, 12C	Typic Ustifluent.	crop		Water 1:2.5	0.8	46	7.8	0.2	0-20	Linear	1.01	0	85.66
e	Thompson et al., 2004 - Site One	Alabama, USA			crop			0.4	71			*11	Spherical	0.05	0.71	186.2
f	Pierce et al. 1995 (Durand)	Durand, USA		Alfisol, fine loam	crop			16	165	6.6	0.9	0-5	Spherical	0.13	0.47	354
g	Machado et al., 2007	Uberlandia, Brazil	tropical humid with dry season,	Red Latosol, moderate clayey texture	crop		water: 1:1	25	121	6	0.4	0-20	Spherical	0.07	0.51	150
h	Thompson et al., 2004 (Site Three)	Alabama, USA			crop			0.4	48			11	Spherical	0.11	0.43	168.9

i	Mulla, 1993	Washington, USA		Ultic Haploxeroll	crop			8	172	6.1	0.7	0-30	Spherical	0.17	0.26	132
j	Pierce et al., 1995 (Adrian)	Adrian, USA		Alfisol, loam	crop			10	74	6.5	0.9	0-5	Spherical	0.08	0.32	95
k	Camacho - Tamayo et al., 2007 (Site One)	Puerto L $\frac{1}{2}$ pez, Colombia	2,375 mm 27C	Typic Haplustox	crop	May-04	water (1:1) potentiometer	1.875	42	5.1	0.4	0-10	Exponential	0.09	0.31	410
l	Webster & McBratney 1987	Suffolk, England			crop		water	77	436	7.7	0.6		Spherical	0.02	0.33	185
m	Uehara, et al. 1985	Sitiung, Indonesia			crop			0.0784	137				Experimental	0	0.35	4
n	de Souza et al. 2010 (Site One)	Araras, SouthEast Brazil	wet summer, dry winter	Oxisol (Typic Haplustox)	crop	fall of 2003		20	80	5.6	4	0-20	Exponential	0.07	0.23	148
o	Adderley et al. 1997	Nigeria			forestry			30	480	6.3	0.5	0-10	Exponential	0.15	0.1	250
p	de Souza et al, 2010 (Site Two)	Araras, SouthEast Brazil	wet summer, dry winter	Oxisol (Typic Haplustox)	crop	fall of 2004		22	90	5.7	0.5	0-20	Spherical	0.01	0.23	97
q	Pierce et al., 1995 (Plainwell)	Plainwell, USA		Entisol, loamy sand	crop			22	174	6.7	0.4	0-20	Spherical	0.06	0.15	190
r	Thompson et al., 2004 (Site Two A)	Alabama, USA			crop			0.2	124			22	Spherical	0.09	0.1	393.2
s	Birrell 1996	Missouri, USA						28	504			0-15	Spherical	0.06	0.11	125

t	Thompson et al., 2004 (Site Two B)	Alabama, USA		crop				0.4	58			22	Spherical	0.05	0.05	181.1
u	Kristensen et al., 1995 (Riso)	Riso, Denmark		Sandy loam/sandy clay loam	crop			10.9	270			0-25	Exponential	0	0.1	17
v	Kristensen et al., 1995 (Vindum)	Vindum, Denmark		Sandy loam	crop			10	302			0-25	Exponential	0	0.09	19
w	Liu et al., 2008	Henan Province, central China	monsoonal 14.6C, 680mm	clay loam to loam,	crop	Before sowing	water (1: 2.5)	87	81	7.7	0.3	0-20	Spherical	0.01	0.06	308
x	Mondo, et al., 2012	Sao Paulo, Brazil	not specified		crop	after		22	33	5	0.2	0-20	Gaussian	0.02	0.05	650
y	Laslett et al., 1987	Brisbane, Australia			pasture		CaCl2	1	121	4.5	0.2		Spherical	0.02	0.03	55
z	Campbell, 1977 (Pawnee)	Pawnee, Kansas, USA					CaCl2 (1:2)	1.6	160	6.5	0.3		Experimental	0.04	0	0
aa	Silva, et al., 2003	Santa Maria, Brazil		Ultisol dystrophic Hapludalf	crop	before sowing	water 1:1	0.3	192	4.9	0.1	0-20	Spherical	0	0.02	18.66
ab	Campbell, 1977 (Ladysmith)	Ladysmith, Kansas, USA					CaCl2 (1:2)	1.6	160	6.5	0.2		Experimental	0.02	0	0
ac	Shatar, 1996	Moree, Australia		Vertisol	crop		CaCl2 (1:5)	15	114	7.4	0.2	5:30	Spherical	0.01	0.01	310
ad	Tabor et al., 1985	Arizona		Haplargid/Mollisol	crop			13	49	7.3	0.2	0-20	Linear	0.02	0.06	500

ae	Lopez Granados, 2002 (Site One)	– Moncolova, Southern Spain		Alfisol	crop	before sowing	0.1 mol KCl	11.2	80	7.8	0.1	0-100	Spherical	0	0.01	66
af	Lopez-Granados, 2002 (Site Two)	Caracol, Southern Spain		Vertic Xerochep	crop	before sowing	0.1 mol KCl	6	84	7.7	0.1	0-100	Nugget	0.01	0	0
ag	Shukla et al., 2004	Gross-Enzersdorf, Austria	510mm 10C	loam to loam	sandy	crop	May	6.25	60	NA	NA	0-15	Spherical	0.01	0	158
ah	Ayoubi et al., 2007	Golestan province, Iran		Fluventic Haploxerepts.	crop	before sowing	0.1 mol KCl	1.8	101	7.9	0	0-30	Spherical	0.001	0.001	24.39

Table 6.5. Compilation of key properties for carbon variograms

	Reference	Location	Climate#	Soil Type	Land Use	Timing	Measurement Method *	Study Area (ha)	Sample Size	Mean	s.d.	depth (cm)	Model	Nug.	Partial Sill	Range
a	Farooque et al. , 2012 (Site One -1)	central Nova Scotia, Canada		sandy loam, Podzols	orchard	May July 2009	OM (LOI)	1	56	6.6	1.5	0-15	Sph.	1.14		
b	Farooque et al. , 2012 (Site One -2)	central Nova Scotia, Canada		sandy loam, Podzols	orchard	Jun-10	OM (LOI)	1	56	6.6	1.4	0-15	Sph.	1.11	2.28	76.1
c	Panagopoulos & Antunes, 2008	Algarve region of south Portugal	Mediterranean	Mostly Lithosols	forestry, crop		OM (WB-wet)	400	81	1.2	0.5	0-20	Exp.	1.63	2.14	70.23
d	Farooque et al. , 2012 (Site Two -2)	central Nova Scotia, Canada		sandy loam, Podzols	orchard	Jun-11	OM (LOI)	1	56	24	5.7	0-16		0.25	1.95	1997.8
e	Farooque et al. , 2012 (Site Two -1)	central Nova Scotia, Canada		sandy loam, Podzols	orchard	May July 2009	OM (LOI)	1.6	86	4.9	1.3	0-15	Exp.	0.22	1.86	13.7
f	Kilic et al. , 2012 (5 years)	Kaz Lake of Tokat, Turkey	436mm, 12C	Typic Ustifluent.	crop		OM (WB-wet)	0.8	46	1	0.3	0-20	Exp.	0.09	1.82	14.6
g	Nolin et al. , 1996	Quebec, Canada		Aquepts	crop		OC	10	130	2.8	0.7	0 - 15	Sph.	0.08	1.23	224.5
h	Kristensen et al. 1995, (Riso)	Riso, Denmark		Sandy loam - sandy clay loam	crop		OC	10.9	270			0 - 25	Exp.	0	0.61	343
i	Kilic et al. , 2012 (10 years)	Kaz Lake of Tokat, Turkey	436mm, 12C	Typic Ustifluent	crop		OM (WB-wet)	0.8	46	0.7	0.3	0-20	Exp.	0	0.43	99
j	Kilic et al. , 2012 (uncultivated)	Kaz Lake of Tokat, Turkey	436mm, 12C	Typic Ustifluent	crop		OM (WB-wet)	0.8	46	1.6	0.4	0-20	Lin.	0.33	0.35	9.6
k	Mulla, 1993	St. John, Washington, USA		Ultic Haploxeroll	crop		OC	8	172	1.2	0.5	0 - 30	Sph.	0.05	0	85.66
l	Gutierrez et al. 2010	Municipality of Pasca, Colombia	1,800mm, 16-C	Entisols and others	horticulture		OC	1.5	64	6.4	0.3	0-20	Sph.	0.17	0.19	114
m	Nanni et al. , 2011	Sao Paulo state, Brazil	mesothermic climate	Oxisols, Entisols, Alfisols, Ultisols, Inceptisols and Molisols	crop		OM ¹	184	184	0.7	0.4	0-20	Sph.	0.05	0.24	10240
n	Zanão Júnior et al. , 2010	South Eastern Brazil	1,500 mm.	Oxisol Hapludox (medium Clay)	crop	May to June 2003.	OM	25	121	1.7	0.2	0-10	Gaus	0.05	0.15	691

o	Cahn et al. , 1994	0.25	Central Illinois		Mollisol	crop		OC	0.25	200	1.7	0.3	0 - 15	Exp.	0	0.15	539
p	Kristensen et al. 1995, (Vindum)		Vindum, Denmark		Sandy loam	crop		OC	10	302			0 - 25	Exp.	0	0.18	50
q	Shukla et al 2004		Gross-Enzersdorf, Austria	temperate and continental, 510mm 10C	loam to sandy loam	crop	May	OC	6.25	60	1.4	0.2	0-15	Sph.	0.04	0.12	45
r	Rowlands 1, 1998**		Wyalkatchem, WA		Duplex	crop		OC	75	56	0.7	0.2	0-10	Sph.	0.03	0.03	163
s	de Souza et al, 2010 (Site Two)		Araras, SouthEast Brazil	wet summer, dry winter	Oxisol (Typic Haplustox)	crop	fall of 2004	OM	22	90	15.1	9.7	0-20	Sph.	0.02	0.03	638.985
t	Mondo et al., 2012		Sao Paolo, Brazil			crop	after harvest	OM	22	33	0.7	0.2	0-20	Gaus	0.01	0.04	304
u	Camacho-Tamayo et al. , 2008 (Site 1)		Puerto Lopez, Colombia	2,375 mm: 27C	Typic Haplustox	crop	May-04	OC (mod- WB)	1.9	42	1.3	0.2	0-10	Exp.	0	0.05	498.2
v	Shukla et al. 2004		Gross-Enzersdorf, Austria	temperate and continental, 510mm 10C	loam to sandy loam	crop	May	OC	6.25	60	1	0.2	0-15	Sph.	0.02	0.04	22.1
w	Shatar (1996)		Moree, Australia		Vertisol	crop		OC	15	114	1.1	0.2	15 - 30	Sph.	0.01	0.02	184
x	Zhang et al., 2016		Jiangsu Province, China			crop	2012	OM	7	136				Sph.	0	0.03	280
y	de Souza et al. , 2010 (Site One)		Araras, SouthEast Brazil	wet summer, dry winter	Oxisol (Typic Haplustox)	crop	fall of 2003	OM	20	80	10.7	1.4	0-20	Sph.	0.01	0.04	38.6
z	Amirinejad et al. , 2011		Uttar Pradesh, India		Inceptisol	crop		OC (WB)	19.6	145			0-15	Gaus	0.01	0.02	324
aa	Kumhalova, et al. , 2011 (sampled 2005)		Prague, Ruzyne, Czech Republic	526mm: 7.9C	Haplic Luvisol.	crop		OC	11.5	70	2.1	0.2		Sph.	0.02	0.02	380.73
ab	Camacho - Tamayo et al. , 2008 (Site 2)		Puerto Lopez, Co lombia	2,375 mm, 27 C	Typic Hapludox	crop	Aug-04	OC (mod- WB)	1.875	42	1.6	0.1	0-10	Sph.	0	0.01	240.5
ac	Liu et al. , 2010		Henan Province, central China	monsoon climate 14.6C, 680mm	Sandy to medium clay loam	crop	After harvest,	OM (WB-wet)	4	111	1	0.1	0-20	Sph.	0.01	0.02	33.5
ad	Liu et al. , 2008		Henan Province, central China	monsoon climate 14.6C, 680mm	clay loam to loam	crop	Before Sowing	OM ²	87	81	0.7	0.1	0-20	Sph.	0.01	0.01	56.5
ae	Ayoubi et al. , 2007		Golestan province, Iran		Fluentic Haploxerepts.	crop	before planting	OM (WB)	1.8	101	1.5	0.1	0-30	Sph.	0.01	0.01	556
af	Silva et al., 2003		Santa Maria, Brazil		Ultisol dystrophic Hapludalf	crop	before sowing	OM ³	0.3	195	1.6	0.1	0-20	Gaus	0.01	0.01	29.28
ag	Kumhalova et al. , 2011 (sampled 2004)		Prague, Ruzyne, Czech Republic	526mm: 7.9C	Haplic Luvisol	crop		OC	11.5	70	1.7	0.2		Sph.	0.01	0.01	9.5

ah	Kumhalova et al. , 2011 (sampled 2006)	Prague, Ruzyně, Czech Republic	526mm: 7.9C	Haplic Luvisol	crop		OC	11.5	70	1.9	0.2		Sph.	0.01	0.01	274.6
ai	Goovaerts & Chiang, 1993 (average)	Belgium		Typic Hapludalf			OC	0.16	73	0.7	0.1	0 - 20	Sph.	0.01	0.05	244.7
aj	Chung et al. 2008	Korea	12.7C, 1560*	Coarse, loamy, mixed, non acid, mesic	crop	after harvest	OM ⁴	0.3	246	1.3	0.1	0-15	Lin.	0.01	0	11.5
ak	Granados - 2002 Site One	monclova, Southern Spain		Alfisol	crop	pre planting	OM ⁵	11.2	80	0.9	0.1	0-10	Nug.	0.01	0	NA
al	Lopez-Granados - 2002 Site Two	Caracol, Southern Spain		Vertic Xerochep	crop	pre planting	OM ⁵	6	84	0.8	0.1	0-10	Sph.	0	0	0
am	Chatterjee et al. , 2015	West Bengal, India	1443 mm, hot and humid		crop	after harvest	OC (WB)	81	100	0.5	0.1	0-15	Lin.	0	0.01	44.8
an	Kumhalova et al. , 2011- (sampled 2007)	Prague, Ruzyně, Czech Republic	526mm: 7.9C	Haplic Luvisol	crop	not specified	OC	11.5	70	2	0.2		Sph.	0	0.01	58
ao	Bai & Wang, 2011	Shaanxi Province, China	393 mm	Silty loams	orchard		OC ⁶	0.275	125	0.3	0.1	0-10	Exp.	0	0.07	247.1

* Measurement Method refers to the original property which was measured. All values have been converted into OC.

** Unpublished data provided provided by Pringle for original article

¹ Organic matter (OM), total and effective acidity (determined by 1 M calcium acetate - Ca(CH₃COO)₂ H₂O and 1M KCl titulometric method, respectively),

² potassium bichromate titrimetric method

³ photolorimetry

⁴laboratory analysis was completed by the Soil Management Division - NIAST, RDA

⁶ oil bath titration

Table 6.6. Compilation of key properties for available nitrogen variograms

	Reference	Location	Climate#	Soil Type	Land Use	Timing	Measurement Method	Study Area (ha)	Sample Size	Mean	s.d.	depth (cm)	Model	Nug.	Partial Sill	Range
a	Liu et al. , 2010	Henan Province, Central China	monsoon climate 14.6C, 680mm	Sandy to medium clay loam	crop	After harvest	Alkaline hydrolyzable N (AN) ¹	4	111	75	14.3	0-20	Spherical	105.6	127.3	112.6
b	Liu et al. , 2008	Henan Province, Central China	monsoon climate 14.6C, 680mm	clay loam to loam	crop	Before Sowing	alkalytic (AN) ¹	N 87	81	70.6	10.3	0-20	Linear	110.46	0	NA
c	Lopez-Granados, 2002 (Site Two)	Caracol, Southern Spain		Vertic Xerochep	crop	before winter sowing	Nitrate ²	6	84	23.2	10.2	0-10	Exponential	10	91	31.7
d	Chatterjee et al, 2015	West Bengal, India	hot and humid		crop	after harvest	Available N ³	81		76.7	7.8	0-15	Spherical	17.38	45.26	43
e	Shire 3*, 1997	Wyalkatchem, Western Australia		Duplex	crop		Nitrate	90	88	22.9	7.6	0-10	Spherical	22.14	36.86	281.432
f	Lopez-Granados, 2002 Site One	Moclova, Southern Spain		Alfisol	crop	before winter sowing	Nitrate ²	11.2	80	7.1	5.3	0-10	Nugget	27.2	0	0
g	Cahn et al. , 1994 0.25 ha	Central Illinois		Mollisol	crop		Nitrate	0.25	200	6.2	3.7	0 - 15	Experimental	7	3	5
h	Everett & Pierce, 1996	Michigan		Loamy sand, sandy loam	crop		Nitrate	22.6	60	6.2	2.2	0 - 30	Spherical	3.05	3.7	167.05
i	Tabor et al. , 1985	Arizona		Haplargid/Mollisol	crop		Nitrate	13	49	13.6	4.2	0 - 20	Linear	6.66	11.12	200

j	van Meirvenne & Hofman, 1989	Belgium	Udifluent	horticulture	Nitrate	1	247	8.9	2.7	0 - 100	Experimental	2.25	4.25	25
k	Wade et al., 1996 (Pasture)			pasture	Nitrate		86	0.8	0.8	0-10	Experimental	0.44	0.57	120
l	Cambardella et al., 1994	Iowa	Udic/argic mollisols	crop	Nitrate	10	72	7.2	1.3	0 - 15	Spherical	0.14	0.2	201
m	Wade et al., 1996, (Arable)	Warwickshire, England			Nitrate		81	0.7	0.5	0-10	Experimental	0	0.3	60

* Unpublished data provided provided by Pringle for original article

¹ Alkaline hydrolyzable N was measured using the alkaline hydrolysis diffusion method (Bao, 2005).

² Nitrate determined by colorimetry in SKALAR.

³ Available N content was determined by alkaline per- manganate method as described by Subbiah and Asija (1956).

Table 6.7. Compilation of key properties for total nitrogen variograms

Reference	Location	Climate#	Soil Type	Land Use	Timing	Measurement Method	Study Area (ha)	Sample Size	Mean	s.d.	depth (cm)	Model	Nug.	Partial Sill	Range
a Ganawa et al. , 2003	Sawah Sempadan Malaysia		Jawa, Teluk, Karang, Sempadan and Sedu	crop	Before Planting	¹	2300	120	4140	870	0-20	Spherical	100,000	700,000	460
b Yana et.al. 2000	Takatsuki, Japan	15.8°C, 1,240 mm	Clay loam		after transplanting	dry combustion	0.5	91	3100	449.5		Spherical	30,000	270,000	35.5
c Yana et.al. 2000	Takatsuki, Japan	15.8°C, 1,240 mm		crop	after harvest	dry combustion	0.5	91	3400	452.2		Spherical	80,000	200,000	19.5
d Zhang et al., 2016	Jiangsu Province, China			crop			7	136				Exponential	0	180,000	39.08
e Shukla et al. , 2004	Gross-Enzersdorf, Austria	510mm, 10C	loam to sandy loam	crop	May	Kjeldahl method	6.25		1328.6	381	0-15	Spherical	106,576	31,746	243.6
f Nouri et al. , 2010	Fesaran village, Esfahan		clay loam and loam	horticulture	Before fertigation	Nitrate	87	60			0-30	Spherical	30,000	30,000	141.8
g Liu et al. , 2008	Henan Province, central China	monsoon climate 14.6C, 680mm	clay loam to loam	crop	Before sowing	Kjeldahl method	87	81	730	100	0-20	Spherical	2,000	9,000	274
h Ayoubi et. al, 2007	Golestan province, Iran		fine, mixed, thermic, Fluventic Haploxerepts.	crop	before sowing	Kjeldahl method	1.8	101	1300	110	0-30	Gaussian	600	10,000	23.99

i	Chung et al. , 2008	Korea	12.7C , 1560mm*	Coarse Loamy	crop	after harvest	²	0.3	246	1500	100	Exponential	0	0	4.5
---	---------------------	-------	--------------------	--------------	------	---------------	--------------	-----	-----	------	-----	-------------	---	---	-----

¹sulfuric-salicylic acid digestion method

²laboratory analysis was completed by the Soil Management Division - NIAST, RDA

Table 6.8. Compilation of key properties for phosphorus variograms

	Reference	Location	Climate#	Soil Type	Land Use	Timing	Measurement Method	Study Area (ha)	Sample Size	Mean	s.d.	depth (cm)	Model	Nug.	Partial Sill	Range
a	McBratney et al. 1985	Narrabri, NSW, Australia		Vertisol	crop		P (NaHCO ₃ soluble)	1	386	129.6	58.8	0-7.5	Gaussian	152.85	7489.55	109.64
b	Chatterjee et al. , 2015	West Bengal, India	hot and humid 1443 mm		crop/ horticulture	after harvest	Available P ₂ O ₅ ¹	81		172.4	82.4	0-15	Spherical	3700.68	3925.85	283
c	Mondo et al. , 2012	Sao Paulo, Brazil			crop	After harvest	P resin	22	33	239.6	59.6	0-20	Spherical	1484.69	2030.1	89.9
d	Cambardella et al. , 1994 (Pothole field)	Iowa, USA		Udic/Aquic mollisols	crop		P (Bray No. 1)	6.25	241	126	55.6	0-15	Spherical	596.9	2839	71
e	Delcourt et al. , 1996	Leefdael, Belgium		Silty	crop		P (colorimetric)					0 - 25	Gaussian	310	850	74.5
f	Cahn et al. , 1994, 0.25 ha	Central Illinois, USA		Mollisol	crop		P (Bray No. 1)	0.25	200	74	26.8	0-15	Experimental	390	760	50
g	Pierce et al. 1995, (Plainwell)	Plainwell, USA		Entisol, loamy sand	crop		P (not specified)	22	174	124	32	0 - 20	Spherical	233	844	172
h	Camacho - Tamayo et al. , 2008 (Site Two)	Puerto Lopez, Colombia	2 375 mm 27 C	Typic Hapludox	crop	Aug-04	P (Bray II)	1.875	42	28.8	25.8	0-10	Spherical	2	660.5	38.4

i	Ganawa, et al. , 2003	Sawah Sempadan Malaysia	Jawa, Karang, Sempadan and Sedu	Teluk, and	crop	Before Planting	available NH4 ²	P	2300	120	50.2	22.5	0-20	Spherical	69	422	597
j	Nolin et al. , 1996	Quebec, Canada	Aquepts		crop		P (Melich III)		10	130	52	18.5	0-15	Exponential	35.1	255.5	13
k	Chung et al. , 2008	Korea			crop	after harvest	³		0.3	246	119	15.5		Spherical	17.8	210.3	4
l	Pierce et al. , 1995 Durand	Durand, USA	Alfisol, fine loam		crop		P (not specified)		16	165	35	21	5:20	Linear	223	163	294
m	Camacho - Tamayo et al. , 2008 (Site One)	Puerto Lopez, Colombia	2 375 mm 27 C	Typic Haplustox	crop	May-04	P (Bray II)		1.875	42	11.1	14.2	0-10	Linear	154.4	262.9	373.4
n	Frogbrook et al. 2002 (sampled 1998)					before fertilisation			16.5					Exponential	17.95	131.5	17.07
o	Frogbrook et al. 2002 (sampled 1999)								16.5					Spherical	54.58	66.61	54.9
p	Frogbrook et al. 2002 (sampled 1997)								16.5					Spherical	56	59.72	49.95
q	Kristensen et al. 1995 (Riso)	Riso, Denmark	Sandy loam/sandy loam	clay	crop		Available P		10.9	270			0 - 25	Exponential	0	110	60

r	Shatar 1996	Moree, Australia		Vertisol			Available P	15	114	18	1	15 - 30	Spherical	55	50	290	
s	Sidorova et al., 2012	Northwestern Russia			crop		available P ⁴		72	484.9	65.6		Spherical	11	93	63.7	
t	Pierce et al. 1995 (Adrian)	Adrian, USA		Alfisol, loam	crop		P (not specified)	10	74	23	9	0 - 5	Exponential	23.6	60.49	68	
u	Machado et.al. 2007	Uberlandia, Brazil	tropical humid with dry season,	Red Latosol, moderate clayey texture	crop			25		12.4	9.1	0-20	Linear	82.33	0	NA	
v	Mulla, 1993	St. John, Washington, USA		Silt loam (Ultic Haploxeroll)	crop		P (acetate extractable)	8	172	15.2	7.7	0 - 30	Spherical	27.58	35.8	145	
w	Rowlands 1*, 1998	Wyalkatchem, WA, Australia		Duplex	crop		P (not specified)	75	56	31.9	7	0 - 10	Spherical	22.32	28.72	414.604	
x	Kristensen et al. 1995 (Vindum)	Vindum, Denmark		Sandy loam	crop		Available P	10	302			0 - 25	Exponential	0	45	148	
y	Liu et al., 2008	Henan Province, central China	monsoon climate 14.6C, 680mm	clay loam to loam,	crop	Before Sowing,	Available P ⁵	87	81	16.1	5.9	0-20	Spherical	13.4	22.59	337	
z	Lopez-Granados - 2002 (Site Two)	Southern Spain (Caracol)		Vertic Xerochep	crop	before crop	Available P ⁶	6	84	11.3	5.6	0-10	Exponential	0.7	33.3	28.3	
aa	Lopez-Granados - 2002 (Site One)	Southern Spain (Monclova)		Alfisol	crop	before crop	Bray extractable P ⁶		11.2	80	15.5	4.4	0-10	Exponential	0.6	18.6	27.4

ab	Ayoubi et al. , 2007	Golestan province, Iran	fine, thermic, Haploxerepts.	mixed, Fluventic	crop before crop	Available P ⁷	1.8	101	27.2	1.3	0-30	Spherical	1.08	0.57	35.58
----	-------------------------	----------------------------	------------------------------------	---------------------	---------------------	--------------------------	-----	-----	------	-----	------	-----------	------	------	-------

* Unpublished data provided by Pringle for original article

¹ Available P₂₀₅Olsen method by way of extracting 2.5 g of soil with 50 ml of 0.5MNaHCO₃ (pH 8.5) for 30 min and determining the phosphorus in the extract by the L-ascorbic acid method (Murphy and Riley 1962).

² available P NH₄F-HCl extraction method

³ laboratory analysis was completed by the Soil Management Division - NIAST, RDA

⁴ Available P (the Tsl- NAO modification of the Kirsanov method).

⁵ Available P Olsen extraction method using alkaline sodium bicarbonate as the extractant in a 20:1 ratio

⁶ Bray extractable P measured by colorimetry using ascorbic acid, ammonium molybdate reagents

⁷ Available P measured by colorimetry using ascorbic acid-ammonium molybdate reagents (Olsen, 1982)

Table 6.9. Compilation of key properties for potassium variograms

	Reference	Location	Climate#	Soil Type	Land Use	Timing	Measurement Method	Study Area (ha)	Sample Size	Mean	s.d.	depth (cm)	Model	Nug.		
a	Lopez-Granados, 2002 (Site Two)	Caracol, Southern Spain		Vertic Xerochep	crop	before planting	exchangeable K ¹	6	84	741	156	0-0.10	Spherical	0	15210	54.6
b	Lopez – Granados, 2002 (Site One)	Monclova, Southern Spain		Alfisol	crop	before planting	exchangeable K ¹	11.2	80	468	117	0-0.10	Exponential	0	15210	34.5
c	Cahn et al., 1994 (0.25 ha)	Central Illinois, USA		Mollisol	crop		K (not specified)	0.25	200	268.2	114.9	0 - 15	Experimental	5000	7500	50
d	Pierce et al. 1995 (Adrian)	Adrian, USA		Alfisol, loam	crop		K (not specified)	10	74	210	71	0 - 5	Exponential	1850	4168	93
e	Frogbrook et al., 2002 (sampled 1997)			clay loam		before fertilisation		16.5	110				Spherical	994.5	1831	55.09
f	Chatterjee et al., 2015	West Bengal, India	hot and humid, 1443 mm		crop/horticulture	after harvest	Available K ₂ O	81		134.8	51.9	0-15	Exponential	1864.51	923.4	55
g	Chung et al., 2008	Korea	12.7C, 1560*	Coarse, loamy, mixed, non-acid, mesic	crop	after harvest		0.3	246	269.1	27.3		Gaussian	304.2	2281.5	32.9

h	Frogbrook et al. , 2002 (sampled 1998)						before fertilisation	K ²	16.5						Circular	1121	1266	57.71
i	Frogbrook et al. , 2002 (sampled 1999)						before fertilisation		16.5						Penta-Spherical	1050	1034	79.03
j	Nanni et al. , 2011	Sao Paulo state, Brazil	mesothermic climate	Oxisols, Entisols, Alfisols, Ultisols, Inceptisols and Molisols		crop			184	184	61.3	44.6			Spherical	706.18	1373.56	353
k	Pierce et al. , 1995 (Plainwell)	Plainwell, USA		Entisol, loamy sand		crop		K (not specified)	22	174	121	35.9	0 - 20		Spherical	887	391	157
l	Ferraz et al. 2012 (sampled 2008)	Tres Pontas, Brazil	mild tropical altitude	Red-Yellow Latosol.		crop		K Mehlich 1	22	48	7.1	6.5	0-20		Spherical	0	1268.37	437
m	Liu et al. , 2010	Henan Province, central China	monsoon climate 14.6C, 680mm	Sandy medium loam	to clay	crop	after harvest	Available K ³	4	111	161.4	30.8	0-20		Spherical	435	744.1	312.4
n	Silva et al. , 2003	Santa Maria, Brazil		Ultisol dystrophic Hapludalf		crop	before sowing	Available K (flame photometry)	0.3	194	111	31.9	0-20		Gaussian	527	619	16.6

o	Pierce et al. 1995, (Durand)	Durand, USA		Alfisol, fine loam	crop		K (not specified)	16	165	97	31	5 - 20	Spherical	302	833	174
p	Delcourt et al. 1996	Leefdael, Belgium		Silty	crop		K (AES)			NA	NA	0 - 25	Spherical	425	565	149.7
q	Rowlands 1*, 1998	Wyalkatchem, WA		Duplex	crop		K (not specified)	75	56	59.1	24.7	0 - 10	Spherical	185.17	581.23	800
r	Camacho-Tamayo et al. , 2008 (Site Two)	Puerto Lopez, Colombia	2 375 mm 27C	Typic Hapludox	crop	Aug-04	K ⁴	1.875	42	74.1	15.6	0-10	Exponential	182.52	349.83	366.6
s	Machado et al. 2007	Uberlandia, Brazil	tropical humid with dry season,	Red Latosol, moderate clayey texture	crop		K ⁵	25	121	79	21.5	0-20	Linear	466.4	0	NA
t	Kristensen et al. 1995 (Riso)	Riso, Denmark		Sandy loam/sandy clay loam	crop		Available K	10.9	270			0 - 25	Exponential	0	389	129
u	Kristensen et al. 1995 (Vindum)	Vindum, Denmark		Sandy loam	crop		Available K	10	302			0 - 25	Exponential	0	377	25
v	Ferraz et al. , 2012 (sampled 2007)	Tres Pontas, Brazil	mild tropical altitude	Red-Yellow Latosol.	crop		K Mehlich 1	22	54	11.5	12.5	0-20	Exponential	0	365.82	165

w	Liu et al. , 2008	Henan Province, central China	monsoon climate 14.6C, 680mm	clay loam to loam, and the soil is slightly alkaline (pH , 7.7).	crop	Before Sowing	available (AK) ³	K	87	81	105.9	14.3	0-20	Spherical	66.9	149.2	345
x	de Souza et al. , 2010 (Site One)	Araras, SouthEast Brazil	wet summer, dry winter	Oxisol (Typic Haplustox)	crop	fall of 2003			20	80	3.2	1.3	0-20	Spherical	26.1	103.9	185
y	Sidorova et al. , 2012	Northwester n Russia			crop		exchangeable K ⁶			72	202.5	36.2		Exponential	7	106	72.8
z	Ayoubi et al. , 2007	Golestan province, Iran		fine, mixed, thermic, Fluventic Haploxerepts.	crop	before sowing	available K ⁷		1.8	101	334.6	8.1	0-30	Spherical	17.16	62.4	93.9 2
aa	Camacho- Tamayo et al. , 2008 (Site 1)	Puerto Lopez, Colombia	2 375 mm 27C	Typic Haplustox	crop	May-04	K ⁴		1.875	42	70.2	7.8	0-10	Nugget	60.84	0	0
a b	Thompso n et al. , 2004 (Site Two A)	Alabama, USA			crop	January			0.2	124			22	Exponential	0.1	55.1	228. 3
ac	Thompso n et al. , 2004 (Site Two B)	Alabama, USA			crop	January			0.4	58			22	Spherical	23.16	27.52	299

a	de Souza	Araras,	wet	Oxisol	(Typic	crop	fall of 2004	22	90	3.7	1.9	0-20	Exponential	0.9	3.2	121
d	et al. ,	SouthEast	summer, dry	Haplustox)												
	2010 –	Brazil	winter													
	(Site Two)															
ae	Thompso	Alabama, USA				crop	September	0.4	71			11	Spherical	0.01	0.06	295.
	n et al. ,															2
	2004 (Site															
	One)															
af	Thompso	Alabama, USA				crop	September	0.4	48			11	Spherical	0	0.03	160.
	n et al. ,															4
	2004 (Site															
	Three)															

* Unpublished data provided by Pringle for original article

¹ exchangeable K atomic absorption spectrophotometry (AAS) 1

²laboratory analysis was completed by the Soil Management Division - NIAST, RDA 2

³ available K (AK) neutral ammonium acetate extraction method 3

⁴ K extraction with ammonium acetate pH 7.0 (USDA, 2004).6

⁵ HCl 0,05 mol L-1 + H2SO4 0,025 mol L-1 7

⁶ exchangeable K Tsl- NAO modification of the Kirsanov method.4

⁷ available K extraction with ammonium acetate (1N) (Richards, 1954) 5

REFERENCES

- Adderley, W. P., Jenkins, D. A., F.L., S., Stevens, P. A., & Verinumber, I. (1997). The influence of soil variability on tree establishment at an experimental agroforestry site in North East Nigeria . *Soil Use and Management*, 1–8.
- Amirinejad, A. A., Kamble, K., Aggarwal, P., Chakraborty, D., Pradhan, S., & Mittal, R. B. (2011). Assessment and mapping of spatial variation of soil physical health in a farm. *Geoderma*, 160(3-4), 292–303.
- Ayoubi, S., Zamani, S. M., & Khormali, F. (2007). Spatial variability of some soil properties for site specific farming in northern Iran. *International Journal of Plant Production*, 1(2), 225–236.
- Bai, Y. R., & Wang, Y. K. (2011). Spatial Variability of Soil Chemical Properties in a Jujube Slope on the Loess Plateau of China. *Soil Science*, 176(10), 550–558.
- Birrell, S. J., Sudduth, K. A., & Kitchen, N. R. (1996). Nutrient Mapping Implications of Short-Range Variability. *Precision Agriculture, Proceedings of the Third International Conference*, 207.
- Cahn, M. D., Hummel, J. W., & Brouer, B. H. (1994). Spatial Analysis of Soil Fertility for Site-Specific Crop Management. *Soil Science Society of America Journal*, (3), 1240–1248.
- Camacho-Tamayo, J. H., Luengas, C. A., & Leiva, F. R. (2008). Effect of agricultural intervention on the spatial variability of some soils chemical properties in the Eastern Plains of Colombia. *Chilean Journal of Agricultural Research*, 68(1), 42–55.
- Cambardella, C. A., Moorman, T. B., Novak, J. M., Parkin, T. B., Turco, R. F., & Konopka, A. (1994). Field-scale variability of soil properties in central Iowa soils. *Soil Science Society of America Journal*, 58.
- Campbell, J. B. (1977). Spatial variation of sand content and pH within single contiguous delineations of two soil mapping units. *Soil Science Society of America Journal*, 42(3), 460–464.
- Chatterjee, S., Santra, P., Majumdar, K., Ghosh, D., Das, I., & Sanyal, S. K. (2015). Geostatistical approach for management of soil nutrients with special emphasis on different forms of potassium considering their spatial variation in intensive cropping system of West Bengal, India. *Environmental Monitoring and Assessment*, 187(4), 1–17.
- Chung, S. O., Kung, I. K., Sung, K. H., Sudduth, K. A., & Drummond, S. T. (2008). Analysis of Spatial Variability in a Korean Paddy Field Using Median Polish Detrending. *Journal of Biosystems Engineering*, 33(5), 362–369.
- de Souza, Z. M., Cerri, D. G. P., Magalhães, P. S. G., & Siqueira, D. S. (2010). Variabilidade espacial de atributos do solo e produtividade da cultura de cana-de-açúcar em relação a localização topográfica. *Revista Brasileira de Engenharia Agrícola E Ambiental*, 14(12), 1250–1256.
- Delcourt, H., Darius, P. L., & DeBaerdemaeker, J. (1996). The spatial variability of some aspects of topsoil fertility in two Belgian fields. *Computers and Electronics in Agriculture*, 14(2-3), 179–196.
- Everett, M. W., & Pierce, F. J. (1996). Variability of Com Yield and Soil Profile Nitrates in Relation to Site-Specific N Management. *Precision Agriculture, Proceedings of the 3rd International Conference*, 43.
- Farooque, A. a., Zaman, Q. U., Schumann, A. W., Madani, A., & Percival, D. C. (2012). Response of wild blueberry yield to spatial variability of soil properties. *Soil Science*, 177(1), 56–68.
- Ferraz, G., Da Silva, F., Carvalho, L. C. C., Alves, M. D. C., & Franco, B. C. (2012). Spatial and Temporal Variability of Phosphorous, Potassium and of the yield of a coffee field. *Engi. Agríc., Jaboticabal*, 32, 140–150.

- Frogbrook, Z. L., Oliver, M. A., Salahi, M., & Ellis, R. H. (2002). Exploring the spatial relations between cereal yield and soil chemical properties and the implications for sampling. *Soil Use and Management*, 18, 1–9.
- Ganawa, Saeed, E. M., Soom, Amin, M. M., Musa, M. H., Rashid, A., Shariff, M., & Wayayok, A. (2003). Spatial Variability of Total Nitrogen , and Available Phosphorus of Large Rice Field in Sawah Sempadan Malaysia *Science Asia*, 29(2003), 7–12.
- Goovaerts, P., & Chiang, C. N. (1993). Temporal persistence of spatial patterns for mineralisable nitrogen and selected soil properties. *Soil Science Society of America Journal*, 372–381.
- Gutierrez, C. A. G., Cortes, C. A., & Camacho-Tamayo, J. H. (2010). Spatial Variability of Some Chemical Properties in an Entisol. *Revista U.D.C.A Actualidad & Divulgación Científica*, 13, 87–95.
- Kerry, R., & Oliver, M. A. (2003). Variograms of ancillary data to aid sampling for soil surveys. *Precision Agriculture*, 4(3), 261–278.
- Kerry, R., & Oliver, M. A. (2004). Average variograms to guide soil sampling. *International Journal of Applied Earth Observation and Geoinformation*, 5(4), 307–325.
- Kerry, R., & Oliver, M. A. (2007). Comparing sampling needs for variograms of soil properties computed by the method of moments and residual maximum likelihood. *Geoderma*, 140(4), 383–396.
- Kerry, R., & Oliver, M. A. (2008). Determining nugget:sill ratios of standardized variograms from aerial photographs to kriging sparse soil data. *Precision Agriculture*, 9(1-2), 33–56.
- Kilic, K., Kilic, S., & Kocuyigit, R. (2012). Assessment of Spatial Variability of Soil Properties in Areas Under Different Land Use, *Bulgarian Journal of Agricultural Science*, 18(5), 722–732.
- Kristensen, K., Simmelsgaard, S. E., Djurhuus, J. D., & Olesen, S. E. (1995). Spatial variability of soil physical and chemical parameters. *Proceedings of the Seminar on Site Specific Farming*, 39–55.
- Kumhalova, J., Kumhala, F., Kroulik, M., & Matejkova, S. (2011). The impact of topography on soil properties and yield and the effects of weather conditions. *Precision Agriculture*, 12(6), 813–830.
- Laslett, G. M., McBratney, A. B., Pahl, P. J., & Hutchinson, M. F. (1987). Comparison of several spatial prediction methods for soil pH. *European Journal of Soil Science*, 38(2), 325–341.
- Liu, G.-S., Jiang, H.-L., Liu, S.-D., Wang, X.-Z., Shi, H.-Z., Yang, Y.-F., ... Gu, J.-G. (2010). Comparison of Kriging Interpolation Precision With Different Soil Sampling Intervals for Precision Agriculture. *Soil Science*, 175(8), 405–415.
- Liu, G.-S., Wang, X.-Z., Zhang, Z.-Y., & Zhang, C.-H. (2008). Spatial Variability of Soil Properties in a Tobacco Field of Central China. *Soil Science*, 173(9), 659–667.
- Lopez - Granados, F., Jurado-Exposito, M., Atenciano, S., Garcia-Ferrer, A., Sanchez de la Orden, M., & Garcia-Torres, L. (2002). Spatial variability of agricultural soil parameters in southern Spain. *Plant and Soil*, 1, 319–326.
- Machado, L. de O., Lana, Â. M. Q., Lana, R. M. Q., Guimarães, E. C., & Ferreira, C. V. (2007). Variabilidade espacial de atributos químicos do solo em áreas sob sistema plantio convencional. *Revista Brasileira de Ciência Do Solo*, 31(3), 591–599.
- McBratney, a. B., & Pringle, M. J. (1999). Estimating Average and Proportional Variograms of Soil Properties and Their Potential Use in Precision Agriculture. *Precision Agriculture*, 1, 125–152.
- McBratney, A., Clarke, S. F., & Thomson, H. M. (1985). pH, Electrical Conductivity and Bicarbonate-Extractable Phosphorus Values for Soil Specimens From a One Hectare Area at Myall Vale

- Research Station, Narrabri. *CSIRO Division of Soils Technical Memorandum*, 25, 1985.
- Miller, M. P., Singer, M. J., & Nielsen, D. R. (1988). Spatial Variability of Wheat Yield and Soil Properties on Complex Hills. *Soil Science Society of America Journal*, 52(4), 1133.
- Molin, J. P., Di, G., & Faulin, C. (2013). Spatial and temporal variability of soil electrical conductivity related to soil moisture. *Scientia Agricola*, 70(February), 1–5.
- Mondo, V. H. V., Gomes Junior, F. G., Pinto, T. L. F., Marchi, J. L. de, Montomiya, A. V. de A., Molin, J. P., & Cicero, S. M. (2012). Spatial variability of soil fertility and its relationship with seed physiological potential in a soybean production area. *Revista Brasileira de Sementes*, 34(2), 193–201.
- Mondo, V. H. V., Gomes Junior, F. G., Pinto, T. L. F., Marchi, J. L. de, Motomiya, A. V. de A., Molin, J. P., & Cicero, S. M. (2012). Spatial variability of soil fertility and its relationship with seed physiological potential in a soybean production area. *Revista Brasileira de Sementes*, 34(2), 193–201.
- Mulla, D. J. (1993). Mapping and managing spatial patterns in soil fertility and crop yield. *Soil Specific Crop Management*, 15.
- Nanni, M. R., Povh, F. P., Demattê, J. A. M., Oliveira, R. B. De, Chicati, M. L., & Cezar, E. (2011). Optimum size in grid soil sampling for variable rate application in site-specific management. *Scientia Agricola*, 68(3), 386–392.
- Nolin, M. C., Guertin, S. P., & Wang, C. (1996). Within field spatial variability of soil nutrients and corn yield in a montreal lowlands clay soil. *Precision Agriculture, Proceedings of the 3rd International Conference*, 257–270.
- Nouri, H., Amin, M. S. M., Razavi, S. J., Anuar, A. R., Aimrun, W., & Borujeni, S. C. (2010). Sugar Beet Performance Affected by Uniformity of N Fertigation. *American Journal of Applied Sciences*, 7(3), 366–370.
- Oliver, M. A., & Webser, R. (1987). The elucidation of soil pattern in the Wyre Forest of the West Midlands, England. I. Multivariate distribution. *Journal of Soil Science*, 38(2), 279–291.
- Oliver, M. A., & Webster, R. (2014). A tutorial guide to geostatistics: Computing and modelling variograms and kriging. *Catena*, 113, 56–69.
- Panagopoulos, T., & Antunes, M. D. C. (2008). Integrating Geostatistics and GIS for Assessment of Erosion Risk on Low Density Quercus Suber Woodlands of South Portugal. *Arid Land Research and Management*, 22(2), 159–177.
- Pettitt, A.N., & McBratney, A. B. (1993). Spatial Sampling Designs for Estimating Variance Components. *Journal of the Royal Statistical Society. Series C (Applied Statistics)*, 42(1), 185–209.
- Pierce, F. J., Warnke, D. D., & Everett, M. W. (1995). Site Specific Management for Agricultural Systems, 133.
- Pribyl, D. W. (2010). A critical review of the conventional SOC to SOM conversion factor. *Geoderma*, 156(3-4), 75–83.
- Shatar, T. M. (1996). Site Specific Crop Management - Relationships between Edaphic Factors and Sorghum Yield. The University of Sydney, Australia.
- Shouse, P. J., Gerik, T. J., Russell, W. B., & Cassell, D. K. (1990). Spatial Distribution of Soil Particle Size and Aggregate Stability Index in a Clay Soil. *Soil Science*. (149) 351-360.

- Shukla, M. K., Slater, B. K., Lal, R., & Cepuder, P. (2004). Spatial Variability of Soil Properties and Potential Management Classification of a Chernozemic Field in Lower Austria. *Soil Science*, 169(Cv), 852–860.
- Sidorova, V. a., Zhukovskii, E. E., Lekomtsev, P. V., & Yakushev, V. V. (2012). Geostatistical analysis of the soil and crop parameters in a field experiment on precision agriculture. *Eurasian Soil Science*, 45(8), 783–792
- Silva, V. R., Reichert, J. M., Storck, L., & Feijo, S. (2003). Seção Iv - Fertilidade Do Solo E Nutrição De Plantas Ao Potássio Em Um Argissolo Sob. *Revista Brasileira de Ciência Do Solo*, (5), 565–571.
- Tabor, J. A., Warrick, A. W., Myers, D. E., & Pennington, D. A. (1985). Spatial Variability of Nitrate in Irrigated Cotton: II. Soil Nitrate and Correlated Variables¹. *Soil Science Society of America Journal*. (49) 390-394
- Thompson, A. N., Shaw, J. N., Mask, P. L., Touchton, J. T., & Rickman, D. (2004). Soil sampling techniques for Alabama, USA grain fields. *Precision Agriculture*, 5(4), 345–358.
- Truong, P. N., Heuvelink, G. B. M., & Gosling, J. P. (2013). Web-based tool for expert elicitation of the variogram. *Computers and Geosciences*, 51, 390–399.
- Uehara, G., Trangmar, B. B., & Yost, R. S. (1985). Soil Spatial Variability. (D. R. Nielsen & J. Bouma, Eds.). PUDOC Netherlands.
- van Meirvenne, M., & Hofman, G. (1989). Spatial variability of soil nitrate nitrogen after potatoes and its change during winter. *Plant and Soil*, 120, 103.
- Wade, S. D., Foster, I. D. L., & Baban, S. M. J. (1996). The spatial variability of soil nitrates in arable and pasture landscapes: implications for the development of geographical information system models of nitrate leaching. *Soil Use and Management*, 12.
- Webster, R., & McBratney, A. B. (1987). Mapping soil fertility at Broom's Barn by simple kriging. *Journal of the Science of Food and Agriculture*, 38(2), 97–115.
- Webster, R., & Oliver, M. (2001). *Geostatistics for Environmental Scientists*. West Sussex, England: John Wiley & Sons, Ltd.
- Williams, R. D., Ahuja, L. R., Naney, J. W., Ross, J. D., & Barnes, B. B. (1987). Spatial Trends and Variability of Soil Properties and Crop Yield in a Small Watershed. *Transactions of the ASAE*, (306), 1653–1660.
- Yana, J., Lee, C. K., Umeda, M., & Kosaki, T. (2000). Spatial variability of soil chemical properties in a paddy field Spatial Variability of Soil Chemical Properties. *Soil Science and Plant Nutrition*, 46:2, 473-482.
- Zanão Júnior, L. A., Lana, R. M. Q., Carvalho-Zanão, M. P., & Guimarães, E. C. (2010). Variabilidade espacial de atributos químicos em diferentes profundidades em um Latossolo em sistema de plantio direto. *Revista Ceres*, 57(3), 429–438.
- Zhang, X., Jiang, L., Qiu, X., Qiu, J., Wang, J., & Zhu, Y. (2016). An improved method of delineating rectangular management zones using a semivariogram-based technique. *Computers and Electronics in Agriculture*, 121, 74–83.

Chapter 7:

Concluding Remarks and Future work

You live out the confusions until they become clear

Anais Nin 1941

7.1 Overview

Understanding how soil variability changes with scale is fundamental to our attempts to study the soil. The extrapolation of data from individual soil cores to larger scales in the form of field, regional, national or even global soil maps relies on our assumptions about soil variability. Without understanding how variability changes between scales, we cannot know how much information is lost in any process of averaging (such as compositing), how accurate any interpolation is (such as those made between soil observations in kriging) or accurately understand the trade-offs between information lost and accuracy gained when selecting a resolution at which to produce any soil map. As we outlined in the introduction, the cost of multiscale sampling limits the production of empirical work examining the scaling properties of soil variability. As we outlined in Chapter 1, the studies in this topic provide valuable insights into particular fields or regions, but they tend not to be generalisable, and tend not to cover more than three scales (i.e., small farm, large farm, field).

Increasing volumes of soil data stored in georeferenced electronic databases have introduced a new source of information that has helped us to better understand the relationship between soil variability at different scales. In this thesis, we have used a combination of legacy data, remotely observed data and published information to address the following questions.

- *How variable is the soil at different spatial scales?*
- *Can we develop a general model to describe how soil variability changes across spatial scales?*
- *How does soil variability compare with the variability of other environmental properties across spatial scales?*

In this concluding chapter we highlight the contributions this thesis makes towards each of these questions, identify unresolved questions, and highlight promising directions for further development of this work.

7.1.1 How variable is the soil at different spatial scales?

It is generally accepted that soil is highly variable at fine scales. Studies that consider fine scale variability of soil tend to find a high proportion of variability occurs within a few meters (Beckett & Webster, 1971; Le Guen et al., 2017; Šamonil et al., 2011). This result lies in some contrast to studies that consider large scale variability of the soil which find significant proportions of the total variability occurs at large scales (Y. Liu, et. al 2013; Z.-P. Liu, et.al. 2013). In Chapter 2 we bridged the gap between field scale studies and regional scale studies and extended the modelling of spatial variability to the continental scale.

We found that of the total variability found in soil texture in the Australian continent (maximum extent 4,000km), 20% occurs within 1km and 50% occurs within 10km. When we calculate global scale variograms (Chapter 5) they show similar maximum variability to the variograms calculated for the Australian continent. Half of the average expected variability in soil texture across the whole globe is found within a separation distance of 10km.

In Chapter 6 we used a different approach to focus on field scale. In Chapters Two through Five, we focused on quantifying the average or expected variability at different separation distances. In Chapter 6, we examined the variability at a single scale, but under different studies. We found several orders of magnitude difference in the variability for all soil properties we considered (including soil texture). This large range in variability highlights the distinction between the general model that we developed in Chapter 2 and applied through Chapter 5, and the site specific variograms we considered in Chapter 6. In Section 7.4., we propose further development of our understanding of spatial variability from legacy data by disaggregating spatial data by covariate.

Chapter 6 also highlighted the strong tendency for variograms to reach a sill. Only a very small number of variograms modelled did not reach a sill within the 1km extent. In Chapter 6, we referred to this as the local sill, to highlight the fact that we expected greater variability to be reached as the extent increases. We have not yet fully resolved the question of whether these local sills occur as a true representation of a local maximum of variability, or whether there is something intrinsic to the process of modelling the variogram which promotes the appearance of finite variance.

7.1.2. Can we develop a general model to describe how soil variability changes across spatial scales?

We developed a model based on the Hausdorff Besicovitch Dimension (D Value) and the Hurst exponent. These tools have been used to quantify the relative importance of short range and long range dependence in spatial or temporal variables. These tools also provide a measure of roughness or stochasticity that does not depend upon the unit of measure, making comparisons between properties easier. Our model shared these features, but adapted the framework of these tools by allowing the modelling of a gradual change in stochasticity (or roughness, or the relative importance of short and long range variability). The gradual change in stochasticity or roughness is a conceptual departure from the multi-fractal framework introduced by Burrough (1983) and subsequently used by other soil scientists. The multi-fractal framework assumes stochasticity remains constant for several spatial scales and then has a relatively abrupt transition to another range of stochasticity. This result

held for the majority of the environmental properties that we considered. While these results are preliminary, they might hold interesting implications for the use of fractals in environmental modelling.

Using proxy data, we tried alternative sampling designs to ensure this departure was not dependent upon the irregular sampling design of the NSSC dataset (Chapter 3). When applied to different environmental variables, we found again that a model of continuous change in variability provided a very close fit to the data for several other environmental properties (Chapter 4). At the global scale our model of spatial scaling appeared to find its limits. This raises the question of whether the model we developed in Chapter 2 would appropriately model scaling properties of variability on other continents or whether it is for some reason only specific to Australia.

Our model was limited in resolution by bin sizes of one meter. At this resolution there was a large degree of variability in the empirical variogram itself. And we had no capacity to model at finer scales. In Chapter 2 we discussed the shape of the roughness index at the finest scales. The shape of the roughness index at fine resolutions suggested unresolved spatial trend at these very fine scales. As discussed above, trends in very fine scale variability still remain poorly understood. Understanding very fine scale variability is of particular interest because the very fine lateral support of a soil core, and practical limitations on frequency of spacing mean that very fine scale variability may often be missed. If very fine scale variability is an important proportion of overall variability then missing it will mean losing valuable information, and not aggregating appropriately might mean incorporating noise as trend.

7.1.3 How variable is the soil compared to other soil properties?

Our results from Chapter 4 suggest that soil is not much more variable than other environmental properties, except at the finer scales. It is very possible that results at the finer scales are likely to be affected by the different supports of the different environmental variables.

We found that the relationship of scale to variability (that is the relative importance of short range and long range variability with changing distance) was very similar for the following properties Enhanced vegetation index, soil texture % from the NSSC dataset, fine range slope, fine range elevation. Only rainfall and elevation above sea level showed much lower levels of stochasticity (or a stronger importance of long range variability).

We noted the strong similarity between the roughness index of the soil texture and the roughness index for micro-topography, at all but the very finest scales. Having the strong linkage in variability

across so many scales might mean that this provides a useful avenue as a proxy for soil. Modelling micro-topography is important for understanding sedimentary processes (Eltner et al., 2018). Microtopography can also exert an influence on plant species composition (Álvarez-Rogel et al., 2007).

7.2 Future work

As described above, the conclusions we have developed from this thesis have opened up a number of further questions and directions for inquiry. We suggest below several directions for further research. These are not comprehensive, but indicate in our opinion the logical next stages of development of this research.

7.2.1 Develop understanding of drivers of spatial variability of soil texture

Our characterization of soil spatial variability in Chapter 2 is highly general. That is, it does not differentiate between regions, climatic zones, land use type or any other factor. All pairs of observations with the same lag were included in the calculation of the semivariance for that lag. This is one of the strengths of the analysis, as it ensures the results are generalisable, but there is a sacrifice in specificity, and potentially in the applicability of the results. Disaggregating the data and testing whether similar degrees of variability occur within the disaggregated data is a logical step in developing this data to a stage that can be used for prediction.

As a starting point we propose bioregion, geology and topography as potentially useful covariates for the disaggregation of the data. Categorical maps of bioregion (Australian Government, 2012) and geology (Geoscience Australia, 2012) will make disaggregation based on these environmental factors relatively straightforward. Disaggregation by local topography would be more complex. Unlike climatic region and underlying geology, local topography cannot be easily spatially disaggregated. It may be more appropriate to consider the covariation of local topography than to disaggregate the texture data based on this metric.

Ideally, we would be able to disaggregate the data based on agricultural management. However, because the NSSC dataset has been sampled primarily from agricultural regions, if we wish to compare managed versus natural soil within Australia, we will need to use a different source of information. It might be possible to conduct this analysis with Gamma Radiometric data (as per Chapter 3), although as discussed in Chapter 5, the wide support and diffuse boundaries make it difficult to observe and predict fine scale variability. Stockmann, et al. (2015) illustrate the potential to combine proximal soil sensing with remote sensing where increased resolution is required.

Disaggregation of the soil texture data will improve our ability to characterise soil variability. It will also allow us to test the applicability of the roughness index model in more specific settings.

7.2.2. Extend the analysis beyond Australia

With the exception of Chapter 5 and 6, the analysis presented in this thesis focuses on the continent of Australia. Access to the WoSIS dataset, which includes very heavy sampling on the North American continent introduces the possibility of conducting an analogous analysis using North American data. A comparison of the average variability across scales is likely to be illuminating. Even more intriguing, this will allow us to test whether the roughness index model we've developed is specific to Australia or whether it applies from field to continental scales across other continents. As we've indicated, the usefulness of this analysis will likely be increased if we consider other environmental factors when we characterise variability. It would be logical to include a similar extension to the one we've described in Section 7.4.1. to the North American dataset. This analysis would be illuminating in its own right. Also, having a comparison to a continent of a similar size, but different geology, climate, and dominant soil types could provide very illuminating information about the scaling properties of variability under different conditions.

7.2.3. Improve understanding of very fine scale variability

Several components of this thesis point to a need for a more focused strategy if we are to improve our understanding of fine scale variability. The roughness index model we fit in Chapter 2 suggested that there was unresolved spatial variability at scales finer than we were able to model. The wide range of field scale variograms in Chapter 6 highlight the importance of site specificity for field scale variability. Finally, as we describe in Chapter 2, the sampling designs of the variograms we collect in Chapter 6 vary significantly. While this may be in part, due to differing aims between studies, we suspect that this is, at least in part informed by different opinions about the importance of fine scale variability. Studies that aliquot data (average several observations taken within a small area) are inherently implying that very fine scale variability is noise that should be removed to allow more accurate predictions. Studies that make predictions from single very small support (i.e. 10cm, the typical radius of a soil core) are inherently implying that the information in that small support is representative enough of the surrounding area to make predictions from. A better understanding of fine scale variability, and its relationship to other scales of variability will allow us to make better decisions about support and sampling. It will also allow us to better understand the impact of support when we are dealing with very different types of data (as per Chapter 5).

Formalising the relationship between variability across scales and information will be critical to ensuring that enhanced understanding of fine scale variability leads to better outcomes. Bishop, et al. (2001) propose a modification to Shannon's information criterion explicitly for evaluating mapping accuracy and informing decisions around grid size in map production. An extension of this framework to take into account support size would also be useful. Combining the development of a formal framework for linking variability to information content at fine scales with a better characterisation of variability at fine scales would be ideal. Before undertaking significant for purpose field studies (with the associated expense) it would be desirable to extend efforts to gather existing information. It might be possible to extend the analysis in Chapter 6 by seeking out raw spatial observations in place of calculated variograms. A focused meta-analysis of studies that explicitly consider very fine scale scaling, as opposed to precision agriculture studies may also provide useful results.

7.2.4. Develop links between variability, scale and process

One of the eventual long term aims of improving our ability to accurately describe soil variability across multiple scales is improving our ability to link variability, scale and process. Our results from Chapter 2 suggest one possible avenue for this. When soil variability is described as multi-fractal in nature, an appealing explanation is that soil variability across particular scales is controlled by specific environmental factors. Abrupt changes in soil variability are associated with a change in the dominant control. Our theory of more gradual change in soil variability with scale suggests that different interpretations might be necessary. Our results from Chapter 4 suggest that the variability of environmental factors themselves might change in a more gradual way than is implicit in Burrough's (1983) theory. The view of the soil as an inert substance controlled by environmental factors is shifting to a more dynamic role, where the soil exerts control on other environmental factors, in particular vegetation and climate, examples include Govindasamy et al. (1999) and Osborne et al. (2004). Specific mechanistic studies designed to better understand the specific effects and feedbacks of particular variables provide valuable insights into some deterministic components of soil variation and variability. Better understanding variability of soil and other properties across scales and with relation to each other²⁷ will complement these mechanistic studies.

²⁷ We've made some suggestions in 7.4.1.

7.3 Final remarks

This thesis has successfully exploited legacy data to push forward our understanding of the behaviour of soil variability across scales. Further development of this understanding should move us towards a model that can serve to enhance soil sampling methods.

REFERENCES

Álvarez-Rogel, J., Carrasco, L., Marín, C. M., & Martínez-Sánchez, J. J. (2007). Soils of a dune coastal salt marsh system in relation to groundwater level, micro-topography and vegetation under a semiarid Mediterranean climate in SE Spain. *Catena*, 69(2), 111–121.

Australian Government, (Department of Environment and Energy). (2012). Interim Biogeographic Regionalisation for Australia. Retrieved from <http://www.environment.gov.au/land/nrs/science/ibra>

Beckett, P. H. T., & Webster, R. (1971). Soil Variability: A review. *Soils and Fertilisers*, 34, 1–15.

Bishop, T. F. A., McBratney, A. B., & Whelan, B. M. (2001). Measuring the quality of digital soil maps using information criteria. *Geoderma*, 103, 95–111.

Eltner, A., Maas, H. G., & Faust, D. (2018). Soil micro-topography change detection at hillslopes in fragile Mediterranean landscapes. *Geoderma*, 313(October 2017), 217–232.

Geoscience Australia (2012). Surface Geology of Australia 1:1 million scale dataset 2012 edition.

Govindasamy, B., Wehner, M. F., Mchoso, C. R., & Duffy, P. (1999). The influence of a Soil-Vegetation-Atmosphere Transfer scheme on the simulated climate of LLNL/UCLA AGCM. *Global and Planetary Change*, 20(1), 67–86.

Le Guen, M., Herrmann, L., Robain, H., Wiriyaakitnateekul, W., Oliveira, T. De, Robin, A., Lesueur, D. (2017). Geoderma Relevance of taking into account the fine scale soil variability to assess the effects

of agricultural inputs on soil characteristics and soil microbial communities : A case study of biochar application in a rubber plantation in North East Thailand. *Geoderma*, 305, 21–29.

Liu, Y., Lv, J., Zhang, B., & Bi, J. (2013). Science of the Total Environment Spatial multi-scale variability of soil nutrients in relation to environmental factors in a typical agricultural region , Eastern China. *Science of the Total Environment*, 450-451, 108–119.

Liu, Z.-P., Shao, M.-A., & Wang, Y.-Q. (2013). Spatial patterns of soil total nitrogen and soil total phosphorus across the entire Loess Plateau region of China. *Geoderma*, 197, 67–78.

Osborne, T. M., Lawrence, D. M., Slingo, J. M., Challinor, A. J., & Wheeler, T. R. (2004). Influence of vegetation on the local climate and hydrology in the tropics: Sensitivity to soil parameters. *Climate Dynamics*, 23(1), 45–61.

Šamonil, P., Valtera, M., Bek, S., Šebková, B., Vrška, T., & Houška, J. (2011). Soil variability through spatial scales in a permanently disturbed natural spruce-fir-beech forest. *European Journal of Forest Research*, 130(6), 1075–1091.

Stockmann, U., Malone, B. P., McBratney, A. B., & Minasny, B. (2015). Landscape-scale exploratory radiometric mapping using proximal soil sensing. *Geoderma*, 239-240, 115–129.